AD 746335

AFAPL - TR - 72 - 35

NICKEL HYDROXIDE BATTERY ELECTRODE DEVELOPMENT

Dr. H. H. Kroger

General Electric Company
Battery Products Section
Gainesville, Florida

Technical Report AFAPL - TR - 72 - 35

July, 1972

Approved For Public Release; Distribution Unlimited

Air Force Aero Propulsion Laboratory
Air Force Systems Command
Wright-Patterson Air Force Base, Ohio

NOTICE

When Government drawings, specifications, or other data are used for any purpose other than in connection with a definitely related Government procurement operations, the United States Government thereby incurs no responsibility nor any obligation whatsoever; and the fact that the government may have formulated, furnished, or in any way supplied the said drawings, specifications, or other data, is not to be regarded by implication or otherwise as in any manner licensing the holder or any other person or corporation, or conveying any rights or permission to manufacture, use, or sell any patented invention that may in any way be related thereto.

Copies of this report should not be returned unless return is required by security considerations, contractual obligations, or notice on a specific document.

UNCLASSIFIED
Security Classification

DOCUMENT CONTROL DATA - R&D

(Security classification of title, body of abstract and indexing annotation must be entered when the overall report is classified)

1. ORIGINATING ACTIVITY (Corporate author) General Electric Company Battery Products Section P.O. Box 114, Gainesville, Florida 32601	2a. REPORT SECURITY CLASSIFICATION Unclassified 2b. GROUP None

3. REPORT TITLE
NICKEL HYDROXIDE BATTERY ELECTRODE DEVELOPMENT

4. DESCRIPTIVE NOTES (Type of report and inclusive dates)
Final Technical Report - 1 January, 1971 - 31 January, 1972

5. AUTHOR(S) (Last name, first name, initial)
Dr. Hanns H. Kroger

6. REPORT DATE	7a. TOTAL NO. OF PAGES	7b. NO. OF REFS
February, 1972	235	None

8a. CONTRACT OR GRANT NO. F33615-69-C-1312	9a. ORIGINATOR'S REPORT NUMBER(S) 72 BPS 02
b. PROJECT NO.	
c.	9b. OTHER REPORT NO(S) (Any other numbers that may be assigned this report)
d.	AFAPL-TR-72-35

10. AVAILABILITY/LIMITATION NOTICES
Approved for public release; distribution unlimited

11. SUPPLEMENTARY NOTES	12. SPONSORING MILITARY ACTIVITY
None	Air Force Aero Propulsion Laboratory Wright Patterson Air Force Base, Ohio

13. ABSTRACT
An electro-deposition process for nickel hydroxide nickel sinter electrodes was improved with regard to ease of manufacturing. The master plaque concept was employed and the resulting electrode materials had a very uniform composition and an increased utilization. Difficulties encountered in building 20 Ah and 50 Ah cells were overcome; however, these problems deserve further attention. The new positive electrode material permitted the introduction of an extra pair of electrodes into one sample cell, thus increasing the energy density based upon unit volume. 20 Ah cells performed well on all repetitive regimes, but showed indications of memory upon discharge. 50 Ah cells did not meet the requirements of their regime. They were also memorized and had to be removed from repetitive cycling. The severity of the effect appears to be related to cell geometry and design. It is of a temporary nature and can be remedied by suitable means. Chemical analysis detected significant amounts of uncharged positive active material in memorized cells; thus memory is caused by a decay in the charge acceptance of the positive electrodes under the experimental conditions applied.

DD FORM 1 JAN 64 1473

UNCLASSIFIED
Security Classification

14. KEY WORDS	LINK A ROLE	LINK A WT	LINK B ROLE	LINK B WT	LINK C ROLE	LINK C WT
Nickel hydroxide nickel sinter electrodes						
Electro-deposition process						
20 Ah sealed cells						
50 Ah sealed cells						
Energy density						
Repetitive cycling						
Memory phenomenon						
Causes for memory						
Chemical analysis						

INSTRUCTIONS

1. ORIGINATING ACTIVITY: Enter the name and address of the contractor, subcontractor, grantee, Department of Defense activity or other organization (*corporate author*) issuing the report.

2a. REPORT SECURITY CLASSIFICATION: Enter the overall security classification of the report. Indicate whether "Restricted Data" is included. Marking is to be in accordance with appropriate security regulations.

2b. GROUP: Automatic downgrading is specified in DoD Directive 5200.10 and Armed Forces Industrial Manual. Enter the group number. Also, when applicable, show that optional markings have been used for Group 3 and Group 4 as authorized.

3. REPORT TITLE: Enter the complete report title in all capital letters. Titles in all cases should be unclassified. If a meaningful title cannot be selected without classification, show title classification in all capitals in parenthesis immediately following the title.

4. DESCRIPTIVE NOTES: If appropriate, enter the type of report, e.g., interim, progress, summary, annual, or final. Give the inclusive dates when a specific reporting period is covered.

5. AUTHOR(S): Enter the name(s) of author(s) as shown on or in the report. Enter last name, first name, middle initial. If military, show rank and branch of service. The name of the principal author is an absolute minimum requirement.

6. REPORT DATE: Enter the date of the report as day, month, year, or month, year. If more than one date appears on the report, use date of publication.

7a. TOTAL NUMBER OF PAGES: The total page count should follow normal pagination procedures, i.e., enter the number of pages containing information.

7b. NUMBER OF REFERENCES: Enter the total number of references cited in the report.

8a. CONTRACT OR GRANT NUMBER: If appropriate, enter the applicable number of the contract or grant under which the report was written.

8b, 8c, & 8d. PROJECT NUMBER: Enter the appropriate military department identification, such as project number, subproject number, system numbers, task number, etc.

9a. ORIGINATOR'S REPORT NUMBER(S): Enter the official report number by which the document will be identified and controlled by the originating activity. This number must be unique to this report.

9b. OTHER REPORT NUMBER(S): If the report has been assigned any other report numbers (*either by the originator or by the sponsor*), also enter this number(s).

10. AVAILABILITY/LIMITATION NOTICES: Enter any limitations on further dissemination of the report, other than those imposed by security classification, using standard statements such as:

(1) "Qualified requesters may obtain copies of this report from DDC."

(2) "Foreign announcement and dissemination of this report by DDC is not authorized."

(3) "U. S. Government agencies may obtain copies of this report directly from DDC. Other qualified DDC users shall request through ________________."

(4) "U. S. military agencies may obtain copies of this report directly from DDC. Other qualified users shall request through ________________."

(5) "All distribution of this report is controlled. Qualified DDC users shall request through ________________."

If the report has been furnished to the Office of Technical Services, Department of Commerce, for sale to the public, indicate this fact and enter the price, if known.

11. SUPPLEMENTARY NOTES: Use for additional explanatory notes.

12. SPONSORING MILITARY ACTIVITY: Enter the name of the departmental project office or laboratory sponsoring (*paying for*) the research and development. Include address.

13. ABSTRACT: Enter an abstract giving a brief and factual summary of the document indicative of the report, even though it may also appear elsewhere in the body of the technical report. If additional space is required, a continuation sheet shall be attached.

It is highly desirable that the abstract of classified reports be unclassified. Each paragraph of the abstract shall end with an indication of the military security classification of the information in the paragraph, represented as *(TS), (S), (C), or (U)*.

There is no limitation on the length of the abstract. However, the suggested length is from 150 to 225 words.

14. KEY WORDS: Key words are technically meaningful terms or short phrases that characterize a report and may be used as index entries for cataloging the report. Key words must be selected so that no security classification is required. Identifiers, such as equipment model designation, trade name, military project code name, geographic location, may be used as key words but will be followed by an indication of technical context. The assignment of links, rules, and weights is optional.

NICKEL HYDROXIDE BATTERY

ELECTRODE DEVELOPMENT

Dr. H. H. Kroger

July, 1972

iia

FOREWORD

This Final Technical Report covers work performed from 1 January 1969 to 31 January 1972 under Contract No. F33615-69-C-1312, Project 3141, "Nickel Hydroxide Battery Electrode Development". It was prepared by General Electric Company, Battery Products Section, Gainesville, Florida for the Department of the Air Force, Headquarters, Air Force Aero Propulsion Laboratory, Wright-Patterson Air Force Base, Ohio. The program monitors were Mr. J. E. Cooper, until April, 1971, and Mr. R. L. Kerr for the remainder of the contract work, respectively.

Dr. H. H. Kroger, General Electric Company, Battery Products Section, was program manager.

The contribution and assistance of the following Battery Products Section personnel is gratefully acknowledged:

Mr. S. F. Acree
Mr. A. P. Akridge
Mr. R. E. Bartholomew
Mr. A. J. Catotti
Mr. T. R. DeMoully
Mr. J. M. Evjen
Mr. R. J. Lehnen
Dr. S. F. Pensabene
Mrs. S. F. Pulliam
Mr. G. G. Rampel
Mr. J. L. Sturgeon
Mr. C. T. Tillis
Mr. J. R. Young

This report was submitted by the author on 17 March, 1972.

Publication of this report does not constitute Air Force approval of the Report's findings and conclusions. It is published only for the exchange and stimulation of ideas.

James D. Reams
Chief
Energy Conversion Branch
Aerospace Power Division
Air Force Aero Propulsion Laboratory

ABSTRACT

An electro-deposition process for nickel hydroxide nickel sinter electrodes was improved with regard to ease of manufacturing. The master plaque concept was employed and the resulting electrode materials had a very uniform composition and an increased utilization. Difficulties encountered in building 20 Ah and 50 Ah cells were overcome; however, this problem deserves further attention. The new positive electrode material permitted the introduction of an extra pair of electrodes into one sample cell, thus increasing the energy density based upon unit volume. 20 Ah cells performed well on all repetitive regimes, but showed indications of memory upon discharge. 50 Ah cells did not meet the requirements of their regime. They were also memorized and had to be removed from repetitive cycling. The severity of the effect appears to be related to cell geometry and design. It is of a temporary nature and can be remedied by suitable means. Chemical analysis detected significant amounts of uncharged positive active material in memorized cells; thus memory is caused by a decay in the charge acceptance of the positive electrodes under the experimental conditions applied.

TABLE OF CONTENTS

Preceding page blank

TABLE OF CONTENTS (Continued)

TABLE OF CONTENTS (Continued)

TABLE OF CONTENTS (Continued)

TABLE OF CONTENTS (Continued)

LIST OF ILLUSTRATIONS

LIST OF TABLES

LIST OF TABLES (Continued)

LIST OF TABLES (Continued)

LIST OF TABLES (Continued)

LIST OF TABLES (Continued)

SECTION I

INTRODUCTION

This report terminates the work on a three-year program aimed at the development of an improved nickel hydroxide electrode for the use in rechargeable alkaline batteries for aerospace applications. The improvements sought in this study were primarily concerned with achieving a better nickel electrode performance with respect to energy density, charge efficiency, and capacity reproducibility. The specific objectives of this program were the development of nickel hydroxide electrodes

- With a minimum of a specific capacity of 8 Ah/in^3 when discharged at the 5-hour rate at room temperature

- With a charge efficiency of 98% when charged at room temperature at the 5-hour rate

- With a discharge capacity uniformity of ± 1% after a minimum of 200 cycles at a depth of discharge of 50 percent at the 5-hour rate at room temperature

- By means of a process offering maximum ease of manufacturing

The first year's effort was a research program which was devoted to a critical examination of the electrode structure, alternative fabrication techniques and the role of additives. The purpose of this initial phase of the program was to identify the most promising electrode design and fabrication technique in order that subsequent work could be directed towards intensive electrode and cell testing, additional electrode and process development refinements, and, finally, to the production of sealed cells with nominal capacities of 20 Ah and 50 Ah, respectively, and their subsequent testing on application cycling regimes.

At the outset of this study an extensive literature search was conducted and the pertinent reference works have been discussed in the appropriate technical sections of the first interim report issued under this contract (February, 1970). Additional references, with titles, which were not cited have been arranged in the bibliographic section (Appendix I) of the first interim report.

Voltammetric cycling techniques were used to assess the various effects of cobalt and other additives to the active electrode material. That work included a determination of the extent and the effect of zinc-oxide absorption in nickel hydroxide electrodes when coupled with zinc plates as negative electrodes. Chemical, physical, crystallographic and electrochemical aspects of the nickel hydroxide electrode were also explored

in an effort to better understand the possible mechanisms associated with the operation of this electrode and the role of additives in general. While voltammetric cycling of planar electrodes was found to offer a convenient method for studying the electrochemical aspects of the electrode mechanism, it appeared that further experimental work would be required to fully interpret the results obtained from porous electrode structures in terms of actual battery usage. It was felt that with additional efforts such work could lead to useful correlations with more conventional battery tests and that modified voltammetric methods could be successfully used for accelerated life testing and for the study of phenomena like memory.

In general, the results of the voltammetric cycling studies showed that all deliberate additions of cations (cobalt, zinc, cadmium, aluminum, and lithium) to the active material have a beneficial effect on the performance of the nickel hydroxide electrode. None of the additives studied showed any negative effects. Cobalt and zinc were the most effective with regard to better utilization of the active material, capacity maintenance with cycling, and charge efficiency, especially at elevated temperatures of 45°C.

The optimum amount of cobalt additive was found to be between 8 and 10% of the total active material. A uniform distribution of this additive within the active material was found to be essential for maximum benefit. Such homogenity cannot be achieved in commercially impregnated plates in which a significant portion of their active materials stems from the corrosion of the nickel sinter structure.

The extent of the zinc absorption in the positive plate during the operation of a nickel zinc cell was found to be 20% of the "active" cation content after about 400 hours of cell operation. The absorption was found to have no detrimental effect on the performance of the nickel electrode. In fact, the voltammetric performance of the nickel hydroxide electrodes appeared to be enhanced by the presence of ZnO dissolved in the electrolyte.

The corrosion resistance of various candidate substrate materials was evaluated as one means of meeting the capacity reproducibility goal of this project. Since it was known that pure nickel will corrode to some extent during cycling, alternatives to conventional nickel substrate materials were briefly examined. From technical considerations alone, platinum represented the best possible material because of its high oxygen overvoltage and chemical stability. From economical considerations, however, pure nickel appeared to be the only suitable choice for the material. The additional cost associated with the search for other alloys or surface treatments in lieu of pure nickel did not appear to be warranted at the time of this investigation.

A theoretical analysis was conducted to identify and characterize the "ideal" electrode structure in terms of the effects of pore size, porosity, plate thickness, and the relative amounts of conductor and active material on the available electrode energy density. These results showed that a high active material/conductor interface area and maximum substrate porosity are the primary prerequisites for achieving good active material utilization and high electrode energy density in sintered structures. The physical properties of currently available nickel battery plaques appeared to be optimum with respect to those criteria. Little or no improvement in electrode performance was expected to result from any modification in such plaque materials or from the use of other forms of porous carriers. Highest electrode energy densities were obtained with sintered porous bodies having an average pore diameter of 8-12 microns, all other things being equal.

Experiments in which electrodes were first prepared by various methods and then electrochemically and chemically analyzed to determine the optimum plate fabrication and active material loading technique with respect to the overall goals of the program involved the preparation of conventional electrodes as well as electro-deposited and pasted structures. The most promising plates were then subjected to a pretesting phase under sealed cell conditions. These tests used various experimental nickel hydroxide plates of a size suitable for 20 Ah cells in conjunction with commercially available cadmium counter electrodes.

While pasted plates initially appeared to offer the greatest promise from the standpoint of ease of fabrication, production cost, and capacity uniformity, the preparation of such electrodes was found to involve a great deal of art and resulted in specific electrode capacities which at best could only approach that of the sintered plate structures.

Accordingly, an electrochemical precipitation technique was developed for use with the sintered plaque electrodes which appeared to offer two distinct advantages over the typical commercial chemical impregnation processes:

- Three electrochemical precipitation cycles requiring a total of nine hours versus five to eight chemical impregnation cycles at about three hours per cycle

- The distribution of the additives in the active material would be improved by the new method and little if any corrosion of the sinter would occur during the impregnation proper

The specific electrode capacities obtained by the electrochemical precipitation technique were found to be as high as 6.5 Ah/in^3 initially; charge efficiencies of over 98% were achieved for these electrodes when charged to 95% of full capacity; when fully charged, efficiencies of

over 96% were demonstrated for electrodes containing an eight percent cobalt additive. Capacity maintenance of ± 1 percent was demonstrated for 100 cycles at 70% depth of discharge for the electrochemically prepared plates.

In view of these tentative results, it was recommended that work on the electrochemically impregnated sintered plates should be continued in order to develop further refinements in this promising fabrication process. Specifically, these efforts were to be aimed at examining, in greater detail, the effects of other precipitation current densities and conditions, such as pulsed currents, the application of vacuum and the use of surfactants and other additives to the impregnation solution.

In the first year of work, some efforts were also undertaken to elucidate the phenomenon of memory. Commercially available C_s-size cells with nominal capacities of 1 Ah were submitted to a systematic cycling regime. At regular intervals cells were removed from the regime and electrically and chemically analyzed in order to check on a possible capacity loss with cycling. Particular attention was given to the postive electrode in order to determine whether it is the contributing factor to the phenomenon of memory commonly experienced in rechargeable nickel-cadmium cells.

No evidence for the presence of memory was obtained after more than 700 partial depth of discharge cycles. This was actually very surprising since it was thought that such a cycle regime really should induce the effect rather rapidly. Only small, temporary losses in discharge voltage and capacities were observed with repetitive cycling and these could be easily removed by means of a single rejuvenation process. Although the results were disappointing in the sense that memory could not be induced and its causes consequently studied, it was decided to continue with the respective efforts also in the second year of contract work.

For this purpose, two different types of positive electrodes were used, namely:

- Electrodes made by the conventional impregnation process, and

- Electrodes made by a modified electrochemical impregnation process

These cells were then used under a variety of experimental conditions in efforts to induce the memory effect. However, as observed in the previous tests, neither significant losses in discharge capacity nor continuous decay of the end of discharge voltage at the end of the normal discharge periods could be observed. These two deviations are required by the working definition adopted at that time. The only irregularity observed was a step of about 50-60 mV in the voltage versus time curves in the vicinity of the normal end of discharge once the usual depth

of discharge was exceeded. The origin could be traced back to the positive electrodes by means of reference electrode measurements, however, a cause for the step could not be established.

Various modification attempts of the existing three-cycle electrode-deposition process did not succeed in making this process capable of producing nickel hydroxide-nickel sinter electrodes meeting the contract goal of a specific capacity of the positives in the 8-10 Ah/in^3 range. A thorough investigation of the operating conditions of the old constant current process led to the development of a new electro-deposition process of constant potential basis. The application of this novel process supplied positive electrodes with specific capacities approaching and slightly exceeding the lower limit of the range specified. Repetitive cycle testing was conducted with the new experimental plate material on a limited scale and the plates were chemically analyzed prior to and after those experiments. The role of the cobalt additive was also briefly investigated and its level was found to be optimized in the 8-10% range in the same manner as previously found for planar electrodes.

Almost 300 individual electrodes of C_s size were produced by means of the new electro-deposition process based upon the constant potential concept. The resulting cells with maximum specific capacity in the positive electrodes were used for a variety of tests such as repetitive cycling, charge retention, input-output analysis, and memory study as mentioned above. The experimental details involved and the results obtained have been presented and discussed in the respective technical sections of the Second Interim Report (AFAPL-TR-71-12, Issued January, 1971).

An amount of about 30 thicker plates was processed into cells with maximum absolute capacity which had average discharge capacities of 1.5 Ah/cell.

In anticipation of the needs of the third year of contract work scale-up attempts were undertaken. For that purpose about 100 individual plates of 20 Ah-size, i.e., 95 cm^2 geometric surface area each, were individually impregnated using the electro-deposition process on constant potential basis. The electrodes are about twice the size of the previously built C_s size and it was of interest to find out whether or not the distribution of the active material and additive remained uniform. A comprehensive chemical analytical program was conducted which indeed showed the uniformity of the distribution of the active material and its cobalt additive across the surface of the plates. Multi-plate cells with nominal capacities of 20 Ah were built from this plate material and were then cycled on a limited scale. The four sealed cells had an average capacity of 26.0 Ah or a specific capacity of the positive electrodes of 7.8 Ah/in^3, while the four flooded cells of this series had an average capacity of 34.2 Ah or a specific capacity in the positives of 10.3 Ah/in^3.

Concurrent with those scale-up and cycling tasks, the concept of plates made by means of a pasting procedure was studied as a second source for experimental plates. These electrodes delivered only discharge capacities which were equivalent to specific capacities of 5 Ah/in^3. The electrodes consisted of mixtures of freshly prepared nickel hydroxide monohydrate, metallic nickel powder, and a binder which was mechanically impregnated into a porous structure. After drying, the plates were compressed to about 90% of their theoretical density. Limited amounts of cycling showed that the active material was completely utilized and that the corresponding specific capacities were in good agreement with the respective predictions.

Efforts to achieve greater electrode energy densities by dehydration of the active material or by a reduction of the nickel powder content were unsuccessful due to a reduction in the utilization of active materials. Additional attempts to achieve a high material utilization with low conductor levels in the paste were made by decomposing nickel carbonyl on the active material prior to the pasting step. The performance of the resulting nickel cladded active material was found to be identical to that of the mixed powder paste having the same fraction of nickel conductor.

The feasibility for producing high energy density nickel hydroxide electrodes by leaching the aluminum from cast Raney alloys was also examined. This technique was found to be unsuitable as an electrode fabrication process due to the extreme brittleness of the alloys and the inability to completely leach the aluminum.

The third year of contract work is described in detail in the body of this final report.

The actual work was started with continued attempts to further modify and improve the impregnation process proper, especially with respect to ease of manufacturing. At the end of the preceding report period, a six-cycle impregnation process was available which was capable of producing 20 Ah-size experimental electrodes on an individual basis. The process comprised some undesirable steps, like treatment of plates with hot concentrated caustic, vacuum treatment prior to deposit, and above all, was restricted to the impregnation of electrodes of the final size.

The large number of both 20 Ah-size and 50 Ah-size plates required for the final cell cycling testing of the program made it mandatory to take care of these problems in order to cut the span for the impregnation process down to a manageable length. The result of these pertinent efforts was a four-cycle impregnation process both without application of vacuum and caustic conversion step which employed so-called master plaques as electrode raw material.

The term master plaque is defined as a piece of unimpregnated porous nickel sinter structure which contains more than one electrode area of the final size to be made. In the case of the 20 Ah-size a master plaque contained six individual electrodes, and in the case of the 50 Ah-size electrodes, three of that kind. By means of appropriate chemical analysis it could be shown that the further increase in electrode size to be impregnated did not lead to a non-uniformity with respect to the distribution of the active material.

In the subsequent plate making phase, a total of 40 master plaques for 20 Ah cells plus 26 master plaques for 50 Ah cells were impregnated without any difficulties. At a typical lab bench style operation enough electrodes for two cells with 20 Ah nominal capacity were produced per day and electrodes for 1-1/3 cells of nominal 50 Ah cell capacity every other day. This amounted to about roughly 12 square feet of electrode area finished per five-day working week. As done in the preceding scale-up and modification tasks, the uniformity of the plate material with respect to its chemical composition was closely monitored by means of appropriate analyses. The composition of the impregnation solution was also controlled by means of analysis.

In the course of the subsequent cell building task, the experimental positive electrodes made by the electrodeposition process were combined with negative cadmium counter electrodes of conventional design and assembled into sealed cells of the two nominal capacities. The assembly process was rather tedious due to the fact that the substrate used tended to produce numerous internal shorts which in turn required a significant amount of cell rebuilding to be overcome.

The formation process in the flooded state produced discharge capacities to one volt at the nominal two-hour rate which were exceptionally good, namely:

- 25.4 Ah average for 20 Ah cells which was equivalent to a specific capacity of 7.7 Ah/in^3 for the positive electrodes.

- 54.2 Ah average for 50 Ah cells which in turn represented a specific capacity of the positives of 8.2 Ah/in^3.

The cells of both 20 Ah and 50 Ah nominal capacity were then assigned to various repetitive cycling regimes at 50 percent or less depth of discharge. Details of the regimes and the pertinent results obtained are discussed in the corresponding chapters. However, the outstanding common denominator of the test program phase is the occurrence of memory. As mentioned in the pertinent paragraphs above, memory did not occur when cells were tested under various conditions which contained only one electrode of each polarity and which were only of moderate geometric size.

The long elusive phenomenon has obviously numerous aspects, but it appeared to be common to all cases involving multiplace stacked designs with large geometric electrode areas. This finding is even more striking since the positive plates for the wound and planar designs were made by similar impregnation processes. In a concerted effort of both chemical analyses and electrochemical discharges, the memory effect can be reduced to two basic facts, namely:

- Under the conditions applied, the positive electrodes suffer a decay in charge acceptance, and consequently at the end of a given charge period are no longer completely charged.

- Under the same experimental conditions, the negative electrodes are no longer capable to deliver their useful charge at normal potential readings. This occurred at the end of a charge period and resulted in distortions of the cell voltage versus time curves on discharge.

The chemical analyses applied to both cycled and uncycled cells definitely detected the causes for the occurrence of memory. The various methods of rejuvenation, that is to say, to get rid of the memory phenomenon,are described in detail, too. However, it appears that even if the symptoms of memory are eradicated, the imprint of the transient effect still prevails in the composition of the electrode material.

In an addendum to the final report, the more pertinent details of the impregnation process proper have been discussed and a schematic flow sheet of the procedure is also provided.

SECTION II

PROCESS MODIFICATION AND SCALE-UP

1. GENERAL REMARKS

An electrodeposition process, based upon the constant potential concept, was developed in the course of the second year of the contract work which enabled us to produce nickel hydroxide-nickel sinter electrodes with specific capacities in the 8 - 10 Ah/in^3 range.

This process, however, at the onset of this task, required six consecutive impregnation cycles with various lengths of time and potential settings in order to achieve the desired loading of the plates with active material. In each impregnation cycle, a treatment of the impregnated plates with concentrated hot caustic was needed for the conversion of the deposits into the β-modification.

Porous nickel sinter plaques of the final size of the respective electrode type were impregnated in individual vessels, and although up to six such impregnation containers could be electrically connected in series in order to increase the material output per unit of time, the physical handling of the numerous specimens involved proved to be a rather cumbersome procedure.

The predeposition treatment of the plaques by means of a vacuum impregnation in the same type of solution used in the subsequent electrodeposition steps aggravated the situation even more.

In order to achieve a greater ease of manufacturing, the following improvement goals were set:

- Elimination of the predeposition vacuum step.
- Reduction of the number of impregnation cycles.
- Elimination of the treatment with hot caustic.
- Impregnation of plaque sizes containing more than one electrode area of a given type.

2. EXPERIMENTAL APPROACH

a. Variation of Experimental Conditions

Our first experiment dealt with the influence of a wetting agent on the plaque soaking step, i.e., the impregnation with nitrate solution immediately preceding the cathodization step. For this purpose C_S-size plaques were treated with four molar Ni/Co nitrate solution

either as prepared, or containing 3 drops per liter of Tergitol NPX (Union Carbide Co.), as a wetting agent. This treatment was done either at atmospheric pressure or under application of vacuum. Since only relative gains in weight were of interest, we refrained from converting the nitrate to hydroxide and weighed the wet plaques after a 15 second dripping period.

The results are presented in Table 1. Column "Plaque Number" is followed by the impregnation technique applied. The last three columns contain the gains in weight in grams for individual plates and its average per group, the latter in rounded-off form.

As can be seen, the application of the wetting agent did not affect the gains in weight. However, the plates treated this way had a cleaner appearance after an additional drying. This can indicate that more active material was confined to the interior of the plates.

Highest relative gains in weight were observed with the application of vacuum. The difference to five minute atmospheric treatment was almost 10%, but became considerably smaller when the treatment time at atmospheric pressure was extended to ten minutes. Since the elimination of a vacuum impregnation prior to cathodization could be considered a step into the direction of ease of manufacturing, especially with regard to the larger master plaque, it was decided at this point to discontinue the vacuum treatment in all future work.

In order to support this decision, the vacuum impregnation step was eliminated in the next set of actual C.P.E.D. experiments. The sequence of constant potential setting was the same as always; namely,

3.0 V at cycle one

2.75 V at cycle two

2.5 V at cycles three through six.

The reaction time was different, with subgroups of two plates always being cathodized for 30, 37-1/2, or 45 minutes, respectively. Upon completion of the actual impregnation process, some plates were submitted to the formation in the flooded state, i.e., to the transition from "green" to "black" active material.

In Table 2, the results pertaining to incremental and cumulative gains in weight and calculated theoretical capacities, C_t, are presented. For comparison, average results obtained during the preparation of 300 plates are also given. Those impregnations were done with a vacuum step prior to each cathodization.

TABLE 1

VARIATION OF PREDEPOSITION CONDITIONS

PLAQUE NO.	TECHNIQUE	GAIN IN WEIGHT; GRAMS INDIV.	AVG.	ROUND-OFF
1	5 Minutes Vacuum	3.979	4.087	4.1
2		4.194		
3	5 Minutes Vacuum +	4.006	4.017	4.0
4	NPX *	4.027		
5	5 Minutes Atmosphere	3.631	3.707	3.7
6		3.783		
7	5 Minutes Atmosphere +	3.603	3.683	3.7
8	NPX *	3.762		
9	10 Minutes Atmosphere +	3.865	3.855	3.9
10		3.844		
11	10 Minutes Atmosphere +	3.744	3.831	3.8
12	NPX *	3.919		

* NPX denotes presence of wetting agent

TABLE 2

GAINS IN WEIGHT AND THEORETICAL CAPACITIES Ah/PLATE

GROUP	PLATE	t*	CYCLE: 1	2	3	4	5	6	GREEN	BLACK	C_t
			INCREMENTAL GAINS IN WEIGHT								
OLD	AVG#	30	3402	1505	653	489	272	117	6438	5897	1.70
I	A	30	2909	1559	874	621	336	169	6468		
	B	30	2896	1559	787	606	457	164	6469	6219	1.80
	C	37.5	3227	1590	771	603	317	139	6647		
	D	37.5	3214	1538	791	590	341	127	6601	6309	1.82
	E	45	3494	1570	764	588	241	46	6703		
	F	45	3498	1660	775	629	182	76	6820	6300	1.28

* Cathodization time, t, in minutes for all cycles of a given experiment.

Refers to results obtained previously.

All weight numbers are mg/plate

The 30-minute duration cycles resulted in the same amount of green material for both vacuum and atmospheric impregnation; however, the latter obviously retained more active material in the inside in the course of the flooded formation. This resulted in a significantly greater value for C_t, i.e., 1.80 Ah versus 1.70 Ah.

The increase in cathodization time did not bring the expected results, inasmuch as the gains were more in the "green" form of the active material and apparently externally deposited. Common to all new experimental runs was the sharp decline of incremental gains in weight with increasing number of cycles. This appears to be inherent with the process and was already observed in the course of our previous work on the subject contract.

Since this phenomenon persisted through all the other experimental runs performed, we refrain from presenting any more incremental gains in weight, but in subsequent tables will present cumulative ones only together with calculated theoretical capacities, C_t. More emphasis, however, will be put on the experimental conditions applied and their respective variations. These results are presented in the following two tables where every time the respective results and experimental data from previous runs are given for comparison.

Common to all experiments presented in Table 3 was the final formation in the flooded state following the completion of the respective impregnation procedures.

A comparison of Groups OLD and I has already been performed above and resulted in the replacement of the vacuum impregnation step by a soaking at atmospheric pressure for five minutes.

The plates of Group II were soaked only prior to the cathodization in solutions containing about 3 drops per liter of Tergitol NPX as wetting agent. The impregnation solution in the reaction vessels did not contain any additional wetting agent.

Although the "green" weights, Δ WG, are comparable with those of Group II, the internally affixed amount of active material was lower here. Since this indicates that surfactants favor the undesired external deposition, the use of this type of additives was discontinued.

Plates of Group III were treated for four cycles with a combination of a constant potential and a constant current regime. After 15 minutes C.P. operation at the levels indicated, the mode was switched at this particular time. Naturally, the reaction cell voltages obviously rose through "critical" levels as indicated by the large portions of external scaling.

TABLE 3

RESULTS & CONDITIONS OF IMPREGNATION VARIATIONS I

GROUP	PLATE	ΔW_G	ΔW_B	C_t	NOC	CONDITIONS
OLD	AVG#	6.44	5.90	1.70	6	30 min STD SEQ VACUUM
I	A	6.47			6	30 min STD SEQ w/o VACUUM
	B	6.47	6.22	1.80		
	C	6.65			6	37.5 STD SEQ w/o VACUUM
	D	6 63	6 31	1.82		
	E	6.70			6	45 STD SEQ w/o VACUUM
	F	6.82	6.30	1.82		
II	G	6.34	5.59	1.62	6	30 min STD SEQ w/o VAC w/NPX
	H	6.32	5.71	1.65		
	I	6.51	4.61	1.62	6	37.5 STD SEQ w/o VAC w/NPX
	J	6.66	5.90	1.70		
	K	6.68	5.89	1.70	6	45 STD SEQ w/o VAC w/NPX
	L	6.88	5.87	1.69		
III	M	9.03	5.43	1.57	4	15 min 3V →45 m CC w/o VAC
	N	8.67	5.52	1.59		
	O	7.65	5.32	1.54	4	15 2.75V→45 m CC w/o VAC
	P	8.57	5.50	1.59		
	Q	7.15	5.17	1.50	4	15 2.5V→45 m CC w/o VAC
	R	6.47	5.55	1.60		
IV	S	8.17	5.33	1.54	4	15 min 3.0V→45 m CC one-sided w/o VAC
	T	6.80	5.48	1.58	4	15 2.75V→45 m CC "
	U	4.99	4.94	1.43	4	15 2.5V→45 m CC "
V	W	6.19	5.63	1.63	6	1st cycle 30 min 3V →30 m CC
	X	7.22	5.84	1.69	6	2-6 cycle 30 min 2.75V→30 m CC
	Y	6.57	5.71	1.65	6	w/o VAC

Refers to results obyained previously
STD SEQ Refers to the setting of constant potential
i.e. 3.0,2.75,2.5,2.5,2.5,2.5V per cycle

Group IV is a repetition of the experiments of the preceding group; however, the plaques to be impregnated were only faced on one each of its sides. The eventually obtained theoretical capacities, C_t, are too low in comparison with group "OLD", and besides that, large amounts of external deposition were encountered.

Group V cells were treated by a different combination of C.P. and C.C. Resulting C_t values are below expectations, and as seen at the ΔW_G values, the overall deposition of active material was rather wide-ranged.

As a consequence of the results reported in Table 3, the method as described for group I was tentatively selected for future work, or in other words, the process of last year without vacuum impregnation, but pre-cathodization soaking in the impregnation vessels.

b. Replacement of Caustic Conversion Step

The conversion of the electrochemically deposited α - $Ni(OH)_2$ to the normal β - modification cannot only be obtained by treatment with hot caustic, but also by means of a charging and discharging in caustic at room temperature. Corresponding results are presented in Table 4. Following each impregnation cycle, the plates were pulse-charged and discharged. Currents for charge were based upon average gains observed previously and the number of pulses limited so that about 45% of the theoretical plate capacity was applied. Discharge was at three-fourths of the value of charge current to the breaking of the plate potential.

Naturally, no gain in weight values for "green" material could be obtained in this manner as indicated by the "-" mark in the ΔW_G column. Results and condition of last year's efforts are again given for comparison.

The conditions applied to group VI plates were identical with those for group V with the exception of the conversion treatment. Final loadings with active material obtained were slightly lower for group VI material.

Groups VII and VIII were merely trials to improve early cycle loadings over established levels. Since they failed to raise the amounts of active material internally deposited, these attempts were terminated after one or two cycles, respectively.

The next three groups, IX, X, and XI, respectively, were submitted to additional combinations of the C.P. plus C.C. concept. The resulting theoretical capacities, C_t, approached, but did not quite reach, last

TABLE 4

RESULTS & CONDITIONS OF IMPREGNATION VARIATIONS II

GROUP	PLATE	ΔW_G	ΔW_B	C_t	NOC	CONDITIONS
0	AVG#	6.44	5.90	1.70	6	30 min STD SEQ VACUUM
VI	1	-	5.46	1.58	6	1st cycle 30 min 3V→30 min CC
	2	-	5.39	1.56	6	2-6 cycle 30 min 2.75V→30 min CC
	3	-	5.47	1.58	6	El chem pulsing
VII	4	-	4.68	1.35	2	1st 15 min 3V→45 min CC
	5	-	4.62	1.33	2	2nd 15 min 2.75V→45 min CC
	6	-	4.61	1.33	2	El chem pulsing
VIII	7	-	3.72	1.07	1	30 min 3.0V→30 min CC
	8	-	3.63	1.05	1	
	9	-	3.41	.99	1	El chem pulsing
IX	10	-	5.74	1.66	6	1st cycle 15 min 3V→45 min CC
	11	-	5.68	1.64	6	2-6 cycle 15 min 2.75V→45 min CC
	12	-	5.75	1.66	6	El chem pulsing
X	13	-	5.21	1.51	6	1st cycle 30 min 3V→30 min CC
	14	-	5.32	1.54	6	2-6 cycle 30 min 2.75V→30 min CC
	15	-	5.40	1.56	6	El chem pulsing
XI	16	-	5.75	1.66	6	1st cycle 15 min 3V→15 min CC
	17	-	5.72	1.65	6	2-6 cycle 15 min 2.75V→15 min CC
	18	-	5.66	1.63	6	El chem pulsing
XII	19	-	6.13	1.77	5	30 min cycle STD SEQ
	20	-	5.40	1.56	5	
	21	-	6.26	1.81	5	El chem pulsing
XIII	22	-	5.92	1.71	6	30 min cycle STD SEQ
	23	-	6.14	1.78	6	
	24	-	6.15	1.78	6	El chem pulsing

\# Refers to results previously obtained

STD SEQ Refers to sequence of potential settings

year's level of 1.70 Ah/plate. In addition to that, it was found that a midstream switch from one operation mode to another requires too much attention by the equipment operator.

Group XII plates produced acceptable C_t values, but with too wide a spread between 1.56 and 1.81 Ah. Test terminated after five cycles due to operator error which led to plate blistering.

Group XIII was consequently processed as a back-up for the group XII plates. As can be seen, C_t values and their range are good, so that the pulsing electrochemical process can successfully replace the treatment with hot caustic. This change is considered as a significant step in the direction of facilitating the overall process.

c. Impregnation at Elevated Temperature

A limited number of experiments were also run at elevated temperatures. The impregnation solution was kept in the 95 - 105°C range, i.e., just below its boiling point. Both C.C. and C.P. mode of operations were used and the respective results are presented in Table 5.

As can be seen, remarkable gains in weight and corresponding theoretical capacities, C_t, were obtained in only two impregnation cycles. However, considerable portions of the active material were deposited externally, and were not removed by either the treatment with hot caustic or the final formation in the flooded state. Actually, the second procedure failed to change the color of the deposits from green to black. In addition, large amounts of green solids were produced in the course of the cathodization and floated freely around in the impregnation vessels. The amount of external deposition and these solids in the solution indicate a low efficiency of the process, and we therefore decided not to pursue this approach any longer.

d. Impregnation of Master Plaques

The term, "Master Plaque", refers to a piece of porous nickel sinter which contains a multitude of individual electrode areas. Such a master plaque is submitted to the impregnation process as a unit, and only at the completion of the process (at this time it might also be referred to as "Master Plate") is it cut into single electrodes.

In the case of the 20 Ah-size electrodes, a master plaque contained six electrodes, and in the case of the 50 Ah-size electrodes, only three individual areas.

Utilizing the experience gained in the experiments described above, a total of 12 master plaques for 20 Ah electrodes were now impregnated under a variety of conditions.

TABLE 5

RESULTS & CONDITIONS OF IMPREGNATION VARIATIONS III

ELEVATED TEMPERATURE

GROUP	PLATE	ΔW_G	ΔW_B	C_t	NOC	CONDITIONS
XIV	H1	5.08	4.60	1.33	2	15 min 16 A caustic treatment
	H2	6.29	5.54	1.60	2	20 min 16 A caustic treatment
	H3	7.40	7.09	2.05	2	30 min 16 A caustic treatment
XV	H4	4.72	4.32	1.25	2	10 min 2.75 V caustic treatment
	H5	6 06	5.24	1.51	2	20 min 2.75 V caustic treatment
	H6	6.01	5.75	1.66	2	30 min 2.75 V caustic treatment
XVI	H7	4.49	4.36	1.26	2	10 min 2.5 V caustic treatment
	H8	5.75	5.27	1.52	2	20 min 2.5 V caustic treatment
	H9	6.22	5.89	1.70	2	30 min 2.5 V caustic treatment

Following the impregnation, the six plates from a given master were assembled into a flooded cell and submitted to three charge-discharge cycles. Results are presented in Table 6, which also contains in the line marked "OLD" the prorated discharge capacity of plates made on a one-by-one basis last year. The table is organized as follows:

Plate number in Roman numerals, incremental gain in weight per master plaque, cumulative gain in weight in the "green" state, ΔW_G and gain in weight in the "black" state, ΔW_G, all three columns expressed in grams. Discharge capacities, $C_{.6}$, in Ah to an end point of .6V are stabilized third cycle values. They were obtained at a discharge current of seven amperes following a 20-hour charge at 1.5 amperes. The conditions shown for each impregnation cycle are minutes of cathodization time and C.P. setting in volt.

For the material conversion, three different treatments were applied; namely,

CAUSTIC	A one-hour soaking in 31% KOH at 80°C.
PULSE	A charge-discharge regime in 31% KOH at room temperature by means of constant current pulses.
CHARGE	A charging only in 31% KOH at room temperature.

One of these treatments was applied after each cathodization and was followed by the usual washing, drying, and weighing steps.

Beginning with plaque VII, the end regions of the plaques were coined and the bath temperature during soaking and impregnation was elevated into the 35 - 40°C range.

As can be seen, the incremental gains in weight decreased with an increasing number of cycles, regardless of the experimental conditions applied. It appears that the gains in weight to be expected in cycles five and six, respectively, are more or less random, and we therefore decided to terminate the impregnation process after cycle four. This resulted in discharge capacities of slightly above 16 Ah for a six plate cell and is in good agreement with previous results.

The new concept was then applied to the impregnation of two master plaques containing 50 Ah-size electrodes. Upon the successful completion of this test, the two plates were cut into single electrodes, and a temporary cell was built containing the six individual electrodes and seven negative cadmium electrodes of conventional designs serving as counters.

TABLE 6

GAINS IN WEIGHT & CAPACITIES & CONDITIONS

	Cycle									Conditions												
	1	2	3	4	5	6	ΔW_G	ΔW_B	C_{x6}	1		2		3		4		5		6		TREATMENT
OLD#	-	-	-	-	-	-	-	-	16.6	37	3.0	30	2.75	30	2.5	30	2.5	30	2.5	30	2.5	CAUSTIC
I	38 4	18.9	9.0	4 8	.1	0	71.2	65.6	16.2	45	3.0	45	2.75	45	2.5	45	2.5	45	2.5	4	.5	CAUSTIC
II	39 5	18.1	6.2	4.0	-	-	66.8	64.6	16.0	45	3.0	45	2.75	45	2.75	45	2.75					CAUSTIC
III	27.7	18.4	8.3	5.0	1.8	.6	61.8	61.7	15.8	30	3.0	30	2.75	30	2.5	30	2.5	30	2.5	30	2.5	CAUSTIC
IV	29.2	18.4	8 3	6.7	3.7	7.9	N.A.	74.2	18.9	30	3.0	30	2.75	30	2.5	30	2.5	30	2.5	30	2.5	PULSE
V	33.7	14.4	6.0	7.1	7.3	3.0	N.A	71.6	19.2	45	3.0	30	2.75	30	2.5	30	2.5	30	2.5	30	2.5	PULSE
VI	34.7	17.3	9.4	5.9	3 7	3.0	N.A.	74.0	19.8	45	3.0	30	2.75	30	2.5	30	2.5	30	2.5	30	2.5	CHARGE
VII*	39 3	13.7	6.0	5.3	1.3	1.6	N A	67.1	18.2	45	3.0	45	2.75	30	2.5	30	2.5	30	2.5	30	2.5	PULSE
VIII*	38.4	16.6	7.7	5.5	0	5 8	N.A.	74.0	18.4	45	3.0	45	2.75	30	2.5	30	2.5	30	2.5	30	2.5	CHARGE
IX*	33.1	17.8	7.4	5.8	-	-	N.A.	64.2	16.5	45	3.0	30	2.75	30	2 5	30	2.5					PULSE
X*	34.1	15.6	9.6	7.2	-	-	N.A	66.8	17.4	45	3.0	30	2.75	30	2.5	30	2.5					CHARGE
XI*	42.8	12.3	3.3	5.0	-	-	N A	63.8	16.1	45	3.0	30	2.75	30	2.5	30	2.5					PULSE
XII*	39.3	13.6	9.5	5.5	-	-	N A	67.9	17.9	45	3.0	30	2.75	30	2.5	30	2.5					CHARGE

* Elevated temperature in the 35° - 40° range and coined edges.
\# Refers to results obtained previously

The cell was then cycled in the flooded state for four cycles. The results obtained were favorable and will be presented later on in the plate making section.*

3. CONCLUSIONS

These variations of the experimental conditions led to a considerable process improvement with respect to the ease of manufacturing.

It could be shown that the use of a wetting agent had no beneficial effects on the amount of the active material deposited inside of the pores of the nickel sinter electrode structure.

A soaking of the plaques in the impregnation solution at atmospheric pressure prior to the electrodeposition step was equivalent to the previously applied vacuum impregnation. The vacuum impregnation was henceforth abandoned.

The cumbersome conversion step of the deposited active material by means of hot concentrated caustic could also be eliminated. The two electrochemical procedures investigated, i.e., charging and discharging of the electrodeposited active material by means of constant current pulses and a charging process by constant current only, were equal in efficiency. However, the latter was easier to conduct, and consequently incorporated into the new improved process.

A slight elevation in operating temperature from formerly room temperature into the 35 - 40°C range also proved to be beneficial.

The number of impregnation cycles could be reduced from six to four without any detectable changes in the final quality of the plates.

Master plaques with either six electrode areas of 20 Ah-size or three electrode areas of 50 Ah-size could be impregnated under the conditions of the improved process. The plates from these "preproduction" runs were tested in flooded cells for a limited length of time. The results obtained were so encouraging that the process modification and scale-up phase could be terminated considerably ahead of scheduled time. The time thus saved was later on used in an extension of the cycle testing of actual cells of nominal 20 Ah and 50 Ah capacity containing the experimental positive electrodes.

---

* Prior to this experiment, the impregnation of 50 Ah-size single electrodes was briefly investigated. The plate loadings with active material were very promising, and the approach would have been used in case the master plaque concept for any reason could not have been applied. Now, however, with the two master plaques of this type prepared, the single electrode concept was no longer pursued.

SECTION III

PLATE MAKING

1. GENERAL REMARKS

In the experiments described in this task, the modified constant potential electro-deposition process, in short, C.P.E.D. process for the remainder of this report, was used for the impregnation of numerous master plaques for 20 Ah-size and 50 Ah-size electrodes.

Before the actual impregnation of the master plaques could be started, a sufficient amount of nickel sinter had to be produced in order to meet the following requirements:

- 20 cells of nominal 20 Ah capacity, namely,
  16 cells for various test programs
  4 cells as spares for contingencies

- 4 cells of nominal 50 Ah capacity, namely,
  2 cells for a low earth orbiting regime
  2 cells as spares for contingencies

- Enough single electrodes of both types for replacements which might be required in the cell building process and for chemical analysis purposes.

Following the impregnation process proper, the master plates were cut into individual electrode sizes, then submitted to a formation process in the flooded state and a roller compression-trimming procedure before actually used in the building of sealed cells designated to the various testing conditions.

2. EXPERIMENTAL APPROACH

a. Equipment

The equipment used in the course of the plate making will be described merely to such an extent as to give an idea of its functioning. For more detailed information, we refer here to the addendum to this report.

A suitable power supply for the electrochemical impregnation of master plaques was constructed in accordance with the schematic diagram given in Figure 1. During the operation of the unit, the charger continuously recharged the nominal 34 Ah flooded battery with a constant current of eight amperes. The 19-cell battery was divided into three sections of seven, six, and six cells, respectively, which were connected in series. While one section supplied power to the reaction vessel by means of its individual double pole knife switch,S1-S3, the other two were recharged for subsequent operation. The adjustable resistor permitted the operation of the system either in a constant potential or constant current mode. The reaction vessel voltage was read directly across the electrodes; the current was measured as a voltage drop across the shunt.

Although the arrangement as described worked in a satisfactory manner, it nevertheless required the almost continuous attention of an operator in order to hold the potential across the electrodes really at a constant level. Consequently, it is strongly recommended to use a self-regulating power supply for further applications which meets the appropriate current and voltage requirements.

From the experience gained with the impregnation of single 20 Ah-size electrodes, we anticipated the appearance of initial surge currents of up to 100 amperes and sustained currents in the 60-70 ampere range for this larger plaque material. Consequently, all the wiring was done with No. 8 insulated copper wire.

The impregnation vessels were made of polycarbonate and contained approximately 15 liters (4 gallons) of the four molar nickel nitrate/cobalt nitrate solution made up as done previously. Polycarbonate was chosen over other plastics for its resistance against elevated temperature above the level of boiling water. This was done in anticipation of temperature increases in the course of operation and also for the case that impregnations at higher than room temperature might be undertaken.

The power supply for the subsequent formation of the impregnated plaques in the flooded state initially a set of 15 series-connected 80 Ah cells which operated in parallel with a recharging power supply delivering a continuous current of ten amperes.

SCHEMATIC OF PRECIPITATION POWER SUPPLY

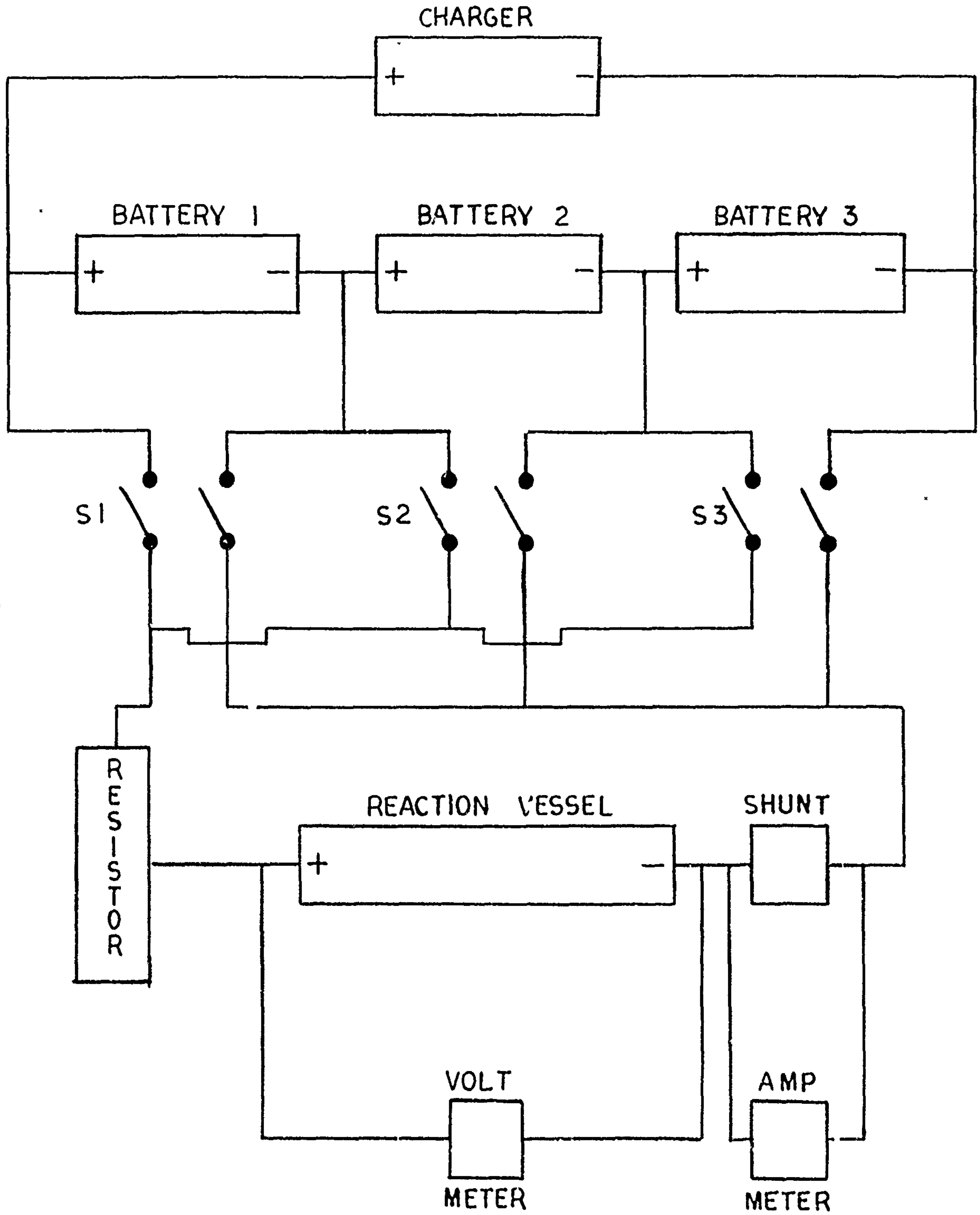

FIGURE 1

In the course of the plate making procedure, these 80 Ah cells were replaced by a self-regulated power supply which was capable of delivering constant currents of up to 30 amperes.

This formation, i.e., charging at constant currents, was conducted at room temperature in polyethylene troughs of the same dimensions used in the impregnation step itself. The lower temperatures encountered here and the high alkalinity of the 31% by weight KOH electrolyte were the causes for selecting this vessel material.

The subsequent washing of the formed plates was also done in polyethylene vessels of the same dimensions. An adequate supply of boiling distilled water, or at least of de-ionized quality, had to be provided by heating it in 4 liter beakers on Bunsen burners and electric hot plates.

A forced air oven set at 110°C for the drying of the washed plates and a top-loading balance for the determination of gain in weights completed the equipment. The latter should be capable of being read at an accuracy of .1 of a gram.

The physical arrangement of all this equipment was done in a manner as to permit a straight-forward transfer of the plaques from one station to the next. It is felt that this definitely was one reason that no operational errors occurred in the course of the impregnation of all these master plaques.

Impregnation, formation,and washing stations existed in duplicate in order to permit the concurrent treatment of two master plaques at each of these steps. From the experience gained with this particular equipment size and arrangement, the increase in material output per unit of time appears feasible by simply employing a greater number of treatment vessels simultaneously at each station.

b. Material

A continuous length of about 50 meters of a porous nickel sinter structure on a nickel wire mesh screen as substrate was produced in a width of 17.1 cm. More pertinent details are to be found in the addendum to this report on page 201

This strip was then cut to the appropriate dimensions to accommodate six 20 Ah-size electrodes or three 50 Ah-size electrodes per master plaque. Metric dimensions are given in Figures 2 and 3, respectively.

As can be seen, one nickel sheet metal strip is provided for each electrode section. It is spot-welded to the compacted section of the nickel sinter along the upper edge of the master plaque. Later on, when cut to appropriate dimensions, part of this strip will serve as tab for the

20 AH MASTER PLAQUE

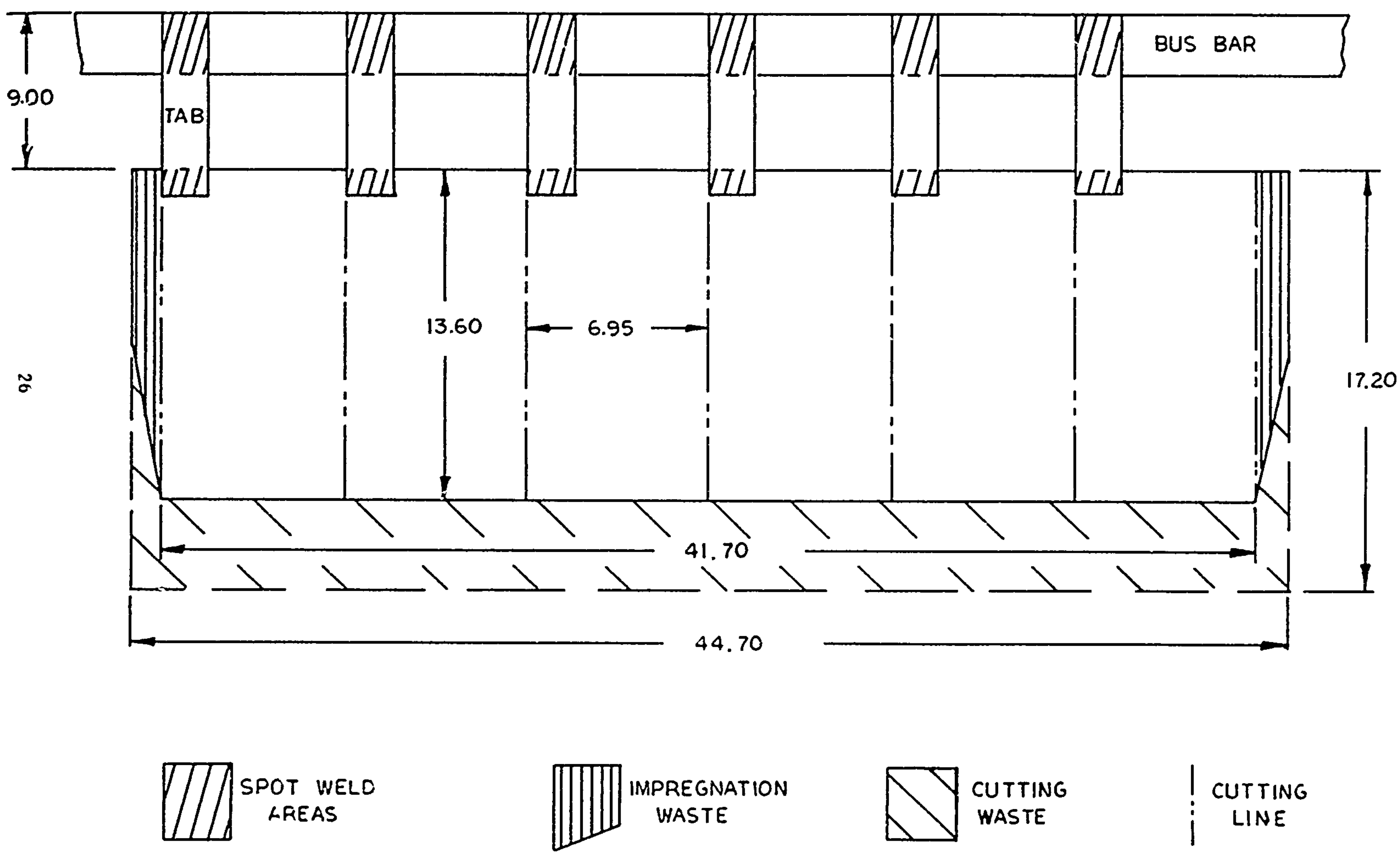

FIGURE 2

50 AH MASTER PLAQUE

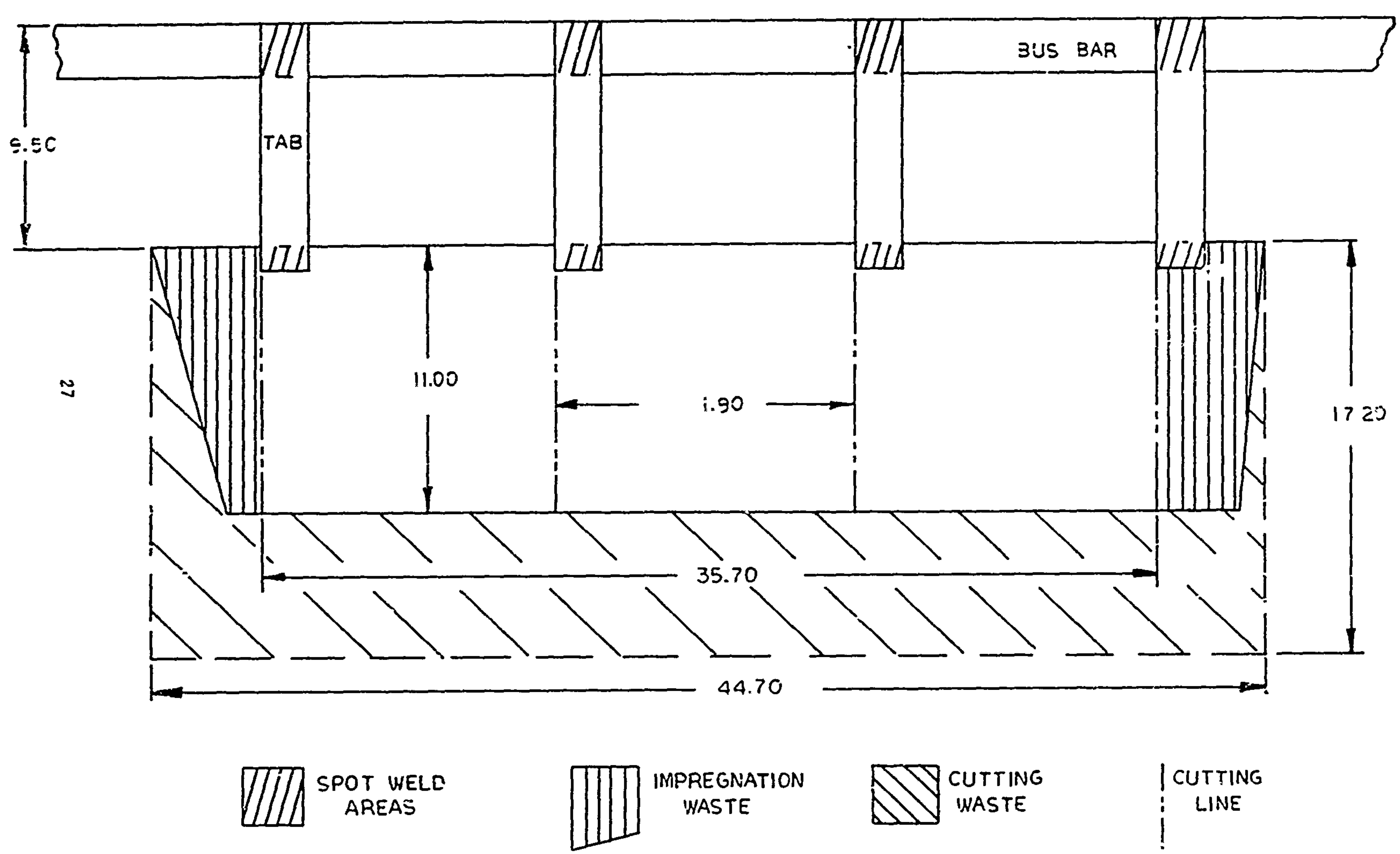

FIGURE 3

electrode.* These strips or tabs extended beyond the surface of the impregnation solution and were again spot-welded to a horizontal piece of nickel strip which ran along the whole length of the plaque, extended beyond the edges of the reaction vessel, and was connected to the negative terminal or the power supply during the electro-deposition step.

Prior to the start of each impregnation step, each master plaque, including its tabs and bus bar, was weighed on a top-loading balance in order to provide a continuous record of its respective gains in weight in the course of the impregnation process.

c. Making of the 20 Ah-Size Electrodes

The C.P.E.D. process was conducted at slightly elevated temperatures in the 34-40°C range. In order to obtain this range in a convenient manner, four out of 28 liters of impregnation solution were preheated to boiling and then remixed with the remainder kept at room temperature. During cycles 1 and 2, the average bath temperature increased slightly from 36.0 to 37.4°C and 39.5 to 39.9°C, respectively, while in the case of cycles 3 and 4, the average temperatures remained constant at 34.8 and 34.1°C, respectively. This performance was not surprising since with increasing number of cycles the average deposition currents produced by the CP mode tended to fall.

To recall the precipitation conditions: At cycle 1, 3.00 volt per cell were applied for 45 minutes; at cycle 2, 2.75 volts per cell for 30 minutes; and at cycle 3, and 4, 2.50 volts per cell for 30 minutes each.

Immediately following each cathodic precipitation, the respective master plaques were charged (anodized) in 31% KOH by weight at room temperature. This treatment always lasted 30 minutes per cycle and was done at constant currents of 30, 20, 15, and 15 amperes for cycles 1, 2, 3, and 4, respectively. The plates were deep black after this treatment and lost most of their external scales.

The subsequent washing of the individual master plaques was done with four liters of hot distilled water for 20 minutes under occasional moving of the plate in the liquid. The temperature dropped from 100°C to almost 80°C in this span. The final pH of the effluent was 11. A second wash under identical conditions lowered the final pH of the liquid to an acceptable value of 8.

---

* To facilitate handling, the 50 Ah master plaques contained one additional vertical strip.

The drying in a forced air oven at 110°C lasted for 20 minutes. After cooling for another 20 minutes, the plates were slightly brushed with a soft brush. The amounts of black scales removed by this procedure were insignificant.

The plates were then weighed and their respective weights recorded. In Table 7, the incremental gains in weight in grams per master plaque of six electrodes are presented as averages of eight plaques which always were processed as a unit. The standard deviations, σ , are expressed in per cent. The last column contains the theoretical capacity, C_t, based upon the final cumulative gain in weight and a conversion factor of .289 Ah/g $Ni(OH)_2$. Its standard deviation, σ , is also given in per cent. The last line of this table contains the overall averages for all plates expressed in the corresponding dimensions and their sigma limits in per cent.

Two things are apparent from these results:

- With increasing number of impregnation cycles, the standard deviations of the incremental gains in weight are increasing substantially.

- However, the average gains in weight per cycle are rather uniform and cumulatively result in theoretical capacities, C_t, with only small sigma limits.

This indicates that the overall process exercised a strong leveling influence as far as the loading of plates with active materials is concerned. That is to say that with individual master plaque a lesser gain in weight following cycle 1 was compensated by a larger gain in weight at a subsequent cycle and vice versa.

The average gain in weight of 66 g per master plaque compared very well with a previously observed gain of 67.9 g (Table 6, line XII) which was obtained under identical experimental conditions. Taking the discharge capacity to .6 volt, $C_{.6}$, of that material of 17.9 Ah, the new material should have

$$\frac{66}{68} \times 17.9 = 17.4 \text{ Ah}$$

or as a flooded 11 plate cell

$$\frac{11}{6} \times 17.4 = 31.9 \text{ Ah}$$

This would be more than one Ah better than a value of 30.5 Ah previously reported for 20 Ah-size electrodes made by means of the

TABLE 7

INCREMENTAL GAINS IN WEIGHT ΔW AND THEORETICAL CAPACITY, C_t

20 Ah MASTER PLAQUE

Cycle	1		2		3		4			
Group	ΔW	σ	ΔW	σ	ΔW	σ	ΔW	σ	C_t	σ
1- 8	34.6	2	16.5	10	8.5	18	5.9	14	18.9	1
9-16	35.0	2	15.5	6	9.2	11	5.5	12	18.9	2
17-24	35.3	2	15.3	5	9.7	11	5.8	12	19.1	1
25-32	35.0	2	16.2	3	9.4	7	6.2	9	19.3	2
33-40	35.3	3	15.7	6	9.8	13	5.6	19	19.2	2
All	35.0	2	15.9	7	9.3	13	5.8	14	19.1	2

C.P.E.D. process on a one-by-one basis (2nd Annual Report, Page 124, Paragraph 4).

In the course of all CP precipitation cycles, the current flow through the impregnation vessels was closely monitored at regular intervals. This served not only as a process control tool, but also permitted to calculate later on the coulombic efficiency of the process. For the second purpose, the average current at each time element was calculated for each of the four impregnation cycles involved. In Figure 4, these currents are plotted versus the respective elapsed impregnation times.

As can be seen, the difference in shape of the curves is striking. During all first cycles the currents slowly declined at a constant potential of 3.0 volts per impregnation cell. At all other cycles, this steady decline was always preceded by steep decay in current during the first five minutes or so from initial values much greater than the starting point of cycle 1 to a point lower than obtained at the same time element for cycle 1.

The explanation for this phenomenon is simple. After each cathodization in the nitrate solution the active material becomes charged in the subsequent anodization step in the caustic solution. Part or all of this charged material survived the following process steps and was then preferentially discharged at the next cathodization in the nitrate solution. This resulted in high "surge" currents for a limited length of time until the normal deposition process took over.

The calculation of process efficiency on a coulomb basis was done as follows:

The theory requires one electron for the production of each hydroxyl ion OH^- or two for the precipitation of one $Ni(OH)_2$ molecule or 2 x 26.8 Ah for 92.7 g $Ni(OH)_2$, that is, 1.73 g per Ah participating at the reaction. The coulombs involved can be easily determined by integrating current-time curves. For cycle 1, an average current can be defined by smoothing the actual curve to a straight line and taking the corresponding value at half-time as its value. The same method can be used for cycles 2-4 when the surge currents are neglected and only the range beyond five minutes is taken into consideration for smoothing out and extrapolation to zero time.

However, in this case, a second possibility existed also, namely, to integrate the complete current-time curves including the surge area. This naturally will result in greater coulomb values for the same gain in weight and, hence, lesser actual utilization.

The insert in Figure 4 contains the appropriate data in the following manner:

AVERAGE PRECIPITATION CURRENTS VS TIME CURVES, C.E.P.D. PROCESS 20 AH MASTER PLAQUES

CYCLE	I AVG.	C AVG.	ΔWP	ΔWA	%TH	%TH*
1	27	20.3	35.1	35.0	100	101
2	19	9.5	16.4	15.9	97	74
3	11	5.5	9.5	9.3	98	91
4	8	4.0	6.9	5.8	84	71
TOTAL 1	-	39.3	67.9	66.0	97	-
TOTAL 2	-	43.0	74.3	66.0	-	89

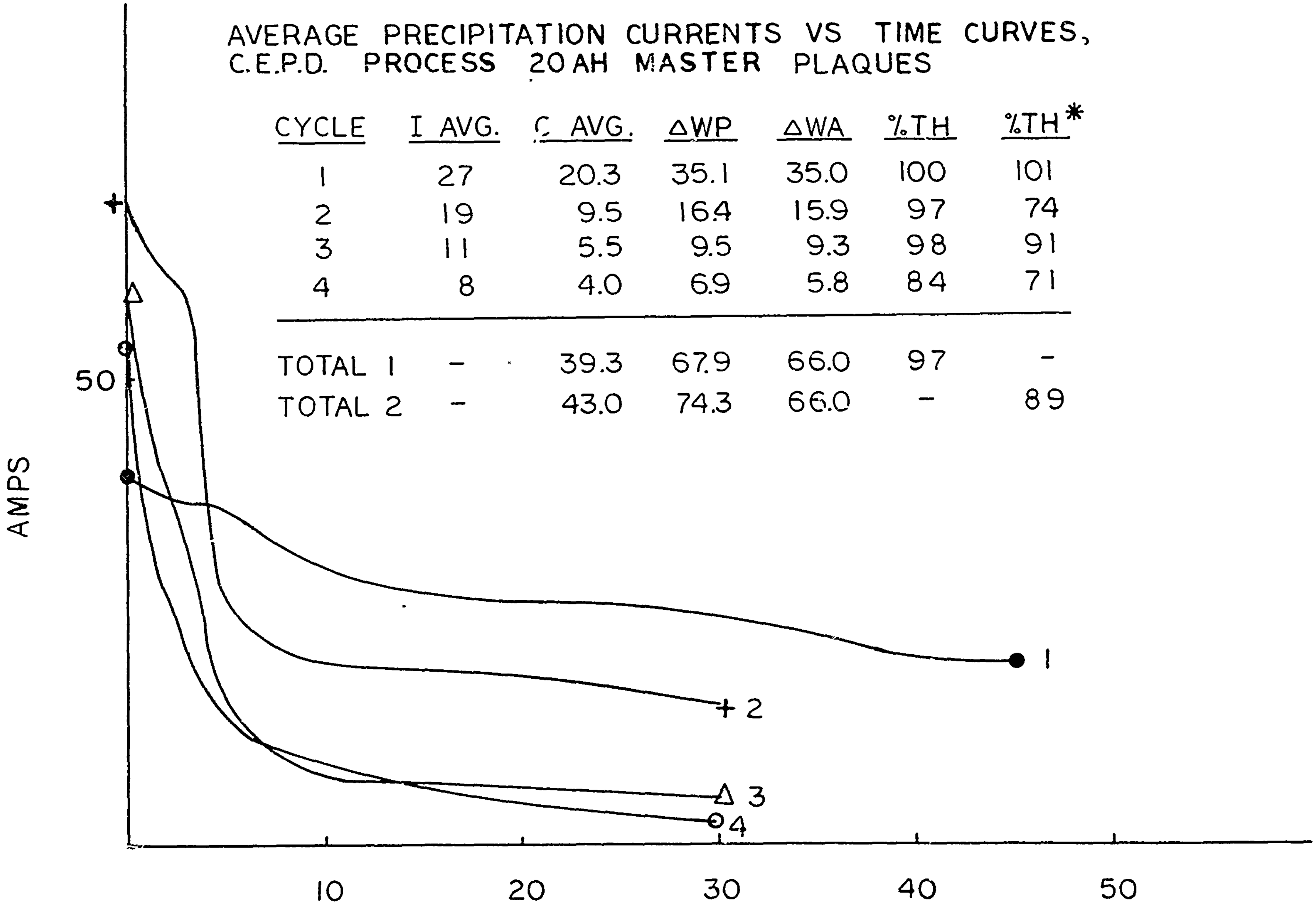

FIGURE 4

I avg	is the average current in amperes at half-time not considering the surge area.
C avg	is the average capacity in Ah obtained by multiplying I avg by the total cycle length.
Δ Wp	is the predicted gain in weight based upon C avg.
Δ Wa	is the actually observed incremental gain in weight also in grams per master plaque.
%Th	is the ratio Δ Wa/Δ Wp expressed in per cent.
%Th*	is the analogous ratio, however, based upon the complete integration of the curves involved.

The lines Total 1 and Total 2 contain overall values to be explained later on.

As can be seen, the agreement between Δ Wp and Δ Wa is excellent as long as the surge current areas are not considered and one consequently observes a very favorably coulombic utilization of 97% for the overall impregnation process as shown by the last entry in line Total 1.

Taking into consideration the surge current areas, the total capacity input per line Total 2 increased from 39.3 to 43.0 Ah with a corresponding ΔWp value of 74.3 grams. This resulted in the slightly lower real overall efficiency of 89% of the theory.

Following the impregnation process, the master plates were cut into individual 20 Ah-size electrodes. One out of 12 electrodes were set aside as spares and for subsequent analysis for composition and uniformity of the active material.

d. Making of 50 Ah-Size Electrodes

The temperature for this experimental section was maintained in the 33 to 38°C range. During cycles 1 and 2 the average temperatures increased only from 35.4 to 35.9°C and from 36.9 to 37.2°C, respectively, while during cycles 3 and 4 constant average values of 34.4 and 33.8°C were obtained.

All subsequent treatments, including the charging in 31% by weight KOH, were identical with those described for the 20 Ah master plaques.

In Table 8, the incremental gains in weight for each cycle, the theoretical capacity, C_t, their overall averages and the corresponding sigma limit are presented in analogy with the 20 Ah material. The re-

TABLE 8

INCREMENTAL GAINS IN WEIGHT ΔW AND THEORETICAL CAPACITY, C_t

50 Ah MASTER PLAQUE

Cycle	1		2		3		4			
Group	ΔW	σ	ΔW	σ	ΔW	σ	ΔW	σ	C_t	σ
1-2	27.8	-	14.9	-	7.5	-	1.2	-	15.4	-
3-10	29.4	2	13.4	3	7.0	12	5.6	13	16.0	2
11-18	29.0	2	13.4	10	8.2	9	5.7	14	16.3	3
19-26	27.7	10	13.3	9	8.7	11	5.5	10	16.3	3
ALL	28.7	6	13.5	8	8.0	14	5.6	12	16.2	3

sults are similar to those, i.e., increase of σ values with cycle number and leveling effect of the process as expressed by the constancy of the C_t values obtained.

It should be noted that master plaques 1 and 2 were prepared ahead of this "production" run in order to obtain some plaque material for preliminary cycling in the flooded state for capacity evaluation. As mentioned above, the six individual plates of these two master plates were assembled into a temporary cell together with seven negative cadmium electrodes of conventional design.

The charging of this cell was done at 2.2 amperes for various lengths of time. The discharge was always to zero volt at ten amperes. Based upon the gain in weight of the individual plates, the theoretical capacity of the test cell was calculated to 27.1 Ah.

The following table contains some pertinent results.

Cycle	$C_{.6}$	% Theory	Charge Time Hours
1	23.2	86	19
2	24.3	90	20
3	24.7	91	20
4	26.1	96	68

As can be seen, the capacity delivered to .6 volt, $C_{.6}$, increased with number of cycles which resulted in the final excellent utilization of the active material of 96% of the theory.

In Figure 5, the voltage versus time curves for the four discharge cycles were presented. They are free of any abnormalities. Extrapolating the final capacity to a 16-plate cell results in a discharge capacity of 69.6 Ah in the flooded state which should be sufficient for the type of cell under consideration.

Figure 6 contains the averaged precipitation currents for identical time elements plotted versus elapsed cathodization time per cycle. Again, the shape of the curve for cycle 1 was different from the other three and cycle 2 produced an average curve with its own uniqueness.

From the insert of this figure we take from line Total 1 that the process efficiency had an overall value of 95 per cent as long as the surge areas were not considered. This coulombic efficiency dropped by about 10 percentage points when this complete course of cell curves was integrated. Although the corresponding efficiency numbers were a bit below those obtained for the preceding group, one can conclude here that both materials were impregnated equally well.

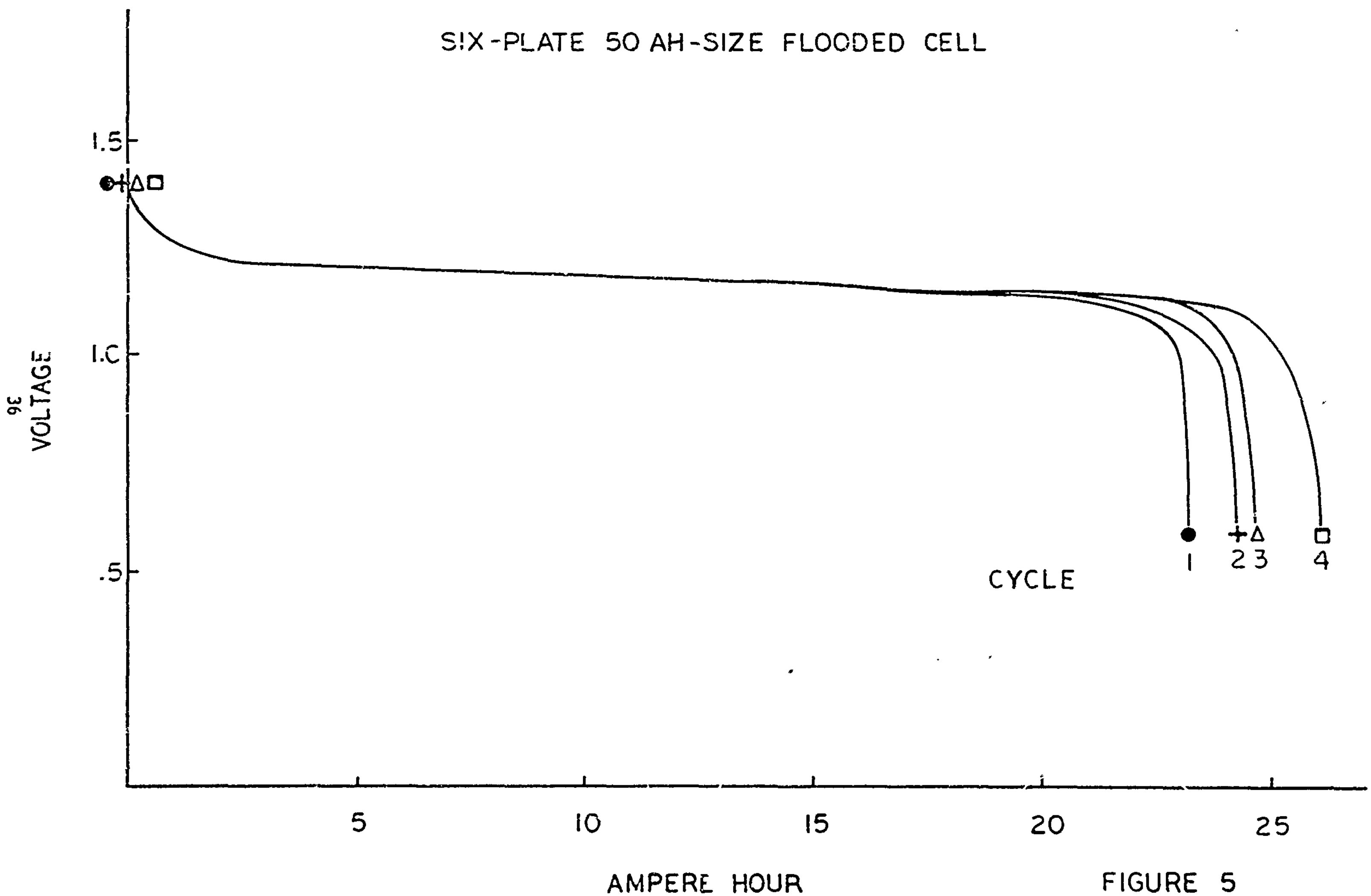
SIX-PLATE 50 AH-SIZE FLOODED CELL
VOLTAGE
1.5
1.0
.5
AMPERE HOUR
5
10
15
20
25
CYCLE
1
2
3
4

FIGURE 5

AVERAGE PRECIPITATION CURRENTS VS TIME CURVES, C.P.E.D. PROCESS 50 AH MASTER PLAQUES

CYCLE	I AVG.	C AVG.	ΔWP	ΔWA	%TH	%TH*
1	23	17.3	29.3	28.7	96	100
2	16	8.0	13.8	13.5	98	62
3	10	5.0	8.7	8.0	92	82
4	7	3.5	6.1	5.6	92	72
TOTAL 1	–	35.8	58.5	55.8	95	–
TOTAL 2	–	38.5	66.5	55.8	–	84

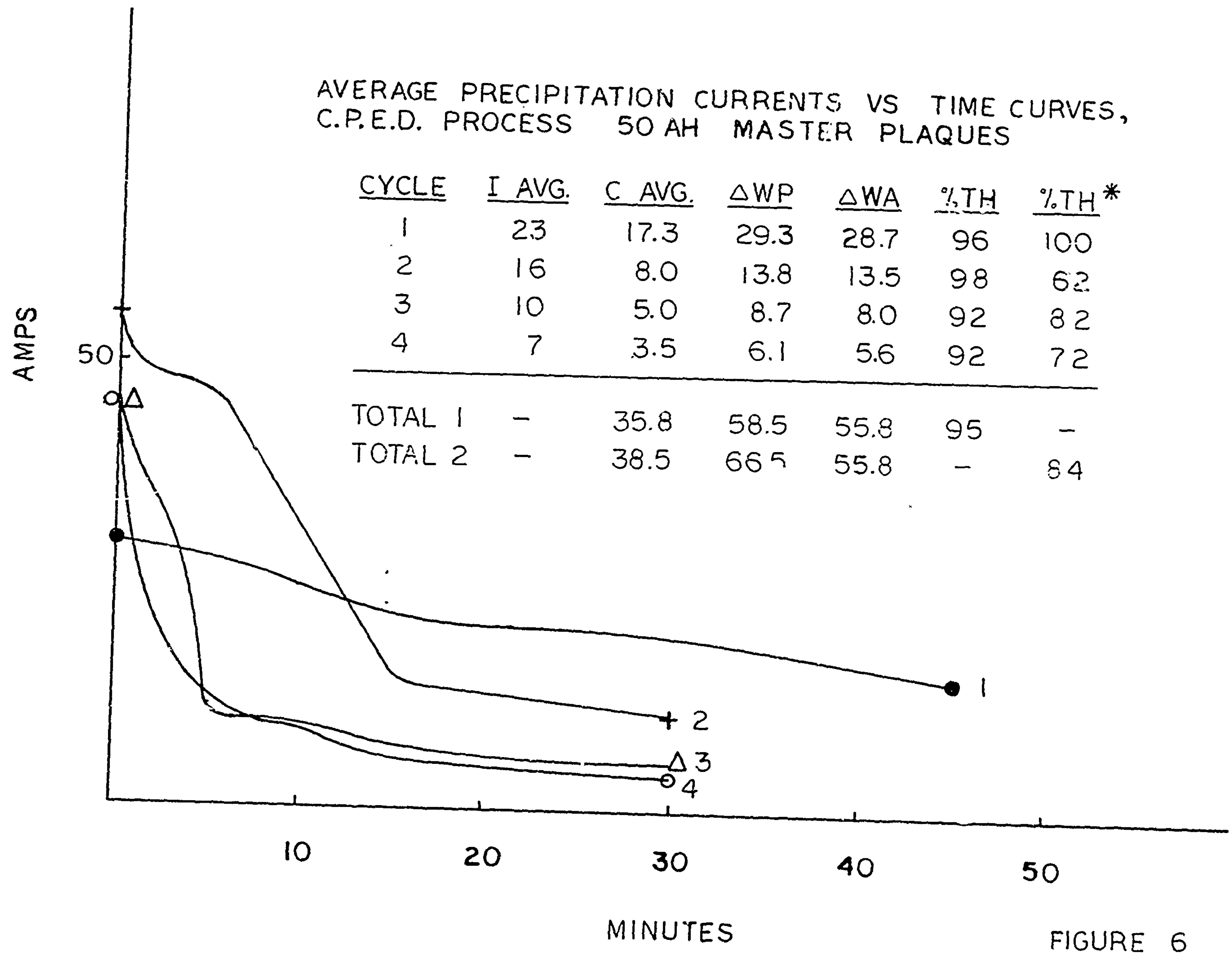

FIGURE 6

Following the impregnation the master plates were cut into individual 50 Ah-size electrodes. Two out of 18 electrodes were set aside as spares and for analytical purposes.

e. Analytical Process Control

As mentioned above on page 23 of the Equipment paragraph, the actual impregnation of the plaques by means of our C.P.E.D. process was done in two polycarbonate vessels containing 14 liters each of the 4+ molar nickel nitrate/cobalt nitrate solution. Although the vessels were electrically connected in series, and consequently an identical amount of charge passed through each one, a filling and mixing regime was applied to help to eliminate possible differences in composition of the solution.

The impregnation solution was kept in two 10-gallon vessels and was approximately two times 35 liters. These tanks were marked "Left" and "Right", respectively. The two impregnation vessels were marked in the same manner and each 14 liters of solution were taken from the storage tank bearing the same marking. At each evening, the two impregnation vessels were drained crosswise, i.e. left vessel into right tank, and vice versa. The two solutions were then well stirred and the vessels refilled from their appropriate tanks.

The composition of the impregnation solution was regularly monitored with respect to the following three points, namely:

Overall Molarity of Ni + Co Ions in the Solution. Prior to each day's impregnation, a one milliliter sample was taken from each of the two cathodization vessels. The sample was diluted to 250 ml in a volumetric flask and two 25 ml parallel runs were titrated with .1 molar EDTA solution with paracatechol violet (PCV) as indicator. The consumption of EDTA in ml is equal to the overall molarity of the impregnation solution and presented in column "Molarity" of Table 9.

Concentration of Cobalt in the Solution. Two ml of the diluted solutions were used for the spectro-photometric determination of cobalt. The results were expressed in per cent of total concentration of heavy metals and presented in column "% Co" in Table 9.

As can be seen, the overall molarity and the cobalt concentration remained virtually constant in the course of the impregnation runs.

The initial overall molarity of 4.6 represents an amount of 4.6 x 35 = 161 moles of heavy metals in each 35 liter batch of 14,920 grams of $Ni(OH)_2$. Twenty master plaques for 20 Ah-cells and 13 master plaques removed a minimum of 20 * 66 + 13 * 56 = 2,048 grams of active material, or approximately 1/7 of the initially present ions.

TABLE 9

CONCENTRATION AND COMPOSITION OF IMPREGNATION SOLUTION

Tank:		Left		Right	
Day		Molarity	% Co	Molarity	% Co
1	20 Ah	4.7	10	4.5	10
2		4.5	10	4.6	10
3		4.7	11	4.6	11
4		4.5	10	4.7	10
5		4.5	10	4.5	11
6		4.6	10	4.7	10
7		4.7	10	4.6	10
8		4.5	10	4.6	10
9		4.6	10	4.5	10
10		4.6	10	4.7	10
11	50 Ah	4.5	9	4.6	9
12		4.4	10	4.6	8
13		4.5	10	4.5	10
14		4.6	10	4.6	10
15		4.6	9	4.6	9
16		4.5	10	4.5	9

Since the EDTA titration certainly would have detected such a decline in the overall molarity, one has to conclude that the constancy observed was maintained by dissolving an appropriate amount of metallic nickel from the counter electrodes in the impregnation vessels.

The removal of a proportional amount of nonreplenished cobalt ions should have resulted in a drop of about 1.3 percentage points. Since the sensitivity of the method can be assumed to be about one percentage point at the absolute concentrations involved, we should expect final values around 9% cobalt. A trend towards that level seems to prevail as manifested by the occurrence of corresponding "Niner" values at higher numbers of days.

Determination of "Free" Acid in the Solution. Since a larger shift of the initial pH value in either direction would have detrimental effects on the efficiency of the electrochemical deposition process, an early detection of such a trend appeared mandatory.

Consequently, each impregnation solution was controlled three times a day, i.e., in the morning prior to the start of the impregnation, at noon at half-time, and in the evening after all runs of the day, by taking a five milliliter sample and titrating it with .1 normal NaOH solution and methyl red as indicator. An increase in NaOH titrant indicates production of acid; a decrease, the consumption of the latter.

The results are presented in Table 10 and two things are evident:

- The value changed significantly in the course of a given impregnation day indicating the production of free acid. This change was more pronounced on odd numbered days when, during impregnation cycles 1 and 2, larger average currents were flowing. The daily mixing of the working solution with those kept in the storage tanks counteracted this trend.

- The initial value remained virtually unchanged with increasing numbers of impregnation days. The passing of 20 x 43 + 13 x 38.5 = 1,360 Ah increased the consumption of titrant by little more than one milliliter from 2.2 to 3.4 ml.

f. Quality Control of Plates

As mentioned above, a certain amount of impregnated plate was not used in the subsequent cell building process, but was rather reserved for chemical analysis and/or as spares to make up for losses encountered in further processing steps.

TABLE 10

FREE ACID IN IMPREGNATION SOLUTION

Tank:		Left			Right		
Day		Morning	Noon	Evening	Morning	Noon	Evening
1	20 Ah	2.2	4.9	6.2	2.2	6.2	6.4
2		3.7	3.8	4.0	4.3	4.2	4.2
3		4.1	6.8	6.3	4.0	6.5	6.6
4		4.8	4.5	4.8	4.7	4.6	4.2
5		4.4	7.4	6.5	4.3	6.5	6.1
6		3.2	3.9	4.2	3.8	3.7	4.4
7		4.1	7.8	6.7	4.2	7.3	8.3
8		5.4	5.4	5.4	5.0	4.4	4.2
9		4.6	7.1	6.2	5.3	8.0	7.7
10		4.6	4.7	5.0	4.8	4.4	4.2
11	50 Ah	3.5	6.4	7.1	3.4	5.5	5.5
12		4.2	4.5	4.8	4.8	4.8	4.9
13		3.9	6.5	7.4	4.1	6.9	7.4
14		4.5	5.2	5.5	5.1	5.1	5.2
15		3.7	6.6	7.2	4.2	6.8	6.6
16		3.4	3.3	3.7	3.3	3.0	3.3

The number of individual plates actually reserved for those purposes were as follows:

- One individual plate out of 12 in the 20 Ah-size group, that is to say, one section per the two master plaques treated concommitantly in the course of the impregnation process.

- Two individual plates out of 18 in the 50 Ah group, in other words, two sections of the six master plaques undergoing an analogous treatment at approximately the same time.

Analytical Results for 20 Ah-Size Electrodes. As mentioned before, the master plaques of this type contained six individual electrode areas which were designated by a letter from A through F. In the course of the impregnation process, the master plaques were always arranged in the same position with respect to vessel and counter electrodes. Six plates, each with a different letter, were selected to cover different times of the impregnation period.

Six 10 cm^2 samples were punched out of each 95 cm^2 plate area and designated with a number from 1 to 6. Care was taken that a given numbered sample always was punched out of the same location of different electrodes. The samples were weighed on an analytical balance and then the mixture of active material and sintered nickel removed from the substrate. The mixture was then analyzed quantitatively for metallic nickel, amount of active material, and per cent of cobalt in the latter.

The corresponding results are presented in Tables 11, 12, and 13, respectively. Average values for lines, i.e., a given plate, and columns, i.e., a given sample location, have been calculated together with their standard deviations which are expressed in per cent.

Table 11 contains the analytical results for metallic nickel. The uniformity of this term, regardless of its origin, is reflected in the small values for the standard deviation. This and the closeness of the overall average value of 7.18 g/cm^2 to the gravimetrically determined average of 7.33 g/dm^2 rules out the possibility of nickel attack in the course of the impregnation and formation process.

In Table 12, the values for active material are presented in $gram/dm^2$ together with their various averages and standard deviations. The active material is the sum of nickel plus cobalt hydroxide and, regardless of their valencies, is calculated as $Ni(OH)_2$.

The distribution of the active material among the several sample locations of a given plate is very uniform as indicated by the

TABLE 11

METALLIC NICKEL CONTENT g/dm^2

20 Ah-SIZE ELECTRODES

POSITION / PLATE	1	2	3	4	5	6	AVG	σ%
A2	7.24	7.34	7.16	7.46	7.20	7.18	7.26	1.5
B28	7.09	7.07	7.43	7 21	7.11	7.26	7.20	1.7
C15	7.26	7.20	7.33	7.26	7.15	7.10	7.22	1.1
D32	7.11	7.14	7.41	7.20	7.29	7.13	7.61	1.5
E22	6.97	6.97	7.02	6 97	6.91	6.18	6.97	.5
F36	7.16	7.27	7.37	7.26	7.10	7.33	7.25	1.3
AVG	7.14	7.17	7.29	7.23	7.23	7.13	7.18	
σ%	1.4	1.7	2.0	2.0	2.0	1.6		1.9

TABLE 12

ACTIVE MATERIAL CONTENT g/dm^2

20 Ah-SIZE ELECTRODES

POSITION / PLATE	1	2	3	4	5	6	AVG	σ %
A2	10.48	10.34	10.16	10.05	10.01	10.07	10.19	1.7
B28	10.81	11.30	10.90	10.50	11.25	10.72	10.91	2.6
C15	10.06	10.33	10.28	10.11	10.16	10.03	10.16	1.1
D32	10.43	10.42	10.42	10.22	10.55	10.31	10.39	1.0
E22	10.68	10.25	10.56	10.36	10.16	10.20	10.37	1.8
F36	10.16	10.31	10.49	10.23	10.30	10.32	10.30	1.0
AVG	10.44	10.49	10.47	10.25	10.41	10.28	10.39	
σ %	2.5	3.5	2.2	1.5	4.0	2.2		2.9

respective standard deviations. The differences are greater from plate to plate, but still have acceptable standard variation limits.

In Table 13, the contents of cobalt additive are presented in per cent of total active material. Since the analytical method permits no more meaningful accuracy than one-half of one percentage point, the values are rounded off accordingly. Consequently, it is not surprising that larger standard deviations are observed.

As can be seen, the percentage of the cobalt additive is in the optimized range which was determined in last year's work.

The results of the chemical analysis of the 20 Ah-size electrode material can be summarized as follows:

- The porous sinter structure was not submitted to any nickel attack.

- The amount of active material was uniformly distributed across the various plate areas.

- The composition of the active material was uniform with respect to cobalt content and the latter was in the optimum range established previously.

Analytical Results for 50 Ah-Size Cells. The master plaques for this type of cell contained three individual electrode areas which were designated by a letter from A to C. Three electrodes were selected and eight samples of 10 cm^2 area were punched out of defined locations. This covers 80 cm^2 out of a total of 131 cm^2.

The analytical procedure was the same as with the 20 Ah-size plates and the results are presented in Tables 14, 15, and 16, respectively.

In Table 14, the values for the metallic nickel content are given. The low standard deviation and the average value of 7.25 g/dm^2 close to the gravimetrically determined average of 7.33 g/dm^2 again rule out any attack on the porous nickel structure.

In Table 15, the amounts of total active material are presented. As indicated by the standard deviations, the distribution was independent from sample and plate location. The overall average of 11.22 g/dm^2 was several percentage points higher than the analogous value for the 20 Ah-size plates of 10.39 g/dm^2.

Table 16 contains the amount of cobalt additive in per cent of the total active material. As can be seen, this additive was again in the optimized range.

TABLE 13

COBALT ADDITIVE CONTENT IN %

20 Ah-SIZE ELECTRODES

POSITION / PLATE	1	2	3	4	5	6	AVG	σ %
A2	9.0	7.0	8.5	8.0	7.0	8.0	7.9	9
B28	9.5	8.0	9.5	8.0	8.0	8.0	8.5	8
C15	7.0	8.0	9 0	8.0	9.0	8.0	8.2	8
D32	8.0	8.0	8.0	8.0	8.0	8.0	8.0	0
E22	8.0	7.0	8.0	8.0	8 0	8.0	7.8	5
F36	9.0	8.0	8.0	9.0	8.0	7.0	8.2	8
AVG	8.4	7.7	8.5	8.2	8.0	7.8	8.1	
σ %	10	6	7	5	7	5		8

TABLE 14

METALLIC NICKEL CONTENT g/dm^2

50 Ah-SIZE ELECTRODES

POSITION / PLATE	1	2	3	4	5	6	7	8	AVG	σ %
A20	7.28	7.33	7.25	7.33	7.29	7.33	7.05	7.20	7.26	1.2
B26	7.12	7.10	7.39	7.18	7.43	7.18	7.14	7.15	7.22	1.7
C3	7.15	7.11	7.43	7.42	7.41	7.24	7.08	7.24	7.26	1.9
AVG	7.18	7.18	7.36	7.34	7.38	7.25	7.09	7.20	7.25	
σ %	1.0	1.5	1.4	.8	.8	.9	.5	.5		1.6

TABLE 15

ACTIVE MATERIAL CONTENT g/dm^2

50 Ah-SIZE ELECTRODES

POSITION / PLATE	1	2	3	4	5	6	7	8	AVG	σ%
A20	11.07	11.49	11.34	11.14	11.44	11.24	11.71	11.69	11.39	2.0
B26	11.25	11.31	11.12	11.14	11.03	11.18	11.10	11.15	11.16	.7
C3	11 43	11.01	11.04	11.07	11.10	11.01	11.01	11.11	11.10	1.6
AVG	11.25	11.27	11.17	11.12	11.19	11.14	11.27	11.32	11.22	
σ%	1.3	1.8	1.1	.3	1.6	.9	2.8	2.3		1.8

TABLE 16

COBALT ADDITIVE CONTENT IN %

50 Ah-SIZE ELECTRODES

POSITION / PLATE	1	2	3	4	5	6	7	8	AVG	σ %
A20	8.0	9.0	8.0	7.0	9.0	9.0	8.0	8.0	8.3	8
B26	8.0	8.0	8.0	8.0	8.0	9.0	8.0	9.0	8.3	5
C3	7.0	9.0	9.0	9.0	8.0	7.0	7.0	8.0	8.0	11
AVG	7.7	8.7	8.3	8.0	8.3	8.3	7.7	8.3	8.2	
σ%	6	5	6	10	6	11	6	6		8

The conclusions to be drawn from these results are the same as for the other material type, i.e., no nickel attack and uniformity of active material distribution and composition.

g. Formation in the Flooded State

Upon the completion of the impregnation process and the cutting of the master plates into individual electrodes of appropriate size, these electrodes were submitted to a conventional formation process in the flooded state. For this purpose, the plates, still accountable by their original impregnation sequence, were assembled into so-called temporary cells together with negative cadmium electrodes of conventional design. The same negative electrodes used in the formation process were later utilized in building the cells of the two nominal capacity levels.

Nominal 20 Ah Cells. In this case, each temporary cell contained 11 experimental positive electrodes and 12 negative cadmium counter electrodes of conventional design. The positive electrodes of each cell were properly identified and in each case stemmed from two simultaneously impregnated master plaques. The results of this three-cycle formation process are presented in Table 17 in the following manner:

Column "Cell" refers to the corresponding temporary cell containing positives of known origin.

Column "$Ni(OH)_2$" contains the average amount of active material in gram per 20 Ah-size electrode. This is based upon the difference in weight between an individual finished electrode and an average for the plaque area.

Column "σ" contains the standard deviation of $Ni(OHO)_2$ values expressed in gram of active material.

Column "C_t" contains the theoretical capacity in Ah of each cell with 11 electrodes. The conversion factor used was .289 Ah/gram of $Ni(OH)_2$.

Column "Cp" contains the actually obtained discharge capacity in Ah at cycle three and at a current of the two-hour rate.

Column "UTIL" contains the ratio C_p/C_t expressed in per cent, i.e., the efficiency of the active material.

Finally, the column averages and their sigma values in per cent are presented at the bottom of the table.

As can be seen, the average gain in weigh[illegible] active material was rather uniform. The sigma limits for the ce[illegible] e in the .22 - .42

TABLE 17

RESULTS OF FLOODED FORMATION

20 Ah CELLS

CELL	$Ni(OH)_2$	σ	C_t	C_p	UTIL.
1	10.56	.34	33.6	30.3	90
2	10.40	.26	33.1	29.9	90
3	10.35	.31	32.9	30.1	91
4	10.75	.24	34.2	30.1	98
5	10.65	.31	33.9	30.8	91
6	10.55	.31	33.6	30.5	91
7	10.41	.42	33.1	30.5	92
8	10.57	.40	33.6	30.7	91
9	10.44	.36	33.2	30.7	92
10	10.88	.27	34.5	30.8	89
11	10.51	.33	33.4	30.8	92
12	10.48	.39	33.3	30.5	91
13	10.52	.37	33.4	30.3	91
14	10.56	.34	33.6	30.5	92
15	10.46	.40	33.2	30.8	93
16	10.73	.35	34.1	30.3	89
17	10.66	.36	33.9	30.8	91
18	10.75	.22	34.2	30.8	90
19	10.73	.24	34.1	30.8	90
20	10.33	.30	32.9	30.7	93
AVG	10.56		33.6	30.5	91
SIGMA %	3.4			.9	2.1

gram, or 2 - 4% range, indicating a good distribution of the active material across the surface of the master plaques. Since the standard deviation for the whole group was of the same order of magnitude, one can also conclude that the process as such provided a uniform electrode material.

The average discharge capacity of 30.5 Ah per cell is identical with the one obtained previously. See, for instance, the 2nd Annual Report, page 124, paragraph 4. However, the average utilization of 91% is almost ten percentage points better than the old value of 82%. This higher utilization offsets the slightly lower loading of the plates with active material.

Before being chemically analyzed, the plates reserved for that purpose were also submitted to a formation in the flooded state.

Two temporary cells, each with ten experimental positives and eleven negative cadmium counter electrodes, were built and submitted to four cycles under the conditions shown in Table 18. Cell 20 - 21 had ten electrodes stemming from master plaques 1 - 12, while cell 20 - 22 had ten plates from the latter plaque 21 - 40 group. The charge for various lengths of time was always with constant current at 2.5 amperes, while the discharge with ten amperes was continued to zero cell voltage . The cells were positive electrode discharge-limiting as measured by means of built-in reference electrodes.

As can be seen, the discharge capacities increased with increasing numbers of cycles. Prorating the values at cycle four for an 11-plate cell results in discharge capacities of 1.0 volt of 31.9 Ah versus 30.5 Ah average for the bulk of the material.

Since it is very unlikely that these superfluous plates really should have had greater capacities than the average of the bulk of the material, a reasonable explanation can be seen in the difference of cycling conditions.

Nominal 50 Ah Cells. The 50 Ah-size electrodes were assembled into four temporary cells each containing 17 negative cadmium counter electrodes and 16 experimental positives with known origin

These cells were then submitted to a conventional three-cycle formation process. The results are presented in Table 19, the organization of which is identical with that of Table 17.

The loading with active material was quite uniform, and both within the plates of a cell and among the four cells, acceptable standard deviations were observed.

TABLE 18

CONDITIONS AND RESULTS OF FLOODED FORMATION II

20 Ah CELLS

	CONDITIONS			CELL 20 - 21		CELL 20-22	
CYCLE	CHARGE h	CHARGE A	DISCHARGE A	C_1 Ah	$C_{.6}$ Ah	C_1 Ah	$C_{.6}$ Ah
1	20	2.5	10	26.5	27.0	27.0	27.4
2	21	2.5	10	27.3	28.1	27.6	28.4
3	20	2.5	10	27.9	29.0	28.4	29.4
4	41	2.5	10	29.0	29.5	29.0	29.7
4TH CYCLE DISCHARGE CAPACITY FOR COMPLETE CELLS				31.9	32.5	31.9	32.6

TABLE 19

RESULTS OF FLOODED FORMATION

50 Ah CELLS

CELL	$Ni(OH)_2$	σ	C_t	C_p	UTIL.
1	16.77	.35	77.5	67.9	88
2	16.62	.56	76.8	68.3	89
3	16.85	.55	77.8	61.9	80
4	16.27	.53	75.2	59.7	79
AVG	16.61		76.8	64.5	84
SIGMA %	3.4		-	3.7	4.5

In spite of this uniformity in the active material level, both cell #3 and #4 delivered discharge capacities to 1.0 volt, which were significantly lower than those of cell #1 and cell #2, respectively. Since the two lower capacity cells required several rebuilding attempts in order to overcome serious internal shorting, one can argue here that prevailing internal shorts, albeit on a very light scale, led to the lower discharge capacity values. The obtained capacity values were nevertheless within the specifications of the test conditions applied, and we consequently refrained from further rebuilding attempts.

The eight plates not used in the building of the four temporary cells and reserved for the chemical analysis were also formed in the flooded state.

The voltage and capacity performance of this eight-plate cell was unsatisfactory and undoubtedly caused by internal shorting. In spite of efforts to remedy this, a fourth cycle capacity to 1.0 volt of only 24.6 Ah was obtained, which is equivalent to 49.2 Ah for a 16-plate cell and considerably below the corresponding results of Table 19.

h. Compression and Sizing of Electrodes

In the course of the second year of contract work, it was established that the goal of 8 - 10 Ah/in^3 in the positive electrode could only be attained when the readily impregnated electrodes were submitted to a roller compression. This processing step typically reduced the initial plate thickness of .064 cm to .052 cm as average values.

Naturally, a reduction in thickness of a given volume of a porous structure will result in an increase of its length and width. These enlarged dimensions have then to be trimmed back to the specifications so that the finished plate fits into the confinement of the cell.

Treatment of 20 Ah-Size Plates. These plates, previously characterized by the formation process in the flooded state, were roller compressed from a nominal thickness of .064 cm to .052 cm. As mentioned above, this reduction in thickness was accompanied by a change in width, initial value 6.95 cm, and a more pronounced change in length, initial value 13.6 cm.

In Table 20, the corresponding measurements after compression are presented together with their respective standard deviations. The table also contains the average specific capacity in Ah/in^3 based upon the final plate volume after trimming to specifications and the average prorated discharge capacity taken from Table 17.

Treatment of 50 Ah-Size Plates. This plate material also required a roller compression of its initial average thickness of .064 cm in order to meet the specific capacity specifications of the contract.

TABLE 20

PHYSICAL DATA OF COMPRESSED 20 Ah-SIZE ELECTRODE

ITEM	DIMENSION		σ %
THICKNESS	.0522	cm	1.3
LENGTH	14.77	cm	1.2
WIDTH	7.02	cm	.8
AREA	103.7	cm^2	1.5
VOLUME	5.41	cm^3	1.7
SPEC. CAP.	8.39	Ah/in^3	

In the course of this processing step, the dimensions of width and length were changed from their initial values of 11.9 cm and 11.0 cm, respectively. The new values obtained are presented in Table 21.

The final plate volume, after trimming to specifications, and a prorated discharge capacity taken from Table 19 have been used in calculating the specific capacity of this electrode material.

3. CONCLUSIONS

A four-cycle C.P.E.D. process was successfully applied in the impregnation of master plaques for 20 Ah and 50 Ah-size, respectively.

The process had a very strong leveling effect with regard to overcoming variations in weight gains in the course of individual cycles. Consequently, the overall gain in weight for all master plates of one size was very uniform.

This uniformity also continued into the area of single electrode size where uniform amounts of active material were deposited across the geometric surfaces of the plates.

The values obtained chemically for the amount of metallic nickel present in the plates upon completion of the impregnation process agreed very well with those found for the raw plaque material. This definitely rules out the occurrence of nickel attack (corrosion) in the course of the impregnation, and further means that all active material stems from the solution.

A further support of this fact was the uniformity of the cobalt additive in the active material. Its level was in the optimized range of 8 - 10% of the total active material and was in good agreement with the amounts originally present in the impregnation solution. If an attack on the nickel sinter ever occurs, the level of the cobalt additive will decrease as a consequence of the "dilution" with pure nickel hydroxide stemming from the sinter structure.

Under the experimental conditions applied, the composition of the impregnation solution remained very stable and did not require any corrective measures.

The results obtained from the formation processes in the flooded state indicated that the plate material of both sizes would at least meet, if not even surpass, the performance of electrodes made previously by means of the old C.P.E.D. procedure.

The final two processing steps, i.e., the roller compacting from .064 cm to .052 cm, and the subsequent cutting of the elongated plates to design size, were conducted without any difficulty.

TABLE 21

PHYSICAL DATA OF COMPRESSED 50 Ah-SIZE E ‿TRODES

ITEM		DIMENSION	σ %
THICKNESS	.0525	cm	1.2
LENGTH	12.96	cm	2.6
WIDTH	12.24	cm	1.7
AREA	156.2	cm^2	2.1
VOLUME	8.19	cm^3	2.6
SPEC. CAP.	8.58	Ah/in^3	-

SECTION IV

CELL BUILDING AND FORMATION

1. GENERAL REMARKS

Both the nominal 20 Ah cells and the nominal 50 Ah cells were of standard construction with the following three exceptions:

1. The positive electrodes were of an experimental nature in accordance with details given in the preceding sections of this report.

2. Each cell contained a reference electrode which was located between the outer negative electrode and the wall of the cell container. A reference electrode consisted of a piece of conventional nickel hydroxide nickel sinter electrode and was enclosed in a bag of the non-woven nylon material which was also used as separators in the cell. The reference electrode was electrically connected to the cover of the cell can.

3. For the whole length of the subsequent cycling, the electrolyte filling tube of each cell remained connected to a pressure gauge - valve assembly. This filling tube is normally pinched closed after the formation process and the assembly removed.

2. BUILDING OF CELLS

a. Nominal 20 Ah Cells

The assembling of the compressed and sized experimental positive electrodes, conventional cadmium counters and separators into electrode packs became rather problematic. The application of standard procedures resulted in a 100% rate of internal shorts. Only by means of a tedious rebuilding process could this phenomenon be overcome. In the course of that process, numerous protruding wire tips had to be removed and the compacting pressure prior to the slipping in the pack into the can had to be reduced considerably.

It should be emphasized here that in future efforts of using the plate material made by this process, it will either be mandatory to change the substrate material and/or alter the appearance of the plate edges, as for instance by means of a coining procedure.

The external appearance of this cell type is presented in Figure 7 together with some pertinent dimension information in inches.

EXTERIOR DESIGN
OF 20AH CELLS

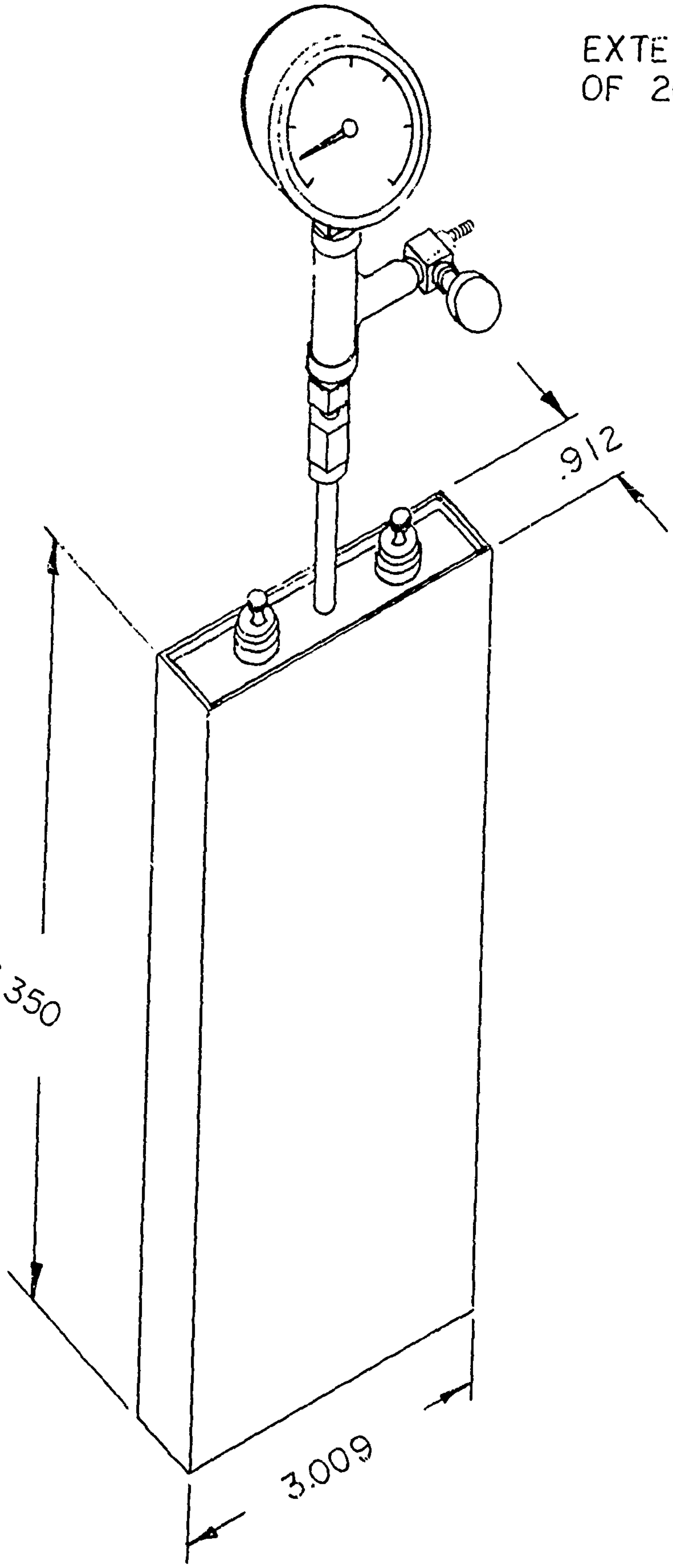

FIGURE 7

The assembled cells were closed by welding along the upper edges of the can, filled with the normal amount of 67 ml of 34% by weight potassium hydroxide as electrolyte, and then the filling tube closed by the aforementioned pressure gauge - valve assembly.

The cells were then ready for the four-cycle formation process.

b. Nominal 20 Ah Cell with Extra Electrodes

A preliminary calculation showed that the overall thickness of an electrode pack consisting of 11 experimental positives, 12 conventional negatives, and the necessary separator material should be smaller than in the case of the use of conventional positives.

Actually, the difference should be large enough as to permit the addition of another experimental positive and a conventional negative plus the necessary amount of separator material.

The calculations proved to be correct and one cell of nominal 20 Ah capacity was built from spare plates and contained this additional plate pair. It received the normal amount and concentration of electrolyte and was then submitted to the four-cycle formation process.

c. Nominal 50 Ah Cells

The dimensional outline of this cell type is given in Figure 8.

The efforts to build the 50 Ah nominal capacity cells with the experimental positive plate material were again affected by the same problems observed with the nominal 20 Ah cells. The protruding wire points at the edges of the plates resulted in a 100% rate of internal short. This could only be overcome by the same elaborate and tedious rebuilding procedure applied previously.

This corroborates the statement made before, that in future applications of this impregnation process for positive electrodes another more suitable substrate has to be used.

These cells received 135 ml of a 34% by weight potassium hydroxide electrolyte and upon closing by means of the usual gauge - valve assembly were submitted to a four-cycle formation process.

3. FORMATION OF CELLS

a. Nominal 20 Ah Cells

The results for this cell type are presented in Table 22, together with group averages and standard deviations. The four cells marked with * were retained as spares and not submitted to any repetitive

EXTERIOR DESIGN
OF 50AH CELLS

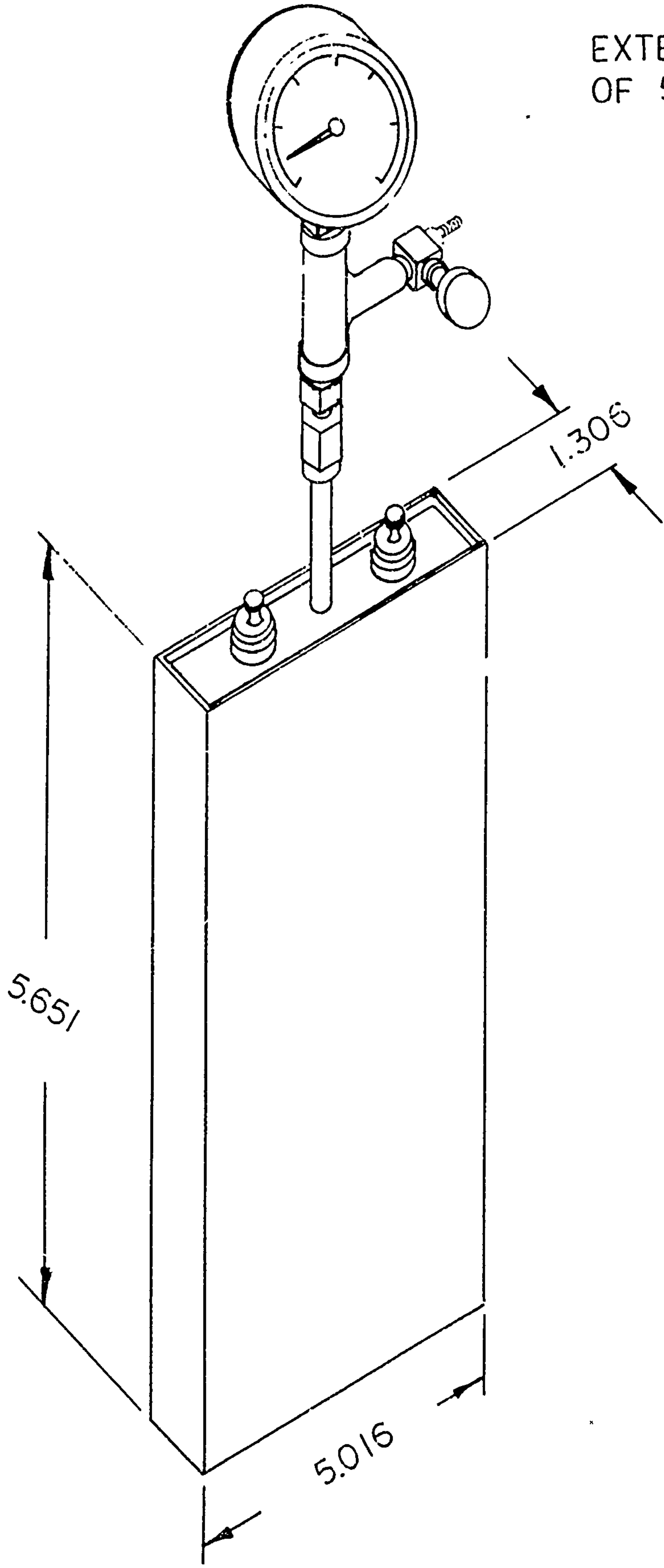

FIGURE 8

TABLE 22

FORMATION RESULTS OF SEALED 20 Ah CELLS

	DISCHARGE CAPACITY TO 1 VOLT Ah/CELL				SPEC. CAPACITY Ah/in^3	EOCV mV	EOCP ##
CELL	CYCLE 1	CYCLE 2	CYCLE 3	CYCLE 4	CYCLE 4	CYCLE 4	
1*	19.2	20.7	21.0	24.7	7.5	1403	7
2*	17.7	20.7	22.0	24.3	7.4	1400	-1
3	19.3	20.8	21.2	25.0	7.6	1404	6
4	19.7	21.0	20.8	25.3	7.7	1402	-3
5	20.0	21.8	22.0	25.3	7.7	1409	2
6*	19.5	21.5	22.2	24.7	7.5	1400	-8
7	19.7	21.2	21.7	25.3	7.7	1404	4
8	19.5	21.2	21.7	25.3	7.7	1404	1
9	19.5	21.3	21.7	25.7	7.8	1404	5
10	19.7	21.8	22.3	25.3	7.7	1403	5
11	19.3	21.0	21.2	25.5	7.7	1400	-1
12	19.8	21.5	21.7	25.7	7.8	1400	11
13	19.7	21.7	22.2	25.3	7.7	1401	2
14*	19.8	21.3	21.0	24.3	7.4	1404	4
15	20.0	21.8	22.0	25.8	7.8	1404	3
16	19.8	22.0	22.3	25.8	7.8	1402	0
17	19.7	21.7	22.0	25.2	7.6	1403	2
18	19.3	21.2	22.0	25.0	7.6	1401	-5
19	19.0	20.3	20.3	25.0	7.6	1408	5
20	19.7	21.2	21.0	25.2	7.6	1406	9
Avg.	19.5	21.3	21.6	25.2 25.4#	7.6 7.7#	1403	-
σ Abs.	.5	.4	.6	.4 .3	.1 .1	2	

* Spare cells not on cycling regimes.

\# Averages without spare cells.

\## Positive values: psig; negative values: inches of vacuum

cycling regimes. They were later on employed as standards in the analytical section of this contract.

All cells were negative electrode discharge-limiting during the first three cycles. Between cycle three and four, the negative electrodes of each cell received a precharge treatment and the cells subsequently became positive electrode discharge-limiting at cycle four.

The discharge capacities at cycle four were very uniform as indicated by the small standard deviation and the average was significantly greater than the corresponding value of 24.3 Ah obtained for the so-called "old" 20 Ah cells built last year.

The specific capacities in Ah/in^3 were calculated using an average thickness of .052 cm, a plate area of 95 cm^2, and the corresponding discharge capacity. The values of 7.6 and 7.7, respectively, constitute a sizeable improvement over the old value of 7.3 Ah/in^3.

End of charge voltages, EOCV, and the corresponding pressures, EOCP, were normal both with respect to magnitude and range.

The efficiency of the active material was calculated in the following manner:

The chemical analysis found an average of 10.39 g of $Ni(OH)_2$ per dm^2 (Table 12) or .95 x 10.39 = 9.87 grams per plate. In the course of the compression, this area was extended to an average of about 104 cm^2 and subsequently trimmed back to specified dimensions. This left 95/104 = 91.5% of the initial amount or .915 x 9.87 = 9.03 grams per plate. For 11 electrodes per cell and a theoretical conversion factor of .289 Ah/g $Ni(OH)_2$, we obtain a theoretical capacity of

$$9.03 \times 11 \times .289 = 28.7 \text{ Ah}$$

The average of discharge capacity of 25.4 then is

$$\frac{25.4}{28.7} \times 100 = 88.5\% \text{ of the theory}$$

This is a considerable improvement of the old value of just 65%, and it is felt that the electrochemical conversion step in the course of the impregnation process is the cause for this improvement.

Up to this point our whole concern was with the specific capacity of the positive electrodes expressed in Ah/in^3. However, for application purposes, the energy density of the whole system on a weight basis might be of interest.

At an average cell weight of 883 grams, this excludes the gauge-valve assembly, and the average discharge capacity of 25.4 Ah to an endpoint of one volt and an average discharge voltage which is conventionally set at 1.2 volts, we can compute an energy density of

34.6 Wh/kg or 15.7 Wh/pound

It appears that these values are significantly above those usually quoted for the nickel-cadmium system for operation in the sealed state.

b. Nominal 20 Ah Cell with Extra Electrodes

The results of the four-cycle formation process for this special cell were as follows:

Capacity Ah Cycle	1	2	3	4	Spec. Cap. Ah/in^3	EOCV mV	EOCP psig
	20.4	22.8	21.8	26.7	7.4	1408	28

The discharge capacity at cycle 4 of 26.7 Ah is 85% of the theory. The latter calculated as

$$9.03 \times 12 \times .289 = 31.33 \text{ Ah}$$

with 9.03 the average amount of active material in grams per single electrode area.

The increase in discharge capacity on the average value of the normal 20 Ah cells is

$$\frac{26.7 - 25.4}{25.4} \times 100 = 5.1\%$$

This is several percentage points lower than one can expect from the increase in plate number, i.e.,

$$\frac{12 - 11}{11} \times 100 = 9\%$$

Although the end of charge pressure was well below the tolerable limit, its value of 28 psig was considerably higher than that of other 20 Ah cells. This and the slighcly lower utilization of the positive active material might indicate that the new design is not optimized.

The inclusion of the additional pair of plates plus the necessary separator material increased the cell weight to 945 grams. The discharge capacity of 26.7 Ah to one volt and the conventionally assumed average discharge voltage of 1.2 volt result in an energy density of

33.9 Wh/kg or 15.4 Wh/pound

These values are slightly below those for the first group of nominal 20 Ah cells. Under the circumstances this is not surprising, because the addition of the extra pair of electrodes failed to raise the discharge capacity to a level which would have been commensurable with the increase in plates.

However, since there was an increase in discharge capacity, the advantage of the addition of an extra pair or more electrodes to a fixed cell volume has to be seen in an increase of the energy density on a volume basis, or by the same token, by the capability to provide the discharge capacity in a correspondingly smaller volume of the cell.

c. Nominal 50 Ah Cells

The results of the analogous formation process are presented in Table 23, together with average values and standard deviations.

Although the cells #3 and #4, respectively, had somewhat lower discharge capacities, they still would meet the specification of 120 minutes discharge time at 25 amperes.

The specific capacity averages for the positive electrodes of 7.9 Ah/in^3 for all four cells and 8.2 Ah/in^3 for cells #1 and #2, respectively, were considerably higher than those of the 20 Ah cells described before.

The calculation of active material utilization had the following results:

The chemical analysis established 11.22 grams $Ni(OH)_2$ per dm^2 or 1.31 x 11.22 = 14.70 grams per plate. Roller compression and subsequent trimming reduced this to

$$\frac{131 \times 14.7}{156} = 12.25 \text{ grams}$$

For 16 plates and the theoretical conversion factor this is equivalent to

$$16 \times .289 \times 12.25 = 56.6 \text{ Ah}$$

Consequently, the discharge capacity of 54.2 Ah was

$$\frac{54.2}{56.6} \times 100 = 95.8\%$$

of the theory.

TABLE 23

FORMATION RESULTS OF SEALED 50 Ah CELLS

	DISCHARGE CAPACITY TO 1 VOLT Ah/CELL				SPEC. CAPACITY Ah/in^3	EOCV mV	EOCP ##
CELL	CYCLE 1	CYCLE 2	CYCLE 3	CYCLE 4	CYCLE 4	CYCLE 4	
1	45.0	47.1	50.8	54.2	8.2	1409	-1
2	43.8	45.8	47.9	54.2	8.2	1410	1
3	43.8	45.4	44.6	50.4	7.6	1407	-8
4	45.0	46.3	44.6	50.4	7.6	1414	-9
Avg.	44.4	46.1	47.6	52.3 54.2#	7.9 8.2#	1407	-
Abs.	.6	.6	2.2	1.9 .0	.3 .0	3	

Average without spare cells.

Positive values: psig; negative values: inches of vacuum.

This is even better than the 88.5% observed for the 20 Ah cells, and again proves the beneficial influence of the electrochemical conversion step.

The energy density of this group was determined with data obtained from cell #3, as follows:

Weight	1.944 grams
Discharge capacity	51.5 Ah to volt (reconditioned)
Average voltage	1.2 volt

This resulted in an energy density of

31.8 Wh/kg or 14.5 Wh/pound.

3. CONCLUSIONS

The cells containing the experimental positive electrodes could not be built in accordance with existing procedures. The protruding wire points at the edges of the plates led to a complete rate of internal shorts. This could only be overcome by means of an elaborate and tedious rebuilding procedure.

The application of the existing impregnation process for positive electrodes in the future will demand the availability of a better suited substrate and/or plaque structure.

Once the difficulties in the actual building of the sealed cells were overcome, the formation process could be successfully applied. Capacities obtained were good, and based upon actual positive plate dimensions, specific capacities were either within the goal of 8-10 Ah/in^3 or only slightly below it.

Energy density for the whole system based upon a weight basis was above the values normally attributed to sealed nickel cadmium cells.

The thinner than usual positive experimental plate structure permitted the incorporation of an additional pair of electrodes plus the necessary separator material. An increase in cell capacity was observed which on one hand was lower than anticipated from the increase in number of plates, but on the other hand proved that an increase of energy density based upon volume was achieved.

SECTION V

CELL TESTING

1. GENERAL REMARKS

At the time of preparing the Second Annual Report on this contract work, eight cells of nominal 20 Ah capacity continued to be on a repetitive cycling regime, and the findings of a subsequent evaluation could not be reported. These cells contained experimental positive electrodes made by the old six-cycle C.P.E.D. process on an individual basis as described previously.

Four of these cells were operated in the flooded state, while the other four were of normal sealed construction. However, like the new cells just described, they had a pressure gauge-valve assembly as closure. All cells were on a five-hour nominal rate of four amperes for both charging and discharging. The depth of discharge was 50% of nominal capacity and the overcharge factor was 1.20. At about half-time of the cycling period, and at the end of the testing, a series of deep discharges was applied.

Upon completion of the final discharges, the flooded cells were submitted to a teardown procedure and to chemical analyses, while the four sealed cells were transferred to a different regime which simulated a low earth orbiting.

The newly built cells, as described in the preceding section, were assigned to the following testing tasks:

- 8 cells of nominal 20 Ah capacity to the same low earth orbiting regime as the old ones, however, about 2,000 cycles behind those.

- 8 cells of nominal 20 Ah capacity to a five-hour rate regime as previously applied to the old cells.

- 4 cells of nominal 20 Ah capacity were kept for contingencies and were stored at room temperature in the discharged state following their fourth formation cycle. These cells were later to be used as standards in the chemical analysis.

- 2 cells of nominal 50 Ah capacity were put on the same low earth orbiting regime, however, at proportionally greater currents for charge and discharge than the 20 Ah cells.

- 2 cells of nominal 50 Ah capacity were kept for contingencies, again at room temperature in a discharged state following their fourth formation cycle.

2. CELL TESTING PROCEDURES

a. Cycle Testing of Old 20 Ah Cells, Part A

Following a formation process and a complete recharge, the cells were initially put on this repetitive cycling regime:

Discharge for 2.5 hours at four amperes = 10 Ah

Charge for 3.0 hours at four amperes = 12 Ah

This was equivalent to a depth of discharge of 50%, based upon the nominal capacity of 20 Ah, and constituted an overcharge factor of 1.20.

Overall test history and capacity performance are presented in Table 24 in the following manner:

Column "Cycle" contains number of cycles at each test sub-section, i.e., formation, F, first series of repetitive cycling, R_1, deep discharges A_1, B_1, and C_1, second series of repetitive cycles, R_2, and final deep discharges, A_2, B_2, and C_2. Column "EDV" pertains to the respective voltages at which discharge capacities were calculated. The next two columns contain the charge currents, I_c, and discharge currents, I_d, in amperes. The discharge capacities, C_d, in Ah are organized by type of cell, i.e., sealed or flooded, and by composition of electrolyte. The cells containing LiOH as additive are marked by the letter L following their cell number.

As can be seen, the discharge capacities of all cells gradually increased in the course of the formation process, i.e., cycle 1F through 3F. In the subsequent 112 repetitive cycles, the conditions as described above were applied.

Capacity Performance. At the deep discharge $113A_1$, the capacities of the sealed cells to 1 volt were generally lower than at the third formation cycle. A recharge for 16 hours at the same current of four amperes not only restored, but even exceeded, the initial capacity in 3 out of 4 cases. Another charge under the same conditions, and a discharge at ten amperes to .6 volt, resulted in capacities comparable to those at the end of formation.

The second series of repetitive cycles induced a considerable loss in discharge capacities at cycle $113A_2$ which could only partially be overcome by the treatment at $113B_2$. The final charge and ten ampere discharge to .6 volt at cycle $113C_2$ resulted in discharge capacities which for cells 1 and 3L were significantly lower than at the beginning.

TABLE 24

DISCHARGE CAPACITIES OF SEALED & FLOODED OLD 20 Ah CELLS

TYPE				SEALED				FLOODED			
CYCLE	EDV	I_c	I_d	1	2	3L	4L	5	6	7L	8L
1F	1	2.5	10	22.9	22.6	22.4	22.1	22.4	22.2	21.6	21.7
2F	1	2.5	10	24.4	23.9	24.5	24.4	24.6	24.8	24.4	24.4
3F	1	12	10	24.5	23.0	25.0	24.8	25.5	25.7	25.4	25.5
plus 112 R_1 repetitive cycles		4	4	10.0	10.0	10.0	10.0	10.0	10.0	10.0	10.0
$113A_1$	1	4	4	21.4	23.6	21.8	22.8	25.9	26.6	28.6	28.7
	.6			23.0	24.5	22.4	23.2	26.2	27.0	28.7	28.8
$113B_1$	1	4	4	25.1	25.4	23.8	25.6	30.5	30.7	34.1	34.0
	6			25.8	26.3	24.2	26.3	30.6	30.7	34.2	34.1
$113C_1$	1	4	10	23.2	23.7	21.4	22.8	28.9	28.9	31.6	31.6
	.6			24.1	24.6	22.3	24.0	29.2	29.[illegible]	32.0	32.0
plus 112 R_2 repetitive cycles		4	4	10.0	10.0	10.0	10.0	10.0	10.0	10.0	10.0
$113A_2$	1	4	4	17.2	19.5	17.2	19.3	21.4	23.3	25.8	26.0
	.6			18.0	20.6	18.0	20.7	22.0	23.4	26.1	26.1
$113B_2$	1	4	4	22.6	24.4	20.8	24.4	31.1	31.0	34.6	34.0
	.6			23.4	25.5	21.7	25.2	31.2	31.2	35.0	34.3
$113C_2$	1	4	10	21.0	21.6	19.9	22.5	31.4	30.8	33.8	33.6
	.6			21.7	22.6	20.8	23.6	31.6	31.3	35.2	34.8

The discharge capacities of the four flooded cells were not adversely affected by the first series of repetitive cycles; on the contrary, they were even higher at cycle $113A_1$ than at formation 3F. Recharging and second discharge at $113B_1$ resulted in even greater capacities than ever before. The third deep discharge cycle resulted in capacities to .6 volt which in all cases were significantly greater than at formation.

The second series of repetitive cycles led to temporary losses in discharge capacity at cycle $113A_2$. In the case of the two cells with normal electrolyte, these values were even below formation performance. However, in the two final deep discharge cycles, considerable improvements beyond formation performance were observed, with the LiOH containing cells about 10% higher capacities than the normal electrolyte cells. In order to establish whether this excellent performance was caused by better utilization or corrosion of the nickel sinter structure and subsequent increase in amount of active material, teardown and chemical analyses were performed with selected cell and electrolyte materials. These results will be reported further below.

It should be noted that in all cases the positive electrodes were discharge limiting. In the case of the flooded cells equipped with reference electrodes, absolute potential readings corroborated this fact. In the case of the sealed cells where the can served as reference, absolute readings could not be obtained, since the potential of the can was unstable. However, the relative changes of the electrode potential versus this reference indicated that the positives were also the discharge limiting factor.

The monitoring of sealed cell pressures showed that on repetitive cycling the pressures were in the -20 to -30 range. At the end of recharge periods for the B and C discharges the pressures were up to +5 to +10 psig; however, upon resuming the cycling, they returned to their former low levels.

<u>Cell Voltage Behavior.</u> The cell voltages at both the end of charge and the end of discharge periods were monitored on a regular basis, and the averages for the four subgroups of two cells each are presented in Table 25.

As can be seen, in the majority of the cases the end of charge voltage for cells with normal electrolyte was a few mV lower than that of their corresponding counterparts with LiOH additive. By the same token, the end of discharge voltage of the normal electrolyte cells was generally a few mV above the value for LiOH containing cells. This first observation has been made before, and was, for instance, reported in Table 29, Second Annual Report.

TABLE 25

VOLTAGE BEHAVIOR OF OLD 20 Ah CELLS

END OF	CHARGE				DISCHARGE			
TYPE	SEALED		FLOODED		SEALED		FLOODED	
ELECTROLYTE	W/O	W / LiOH	W/O	W/LiOH	W/O	W/LiOH	W/O	W/LiOH
CYCLE								
1 R_1	1351	1346	1523	1568	1230	1216	1382	1412
29 "	1422	1425	1641	1651	1211	1207	1199	1196
57 "	1421	1428	1664	1665	1200	1196	1273	1274
89 "	1424	1430	1665	1670	1277	1276	1273	1274
113 "	1427	1430	1664	1677	1187	1171	1198	1195
1 R_2	1421	1421	1645	1640	1220	1219	1222	1223
29 "	1470	1422	1660	1662	1208	1205	1208	1208
37 "	1422	1424	1661	1672	1203	1199	1208	1205
41 "	1423	1425	1668	1673	1200	1196	1205	1205
61 "	1427	1431	1670	1678	1188	1190	1202	1202
97 "	1438	1445	1686	1700	1194	1194	1204	1204
113 "	1423	1428	1668	1692	1190	1198	1202	1201

General trends in the two terms were an increase in EOCV values and a decrease in the corresponding EODV readings with an increasing number of cycles. The series of deep discharges after the first 113 repetitive cycles broke both of those developments. However, the trends reappeared in the second series of repetitive cycling.

Attempts to treat the data with statistical curve fitting procedures were inconclusive, in all likelihood because of the small span of the repetitive cycling involved.

In the next three figures the discharge voltage versus time behavior of the 20 Ah cells is presented for the two series of deep discharges to .6 volt. For comparison, the corresponding curves of the third formation cycle are also given and marked as such.

To recall the nomenclature used: Curves designated with letter A were obtained at a continuation of the discharge beyond the normal cutoff point at 10 Ah. Curves bearing the letter B are deep discharges following a complete recharge for 16 hours at four amperes.

Curves called C are discharges with 10 amperes in lieu of the four ampere currents for curves A and B, respectively. The charge for C was also 16 hours at four amperes. Subscript 1 or 2, respectively, stands for the first or second regime of deep discharge. In Figure 9, typical curves for the four sealed cells are presented. The composition of the electrolyte did not affect the shape of the curves.

Curve A_1 displays a previously observed step in the vicinity of the end of normal shallow discharge, here marked by the arrow. Beyond this point, a considerable depression in voltage could be observed, yet the capacity delivered to one volt was only slightly affected. Curve B_1 constitutes a significant improvement,not only over A_1, but even over the formation performance, which might be due to the lower discharge current, i.e., 4 A versus 10 A at formation. Curve C_1 obtained under conditions similar to those at formation is initially good, then shows a more rounded "knee" in cell voltage, but only small loss in capacity to one volt.

The three curves with subscript 2 are replicas of their corresponding predecessors, i.e., A_2 has the step and low voltages right of the arrow mark; B_2 eliminates the step and improves voltages and capacities, however, to a lesser degree than B_1; C_2 finally is completely identical with C_1.

The performance of the flooded cells made it necessary to distinguish between the composition of the electrolyte in presenting the voltage versus time curve data.

Figure 10 represents the typical curves for the two flooded cells with conventional KOH electrolyte. Curves A_1 and A_2 have a less

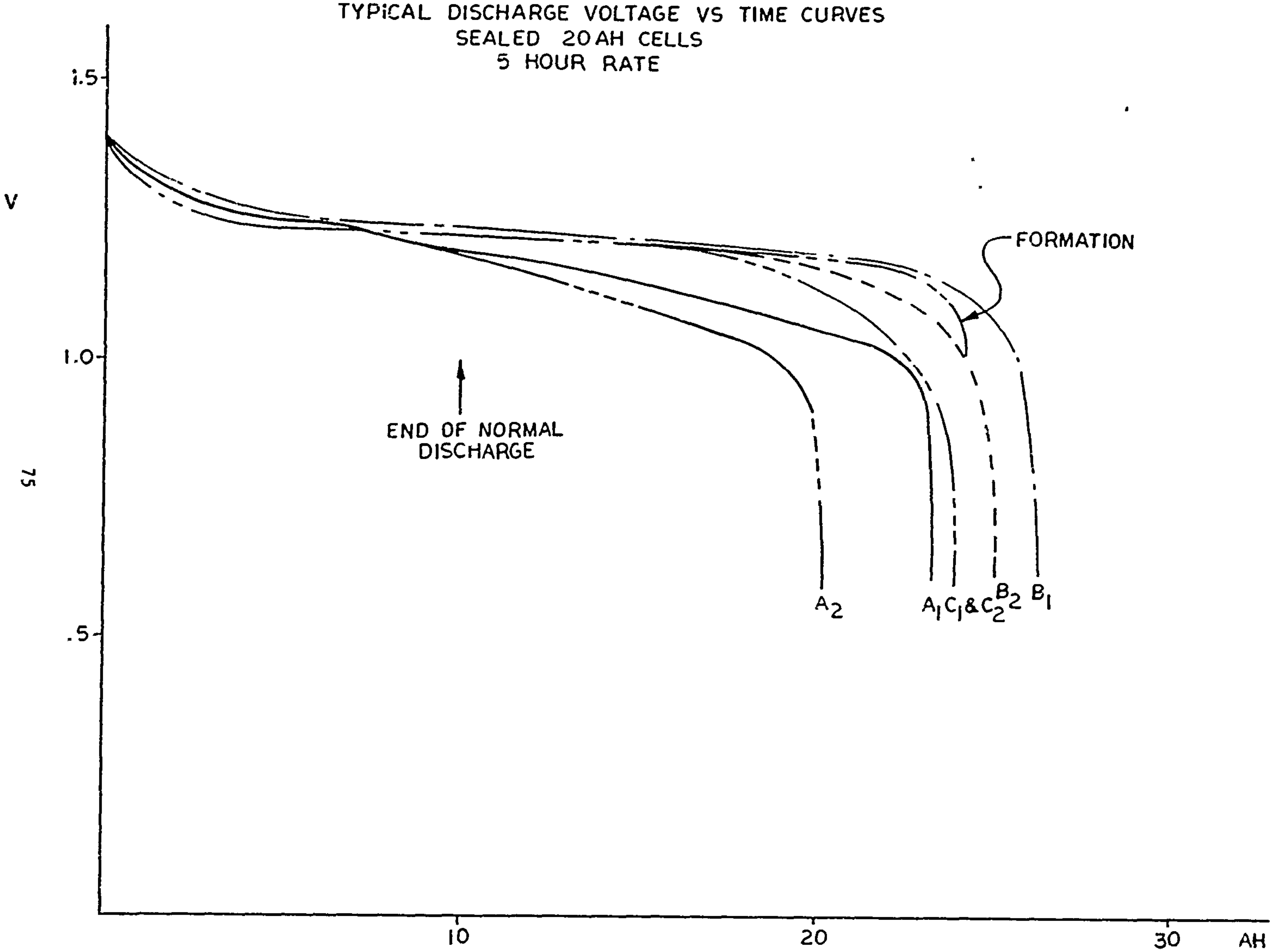
TYPICAL DISCHARGE VOLTAGE VS TIME CURVES
SEALED 20 AH CELLS
5 HOUR RATE
V
1.5
1.0
.5
10
20
30
AH
END OF NORMAL DISCHARGE
FORMATION
A2
A1 C1 & C2
B2
B1

FIGURE 9

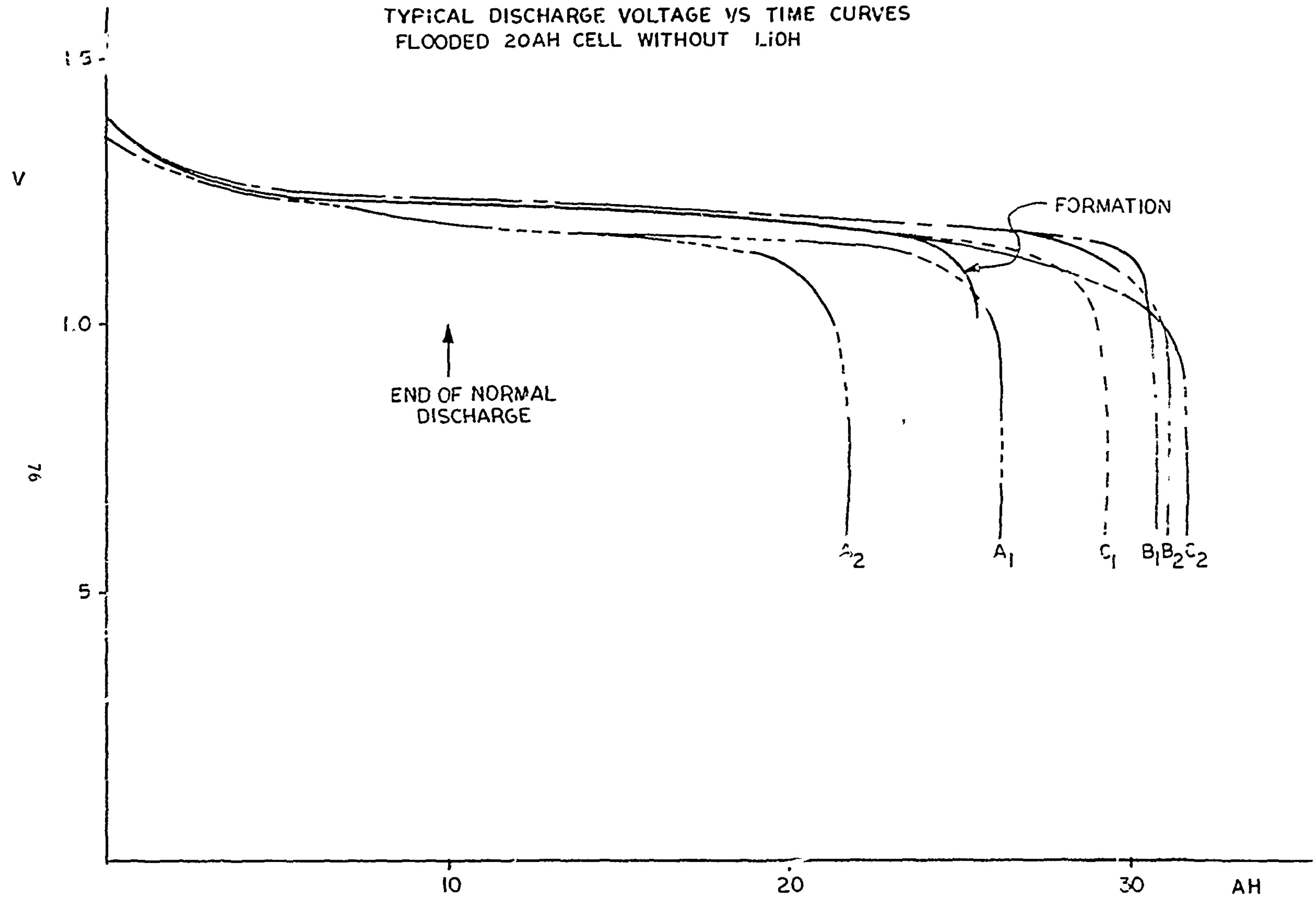
TYPICAL DISCHARGE VOLTAGE VS TIME CURVES
FLOODED 20AH CELL WITHOUT LiOH
V
1.5
1.0
5
FORMATION
END OF NORMAL
DISCHARGE
A2
A1
C1
B1
B2
C2
10
20
30
AH

FIGURE 10

pronounced step in the vicinity of the arrow mark and only slightly depressed voltages beyond that point. Curves B_1 and B_2 are considerable improvements over their forerunners and the formation performance, both with regard to capacities and voltages. Finally, curves C_1 and C_2 significantly surpass the formation behavior at the same discharge current, and voltage-wise are only slightly below the B-curve courses.

In Figure 11, the situation for the two flooded cells with LiOH additive is presented. The A curves have a slight step near the arrow mark, a voltage depression, but show an increase in discharge capacity over the formation process. B curves are flawless with respect to voltage performance and have impressive increases in discharge capacities. C curves are better than formation behavior voltage-wise, and even better with regard to capacity. Interesting to note is the capacity increase from curve C_1 to C_2.

Overall, the behavior of the LiOH containing cells was analogous to that of cells with conventional KOH electrolyte, however, everything was moved to the right, i.e. greater capacity values.

Summary of Results. Here we observed that:

- The application of a limited number, i.e., 112, of repetitive cycles produced a step in the voltage curves and also subsequent voltage depressions once the discharge was continued beyond the normal endpoint of 10 Ah removal.

- The deviations were more pronounced for sealed than for flooded cells.

- The voltage irregularities and associated losses in discharge capacities were only temporary and could be remedied by a complete recharge and subsequent discharge under the same conditions.

- Discharge capacities immediately after rejuvenation were greater than those at formation. This trend was more pronounced with the flooded cells, and even more with the LiOH containing cells.

- Discharges at formation currents were different for sealed and flooded cells. The first fared slightly worse than before, while the latter exhibited considerable improvements over their formation performance.

- Voltage step and subsequent depression obtained with a multiplate system were similar to those observed with C_5 cells. However, it appears that these phenomena occurred earlier in cycling and were more pronounced.

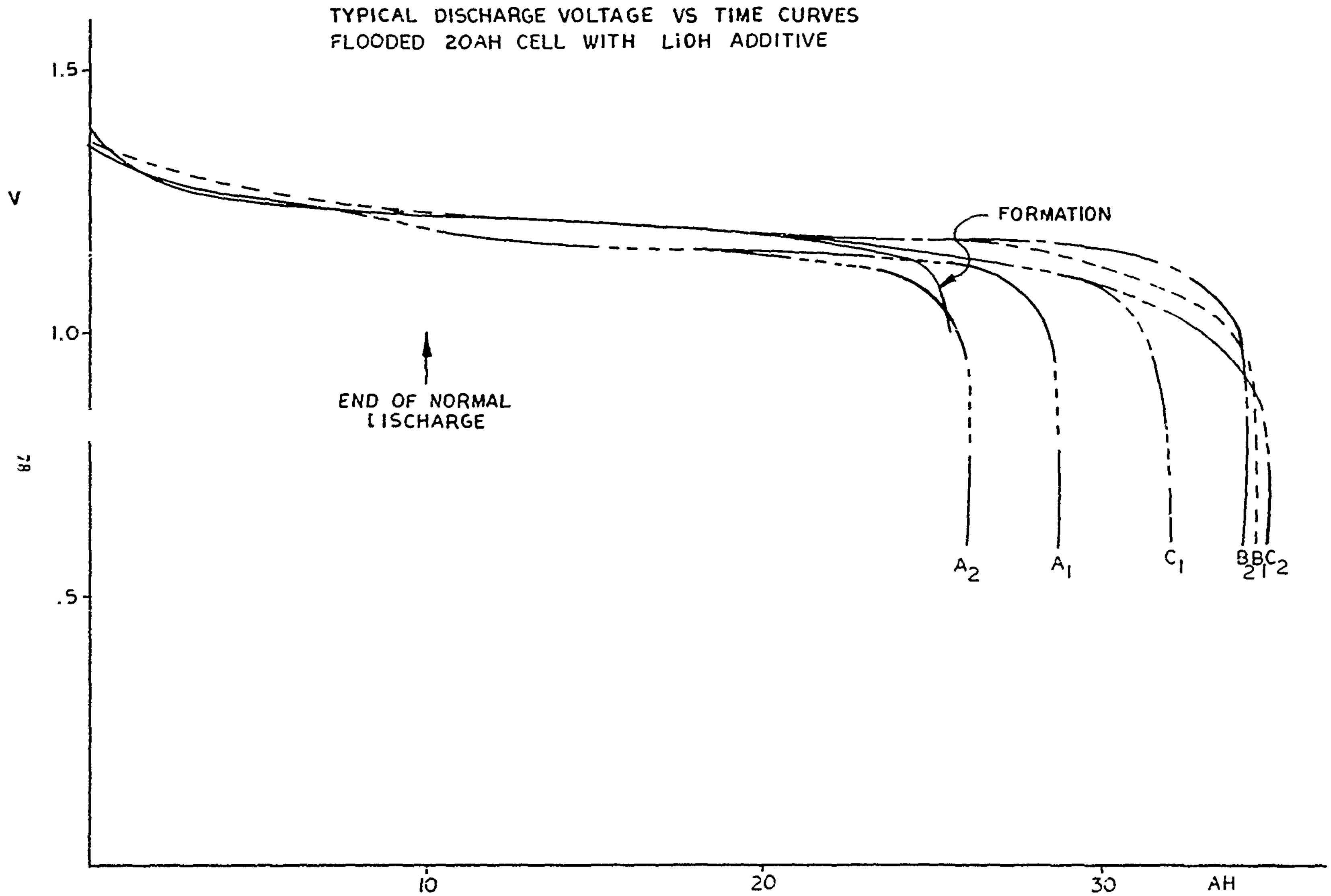
TYPICAL DISCHARGE VOLTAGE VS TIME CURVES
FLOODED 20AH CELL WITH LiOH ADDITIVE
V
1.5
1.0
.5
FORMATION
END OF NORMAL
DISCHARGE
A2
A1
C1
B2
B1
C2
10
20
30
AH

FIGURE 11

- In the future, these new observations might deserve more consideration and might even lead to a redefinition of the "memory" complex.

b. Analysis of Old Flooded 20 Ah Cells

Results of Teardown. One flooded cell each with normal and LiOH containing electrolyte was disassembled following the final discharge at cycle $113C_2$.

The visual inspection of all cell components, i.e., positive and negative electrodes and cellophane and woven nylon separator, revealed no defects of any kind. Specifically, all positive electrodes appeared free from any sign of corrosion or attack on the sinter structure.

Thickness measurements indicated a swelling of the positives in the course of the testing process from the initial compressed thickness of .052 cm to .060 cm for conventional electrolyte to .062 cm for LiOH additive electrolyte, respectively. The final thicknesses stayed below the thickness of .064 cm measured prior to compression.

Results of Chemical Analysis. Since the external appearances of the positives were flawless, only three 10 cm^2 punches were removed from one plate of each cell. According to their location, they were designated as top, middle, and bottom, respectively. The mixture of active material and metallic nickel was carefully removed from the nickel wire substrate and then submitted to chemical analysis for Ni°, total active material, $Ni(OH)_2$, and per cent of residual charge, C_r.

The results obtained are presented in Table 26, together with pertinent data obtained from "black" electrode material prior to compression. All values, with the exception of the residual charge, are in g/dm^2.

As can be seen, the amount of metallic nickel, Ni°, remained virtually unchanged in the course of the cycling regime under the experimental conditions applied, as did the amount of active material, $Ni(OH)_2$. Consequently, an attack on the sinter structure (corrosion) and subsequent increase of amount of active material can be ruled out as cause for the increase in discharge capacities observed. We therefore must assume an increase in the efficiency of the active material proper.

At the end of formation, the four flooded cells had an average capacity to 1.0 volt of 25.4 Ah in a volume of 95 x .052 x 11 = 54.3 cm^3 corresponding to 7.7 Ah/in^3. At the end of cycling, the cells with conventional electrolyte had a capacity to .6 volt of 31.6 Ah at a positive electrode volume of 95 x .060 x 11 = 62.7 cm^3 corresponding to 8.3 Ah/in^3. The cells with LiOH as additive produced 35.2 Ah to .6 volumes at a plate volume of 95 * .062 x 11 = 65.9 cm^3 which is

TABLE 26

CHEMICAL COMPOSITION OF CYCLED FLOODED 20 Ah-SIZE PLATES

		ELECTROLYTE NORMAL			W/LiOH		
TYPE		Ni°	$Ni(OH)_2$	$\%C_R$	Ni°	$Ni(OH)_2$	$\%C_R$
Black		6.66	11.02	28	-	-	-
Cycled	TOP	6.54	11.05	27	6.51	9.83	25
	MID	6.57	10.51	29	6.56	9.73	26
	BOT	6.42	10.53	27	6.49	10.09	26
	AVG	6.51	10.70	28	6.52	9.92	26

Calculation of pre-cycle levels

TOTAL	10.81*	12.25#
-SUBSTRATE	3.40	-
NET	7.40	12.25
-10% ⁑	.74	1.23
FINAL	6.66##	11.02

* See for instance TABLE 50, 2nd Annual Report

$\#$ Average from TABLE 52, ibid.

⁑ Due to necessary compression and subsequent sizing steps, about 10% of the original material per plate is lost.

$\#\#$ Compare for instance with average of 6.6 g/dm^2 for compressed black C_s plates TABLE 45 ibid.

equivalent to 8.9 Ah/in^3. The increase in specific capacity, C_s, with cycling indicates that the increase in discharge capacity more than compensated the increase of plate volume caused by the swelling.

Under the assumption that the results of the chemical analyses are representative for all of the positive plates in the flooded cells, one can perform some calculations pertaining to efficiency aspects of the active material proper.

The results of those computations are presented in Table 27 in the following manner:

The discharge capacity, C_d, from the last deep discharge for cells 5 and 7L, is followed by the amount of active material, $Ni(OH)_2$, determined by chemical analysis and expressed in various ways, and finally, as theoretical capacity, C_t.

The ratio, C_d/C_t, is the efficiency of the active material and is expressed in per cent. For the cell with normal electrolyte, the efficiency is almost theoretical on the basis of one-electron transfer, while for the cell with LiOH additive, an efficiency of 118% is found. This means, of course, that part of the active material must have attained an oxidation level of greater than 3+.

Since in both cases significant amounts of residual charged material were found, i.e., stored electrical charge which did not contribute to the discharge capacity, C_d, the efficiencies found have to be corrected accordingly. In the lower part of the table this is done in the following manner:

The amount of residual charge, C_r, chemically determined and expressed in Ah/dm^2 is converted to Ah/cell which then is subtracted from C_t and yields the corrected theoretical capacity, C_t^{cor}. Dividing the discharge capacity, C_d, by this corrected value results in the corrected efficiency of the "working" active material.

As can be seen, both for normal and LiOH containing electrolyte, the efficiencies are now significantly beyond the 100% theory mark, or in other words, considerable portions of the active material participating in the charge-discharge cycle must have had valencies exceeding 3+. Since intermediate valencies between the 3+ and 4+ level are not possible, 37% of the active material in normal electrolyte cells and 58% of the active material in the LiOH containing cells must have been at the 4+ valency level.

TABLE 27

EFFICIENCY OF ACITVE MATERIAL

	ELECTROLYTE		
	NORMAL	W/LiOH	
TERM	LEVEL	LEVEL	DIMENSION
C_d	31.6	35.2	Ah/cell
$Ni(OH)_2$*	10.7	9.92	g/dm^2
$Ni(OH)_2$*	9.98	9.42	g/plate
$Ni(OH)_2$*	109.8	103.6	g/cell
C_t	31.73	29.94	Ah/cell
C_d/C_t	98	118	% Efficiency
C_R*	.85	.73	Ah/dm^2
C_R*	.808	.693	Ah/plate
C_R*	8.89	7.62	Ah/cell
$C_t^{cor} = (C_t - C_R)$	22.84	22.32	Ah/cell
C_d/C_t^{cor}	137	158	% Efficiency corrected

* From chemical analyses.

Summary of Results. In this chapter one can conclude that:

- The cycle regime applied did not lead to an attack on the sinter structure (corrosion).

- The increase in discharge capacity levels upon cycling was caused by a better utilization or efficiency of the active material.

- The "working" active material, i.e., the portion of the total contributing to the discharge capacity, on an average is at a higher state of oxidation than 3+.

- The presence of LiOH in the electrolyte of flooded cells is clearly beneficial since it enhances the utilization of the active material.

c. Cycle Testing of Old 20 Ah Cells, Part B

The four sealed cells of the first group of nominal 20 Ah cells described above were recharged for 16 hours at two amperes and then put on a simulated low earth orbiting regime consisting of:

Discharge at 10.8 amperes for 35 minutes = 6.3 Ah

Charge at 5.6 amperes for 75 minutes = 7.0 Ah

These conditions corresponded to a depth of discharge of 31.5% based upon the nominal capacity of 20 Ah and an overcharge factor of 1.11.

In the span of about ten months, 4,042 of such uninterrupted cycles were acquired and the cells were then submitted to a final series of deep discharges.

In their cycle life, all cells performed flawlessly as indicated by the values for the end of charge voltages, EOCV, and that of the end of discharge voltages, EODV, presented in Table 28.

It appears that the EOCV values slowly increased with time, but they still remained within acceptable limits. The EODV readings declined within the first week of cycling from an initial value of 1.24 volt to a stabilized value around 1.15 volt. This plateau was temporarily left when at cycle 1,264 the discharge current was found to be too low. A correction of that term brought the EODV readings back to their previous levels.

TABLE 28

VOLTAGE DATA OF FOUR SEALED 20 Ah CELLS

CELL	EOCV				EODV			
CYCLE	3L	1	2	4L	3L	1	2	4L
1	1.44	1.46	1.47	1.44	1.24	1.24	1.23	1.24
86	1.46	1.46	1.46	1.46	1.19	1.16	1.19	1.16
175	1.45	1.46	1.46	1.43	1.19	1.16	1.20	1.16
259	1.44	1.47	1.47	1.48	1.19	1.16	1.18	1.17
429	1.44	1.44	1.44	1.44	1.16	1.14	1.15	1.18
512	1.44	1.44	1.44	1.44	1.16	1.11	1.13	1.16
608	1.44	1.45	1.44	1.44	1.16	1.10	1.11	1.16
679	1.44	1.45	1.44	1.45	1.16	1.10	1.10	1.17
763	1.44	1.46	1.45	1.45	1.16	1.14	1.12	1.16
857	1.44	1.46	1.46	1.45	1.16	1.10	1.10	1.16
935	1.44	1.44	1.44	1.44	1.16	1.14	1.12	1.16
1024	1.44	1.44	1.44	1.44	1.15	1.10	1.10	1.15
1108	1.44	1.44	1.44	1.44	1.15	1.11	1.11	1.15
1191	1.46	1.46	1.45	1.45	1.16	1.13	1.13	1.16
1264*	1.44	1.46	1.45	1.46	1.17	1.15	1.16	1.17
1677	1.45	1.46	1.45	1.48	1.14	1.11	1.11	1.16
1325	1.43	1.44	1.44	1.44	1.10	1.10	1.10	1.10
1352	1.44	1.44	1.44	1.44	1.18	1.17	1.16	1.16
1432	1.44	1.45	1.45	1.46	1.17	1.17	1.16	1.15
1517	1.45	1.47	1.45	1.48	1.14	1.12	1.10	1.14
1615	1.44	1.44	1.44	1.45	1.13	1.10	1.10	1.14
1688	1.44	1.45	1.45	1.45	1.12	1.12	1.12	1.12
17[illegible]	1.44	1.46	1.45	1.46	1.12	1.10	1.10	1.11
18[illegible]	1.44	1.45	1.44	1.46	1.12	1.08	1.12	1.12
1940	1.44	1.45	1.45	1.45	1.12	1.10	1.10	1.11
2023	1.46	1.46	1.44	1.46	1.13	1.10	1.10	1.12
2109	1.43	1.44	1.43	1.45	1.13	1.11	1.11	1.11
2194	1.45	1.45	1.44	1.46	1.13	1.13	1.13	1.15
2277	1.45	1.45	1.44	1.47	1.14	1.13	1.12	1.12

TABLE 28 (Continued)

VOLTAGE DATA OF FOUR SEALED 20 Ah CELLS

CELL CYCLE	EOCV 3L	EOCV 1	EOCV 2	EOCV 4L	EODV 3L	EODV 1	EODV 2	EODV 4L
2372	1.48	1.48	1.47	1.49	1.14	1.13	1.13	1.14
2400	1.46	1.48	1.46	1.49	1.13	1.12	1.13	1.14
2525	1.46	1.48	1.45	1.50	1.11	1.11	1.11	1.12
2600	1.46	1.46	1.45	1.48	1.13	1.12	1.15	1.12
2696	1.46	1.46	1.44	1.46	1.14	1.12	1.17	1.14
2786	1.45	1.45	1.45	1.46	1.14	1.11	1.13	1.14
2878	1.48	1.48	1.47	1.49	1.14	1.12	1.13	1.14
2947	1.46	1.48	1.48	1.49	1.14	1.12	1.15	1.16
3121	1.43	1.40	1.38	1.43	1.14	1.16	1.20	1.19
3199	1.48	1.49	1.50	1.50	1.17	1.16	1.15	1.16
3297	1.47	1.47	1.48	1.49	1.19	1.15	1.14	1.18
3379	1.50	1.50	1.51	1.51	1.17	1.14	1.13	1.17
3470	1.50	1.50	1.49	1.50	1.15	1.12	1.12	1.15
3631	1.49	1.49	1.49	1.50	1.19	1.18	1.17	1.11
3718	1.48	1.47	1.49	1.49	1.15	1.15	1.14	1.15
3789	1.45	1.49	1.50	1.51	1.14	1.11	1.25	1.14
3879	1.48	1.47	1.50	1.50	1.14	1.14	1.14	1.14
3971	1.49	1.49	1.50	1.46	1.17	1.17	1.14	1.17
4043	1.48	1.48	1.48	1.49	REMOVED FROM CYCLING			

* Discharge current too low

As far as these voltage readings were concerned, no differences between cells #1 and #2, with normal electrolyte, and cells #3L and #4L, with LiOH additive in the electrolyte, could be detected.

In Table 29, the corresponding cell pressures are presented for the four cells. The end of charge pressures, EOCP, are always given in psi gauge, while the end of discharge pressures, EODP, are either in inches per sq. inch gauge when having a negative sign or in psi gauge for zero or values with a positive sign.

Both of these terms increased with time, however, which was no cause for concern. A systematic influence of the LiOH additive could not be detected.

At the end of the charge period 4,043, all four cells were removed from the automatic cycling equipment and submitted to manual deep discharges at the same discharge current of 10.8 amperes.

In Figure 12, the respective voltage versus time curves for cells #3L and #1, respectively, are presented together with a typical voltage curve obtained at the formation process.

In this figure, and in all subsequent identical ones, the normal end of discharge, EOD, is marked by an arrow positioned at 6.3 Ah capacity removed. The amount of charge returned, 7 Ah, at every cycle is symbolized by another arrow marked "RECHARGE".

As can be seen, the performances of these cells became unacceptable as soon as the discharge was continued beyond its normal end at 6.3 Ah removed. This statement applies to both capacity and voltage aspects:

- The initial formation capacities of 25.0 Ah and 24.5 Ah, respectively, are reduced to 14.3 Ah for cell #3L and to 11.6 Ah for cell #1.

- The discharge voltage versus time curves are severely distorted.

Although this group of cells did not have a built-in reference electrode like the newer ones, the cans of cells #3L and #4L, but not those of cells #1 and #2, had sufficiently stable potentials as to permit some meaningful measurements. These tracings are superimposed with a straight line at one volt serving as relative potential of the cell can.

Keeping in mind that reference electrode measurements by means of the cell can are not too reliable, two tentative statements can be made, namely:

TABLE 22

PRESSURE DATA OF FOUR SEALED 20 Ah CELLS

CELL CYCLE	EOCP 3L	EOCP 1	EOCP 2	EOCP 4L	EODP 3L	EODP 1	EODP 2	EODP 4L
1	11	9	10	9	-5	-18	-15	-14
86	11	10	10	9	-8	-15	-10	-13
175	11	10	10	10	-8	-16	-10	-13
259	10	13	14	15	-8	-15	-10	-13
429	10	13	14	15	-8	-14	-10	-13
512	8	10	10	10	-8	-15	-17	-11
608	10	14	14	14	-10	-18	-18	-10
679	10	13	15	15	-10	-17	-18	-10
763	10	12	9	15	-10	-17	-17	-10
857	10	13	10	15	-10	-18	-18	- 9
935	9	13	10	15	-10	-16	-18	- 8
1044	12	14	10	18	-9	-14	-18	- 8
1108	12	15	11	16	-10	-14	-19	- 8
1191	11	14	11	15	-8	-11	-18	- 4
1264	18	33	15	35	0	+ 2	-11	+ 5
1277	49	36	20	35	-2	+ 2	-11	+ 4
1325	5	8	2	5	-10	-10	-17	-10
1352	13	13	11	14	-7	-12	-18	-11
1432	23	42	24	39	-10	- 9	-11	-14
1517	19	30	17	31	0	+ 1	-11	+ 2
1615	[illegible]	23	14	25	0	+ 2	- 6	+ 5
1688	12	22	15	22	0	2	-10	5
1772	20	25	12	26	-4	- 3	-12	1
1855	21	27	18	30	-2	- 6	-12	0
1940	20	26	20	27	-4	- 6	-12	- 1
2063	20	24	20	25	-3	- 3	-12	1

TABLE 29 (Continued)

PRESSURE DATA OF FOUR SEALED 20 Ah CELLS

CELL CYCLE	EOCP 3L	EOCP 1	EOCP 2	EOCP 4L	EODP 3L	EODP 1	EODP 2	EODP 4L
2109	25	20	15	30	-5	-6	-10	1
2194	23	21	15	25	0	2	-10	5
2277	21	23	15	20	0	4	-10	5
2372	21	33	15	35	2	4	-10	5
2400	20	30	15	30	0	4	-10	5
2525	20	28	19	26	0	-2	-6	-6
2600	28	34	18	35	0	0	-5	0
2696	33	37	18	40	4	6	-5	9
2786	35	40	20	35	3	7	-8	6
2878	26	33	15	35	2	4	-10	5
2947	36	36	16	36	4	4	-11	6
3121	23	25	5	27	0	0	-15	4
3199	24	27	8	30	5	2	-12	5
3297	30	27	10	35	10	5	-10	10
3470	30	35	15	40	2	5	-10	5
3631	35	43	20	45	7	10	-10	12
3718	33	33	18	43	5	4	-10	10
3789	36	41	24	45	5	3	-12	8
3879	28	31	15	35	5	3	-10	10
3971	30	33	15	37	5	5	-5	10
4043	28	30	15	34	REMOVED FROM CYCLING			

Weight values in inches of vacuum.

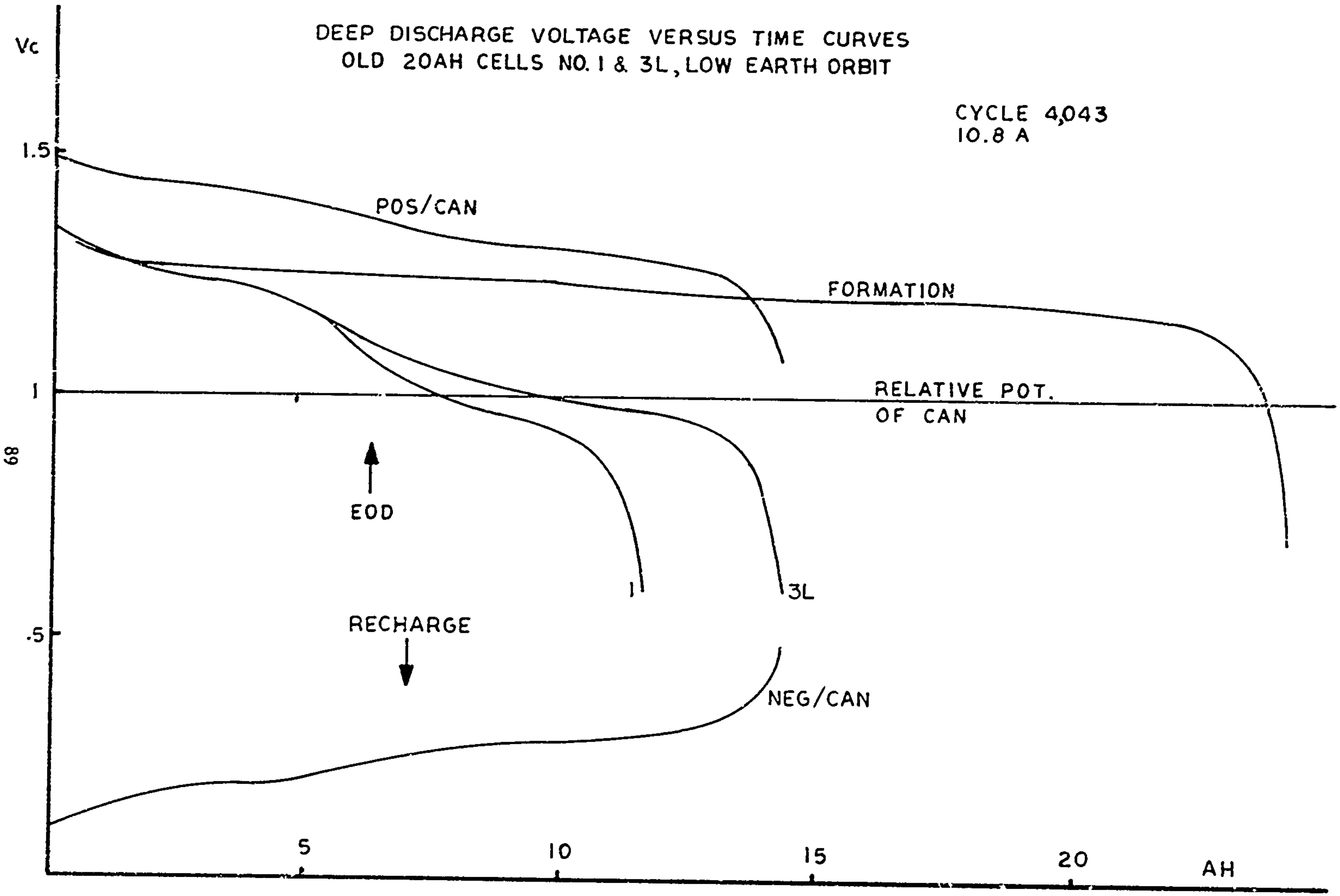
DEEP DISCHARGE VOLTAGE VERSUS TIME CURVES
OLD 20AH CELLS NO. 1 & 3L, LOW EARTH ORBIT
CYCLE 4,043
10.8 A
Vc
1.5
1
.5
POS/CAN
FORMATION
RELATIVE POT.
OF CAN
EOD
1
3L
RECHARGE
NEG/CAN
5
10
15
20
AH

FIGURE 12

- The potentials of both electrodes broke simultaneously at the end of useful discharge.
- The origin of the distortion of the voltage curve is in all probability to be found in the negative electrodes.

It is interesting to note that cells #3L and #4L had an LiOH additive in their electrolytes, while the other two cells of this group contained the normal pure KOH electrolyte. The additive obviously had a beneficial influence on cell performance with respect to cell voltage in the area beyond the normal end of discharge and also on the capacity obtainable. However, the presence of the additive could not prevent the deterioration of the cell performance in the course of deep discharges.

Following these so-called driven discharges, both cells were individually discharged through a two ohm resistor, and the additional capacities obtained were measured by means of ampere-minute meters. In this fashion, increments of 11.2 Ah and 12.1 Ah, respectively, were obtained for the two cells for a total of 25.5 Ah for cell #3L (with LiOH additive) and 23.7 Ah for cell #1 (with normal electrolyte).

The cells were then prepared for chemical analysis. The pertinent results are presented in Tables 37 and 38, respectively.

The other two cells of this group, namely, #2 and #4L, respectively, the latter with LiOH additive in the electrolyte, were submitted to a charge/discharge regime in attempts to restore the initial capacity as follows:

<u>Cycle 4,043</u>

Discharge at 10.8 A to .6 volt
Open circuit rest for 16 hours

<u>Cycle 4,044</u>

Charge at 2.5 A for 20 hours
Discharge at 19.8 A to .6 volt
Resistive discharge to .035 volt

<u>Cycle 4,045</u>

Charge at 2.5 A for 21 hours
Discharge at 10.8 A to .6 volt
Resistive discharge to .035 volt

No chemical analyses were conducted with these cells.

The cell voltage curves obtained for cell #2 are presented in Figure 13. As can be seen, the curve for cycle 4,043 is very similar to that for cell #1, both in shape and capacity aspects.

The subsequent treatment, as outlined above, remedied both shape distortion and increased the capacity towards the initial level. In addition to the capacities to .6 volt, the increments obtained by the resistive discharges are also given.

In Figure 14, the corresponding curves for cell #4L are presented. The shapes of the curves are similar to the ones of cell #3L with capacities to .6 volts slightly greater which obviously was due to the influence of the LiOH additive.

This cell permitted the use of the can as a reference electrode, and the corresponding tracings of positive and negative electrode potentials are given for cycles 4,043 and 4,045, respectively, with the latter in the final region only.

Again we observed a simultaneous break in the electrode potentials toward the end of the discharge period, and we could trace back the distortion in the discharge voltage versus time curve to the negative electrode.

As can be seen, the performance of the cells improved considerably with respect to voltages and capacities in the course of the rejuvenation process. However, the potentials of both electrodes continued to break at the same time, and so terminated the delivery of useful capacity. Significant additional amounts of capacity could be removed from the cells in the course of a resistive discharge at two ohms, but this occurred at unimportant voltages and currents.

These additional capacities are presented in Table 30, together with formation values and deep discharge capacities to various endpoints.

The following observations were made:

- The cells of this group performed satisfactorily under the conditions of the repetitive cycling regime simulating a low earth orbit.

- Upon deep discharge beyond the normal endpoint, all cells exhibited the symptoms of memory.

- Both electrodes were responsible for the end of useful discharge.

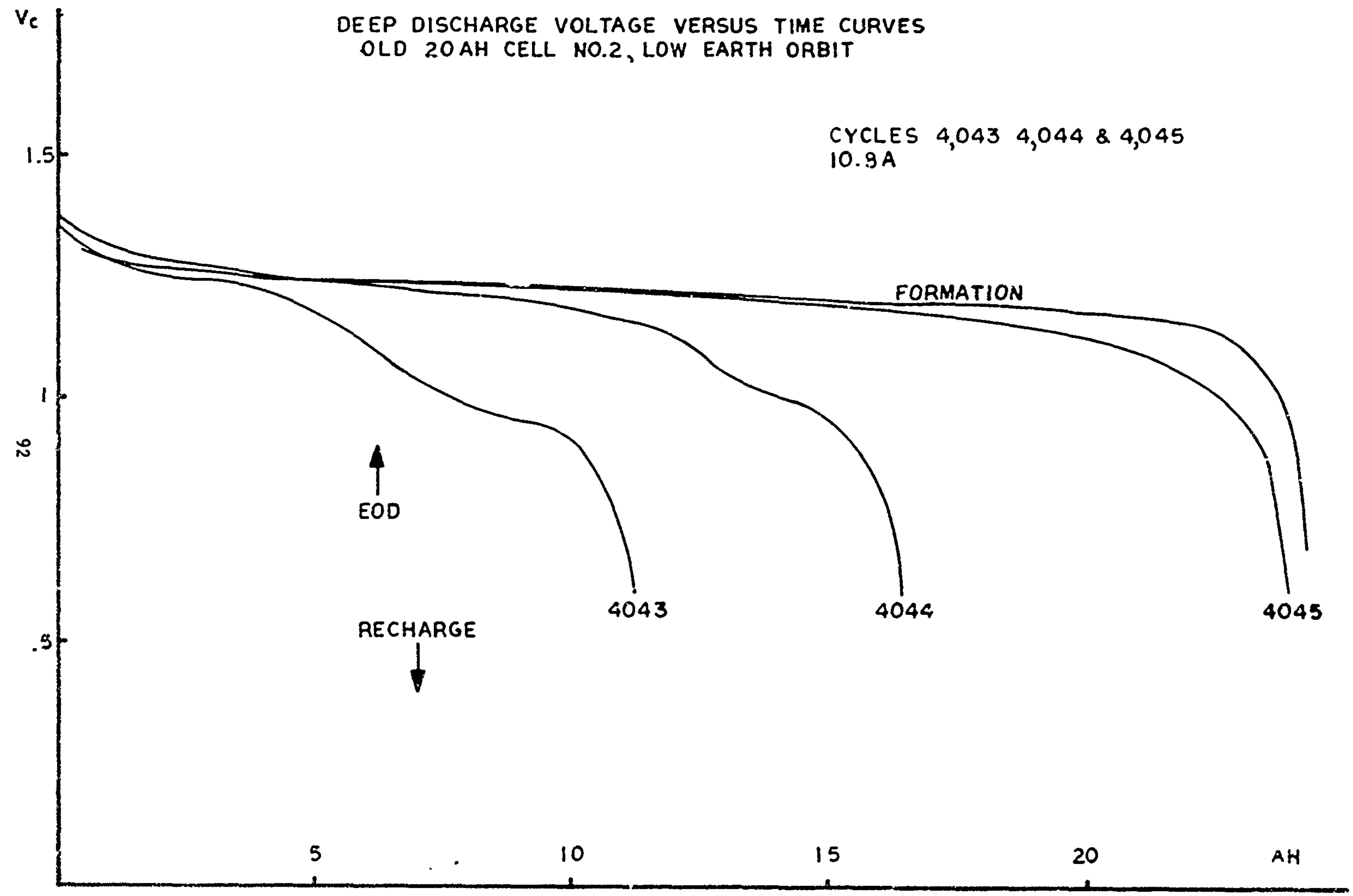
DEEP DISCHARGE VOLTAGE VERSUS TIME CURVES
OLD 20 AH CELL NO.2, LOW EARTH ORBIT
CYCLES 4,043 4,044 & 4,045
10.9A
Vc
1.5
1
.5
FORMATION
EOD
RECHARGE
4043
4044
4045
5
10
15
20
AH

FIGURE 13

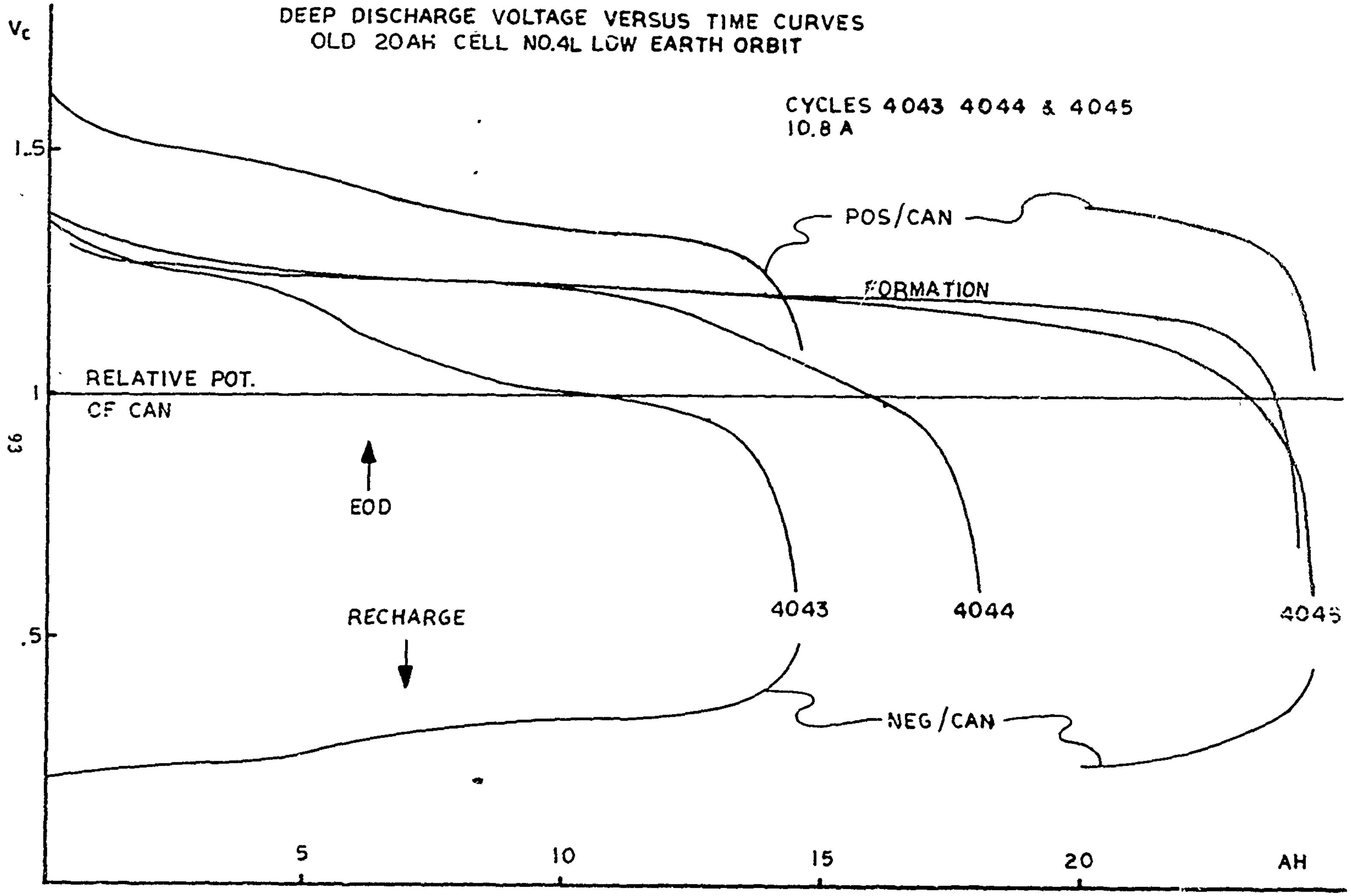
DEEP DISCHARGE VOLTAGE VERSUS TIME CURVES
OLD 20AH CELL NO.4L LOW EARTH ORBIT
CYCLES 4043 4044 & 4045
10.8 A
V_c
1.5
1
.5
POS/CAN
FORMATION
RELATIVE POT.
CF CAN
EOD
RECHARGE
4043
4044
4045
NEG/CAN
5
10
15
20
AH

FIGURE 14

TABLE 30

DISCHARGE CAPACITIES IN Ah

OLD 20 Ah CELLS

CELL		3L	1	2	4L
CYCLE	END POINT V				
Formation	.600	25.3	24.5	23.0	24.8
4043	1.000	10.0	7.7	7.8	10.2
	.600	14.3	11.6	11.1	14.5
	.035#	+11.2	+12.1	- *	-
	Total	25.5	23.7	11.1	14.5
4044	1.000			14.2	15.8
	.600			16.4	18.0
	.035#			+9.9	9.6
	Total			26.3	27.6
4045	1.000			22.7	23.3
	.600			23.9	24.5
	.035#			+6.4	+6.7
	Total			30.3	31.2

* Open circuit rest.

\# Resistive discharge overnight.

- Additional amounts of charge could be removed at subsequent resistive discharges at low currents and cell voltages.

- The loss of discharge capacity and the distortion in the voltage curves could be overcome by a rejuvenation process.

- The presence of LiOH as an additive in the electrolytes of two cells could not prevent the occurrence of memory, but definitely had beneficial effects with regard to voltages and capacities.

- In the course of repetitive cycling, however, the presence of that additive did not produce any visible effects.

d. Cycle Testing of New 20 Ah Cells-Low Earth Orbiting

As mentioned before, this group of eight cells was on the same cycling regime as the preceding group, only about 2,000 cycles behind. At the end of the testing period, they had acquired 1,952 of such cycles without any interruption in the course of about five months.

At about weekly intervals, cell voltages and pressures were measured and recorded. The pertinent data are presented in the following tables:

Table 31:	End of Charge Voltages	EOCV
Table 32:	End of Discharge Voltages	EODV
Table 33:	End of Charge Pressures	EOCP
Table 34:	End of Discharge Pressures	EODP

A review of these data presented resulted in the following statements:

- The end of charge voltage data, EOCV, were independent of the number of cycles and reflect a normal, satisfactory performance of this cell group.

- The end of discharge voltage data, EODV, declined rapidly from their starting level of about 1.27 volt and stabilized around 1.15 volt. Occasional fluctuations did not render the cell performance unacceptable.

- The end of charge pressures, EOCP, were much lower than those observed with the old cells of nominal 20 Ah capacity operating on the same regime. Certain fluctuations occurred, but no trends were detectable.

TABLE 31

END OF CHARGE VOLTAGES, EOCV, IN mV

NEW 20 Ah CELLS, LOW EARTH ORBITING REGIME

CELL CYCLE	4	11	5	9	13	16	17	20
1	1.44	1.44	1.44	1.44	1.43	1.44	1.44	1.44
145	1.43	1.44	1.45	1.45	1.43	1.44	1.43	1.45
246	1.43	1.43	1.44	1.44	1.44	1.44	1.45	1.44
346	1.44	1.44	1.44	1.44	1.44	1.44	1.46	1.44
422	1.45	1.46	1.44	1.44	1.45	1.43	1.46	1.44
517	1.46	1.45	1.44	1.44	1.46	1.43	1.47	1.45
608	1.46	1.45	1.45	1.45	1.45	1.44	1.46	1.44
700	1.43	1.48	1.43	1.44	1.44	1.44	1.45	1.44
768	1.46	1.48	1.45	1.45	1.46	1.46	1.46	1.46
941	1.46	1.45	1.44	1.44	1.44	1.44	1.45	1.45
1015	1.45	1.44	1.45	1.45	1.45	1.45	1.44	1.45
1114	1.43	1.43	1.43	1.45	1.44	1.44	1.44	1.41
1196	1.45	1.48	1.45	1.46	1.46	1.45	1.45	1.45
1288	1.45	1.45	1.45	1.46	1.45	1.45	1.45	1.45
1450	1.45	1.45	1.45	1.45	1.45	1.45	1.44	1.44
1534	1.43	1.43	1.43	1.43	1.43	1.43	1.44	1.44
1600	1.45	1.44	1.45	1.46	1.46	1.46	1.45	1.45
1695	1.44	1.44	1.45	1.46	1.45	1.45	1.45	1.45
1786	1.45	1.45	1.49	1.52	1.46	1.46	1.44	1.44
1869	1.45	1.43	1.45	1.44	1.45	1.45	1.44	1.44
1941	1.44	1.44	1.45	1.45	1.44	1.44	1.45	1.44
1953	REM.	1.44	R	1.45	R	1.44	R	1.44

TABLE 32

END OF DISCHARGE VOLTAGES, EODV, IN mV

NEW 20 Ah CELLS, LOW EARTH ORBITING REGIME

CELL	4	11	5	9	13	16	17	20
CYCLE								
1	1.28	1.27	1.27	1.26	1.28	1.27	1.26	1.27
145	1.17	1.16	1.17	1.17	1.18	1.15	1.16	1.15
246	1.17	1.18	1.16	1.17	1.17	1.16	1.17	1.14
346	1.15	1.15	1.14	1.14	1.14	1.14	1.16	1.13
422	1.15	1.15	1.14	1.14	1.15	1.14	1.16	1.16
517	1.15	1.14	1.15	1.16	1.16	1.15	1.18	1.16
608	1.16	1.14	1.14	1.16	1.16	1.16	1.17	1.15
700	1.17	1.18	1.14	1.16	1.16	1.16	1.17	1.15
768	1.16	1.16	1.12	1.12	1.14	1.16	1.15	1.15
941	1.20	1.20	1.17	1.18	1.19	1.20	1.19	1.20
1015	1.15	1.15	1.14	1.12	1.13	1.12	1.14	1.15
1114	1.15	1.16	1.14	1.13	1.14	1.14	1.15	1.15
1196	1.14	1.17	1.14	1.13	1.15	1.13	1.15	1.14
1288	1.10	1.10	1.09	1.09	1.09	1.07	1.10	1.09
1450	1.14	1.12	1.16	1.13	1.16	1.11	1.14	1.14
1534	1.14	1.13	1.11	1.12	1.10	1.07	1.09	1.09
1600	1.04	1.06	1.03	1.02	1.20	1.06	1.08	1.07
1695	1.07	1.11	.86	1.07	1.08	1.07	1.07	1.06
1786	1.16	1.16	1.13	1.14	1.13	1.13	1.12	1.12
1809	1.14	1.16	1.15	1.15	1.15	1.15	1.15	1.16
1941	REM	1.16	R	1.15	R	1.15	R	1.15
1953	No Automatic Discharges							

TABLE 33

END OF CHARGE PRESSURES, EOCP

NEW 20 Ah CELLS, LOW EARTH ORBITING REGIME

CELL CYCLE	4	11	5	9	10	16	17	20
1	-11	-10	- 5	- 1	- 1	-10	- 1	1
145	2	5	5	2	6	5	2	7
246	0	1	3	5	3	2	5	7
346	5	2	3	6	6	1	5	3
422	0	2	0	4	3	0	5	5
517	0	3	0	4	2	0	5	5
608	0	5	0	6	6	0	5	6
700	0	1	3	5	2	2	5	7
768	0	2	0	3	1	0	4	5
941	-12	0	-10	-10	-10	-15	-10	-10
1015	-10	5	- 2	0	0	- 3	2	0
1114	-10	5	- 2	0	0	- 2	0	0
1196	- 2	5	0	2	2	0	5	5
1288	0	5	0	0	0	0	0	0
1450	0	2	0	0	5	0	5	5
1534	0	2	0	2	2	- 2	5	4
1600	0	5	2	5	4	0	5	5
1695	0	5	0	3	2	0	4	0
1786	0	5	0	2	2	0	4	0
1869	0	5	0	2	2	0	3	3
1941	0	5	0	3	2	0	4	4
1953	REM	5	R	2	R	0	R	1

Positive values in psig.
Negative values in inches of vacuum.

TABLE 34

END OF DISCHARGE PRESSURES, EODP

NEW 20 Ah CELLS, LOW EARTH ORBITING REGIME

CELL CYCLE	4	11	5	9	13	16	17	20
1	-20	-20	-20	-20	-10	-20	-20	-17
145	-20	-20	-20	-20	-10	-20	-20	-17
246	-20	-10	-20	-20	-20	-20	-20	-17
346	-22	-11	-18	-18	-21	-18	-18	-16
422	-25	- 8	-10	-20	-20	-20	-20	-20
517	-25	- 4	-25	-25	-25	-27	-25	-23
608	-20	- 5	-20	-20	-20	-25	-20	-20
700	-20	-10	-20	-20	-10	-20	-20	-17
768	-25	- 4	-25	-25	-11	-28	-25	-24
941	-20	- 5	-22	-20	-20	-25	-20	-20
1015	-20	- 2	-20	-20	-20	-25	-20	-20
1114	-20	0	-20	-20	-20	-25	-20	-20
1196	-20	- 2	-20	-20	-20	-25	-20	-20
1288	-20	- 5	-20	-20	-20	-25	-20	-20
1450	-20	0	-22	20	-20	-22	-20	-20
1534	-20	- 3	-21	-21	-20	-25	-20	-20
1600	-20	- 2	-20	-20	-20	-22	-20	-20
1695	-20	0	-20	-20	-20	-21	-20	-20
1786	-20	0	-20	-20	-20	-25	-20	-20
1869	-20	0	-20	-20	-20	-20	-20	-20
1941	REM	0	R	-20	R	-20	R	-20
1953	No Automatic Discharges							

- The end of discharge pressures, EODP, never exceeded atmospheric levels, i.e., zero readings. The repeated occurrence of vacuum readings in the -20 inch range ruled out the possibility that the low EOCP readings observed were caused by leaking cells. This statement was also corroborated by the fact that no visible signs of electrolyte escape could be detected.

All these observations indicated that the performance of the cells was normal and satisfactory in the course of the repetitive cycling regime applied.

Since all cells of this group were of the same construction, i.e., normal design with built-in reference electrode, and had an additive free KOH electrolyte of 34% by weight, the cells were arbitrarily assigned to two subgroups of four each in order to facilitate their handling during the final deep discharges and subsequent rejuvenation attempts.

Deep Discharges of the First Subgroup. The first subgroup consisting of cells 4, 5, 13, and 17, respectively, received 1,940 repetitive cycles, and at the end of charge period 1,941, was removed from the automatic cycling equipment. The cells were then discharged at the same current of 10.8 amperes used on the repetitive regime to an individual endpoint of .6 volts.

Cell #13 received an additional resistive discharge to 50 mV and was set aside for chemical analysis. Pertinent results are presented in Table 55. The remaining three cells were then kept on open circuit rest for 72 hours before being charged for 21 hours at 2.5 amperes.

At this cycle 1,942, the cells were first discharged at a current of 10.8 amperes to .6 volt and then through a resistor of two ohms, while the incremental capacity removed was measured by means of ampere-minute meters.

The capacities obtained in the course of this procedure are presented on the left side of Table 35, together with the corresponding values of the initial formation procedure. As can be seen, the cells were heavily "memorized" with respect to discharge capacity at cycle 1,941. The three-day open circuit stand did not alleviate this situation in a significant way. Where applied, the subsequent resistive discharges removed substantial amounts of additional charge from each cell, however, at voltages below one volt and at currents never in excess of 500 mA.

In Figure 15, cell voltage curves for typical formation behavior and the two final cycles are presented for cell #4. For the latter ones, tracings of the individual electrode potentials are also

TABLE 35

DISCHARGE CAPACITIES IN Ah, NEW 20 Ah CELLS

LOW EARTH ORBITING REGIME

CELL		4	5	13	17		11	1	16	20
CYCLE	END POINT									
FORMATION	1.000	25.3	25.3	25.3	25.2	FORMATION	25.5	25.7	25.8	25.2
1941	1.000	8.4	7.9	9.4	9.9	1953	8.7	8.3	8.5	9.8
	.600	11.3	9.6	11.8	12.0		11.6	10.3	10.7	12.2
	.000	-	-	-	-		12.4	11.1	11.5	13.0
	Resistor	-	-	+8.5	-		+5.4	+8.7	+9.2	+8.4
	Total	11.3	9.6	20.3	12.0		17.8	19.8	20.7	21.4
1942	1.000	14.2	12.0	A	13.0	1954	20.2	21.1	A	20.8
	.600	15.5	13.3		14.1		20.8	21.8		21.3
	Resistor	+7.7	+7.4		+6.5		+4.2	+4.8		+5.6
	Total	23.2	20.7		20.6		25.0	26.6		26.9

A = Analyzed

DEEP DISCHARGE VOLTAGE VERSUS TIME CURVES
20 AH CELL NO. 4 LOW EARTH ORBIT REGIME

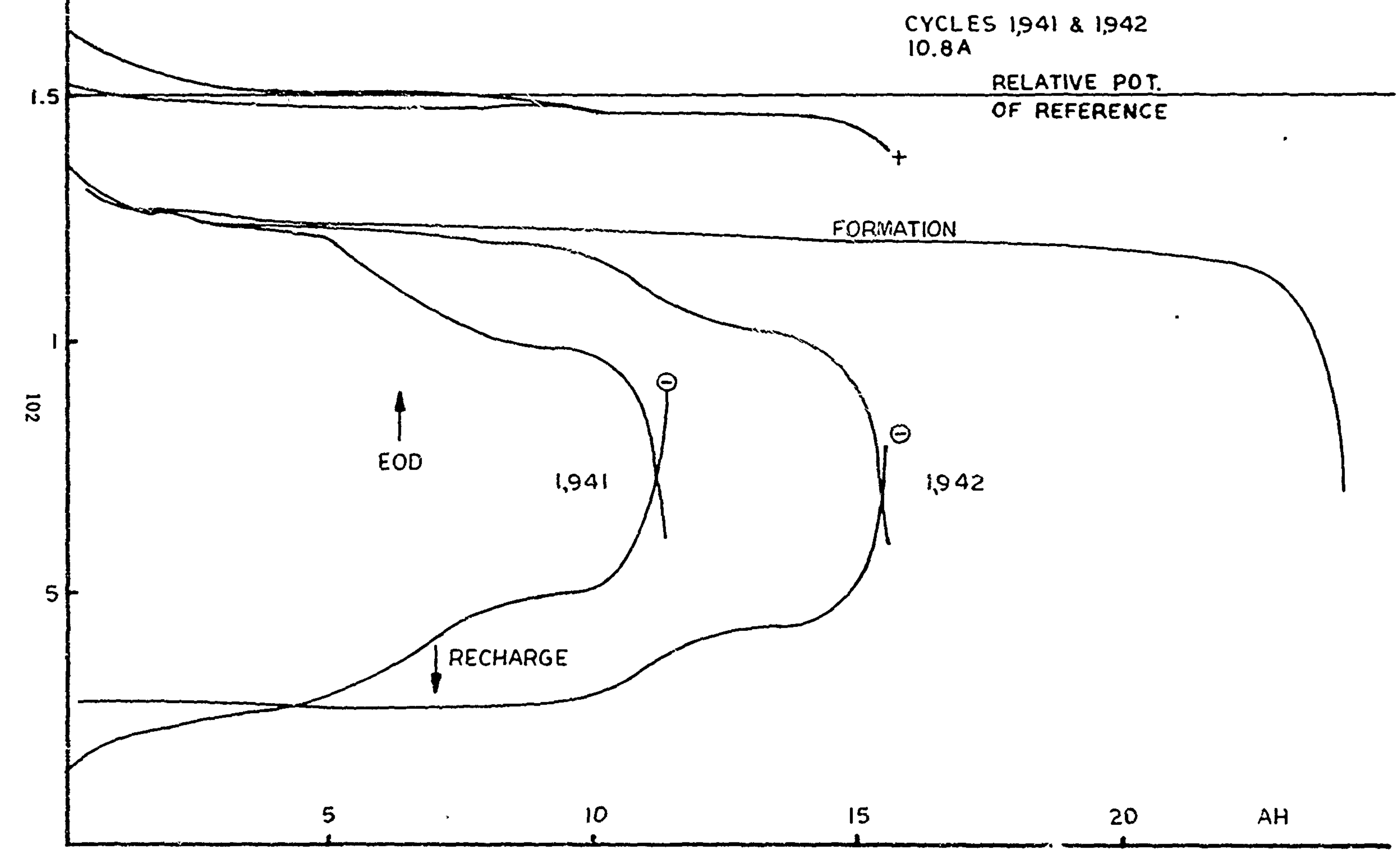

FIGURE 15

included. The curves are also representative for cell #13 at cycle 1,941 and for cell #17 for both final cycles.

Two things are obvious:

- The cells are negative electrode discharge-limiting on deep discharge.

- The distortion in the shape of the cell voltage curves were caused by the negative electrodes.

In Figure 16, the situation for cell #5 is presented.

At cycle 1,941, both electrode potentials deviated from normal behavior and decreased almost continuously. Consequently, there was no voltage plateau in the one volt range as observed with the other three cells of this subgroup.

The three day open circuit stand straightened out the positive electrode potential curve in the truest sense of the word so that the influence of this electrode on the decay of the cell voltage was less on cycle 1,942.

Deep Discharges of the Second Subgroup. Since a prolonged stand on open circuit failed to restore the initial capacity levels and to eliminate voltage distortions, the second subgroup was submitted to a different final treatment as follows:

The cells were removed from the automatic cycler at the end of charge period 1,953 and then manually deep discharged at 10.8 amperes to zero volt. Care was taken not to drive the cell voltage into reverse. Individual discharges by resistor followed while the additional amounts of charge removed were monitored again by means of ampere-minute meters. This discharge was conducted over a weekend, i.e., in 60+ hours. Cell #16 was then prepared for chemical analysis. For results see Table 56.

The other cells were then kept on open circuit for about 8 hours before being recharged on cycle 1,954 at 2.5 amperes for 21 hours. This was then followed by a final discharge at 10.8 amperes to .6 volt and a supplemental resistive discharge over a 24 hour period. Pertinent capacity values obtained are presented on the right side of Table 35.

The results for the first deep discharge are largely identical with those of the first subgroup, and the continuation of the discharge to zero produced only insignificant amounts of capacity at the current of 10.8 amperes.

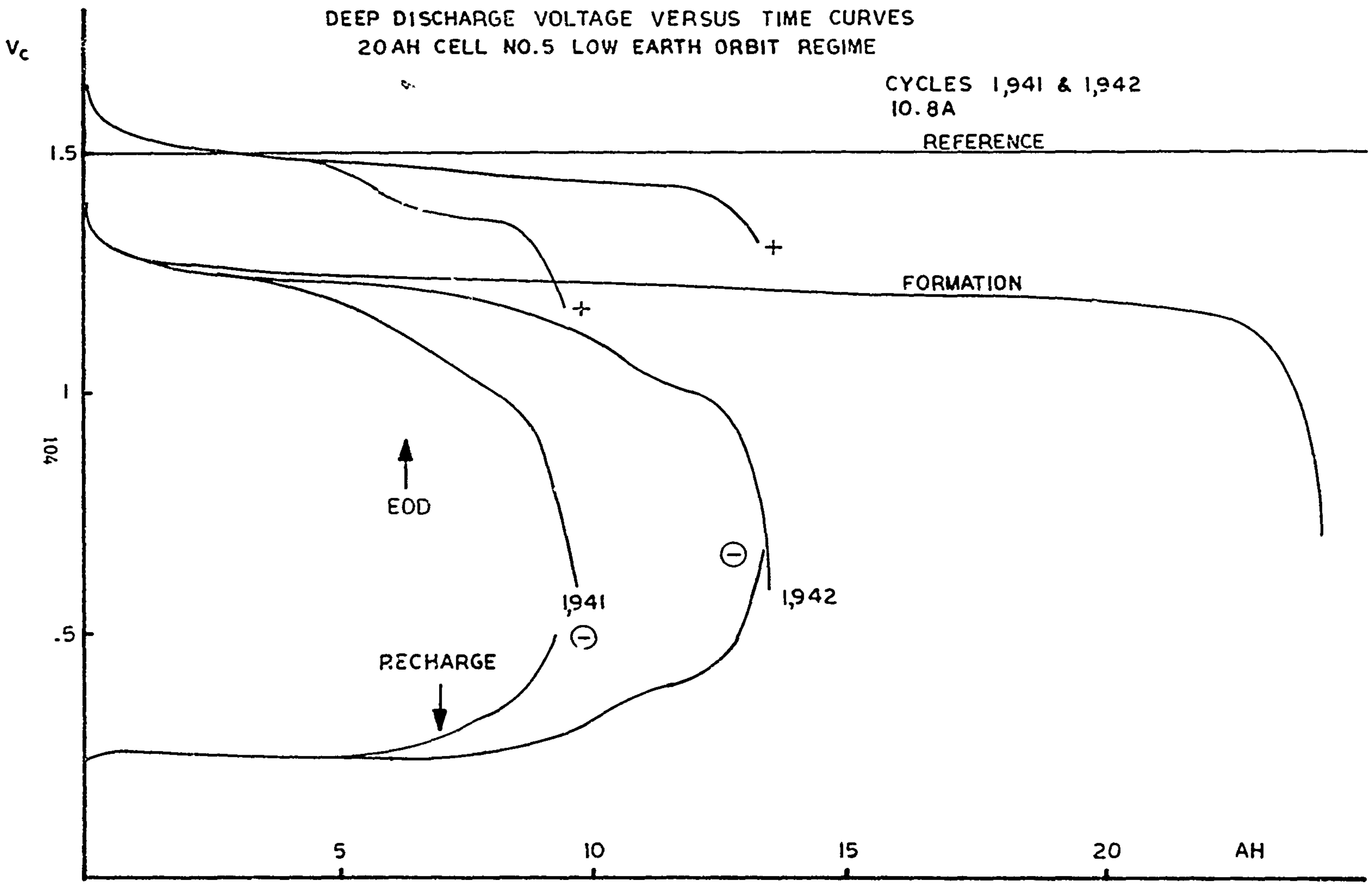
DEEP DISCHARGE VOLTAGE VERSUS TIME CURVES
20AH CELL NO.5 LOW EARTH ORBIT REGIME
CYCLES 1,941 & 1,942
10.8A
V_c
1.5
1
.5
REFERENCE
FORMATION
+
+
EOD
RECHARGE
1,941
1,942
5
10
15
20
AH

FIGURE 16

The subsequent low current discharge obviously was rather beneficial on the capacity performance on cycle 1,954 when values were obtained which are comparable to formation values.

In Figure 17, voltage and potential versus time curves are presented for cell #20 covering formation and final deep discharge. They also pertain to the performance of cells #11 and #16, respectively.

At cycle 1,953, we here observed severe changes in voltage and negative potential curves and also some contributions from the positives to the unsatisfactory cell performance. The treatment following this cycle, and as described above, restored the initial shapes of the curve; however, the cells were still negative electrode discharge-limiting.

Figure 18 shows the performance for cell #9 which is slightly different at cycle 1,954. Capacity and voltage curve shapes are restored to almost normal levels, but the end of discharge is caused by potential breaks of both electrodes, perhaps with an even larger contribution from the positive.

<u>Summary of Results.</u> Pertinent observations were:

- The cells performed flawlessly under the experimental conditions of the cycling regime.
- Deep discharges beyond the point of normal end of discharge revealed the presence of "memory".
- The cells were negative electrode discharge-limiting at the 10.8 amperes discharge current applied.
- The distortions in voltage curves and the loss of capacity are temporary and can be overcome by suitable measures.
- Low current discharge over several days appears to be an effective rejuvenation procedure.
- In the course of this procedure the cells become positive discharge-limiting.

e. <u>Cycle Testing of New 20 Ah Cells, Five-Hour Rate Regime</u>

This group also consisted of eight cells. After a complete charge at two amperes for 16 hours, they were put on the following cycle regime:

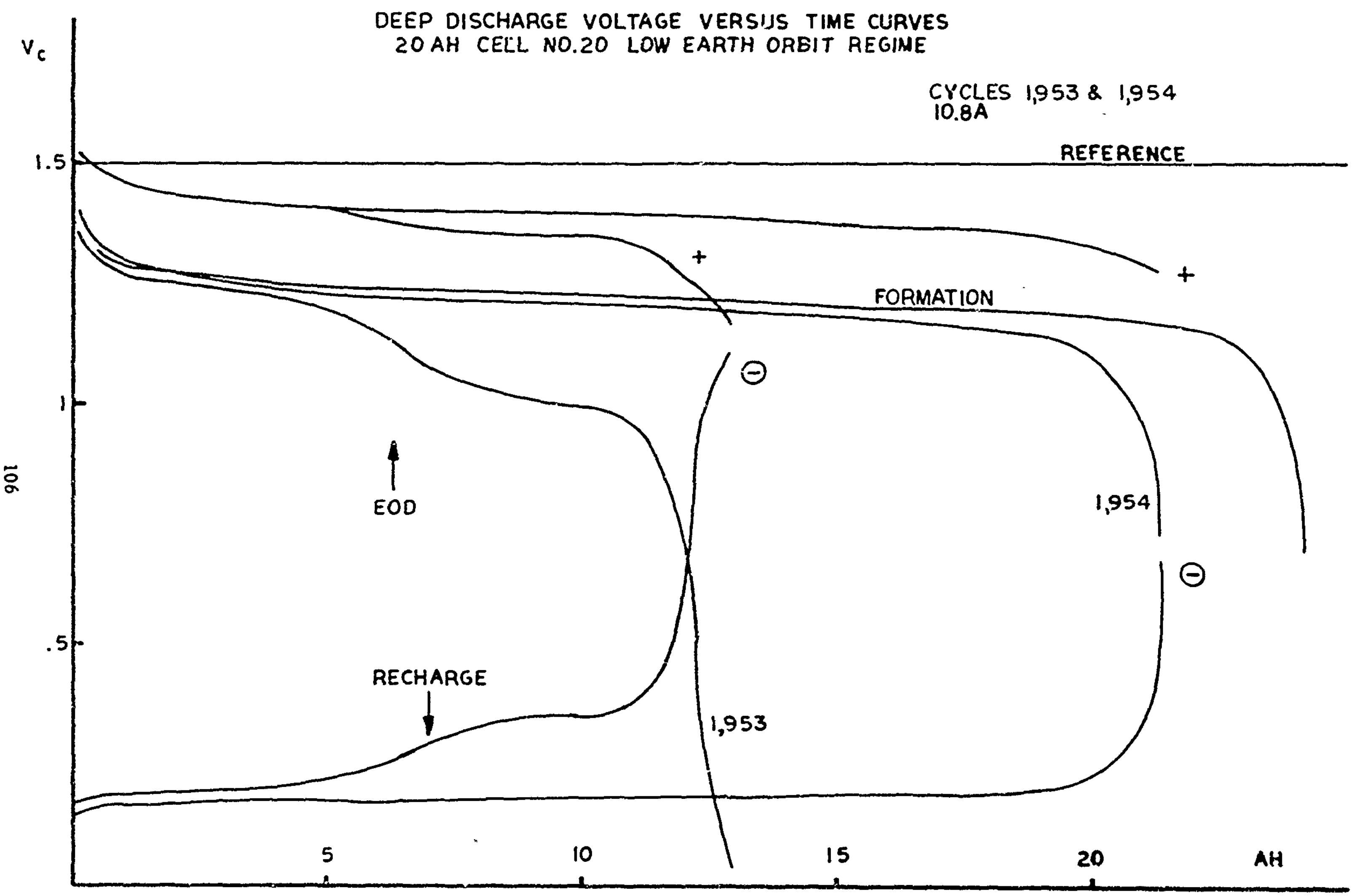
DEEP DISCHARGE VOLTAGE VERSUS TIME CURVES
20 AH CELL NO.20 LOW EARTH ORBIT REGIME
CYCLES 1,953 & 1,954
10.8A
V_c
1.5
1
.5
REFERENCE
FORMATION
+
+
⊖
⊖
EOD
RECHARGE
1,953
1,954
5
10
15
20
AH

FIGURE 17

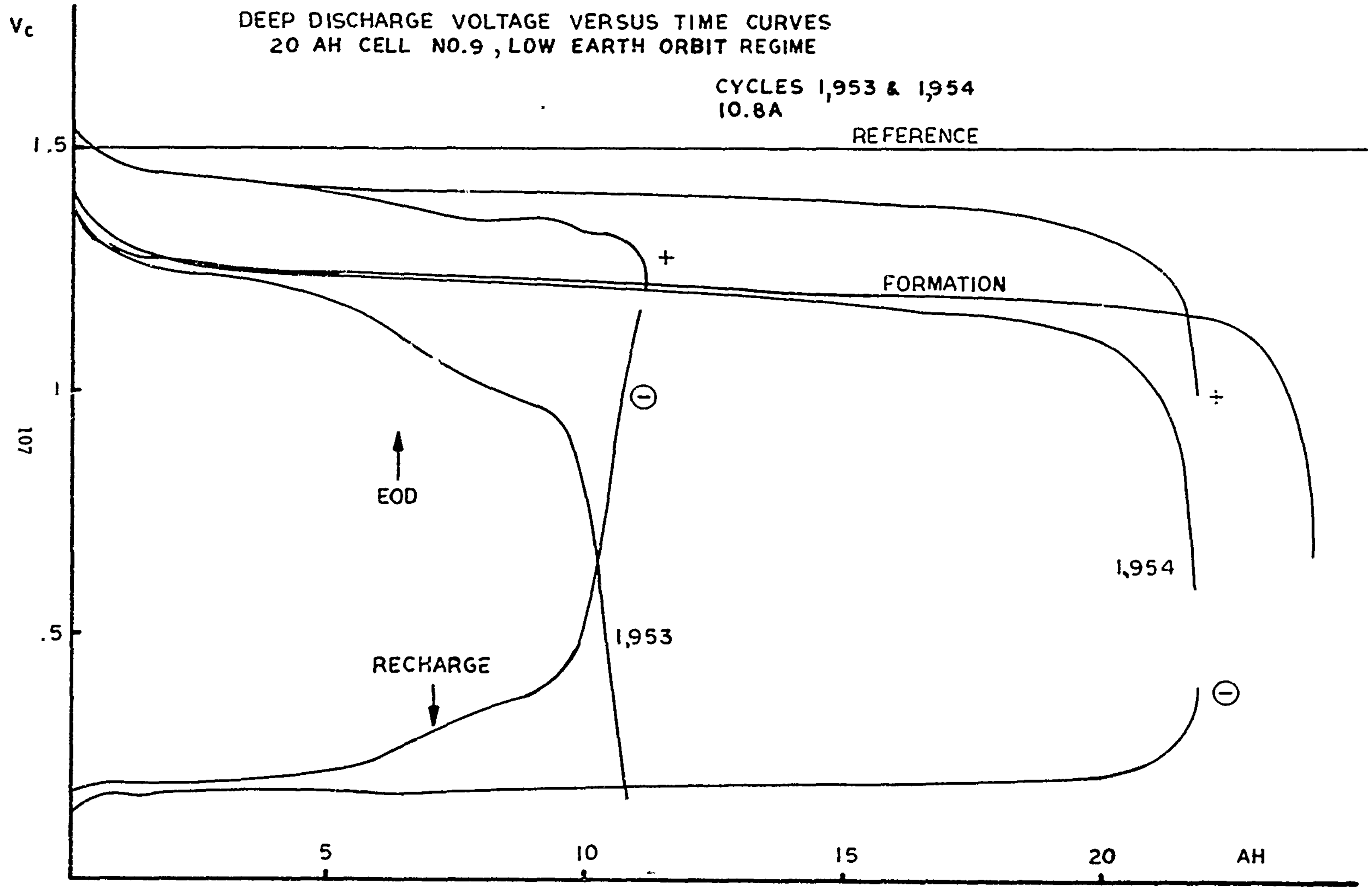
DEEP DISCHARGE VOLTAGE VERSUS TIME CURVES
20 AH CELL NO.9 , LOW EARTH ORBIT REGIME
CYCLES 1,953 & 1,954
10.8A
REFERENCE
FORMATION
V_c
1.5
1
.5
5
10
15
20
AH
+
EOD
RECHARGE
1,953
1,954

FIGURE 18

Discharge at 4 amperes for 2.3 hours = 9.2 Ah

Charge at 4 amperes for 3.2 hours = 12.8 Ah

At about cycle 72, the length of the discharge/charge periods was changed to 2.5 hours and 3.0 hours, respectively, thus providing a realistic overcharge factor of 1.20 at a depth of discharge of 50% based upon a nominal cell capacity of 20 Ah.

Right from the beginning it was planned to interrupt the repetitive cycling at about cycle 200 with a series of deep discharges for capacity determination. Afterwards, the cells were to be returned to their former regime for another series of repetitive cycles.*

In the course of both repetitive cycling phases, cell voltages and pressures were monitored on a regular basis. The accumulated data are presented in the following tables:

Table 36:	End of Charge Voltages	EOCV
Table 37:	End of Discharge Voltages	EODV
Table 38:	End of Charge Pressures	EOCP
Table 39:	End of Discharge Pressures	EODP

A review of these data had the following results:

- The end of charge voltages, EOCV, were unaffected by the number of cycles acquired.
- The end of discharge voltages, EODV, decayed with time, and at the end of the first series of repetitive cycles were slightly below 1.10 volt.
- In the second series of cycles, these voltages appeared to be unaffected by time, and generally fluctuated in the 1.12 to 1.20 volt range.
- The end of charge pressures, EOCP, were very low. However, as with the preceding group, there were no indications of leaking.
- The vacuum readings for the end of discharge pressures, EODP, corroborated the fact that the cells indeed did not leak.

---

* A similar approach had been undertaken in the previous year with C_S-type cells as test vehicles. See, for instance, Second Annual Report, page 74.

TABLE 36

END OF CHARGE VOLTAGES, EOCV, IN mV

NEW 20 Ah CELLS, FIVE-HOUR RATE REGIME

CELL CYCLE	3	7	19	18	15	8	10	12
1	1.43	1.44	1.44	1.44	1.44	1.44	1.44	1.44
72	1.40	1.40	1.41	1.40	1.41	1.41	1.41	1.40
85	1.40	1.41	1.41	1.41	1.40	1.41	1.41	1.41
117	1.42	1.42	1.42	1.42	1.41	1.42	1.42	1.43
151	1.41	1.42	1.42	1.42	1.42	1.41	1.42	1.43
182	1.42	1.43	1.41	1.42	1.41	1.41	1.42	1.43
213 *	1.42	1.43	1.42	1.43	1.42	1.40	1.42	1.43
214 *	1.42	1.42	1.42	1.41	1.42	1.42	1.42	1.41
252	1.41	1.41	1.42	1.41	1.42	1.42	1.42	1.42
320	1.41	1.42	1.41	1.42	1.41	1.42	1.41	1.42
351	1.42	1.43	1.43	1.43	1.43	1.43	1.42	1.43
402	1.33	1.34	1.30	1.34	1.34	1.34	1.34	1.34
404	1.43	1.44	1.44	1.44	1.44	1.43	1.44	1.44
416	1.44	1.44	1.44	1.44	1.44	1.44	1.44	1.44
438	1.44	1.44	1.44	1.44	1.44	1.44	1.44	1.44
460	1.43	1.44	1.44	1.43	1.44	1.44	1.44	1.43
469	1.43	1.43	1.44	1.43	1.44	1.43	1.43	REM
509	1.43	1.44	1.44	1.44	1.44	1.44	REM	
539	1.43	1.43	1.43	1.43	1.43	REM		
565	1.43	1.43	1.43	1.43	1.43			
596	1.43	1.43	1.43	1.43	REM			
631	1.43	1.43	REM	REM				
648	1.43	REM						

TABLE 37

END OF DISCHARGE VOLTAGES, EODV, IN mV

NEW 20 Ah CELLS, FIVE-HOUR RATE REGIME

CELL	3	7	19	18	15	8	10	12
CYCLE								
1	1.24	1.25	1.24	1.25	1.26	1.25	1.25	1.24
72	1.19	1.20	1.19	1.19	1.19	1.19	1.19	1.19
85	1.15	1.16	1.16	1.15	1.15	1.15	1.15	1.15
117	1.14	1.15	1.15	1.14	1.14	1.14	1.15	1.15
151	1.14	1.14	1.15	1.14	1.14	1.15	1.14	1.14
182	1.14	1.14	1.16	1.14	1.15	1.14	1.14	1.15
213 *	1.08	1.10	1.09	1.09	1.08	-	1.07	1.09
214 *	1.24	1.25	1.24	1.25	1.25	1.25	1.25	1.25
252	1.15	1.15	1.17	1.15	1.15	1.16	1.17	1.17
320	1.18	1.17	1.19	1.16	1.19	1.16	1.18	1.17
351	1.17	1.16	1.13	1.18	1.14	1.17	1.16	1.14
402	1.15	1.14	1.12	1.17	1.12	1.15	1.13	1.11
404	1.22	1.22	1.20	1.21	1.22	1.22	1.22	1.22
416	1.20	1.21	1.21	1.20	1.20	1.20	1.21	1.21
438	1.21	1.22	1.22	1.22	1.22	1.22	1.22	1.22
460	1.18	1.19	1.19	1.18	1.18	1.18	1.18	1.18
469	No Readings							REM
509	1.21	1.22	1.22	1.22	1.21	1.21	REM	
539	1.12	1.12	1.13	1.12	1.11	REM		
565	1.21	1.21	1.20	1.20	1.20			
596	1.19	1.17	REM	REM	REM			
631	1.16	1.16						

TABLE 38

END OF CHARGE PRESSURES, EOCP

NEW 20 Ah.CELLS, FIVE-HOUR RATE REGIME

CELL / CYCLE	3	7	19	18	15	8	10	12
1	1	0	- 1	-13	- 1	- 1	- 5	- 1
72	3	6	2	2	5	2	5	6
85	3	4	1	1	5	3	5	5
117	5	5	2	3	6	5	3	7
151	4	4	3	2	5	4	4	6
182	4	5	2	1	4	3	4	5
213 *	3	2	4	1	6	5	6	6
214 *	4	0	5	0	5	5	11	6
252	-1	-3	0	- 3	0	- 3	- 2	- 2
320	0	-1	1	- 5	0	- 5	0	- 2
351	0	0	- 1	0	1	0	- 3	0
402	10	15	20	17	10	15	15	5
404	1	0	4	0	0	0	5	0
416	0	0	0	- 3	0	- 1	2	0
438	0	0	0	- 5	0	0	0	0
460	0	-3	- 5	0	0	- 2	0	- 1
469	0	0	0	- 2	0	- 1	0	REM
509	0	0	0	- 2	0	0	REM	
539	1	0	0	- 2	0	REM		
565	0	0	0	- 2	0			
596	2	0	0	- 2	REM			
631	0	0	REM	REM				
648	3	REM						

Positive values psig.
Negative values inches of vacuum.

TABLE 39

END OF DISCHARGES PRESSURES, EODP

NEW 20 Ah CELLS, FIVE-HOUR RATE REGIME

CELL	3	7	19	18	15	8	10	12
CYCLE								
1	-26	-27	-27	-25	-28	-27	-28	-26
72	-25	-28	-28	-25	-28	-28	-28	-28
85	-26	-26	-26	-24	-26	-26	-25	-25
117	-25	-25	-24	-24	-25	-23	-26	-23
151	-25	-24	-24	-23	-25	-22	-25	-24
182	-25	-25	-25	-24	-25	-23	-26	-25
213 *	-23	-24	-25	-24	-24	-24	-25	-24
214 *	-22	-28	-26	-26	-26	-23	-24	-27
252	-26	-25	-25	-26	-25	-24	-22	-27
320	-25	-20	-20	-20	-20	-19	-20	-20
351	-20	-20	-20	-20	-20	-20	-20	-20
402	- 5	- 3	- 1	- 5	- 8	- 6	- 3	- 1
404	- 7	-10	- 3	-10	- 5	-10	- 4	-20
416	-20	-20	-18	-20	-20	-20	- 8	-20
438	-20	-20	-20	-20	-20	-20	-20	-20
460	-20	-20	-20	-20	-20	-20	-20	-20
469	No Readings							REM
509	-20	-20	-20	-20	-20	-20	REM	
539	-20	-20	-20	-20	-20	REM		
565	-20	-20	-20	-20	-20			
596	-22	-20	REM	REM	REM			
631	-20	-20	REM					
648	No Automatic Discharges							

Positive values psig.
Negative values inches of vacuum.

All these observations permit the conclusion that the cells performed flawlessly under the experimental conditions of this particular repetitive cycling regime.

As initially planned, the repetitive regime was interrupted at cycle 213* by means of continuing the discharge period beyond its normal endpoint of 10 Ah removed. A typical discharge voltage versus time curve for this event is presented in Figure 19.

The normal end of discharge at 10 Ah removed is marked by a vertical arrow. The shape of the curve to the left of this mark is typical for all preceding cycles. To the right, the "knee" is not immediately continued, but replaced by a kind of plateau slightly above 1.0 volt. At this level, between 2 and 4 additional ampere hours were discharged from individual cells before the cell voltages steeply dropped.

Since this change in curve shape occurred very close to the normal end of discharge, and the additionally obtained capacity was rather small in comparison to the nominal cell capacity, we undoubtedly had, ultimately, encountered the phenomenon of "memory". Unfortunately, however, the built-in reference electrode of each cell was not used to determine which electrode was responsible for this effect.

A rejuvenation procedure consisting of an overnight external shorting by a one ohm resistor, and a subsequent charge for 16 hours at the nominal ten-hour rate of two amperes, restored the cell capacities. A typical discharge curve for cycle 214 is also presented in Figure 19.

In Table 40, discharge capacities for some selected cycles are presented together with average values and standard deviations in per cent. At the end of formation, an average of 25.4 Ah was obtained with a sigma limit of 1.2%. At cycle 213*, this term dropped to 12.5 Ah with a standard deviation of 5.2%.# The rejuvenation brought back the average to almost its initial value, 23.3 Ah, and reduced the standard deviation to 1.5%.

This table also contains the corresponding capacities obtained at the final discharges which were performed after a second series of repetitive cycles. As can be seen, all final capacities were affected again by the conditions of the preceding cycling period, thus signaling the reappearance of memory.

The discharge capacity of cell 8 is not included in this calculation. In preparation for the manual discharge, this cell obviously was partially discharged.

DEEP DISCHARGE VOLTAGE VERSUS TIME CURVES
TYPICAL 20AH CELLS ON FIVE HOUR RATE REGIME

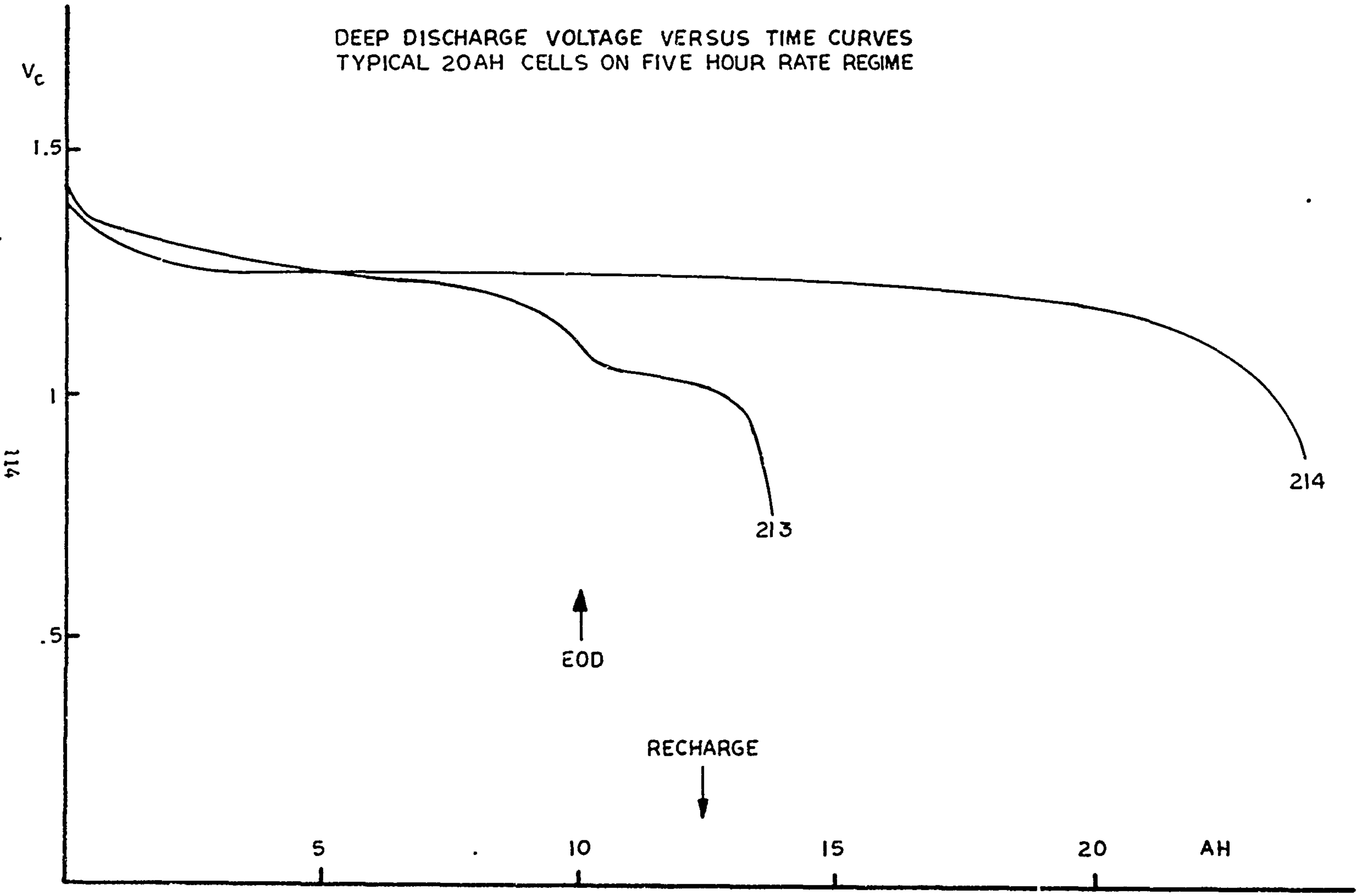

FIGURE 19

TABLE 40

VARIOUS DEEP DISCHARGE CAPACITIES, Ah

NEW 20 Ah CELLS, FIVE-HOUR RATE REGIME

CELL CYCLE	3	7	19	18	15	8	10	12	AVG.	% σ
FORMATION 1V	25.0	25.3	25.0	25.0	25.8	25.3	25.5	25.7	25.4	1.2
213	12.4	11.9	13.7	11.6	12.3	(4.9)	12.9	12.9	12.5	5.2
214	22.6	23.1	23.5	23.2	23.6	23.4	23.6	23.7	23.3	1.5
Final	N.D.	12.5	17.6*	13.2	N.D.	16.6	16.9*	15.2		
Rejuvenation		22.7	24.7	23.8		-		-		

*Resistive discharge included.

f. Performance of Individual Cells.

In order to investigate the causes for this phenomenon, and, if possible, to come up with a remedy, the individual cells received final treatments under a variety of conditions.

The results and observations were as follows:

Cell #12 was the first cycled cell finally being deep discharged after a total of 468 cycles. In Figure 20, the discharge curve for this cycle is presented together with the reference electrode readings for both positive and negative electrodes.

As can be seen, the cell was clearly positive electrode discharge-limiting and provided only 15.2 Ah to .6 volt at a current of four amperes.

The normal end of discharge, EOD, at 10 Ah, i.e., 2.5 hours at four amperes, is marked by an arrow. We observed slightly to the left of this mark a peculiar change in the shape of the voltage curve. This was caused by a change in the negative electrode potential by about 150 mV towards more positive values. When this step was over in the 12 Ah region, the amount of charge normally returned on cycling, the further decay of the cell voltage was caused by the positive electrodes.

The cell was submitted to chemical analysis, the results of which are presented in Table 49.

Cell #10 was deep discharged to .6 volt with four amperes at cycle 509. The respective voltage and potential versus time curves are presented in Figure 21.

Both the capacity and voltage behavior were similar with those observed at cell #12 discharges, and this indicates that the phenomenon is not an incidental one, but the manifestation of a real thing.

In order to determine whether or not there was any dischargeable material left in the cell, the cell was externally shorted by a two ohm resistor and the additional charge removed was measured by means of an ampere-minute meter.

In this manner, about three additional ampere hours could be removed, however, at currents and voltages which are far too low for any practical purposes. The cell was then prepared for chemical analysis (Table 50).

DEEP DISCHARGE VOLTAGE VERSUS TIME CURVES
20 AH CELL NO. 12, FIVE HOUR RATE REGIME

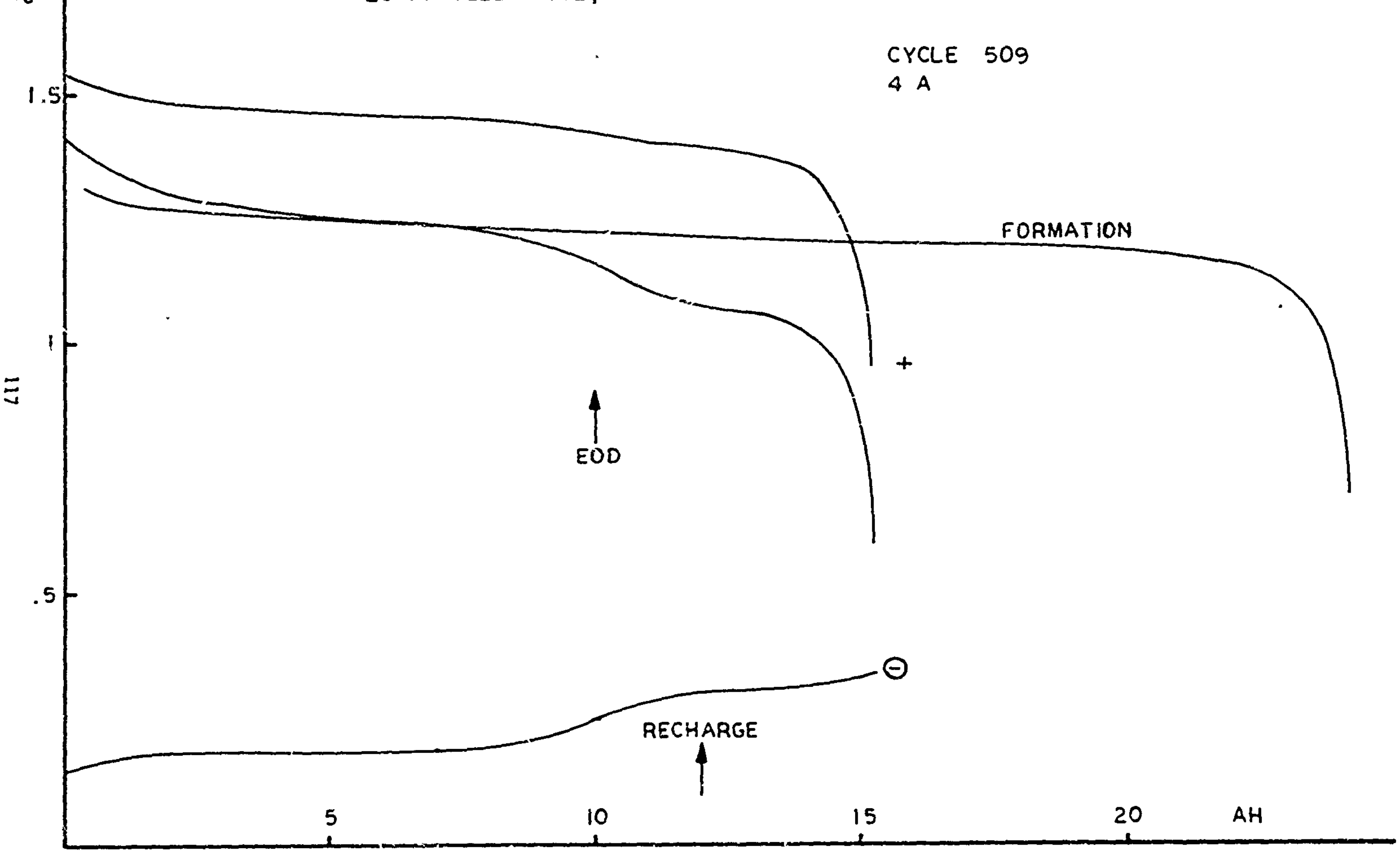

FIGURE 20

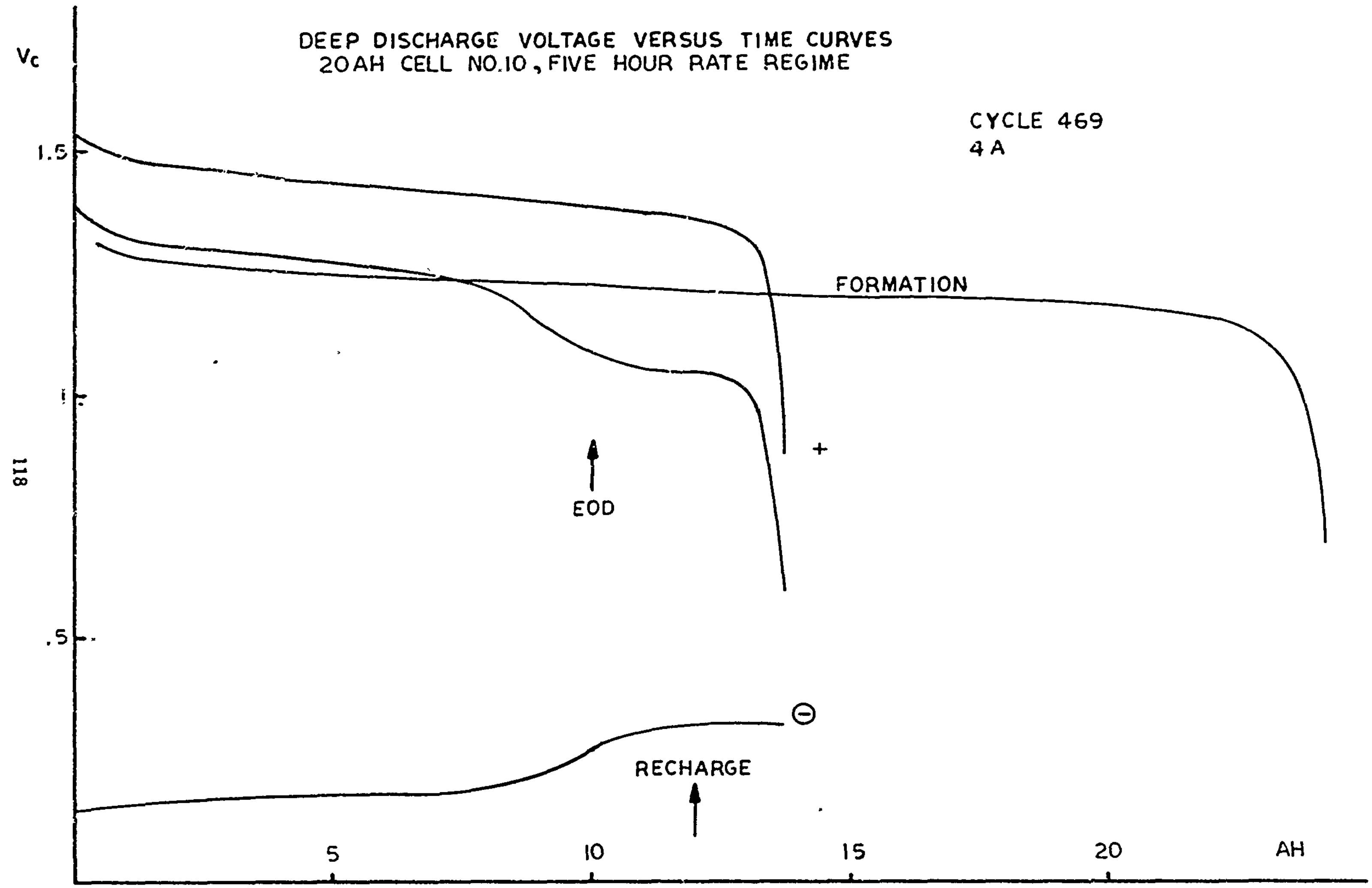
DEEP DISCHARGE VOLTAGE VERSUS TIME CURVES
20AH CELL NO.10, FIVE HOUR RATE REGIME
CYCLE 469
4 A
Vc
1.5
1
.5
FORMATION
EOD
+
⊖
RECHARGE
5
10
15
20
AH
FIGURE 21

Cycled cell #8 was finally deep discharged to .6 volt with four amperes at cycle 534. However, in an attempt to overcome the "memory", the charge period of cycle 534 was doubled, so that an additional amount of 12 Ah were returned to this cell. The corresponding voltage and potential versus time curves for this cell are presented in Figure 22.

As can be seen, these curves were identical with those obtained from the preceding cells, and the capacity delivered to .6 volt was only 16.6 Ah. In other words, the additional 12 Ah charge input increased this term only about 1.4 Ah over a comparable value of 15.2 Ah obtained for cell #12 under similar test conditions.

The cell was then chemically analyzed. The corresponding results are presented in Table 51.

Cell #15 was not discharged, but at the end of charge period 584 was immediately prepared for the chemical analysis. This was done in order to investigate the electrode composition in a "fully" charged state.

Cycled cell #18 was deep discharged at cycle 596 with all indications of memory, i.e., discharge capacity only 13.2 Ah and heavily distorted voltage and potential versus time curves, as indicated in Figure 23.

As a possible remedy for the "memory" phenomenon, the cell was left on open circuit for 69 hours and then recharged for 21 hours at 2.5 amperes. A subsequent discharge at four amperes resulted in 23.8 Ah to .6 volt, i.e., an almost complete restoration of capacity to the 25.0 Ah value at formation.

The voltage curve to about 18 Ah looks normal; 1.2 volt at that point, however, then becomes depressed due to a change in the potential of the negative from here to about 21 Ah. As found on several other occasions, this change in the shape of the negative potential curve is very persistent.

The cell was then prepared for chemical analysis. Results are given in Table 52.

Cell #19 was deep discharged at cycle 596 also with all indications of memory, i.e., capacity of only 14.1 Ah and distorted voltage and potential curves, as presented in Figure 24.

A different remedy was tried by shorting the cell for 69 hours, in which an additional amount of 3.5 Ah was removed and measured by an ampere-minute meter.

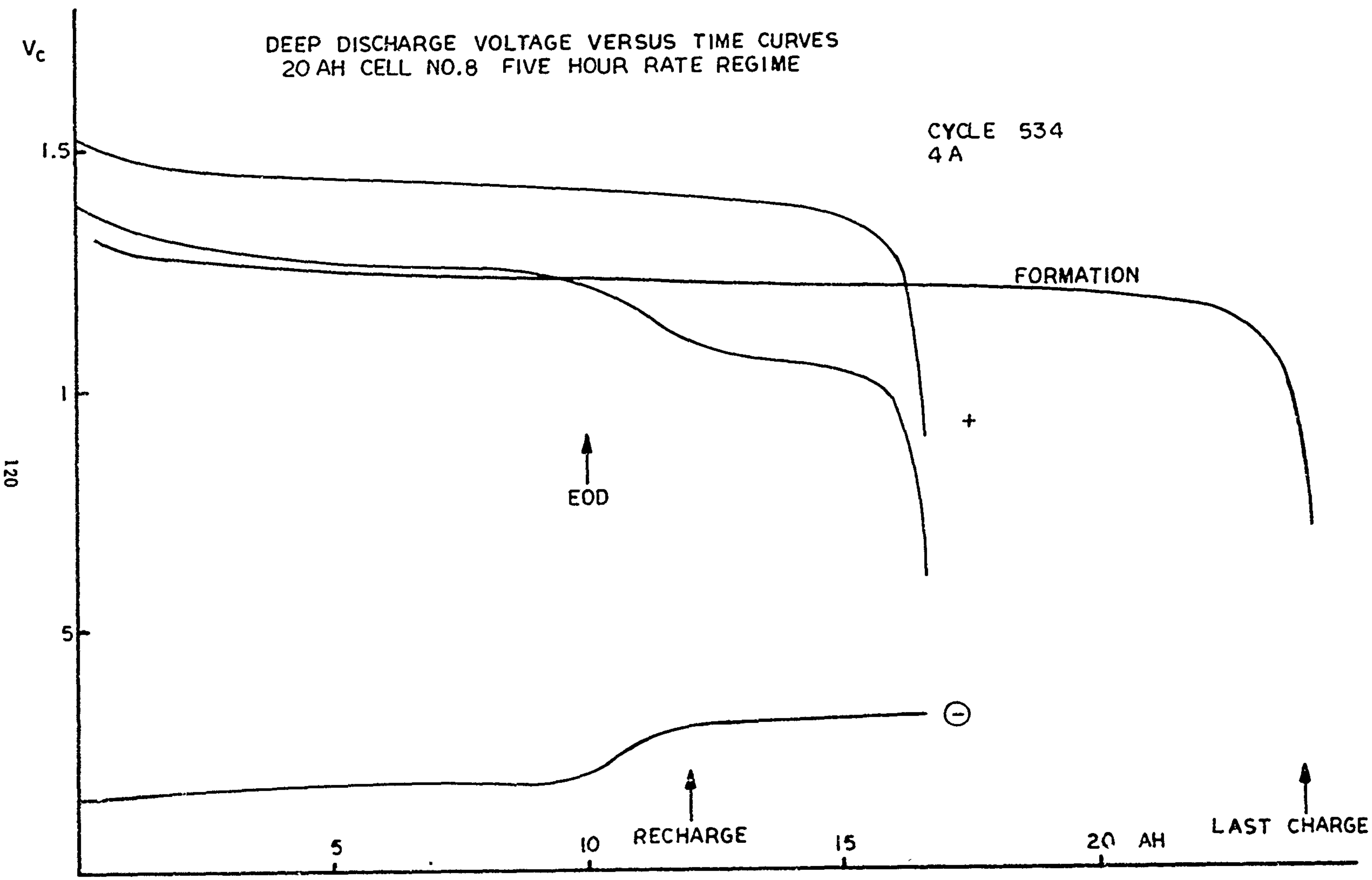
DEEP DISCHARGE VOLTAGE VERSUS TIME CURVES
20 AH CELL NO.8 FIVE HOUR RATE REGIME
CYCLE 534
4 A
V_c
1.5
1
5
FORMATION
+
EOD
⊖
RECHARGE
LAST CHARGE
5
10
15
20 AH

FIGURE 22

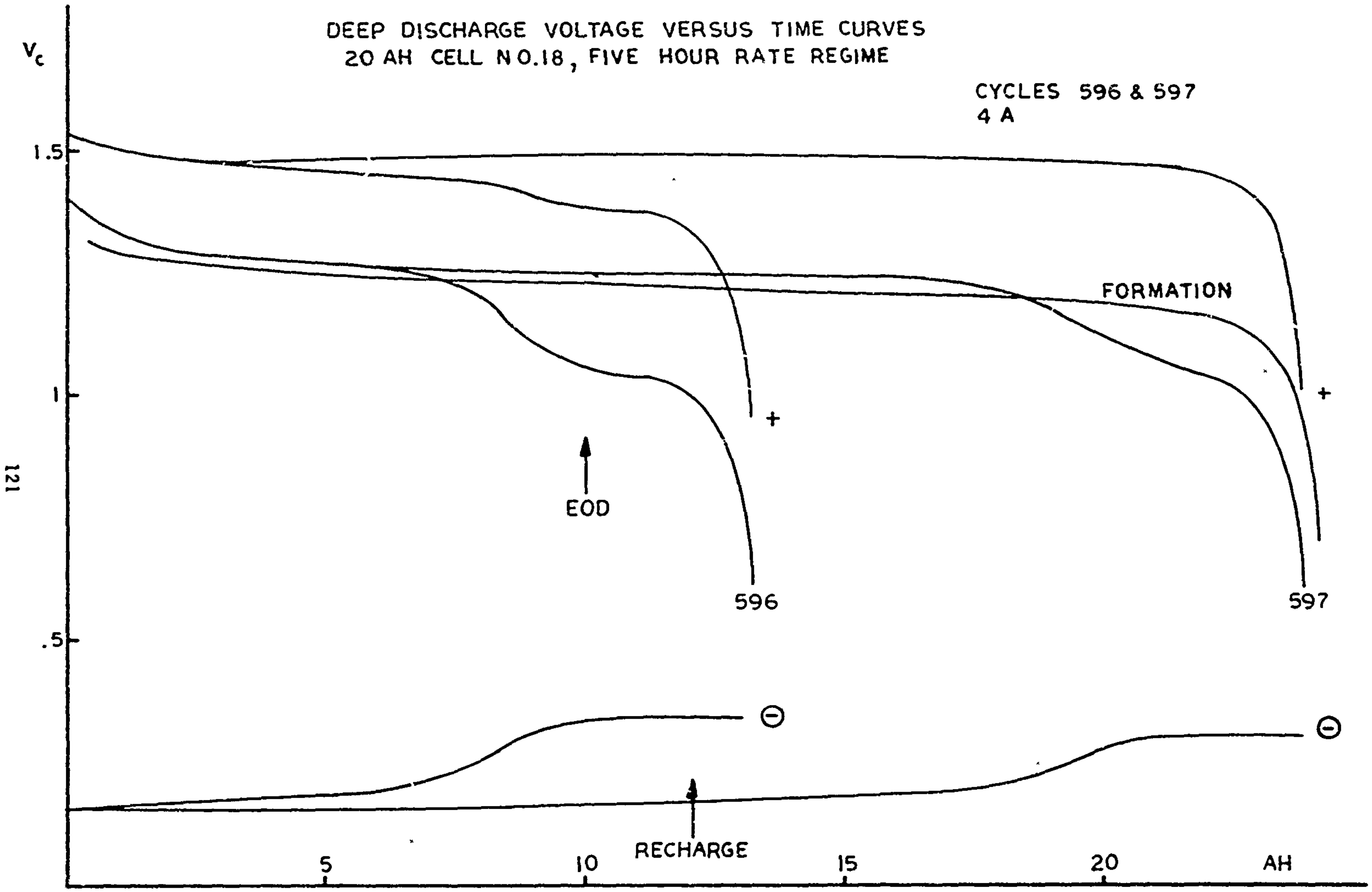
DEEP DISCHARGE VOLTAGE VERSUS TIME CURVES
20 AH CELL NO.18, FIVE HOUR RATE REGIME
CYCLES 596 & 597
4 A
V_c
1.5
1
.5
FORMATION
+
+
EOD
596
597
RECHARGE
5
10
15
20
AH

FIGURE 23

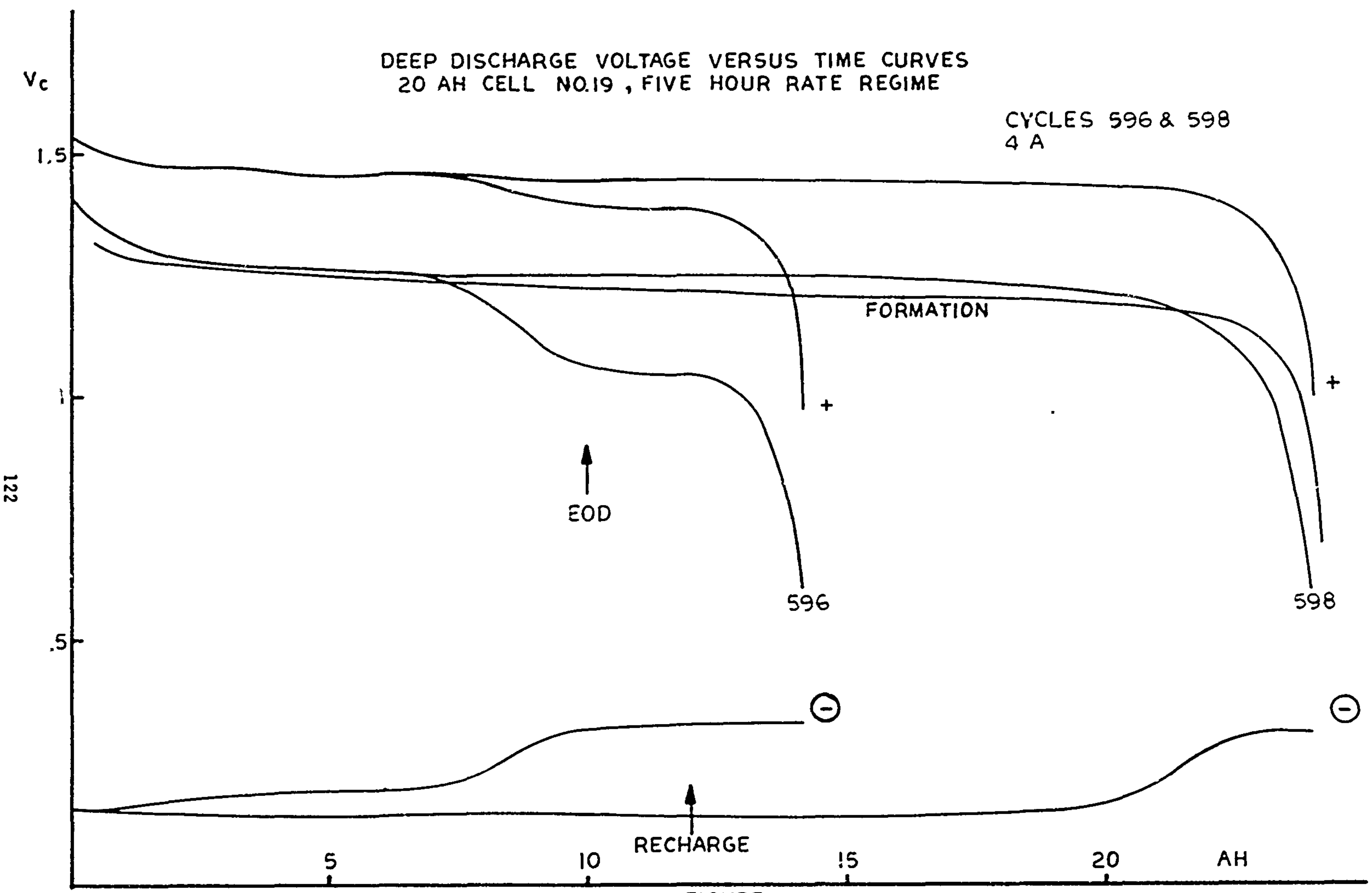
DEEP DISCHARGE VOLTAGE VERSUS TIME CURVES
20 AH CELL NO.19 , FIVE HOUR RATE REGIME
CYCLES 596 & 598
4 A
Vc
1.5
1
.5
FORMATION
EOD
RECHARGE
+
+
596
598
5
10
15
20
AH

FIGURE 24

Recharge was done at 2.5 amperes for 21 hours and a subsequent discharge at four amperes to .6 volts resulted in 24.7 Ah to that point, or an almost complete restoration of the formation capacity of 25.0 Ah. However, again the negative potential curve was distorted in the 20 - 23 Ah range.

The results are the same as obtained with cell #18, i.e., quick restoration of capacity and positive electrode potential curve, but entrenched shape changes in the negative electrode potentials.

Following another resistor discharge which produced an additional capacity of 2.8 Ah, the cell was also prepared for the chemical analysis, the results of which are presented in Table 53.

Cell #7 was removed at the end of charge period 643 and then submitted to a series of charges/discharges in attempts to get rid of the symptoms of memory.

The conditions applied were as follows:

<u>Cycle 643</u>

Charge	3 hours at 4A (automatic)
Discharge	4A to 1.0 volt
Rest	None

<u>Cycle 644</u>

Charge	20 hours at 2.5A
Discharge	4A to .6 volts
Rest	None

<u>Cycle 645</u>

Charge	20 hours at 2.5A
Discharge	4A to .6 volts
Rest	24 hours open circuit

<u>Cycle 646</u>

Charge	20 hours at 2.5A
Discharge	4A to .6 volts

The capacities obtained are presented in Table 41 together with the corresponding values for formation and previous deep discharges. At the first series of deep discharges the cell was heavily memorized, but its capacity could be restored by a 24 hour rest with a one ohm resistor across the terminals.

TABLE 41

VARIOUS DISCHARGE CAPACITIES

NEW 20 Ah CELL #7, FIVE-HOUR RATE REGIME

CYCLE	To 1.0 V	To .6 V	REMARKS
Formation	25.3	-	At 4th cycle
1-212	10.0+		Repetitive regime
213	11.0	13.0	1st deep discharge *
214	23.1	23.4	2nd deep discharge
215-642	10.0+	-	Repetitive regime
643	12.5	-	3rd deep discharge
644	20.2	21.8	4th deep discharge
645	21.3	22.5	5th deep discharge
646	21.8	22.7	6th deep discharge

* Was followed by 24 hour stand with resistor of one ohm across terminals.

As can be seen, the memory situation reoccurred in the course of the second series of repetitive cycling, and most of the capacity lost already could be restored by an immediate recharge at cycle 644. The subsequent cycles brought only marginal additional improvements, at least as far as the capacity aspect is concerned.

In Figure 25, the corresponding voltage and electrode potential curves for the last four deep discharges are presented. It is apparent that it took more than the first recharge at cycle 644 to restore these curves to their original shape. The tracing of the positive electrode regained its normal shape inmediately, while the shape changes in the negatives lingered on even during the last discharge. There were no further attempts made to correct the potential performance of those electrodes.

Cell #3 was not discharged, but at the end of charge period 648 was removed from repetitive cycling and immediately prepared for chemical analysis. This was a repetition of the experiment previously conducted with cell #15 in order to investigate the composition of fully charged cells. Pertinent results are presented in Table 54.

Summary of Results. In this chapter it was found that:

- In analogy to the two preceding groups, these eight cells performed satisfactorily under the conditions of the cycle regime applied.
- Upon deep discharge, the presence of memory was clear.
- The cells were positive electrode discharge limiting and a pronounced step in the negative electrode potential was responsible for distortions in the cell voltage curves.
- This step occurs in the vicinity of the normal end of discharge.
- Repeated charges and discharges restored capacities to formation levels and voltage curves to normal slopes.

f. Reconditioning of New 20 Ah Cells

In order to investigate the changes in the composition of the electrodes with cycling by means of chemical methods, electrode material from so-called uncycled cells had to be provided as standards. Since no really uncycled material was available, the term "uncycled" here refers to those cells which were initially formed but then stored for several months in the discharged state.

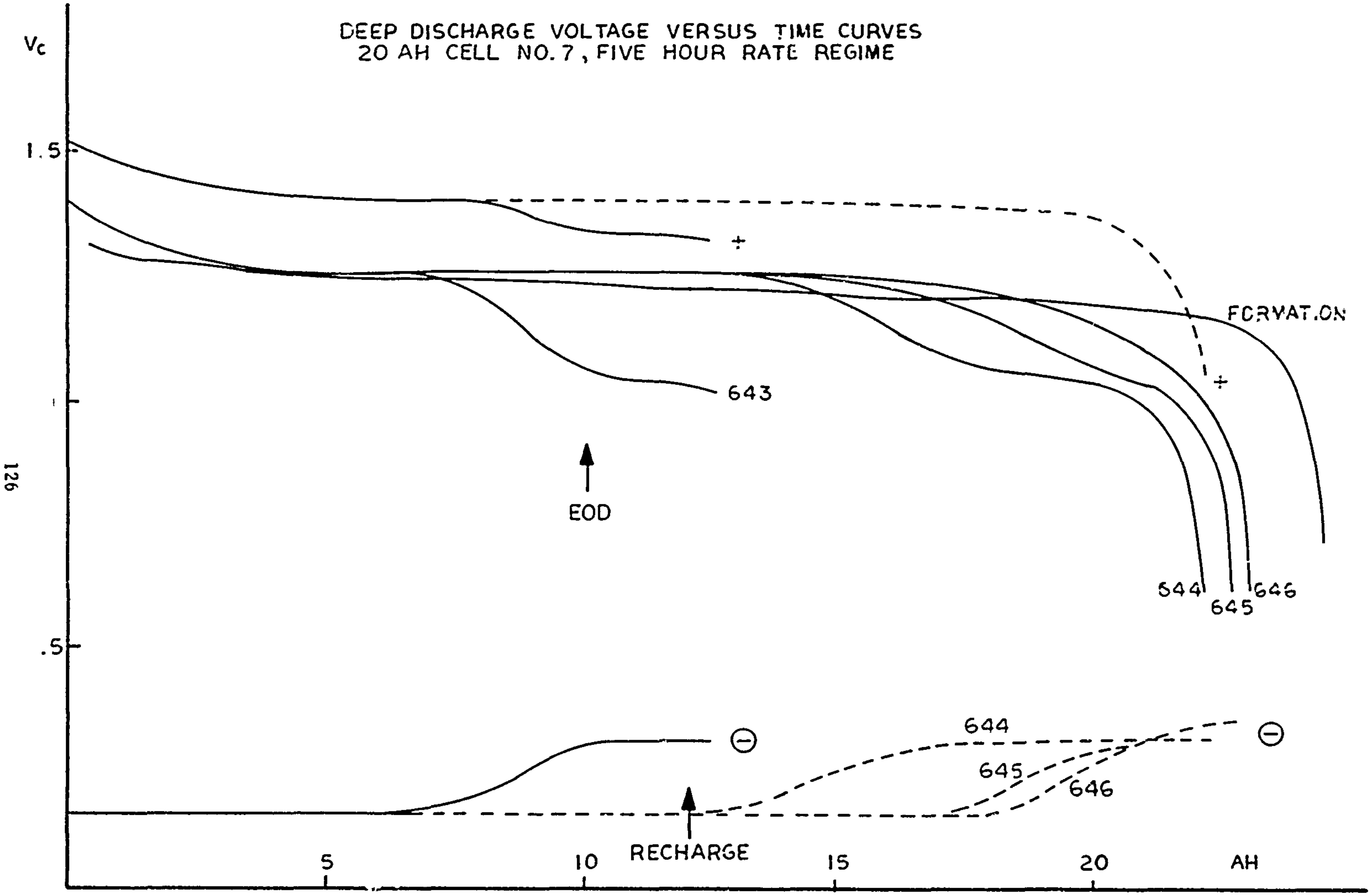

DEEP DISCHARGE VOLTAGE VERSUS TIME CURVES
20 AH CELL NO. 7, FIVE HOUR RATE REGIME

FIGURE 25

After an extended storage period like that, it is always desirable to recondition the cells to assure their proper working. This was done with the four "uncycled" cells in the following manner:

1. Cycle

Charge	40 hours at one ampere
Discharge	to one volt at ten amperes

2. Cycle

Charge	16 hours at two amperes
Discharge	to one volt at ten amperes
Shorting	with one ohm overnight

3. Cycle

Charge	20 hours at two amperes
Discharge	69 .6 volt at four amperes

The discharge capacities in Ah/cell and the corresponding end of charge pressures, EOCP, are presented in Table 42, together with the appropriate values of the fourth cycle of the initial formation.

As can be seen, all end of charge pressures were low and the capacities obtained in the course of the three reconditioning cycles were within a few per cent of the original formation values.

The plotting of the discharge voltages versus time resulted in a normal curve without any steps and inflection points. The final "knee" was sharp. This curve has been used in the corresponding figure of the preceding chapter and was there marked as "FORMATION".

The cells were found to be positive electrode discharge-limiting. For the three cells, 1, 6, and 14, respectively, this was established by means of the built-in reference electrode. The reference electrode of cell 2 did not work properly; it was later found to be shorted against the adjacent negative electrode.

In order to assure that this cell also was positive electrode discharge-limiting under the conditions applied, the discharge-limiting electrode had to be determined by means of gas analysis. For this purpose, the cell was filled with extra electrolyte and the discharge continued with gauge and valve assembly removed. 9.5 Ah were removed at 10 amperes until the cell voltage steeply dropped from -.2 volt to -1.5 volt. During the whole time, H_2 gas was evolved, indicating the positive electrode as being reversed first.

TABLE 42

DISCHARGE CAPACITIES AND END OF CHARGE PRESSURES OF RECONDITIONED CELLS

NEW 20 Ah CELLS

CYCLE	F		1		2		3	
CELL	C_1	P	C_1	P	C_1	P	$C_{.6}$	P
1	24.7	+7	24.0	-5	24.0	+5	23.9	+5
2	24.3	-1	24.2	-11	24.4	-2	24.2	0
6	24.7	-8	24.0	-11	24.4	-3	23.9	0
14	24.3	+4	23.2	-7	23.3	+1	23.2	3

Discharge capacities in Ah/cell.

Pressures: Negative values = inches of vacuum
Positive values = PSIG

Cells #6 and #2, respectively, were then prepared for the chemical analysis to serve as standards in that procedure. The results obtained are presented in Tables 47 and 48, respectively.

It is apparent that the reconditioning process applied restored the performance of the cells to that observed at the initial formation.

All cells were positive electrode discharge-limiting as indicated by either the built-in reference electrode of each cell, or by a driving of the opened cell into complete reversal and the determination of the gas evolved in the period of one-electrode reversal.

g. <u>Cycle Testing of 50 Ah Cells, Low Earth Orbit Regime</u>

Four cells of 50 Ah nominal capacity were initially built and were assigned the numbers 1, 2, 3, and 4, respectively. In combination groups of two, namely, #1 and #2, #3 and #4, they were submitted to three consecutive series of tests on the following low earth orbiting cycling regime:

Discharge	35 minutes at 27 amperes	(all 3 series)
Charge	75 minutes at 14 amperes	(series 1 & 2)
Charge	75 minutes at 15.1 amperes	(series 3 only)

Each series was preceded by a 16-hour charge period at five amperes, i.e., the nominal ten-hour rate.

<u>First Run.</u> As described in previous chapters, the cell voltages and pressures were monitored on a regular basis. In Table 43, the corresponding results for the first series are presented.

Up to cycle 902, the performance of those cells can only be termed as normal; that is to say, the end of charge voltages, EOCV, were constant, the end of discharge voltages, EODV, were stabilized in the 1.10 volt area, and both types of cell pressures were low.

Between that point in cycle life and the next monitored cycle 954, an equipment malfunction occurred. At that time, it was reasoned that, obviously undetected, an additional amount of charge must have been removed from the cells during this disturbance, and the cells were subsequently deep discharged thereafter at each cycle. The overcharge factor of 1.11 was apparently just sufficient to prevent a cell voltage reversal, but on the other hand, not large enough to restore the capacity lost.

TABLE 43

CYCLING DATA OF FIRST RUN

50 Ah CELLS, LOW EARTH ORBIT REGIME

	EOCV		EODV		EOCP		EODP	
CELL	1	2	1	2	1	2	1	2
CYCLE								
1	1.41	1.41	1.25	1.26	-18	-17	-28	-28
100	1.40	1.41	1.14	1.14	0	1	-27	-28
277	1.38	1.41	1.13	1.13	2	6	-26	-26
380	1.42	1.41	1.14	1.13	3	2	-20	-20
476	1.42	1.41	1.13	1.14	0	1	-18	-20
578	1.42	1.41	1.13	1.16	- 1	9	-20	-20
583	1.42	1.41	1.14	1.16	0	0	-20	-20
902	1.43	1.42	1.13	1.10	- 4	- 5	-25	-25
954	1.41	1.42	.25	.30	-	-	-	-
968	1.43	1.43	.20	.25	- 4	- 6	-25	-25

Consequently, this first series of cycles was terminated at cycle 968-1*) when the cells repeatedly had approached zero volt at the end of the normal discharge period.

Second Run. In lieu of applying a rejuvenation procedure consisting of external shorting, recharge, deep discharge, and second recharge, it rather was decided to restart the test using the two back-up cells #3 and #4.

This decision was made under the assumption that the evaluation of the cycle performance of the two spare cells would be better suited to decide whether the failure of cells #1 and #2, respectively, was merely prompted by the cycle equipment malfunction, or whether it was possibly aggravated by the onset of memory.

The two replacement cells, #3 and #4, respectively, were submitted to a reconditioning regime as follows:

1. Cycle

Charge	40 hours at 2.5 amperes
Discharge	to one volt at 25 amperes

2. Cycle

Charge	24 hours at 5.0 amperes
Discharge	to one volt at 25 amperes
Shorting	with one ohm overnight

3. Cycle

Charge	20 hours at 5.0 amperes
Discharge	to .6 volt at 25 amperes

The discharge capacities to one volt at the third reconditioning cycle were with 51.2 and 51.7 Ah, respectively, slightly higher than the formation value of 50.4 Ah for each cell. The cells were positive electrode discharge-limiting as indicated by the built-in reference electrode of each cell.

The cells were then recharged for 16 hours at five amperes and then put on the repetitive low earth orbiting regime.

---

*) The number following the hyphen denotes the serial number of the test.

The monitoring of cell voltages and pressures was again done on a regular basis, and the corresponding results are presented in Table 44.

The end of charge voltages, EOCV, were stable, and the pressure readings made were decreasing from initially high values into ranges of normal operation.

However, the end of discharge voltages, EODV, developed a failing trend, went below one volt, and one can safely assume that a continued approach towards zero would have been only a question of time.

At the end of charge period 347-2, the two cells were removed from the automatic cycler and submitted to a deep discharge at the normal discharge current of 27 amperes.

In Figure 26, the corresponding cell voltage and electrode potential versus time curves are presented for both cells. The discharge capacity to .6 volt was only 17.3 Ah versus a reconditioned value of 51.2 Ah for cell #3 and 17.4 Ah versus 51.7 Ah for cell #4.

Both cells were negative electrode discharge-limiting and displayed severe distortions in the cell voltage curves. This occurred in the vicinity of the normal end of discharge, EOD, marked by an arrow, and according to the reference electrode measurements, had its origin in the negative electrodes. Whatever the underlying reaction mechanisms were, they caused the delivery of charge from these electrodes at a voltage plateau which was 150-200 mV more positive than normal.

The broken line in this figure, starting at about a capacity of 13 Ah removed and in the vicinity of one volt, depicts the final discharge voltage versus time curves for cells #1 and #2, respectively, at cycle 968-1. At that time, the useful discharge of the cells was also limited by the negative electrodes.

Cell #3 was now shorted by a two ohm resistor, and another capacity increment of 17.9 Ah was removed and measured by an ampere-minute meter. In the course of this low current-low voltage discharge, the cell became positive electrode limiting. Following this additional discharge, the cell was prepared for chemical analysis. The results are given in Table 66.

Third Run. In order to continue the cycle testing, the remaining cells 1, 2, and 4 were reconditioned as described previously, and then the cells 1 and 4 returned to the automatic cycler; however, this time the charge current was increased from previously 14 amperes

TABLE 44

CYCLING DATA OF SECOND RUN

50 Ah CELLS, LOW EARTH ORBIT REGIME

	EOCV		EODV		EOCP		EODP	
CELL	3	4	3	4	3	4	3	4
CYCLE								
1	1.43	1.43	1.21	1.22	30	28	10	10
57	1.43	1.43	1.14	1.14	0	0	0	0
146	1.44	1.44	1.17	1.18	12	10	2	0
225	1.43	1.43	1.15	1.15	12	10	4	2
307	1.43	1.43	1.00	1.00	12	5	3	0
346	1.44	1.44	.98	.98	17	15	3	0

All pressures in psig.

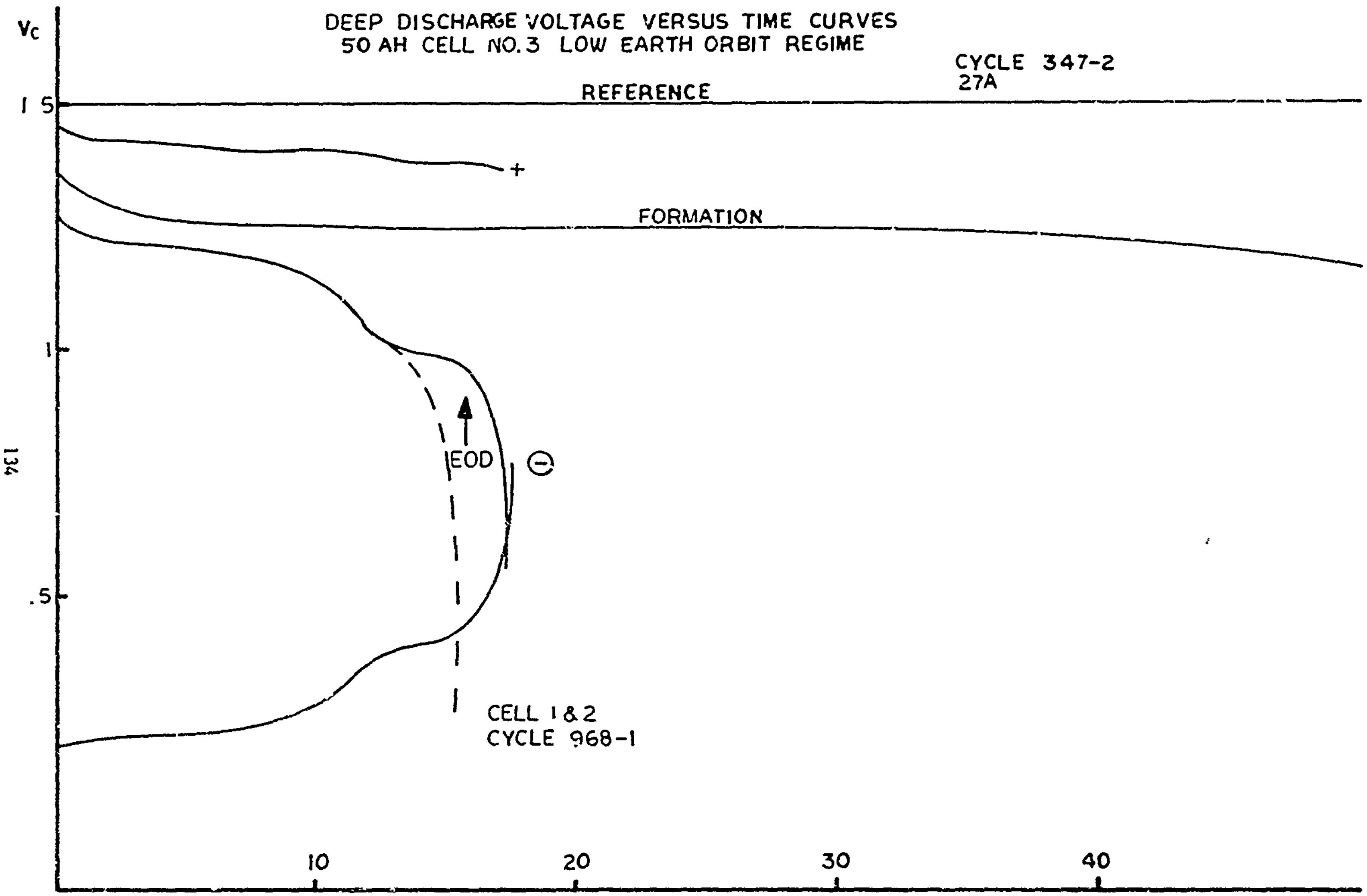

DEEP DISCHARGE VOLTAGE VERSUS TIME CURVES
50 AH CELL NO.3 LOW EARTH ORBIT REGIME
CYCLE 347-2
27A
Vc
1 5
1
.5
REFERENCE
+
FORMATION
EOD
CELL 1 & 2
CYCLE 968-1
10
20
30
40

FIGURE 26

to 15.1 in order to increase the overcharge factor to 1.2 from its previous value of 1.11.

In Table 45, the corresponding cell voltage and pressure data are presented, which undoubtedly indicates a normal cell performance. However, the cell voltage versus time curves obtained during this series had very pronounced steps in the final section of each discharge period, and thus were indicating the presence of memory.

Although these distortions in the voltage curves occurred with increasing numbers of cycles, the cells did not fail on this regime, and they were removed only at the general end of experimentation when they had acquired 589 repetitive cycles. The cells were then submitted to final deep discharges, i.e., two for cell #1 and one for #4. Cell #4 was then prepared for chemical analysis. See Table 67.

In Figure 27, the voltage and potential curves for cell #4 at the final deep discharge at cycle 590-3 are presented. The curves are essentially identical with those given in the preceding Figure 26, only the comparable discharge capacities were about 3 Ah greater than those.

In Figure 28, the final deep discharges for cell #1 are presented and it is obvious that we are confronted with a completely different situation. Not only did this cell deliver at cycle 590-3 twice the amount of capacity than all other 50 Ah cells before under the same conditions, but the end of useful discharge was caused here by the positive electrode which also displayed a step in its potential curve.

The subsequent resistor discharge produced another 7.8 Ah capacity, albeit at low voltage levels. The recharge for 20 hours at 5 amperes reconditioned the cell so that at cycle 591-3 a capacity of 48.6 Ah to 1 volt and 50.0 Ah to .6 volt was obtained. Towards the end of discharge, we here observed the usual step in the negative potential curve and the cell apparently became discharge limited by this electrode.

A possible explanation for this different behavior could be seen in the increase of the overcharge factor in this series of tests. It was obviously a step in the right direction, but individual cells respond to it in various ways. So cell #4 was merely prevented from failing to meet the cycling conditions, while cell #1 was directed towards a behavior pattern as we have seen it with the 20 Ah cells on the five-hour rate regime.

In Table 46, various formation, recondition, and final deep discharge capacities have been compiled for the 50 Ah cells.

As can be seen, the cells were heavily afflicted by the cycling conditions, and with the exception of cell #1 at cycle 590-3,

TABLE 45

CYCLING DATA OF THIRD RUN

50 Ah CELLS, LOW EARTH ORBIT REGIME

	EOCV		EODV		EOCP		EODP	
CELL	1	4	1	4	1	4	1	4
CYCLE								
1	1.44	1.42	1.23	1.23	19	58	0	7
2	1.48	1.47	1.23	1.22	13	43	0	15
4	1.46	1.44	1.22	1.21	15	55	0	20
46	1.44	1.43	1.20	1.14	9	38	0	14
125	1.44	1.43	1.19	1.12	10	39	0	12
219	1.44	1.44	1.19	1.15	7	32	0	0
342	1.43	1.43	1.17	1.09	7	35	0	10
422	1.43	1.43	1.18	1.18	2	25	0	10
519	1.44	1.44	1.20	1.16	5	35	0	13
590	1.41	1.42	-	-	5	30	-	-

All pressures in psig.

DEEP DISCHARGE VOLTAGE VERSUS TIME CURVES
50 AH CELL NO.4 LOW EARTH ORBIT REGIME

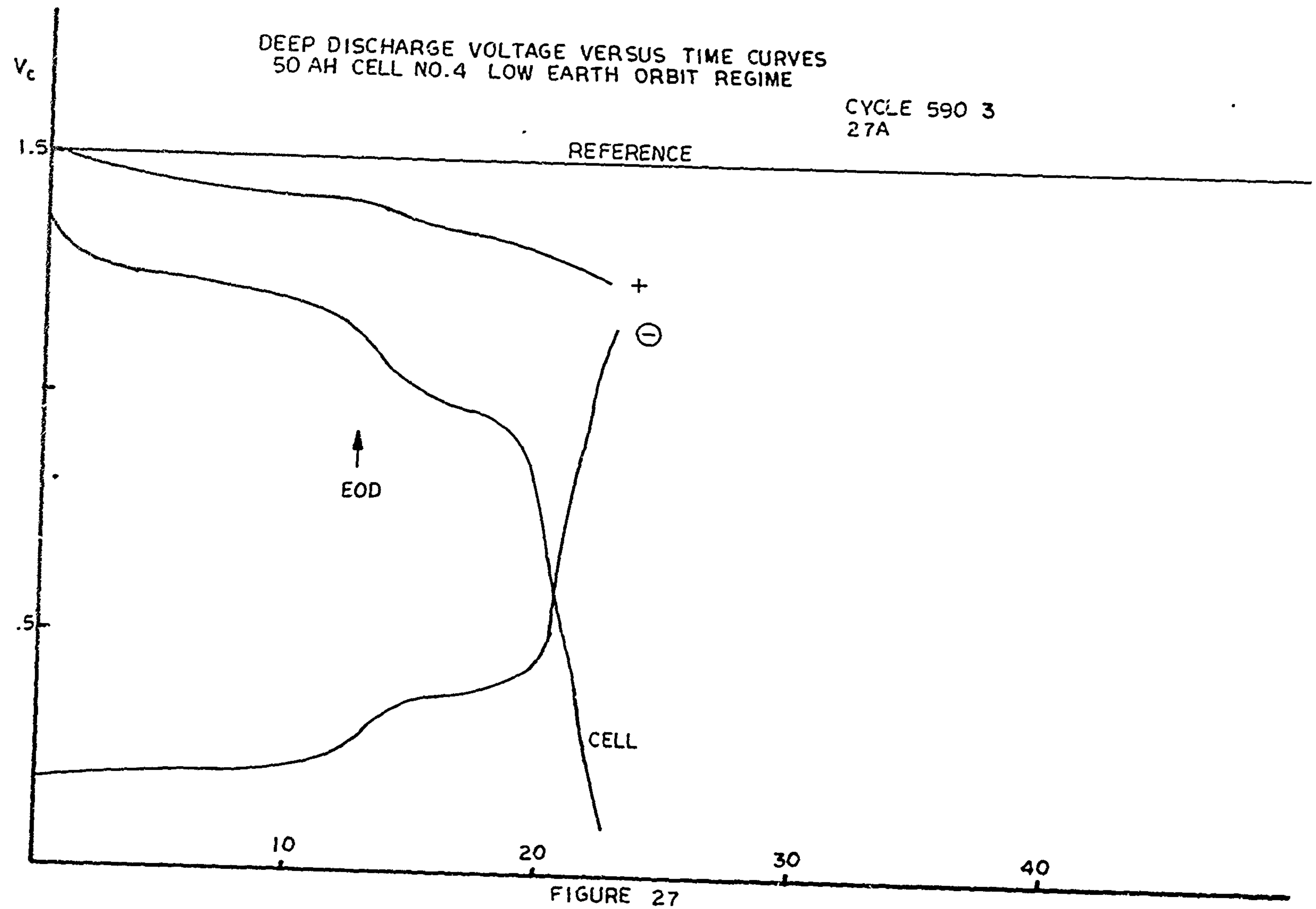

FIGURE 27

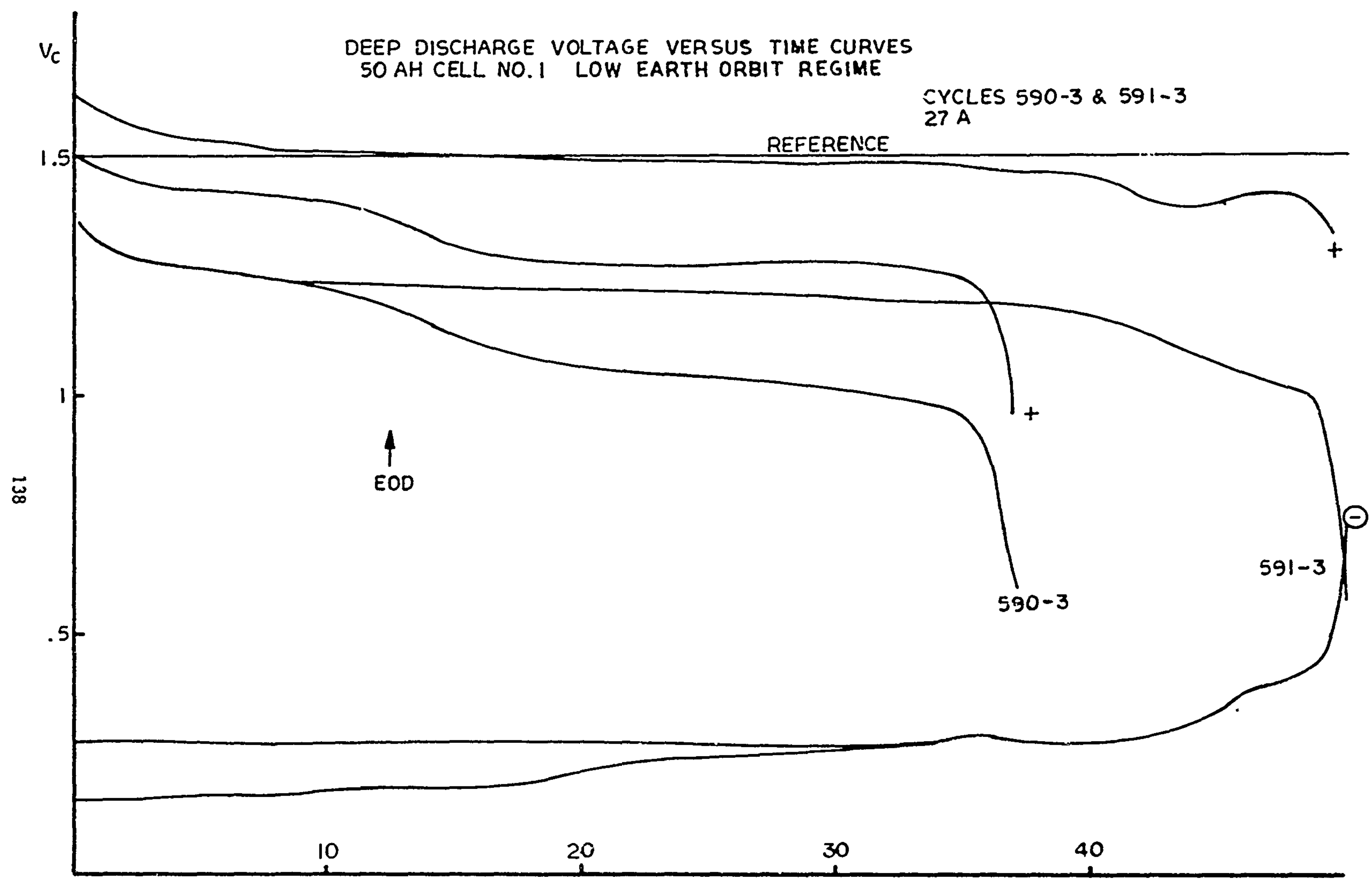
DEEP DISCHARGE VOLTAGE VERSUS TIME CURVES
50 AH CELL NO. 1 LOW EARTH ORBIT REGIME
CYCLES 590-3 & 591-3
27 A
REFERENCE
V_c
1.5
1
.5
10
20
30
40
EOD
590-3
591-3
+
+

FIGURE 28

TABLE 46

VARIOUS DISCHARGE CAPACITIES OF 50 Ah CELL

CAPACITY TO ;

CELL	CYCLE	1.00	.50	.00 V	TOTAL
1	Formation-1	54.2	-	-	
	968-1	-	-	15.8	
2	Formation-1	54.2	-	-	
	968-1	-	-	15.8	
3	Recond.-2	51.2	-	-	
	347-2	13.1	17.3	-	
4	Recond.-2	51.7	-	-	
	347-2	13.0	17.4	-	
1	Recond.-3	52.2	52.5	-	
	590-3	32.5	37.1	-	
				+7.8	44.9
	591-3	48.6	50.0	50.6	
				+8.1	58.7
4	Recond.-3	52.0	-	-	
	590-3	15.5	20.5	22.5	

delivered only small additional amounts beyond the normal end of discharge.

Summary of Kesults. In conclusion of this chapter, one can state that:

- Contrary to the 20 Ah cells, the majority of the 50 Ah cells failed under the conditions of the cycle regime.
- These failing cells were negative electrode discharge-limiting and only on subsequent low current resistor discharges became positive limiting.
- Rejuvenation attempts were always successful and restored both capacity and voltage performance to formation levels.

3. CONCLUSIONS

Under the experimental conditions of the repetitive cycling regimes, all 20 Ah cells performed well, regardless of the origin of their experimental positive electrodes.

However, every time when the discharge was continued, at the same current as used in the respective regime, beyond its normal endpoint, severe performance shortcomings of the cells became obvious. That is to say, capacities delivered were far below those of formation, and the respective voltage and potential versus time curves had more or less severe distortions.

The reason for the discharge limitations varied with regime. It was simultaneous limitation or negative electrode for the low earth orbit and strictly positive for the five-hour rate regime. In all those cases, where additional capacity increments were obtained by means of resistive, low current discharges, all cells became or remained positive electrode discharge-limiting.

The cell voltage distortions observed, usually occurring in the vicinity of the normal end of discharge, were definitely caused by the negative electrodes. Once the normal end of discharge was approached or reached, the negative electrodes started to deliver their useful charge at electrode potentials which were about 150 - 200 mV more positive than normal.

These electrode potential distortions of the negatives were very persistent, and they lingered on even when the capacity performance of the afflicted cells had been restored to normal levels by means of appropriate measures. Under those circumstances, the step in the negative potential still occurred, albeit at larger values of capacity removed.

The restoration of formation behavior with respect to capacity can be done either by a long open circuit stand in the discharged state and, maybe even more effectively, by means of an external short circuiting. Although the gauge-valve assembly of each cell might have permitted it, more drastic rejuvenation attempts, such as complete cell reversal followed by restoration of precharge in the negative electrodes, have not been conducted, since hermetically sealed cells cannot be submitted to such a treatment at all.

The performance of nominal 50 Ah cells with experimental positive electrodes was different. The cells did not meet the requirements of the original low earth orbiting regime conditions.

In the course of all three series of cycling, cell voltage distortions and capacity deficiencies became visible prior to the normal end of discharge, and during the first two series led to an involuntary termination of the tests.

The origin of those voltage distortions could be traced again to the negative electrodes which now also limited the discharge period. Amounts of capacity removed under the conditions of deep discharge were only fractions of the formation and/or recondition capacities, respectively.

The decay in cell performance with respect to capacity and voltages was of a temporary nature. It could be overcome by means of appropriate measures, however, with the deviations in the negative electrode potentials much more persistent than those of cell capacity.

In contemplating the unsatisfactory performance of the 50 Ah cell containing experimental positive electrodes, a striking common denominator begins to emerge in the light of results previously obtained with C_S cells, and now with 20 Ah cells, that is to say, the internal cell geometry, or its design, namely:

- The C_S cells contained only one electrode of each polarity with a total geometric area for both of slightly above one square decimeter, and besides that, they were of a cylindrical, wound construction.

- These cells were free of memory or distortions described above.

- The 20 Ah cells, regardless of the origin of their experimental positive electrodes, have a multitude of electrodes of each polarity. The 11 positives and the 12 negative electrodes account for a total in geometric area of 22 dm^2, and they were arranged in a planar manner.

- These cells performed well under the experimental cycle conditions, but were severely retarded in their performances once they were submitted to deep discharges.

- By necessity, the 50 Ah cells had to have a multitude of electrodes of both polarities. The sum of 16 positive experimental electrodes and 17 negative electrodes of conventional design, with an active geometric area of 131 cm^2 each, constitute a total electrode area of about 43 square decimeters. Contrary to the shape of both C_s electrodes and those of the 20-size design, these electrodes are quadratic.

- This type of cell neither met the conditions of the respective cycling regime under which the 20 Ah cells passed, nor were they positive electrode limiting on discharge.

In the case that these notions actually reflect the real causes for the failure of the 50 Ah cells, it will be worth the consideration to submit cells with large geometric plates to a drastic design review.

SECTION VI

CHEMICAL ANALYSIS AND EVALUATION

1. OBJECTIVE

In this part of the program, the composition of cycled positive and negative electrodes was investigated by means of established chemical analytical methods. The pertinent results were then compared with those obtained from "uncycled" cells which served as standards.

In addition, the disassembled cells were also visually inspected for possible signs of physical deterioration.

At the onset of these efforts, it was argued that the chemical analyses could detect the causes for the peculiar voltage and potential versus time curve distortions, provided, however, that changes in the composition of the respective electrodes were large enough to permit their detection.

If this notion was correct, a solution of the memory problem finally might have been obtained.

2. EXPERIMENTAL APPROACH

The chemical methods applied were directed to resolve the following problems:

- Determination of the total amount of active material in order to permit calculations of material utilization.
- Differentiation between charged and uncharged parts of the active materials of both electrodes.
- Evaluation of the influence of the original sample site on the composition of the specimen.
- Determination of the amount of metallic nickel still present in the cycled electrodes, and comparison with initial amounts, i.e., an evaluation of the corrosion.
- Determination of the actual level of the cobalt additive in cycled positive electrode material.

a. Preparation Procedure

In the course of the preparation of all samples for the chemical analysis, the following procedure was strictly adhered to:

1. Cutting open the stainless steel case within one cm of upper edge of the case.

2. Immediate removal of the electrode pack from the cell case.

3. Extraction of the electrolyte from the electrode pack by means of a thorough wash with distilled water.

4. Separation of the electrodes from their respective terminals with concurrent identification of the individual electrodes.

5. Drying of the electrodes to a constant weight at 110°C.

6. Punching of 10 cm^2 samples from defined plate locations.

7. Preparation of those samples for the chemical analysis proper.

8. Chemical analyses.

9. Evaluation of results.

In order to maintain the identity of the electrodes, the plate packs were always put on the bench in the same manner, namely, with the positive terminal to the left hand of the person disassembling the pack. Upon removal of the electrodes from the terminals, the electrodes were numbered in a consecutive manner, starting with "1" at the top of each polarity pack. The respective numbers were punch-died into the electrode tabs. By means of this method, the actual location of each electrode within a given pack could always be recalled.

b. Sampling Procedure

From each electrode, one 10 cm^2 punch was removed per point #6 of the preparation procedure above. These locations were well defined and identification by one of the letters, A, B, C, and D, respectively, was carried out. In Figure 29, the sampling pattern for the 20 Ah-size electrodes is presented in the full scale of 95 cm^2 geometric area per electrode.

In the right section of the figure, the stack of negative electrodes is depicted. The punching operation started at position "A" of

SAMPLING PATTERN FOR 20 AH SIZE
ELECTRODE

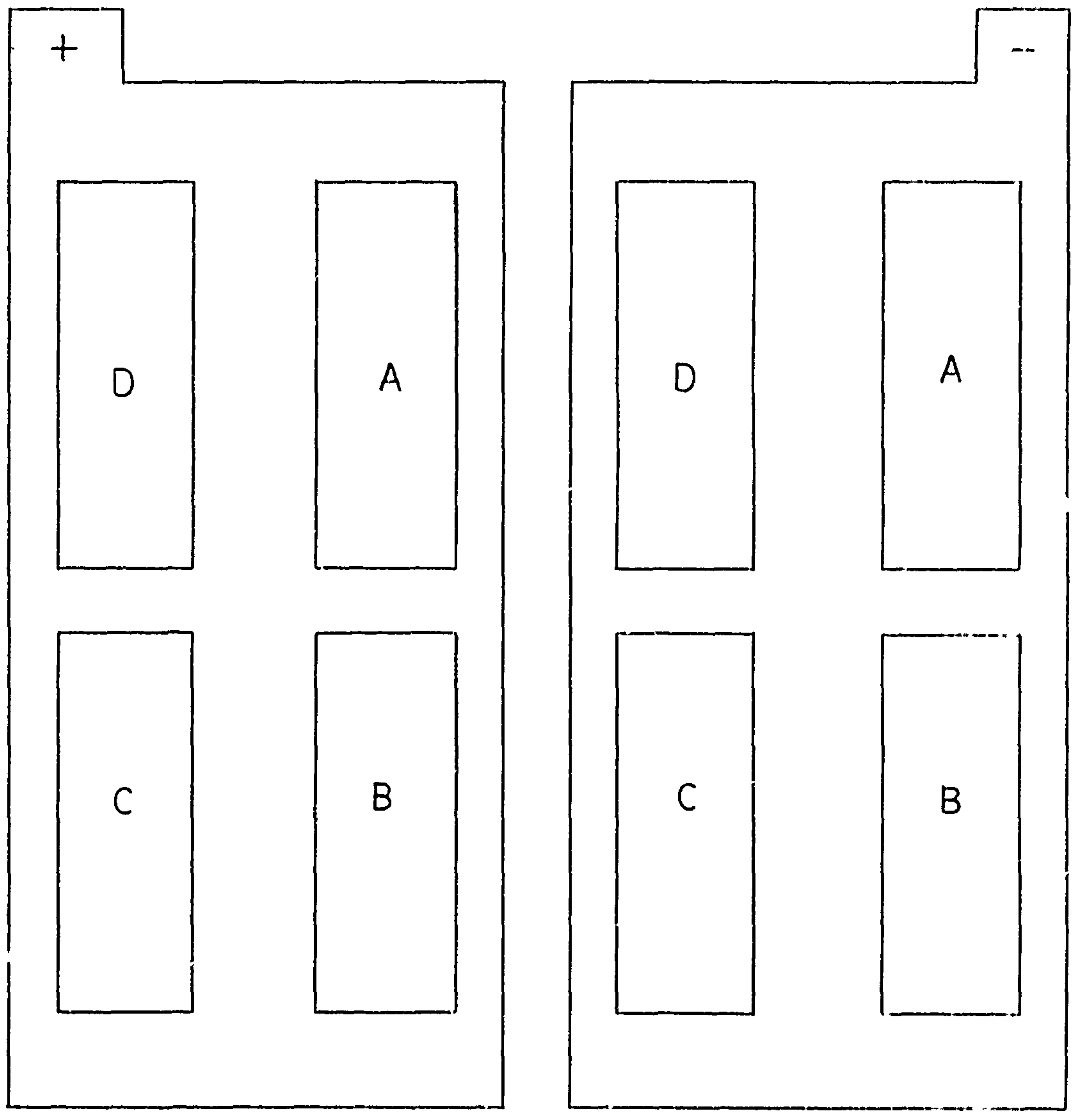

FIGURE 29

plate #1 and moved clockwise by one position for each subsequent electrode, i.e.,

1A, 2B, 3C, 4D, 5A, etc.,

until all 12 plates of this polarity were sampled in a helical manner.

The left section of the figure represents the positive stack. Again, the punching started at position "A" of plate #1 and then proceeded clockwise in the same fashion, i.e.

1A, 2B, 3C, 4D, 5A, etc.,

until all 11 plates of this polarity were sampled.

This sampling procedure provided pairs of punches of opposite polarity which not only had faced each other in the respective electrode packs, but also were very well defined with respect to their location in the pack.

In the case of the 50 Ah-size electrodes, 131 cm^2 geometric area each, the same sampling procedure was applied, however, with a different arrangement of the punch locations. Figure 30 gives the details, again at an actual scale. In trial punches, it was found that this pattern was the only one which provided an easy reproducibility of the punch locations.

The sampling started again at location "A" of the negative plate #1, and proceeded through the sequence,

1A, 2B, 3C, 4D, 5A, etc.,

until all 17 negative plates of a cell were sampled.

With a corresponding procedure for the 16 positive electrodes of each cell, pairs of punches were obtained which had faced each other in the cell during its cycle life and which also stemmed from well-defined locations within the packs.

The preparation of the punches for the chemical analysis, per point #7 of the preparation procedure above, was always done as follows:

1. Weighing of the punch on an analytical balance.
2. Measurements of thickness either on the punches or on the whole electrodes.

SAMPLING PATTERN FOR 50AH SIZE ELECTRODE

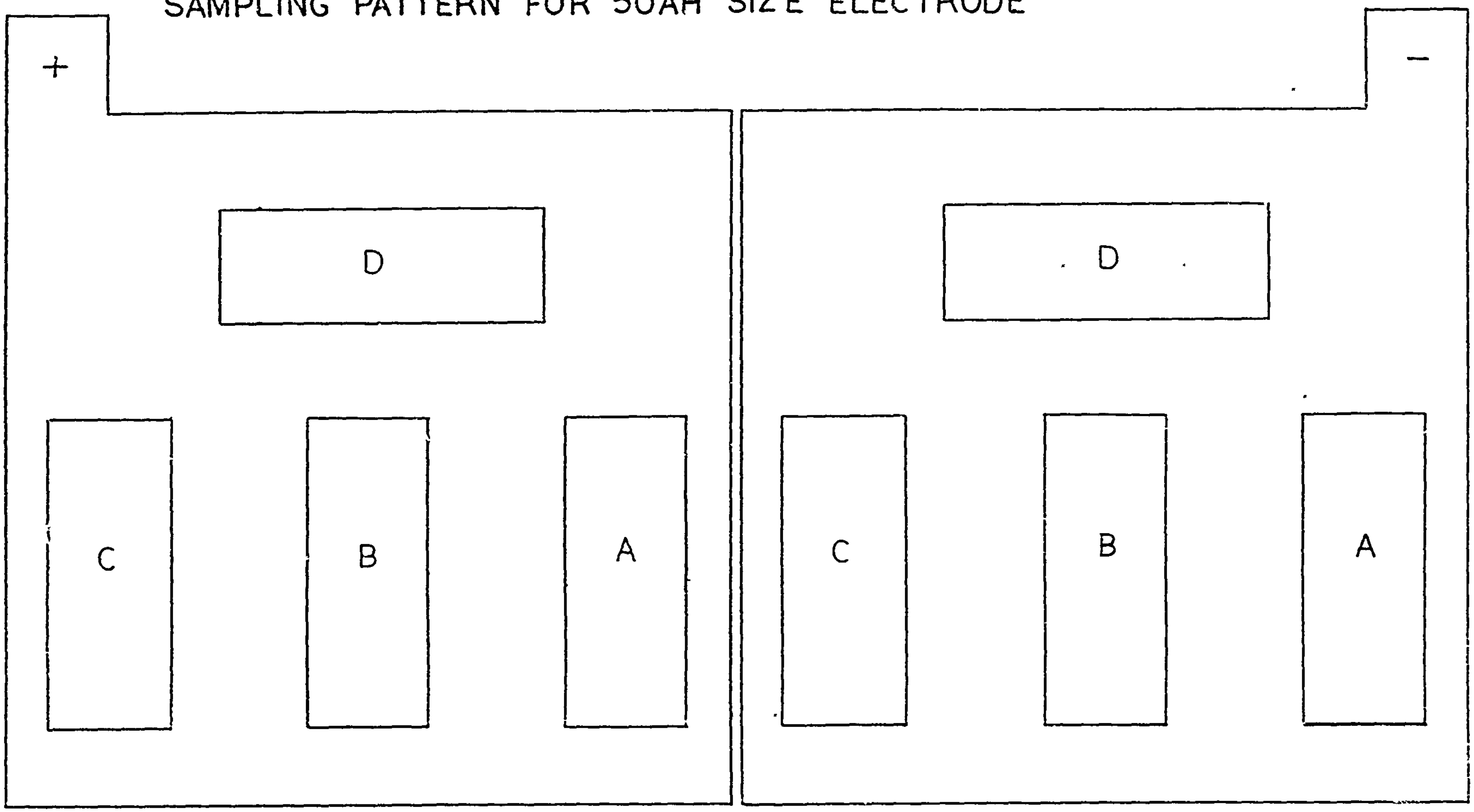

FIGURE 30

3. Removal of the mixture of nickel sinter and active material from the substrate by mechanical means.

4. Determination of the weight of the cleaned substrate.

5. Fine grinding of the mixture and storage in closed vessels until time of the analysis.

The time requirement for the span between cell opening and the availability of all ground samples was about 2-1/2 man-days for each 20 Ah cell, and about 3 man-days for the 50 Ah cells, with their larger number of samples. The actual analysis and the preliminary evaluation of the results took about 3 - 4 man-days per cell. The total was about one week per cell in elapsed time.

3. RESULTS AND DISCUSSIONS

a. General Considerations

The evaluation of the cells was not restricted to chemical aspects, and before we go to the actual chemical analysis results for individual cells, some more general comments appear to be in order.

Level of Cobalt Additive in Positives. In the work done during the second year of the contract, the optimum range for this additive was established to be 8 - 10 per cent of the total amount of active material. In the course of plate making for this year's tasks, we found an average of 8.2% with a standard deviation of 8% of the preceding value (see Tables 13 and 16).

In the course of the final chemical analysis, 18 out of 165 positive samples were analyzed for their cobalt additive content, and we found an average value of 8.3% with a standard deviation of 9.1% of that value.

Since this was identical with the amount originally present, and also was within the optimized range, we refrained from analyzing further samples.

Accuracy of the Chemical Methods. In order to convey a feeling for the accuracy of the chemical results presented later on, the following considerations are made.

The existing computer time sharing program used for converting chemical analysis readings into weights and capacities per dm^2 simultaneously conducts a comparison between the weight of a given sample and the sum of its component weights found analytically. In theory, the ratio R, called R-factor, of weight given to weight found must be unity. In practice we found:

- For 165 positive samples analyzed in the course of this task, the average R-factor was 1.005 with a standard deviation of .016.

- For 168 negative samples analyzed, the R-factor was .990 with a standard deviation of .015.

- For the total population of 333 positive and negative samples, the corresponding numbers were .998 and .017.

The proximity of these results to the theoretical unity value makes the results of the chemical analysis very reliable.

Amount of Metallic Nickel in Positives. The determination of the metallic nickel present in given electrode samples and the subsequent comparison of the results with standards is a good method for the detection of nickel attack or the corrosion of the porous sinter structure.

The initial average value for both 20 Ah and 50 Ah-size electrodes made by the new modified process was 6.46 g metallic nickel/dm^2 of electrode area after compression and trimming. This value was arrived at by prorating the average value of 7.18 g/dm^2 (Table 11) under consideration of the electrode areas lost in the trimming procedure.

In cycled cells, an average value of 6.40 g/dm^2 was found, which ruled out any corrosion or nickel attack in the course of the cycling regimes. The standard deviations of 1.4% at the beginning and 3% at the final analysis are also comparable.

The average value found for cycled cells of 20 Ah with electrodes made by the old 6-cycle process was 5.70 g metallic nickel/dm^2 electrode area, i.e., lower than the initial value found after impregnation. The difference of 6.46 - 5.70 = .76 g/dm^2 is significant. This might indicate the occurrence of corrosion in the course of the cycling.

A conversion of this amount of metallic nickel into oxidized species, not necessarily active in an electro-chemical sense, would have produced

$$.76 \times 1.58 = 1.20\ Ni(OH)_2/dm^2$$

with 1.58 the conversion factor nickel to nickel hydroxide. The amount of nickel found in the analysis, other than metallic nickel, should have been higher by an appropriate amount over the level of active material initially present.

Levels of Total Positive Active Material. In light of the possibility that the metallic nickel structure of the old 20 Ah cells actually was attacked or corroded in the course of the repetitive cycling, a general review of the levels of total active material in the positives appears to be rather interesting. This approach had the following results:

1. New 20 Ah Cells

In Table 12 of this report, an average value at the time of plate making of 10.39 g/dm^2 was reported with a standard deviation of 2.9%. Considering the plate area losses in the trimming procedure, the prorated average would be

9.46 g active material/dm^2.

In cycled cells of this type, an average value of

9.70 g active material/dm^2

was found with a standard deviation of 3.4%.

Even if a few percentage points higher than the initial value, it is identical for all practical considerations.

2. 50 Ah Cells

In Table 15, an average value of 11.22% g active material was reported with a standard deviation of 1.8%. Considering the losses encountered in the compressing-trimming process, this average would have been prorated to

10.21 g active material/dm^2.

Actually found in the two cells analyzed was an average value of

9.97 g active material/dm^2.

This is an agreement as good as one can expect.

3. Old 20 Ah Cells

In Table 26 of this report, an average value of 12.25 g active material/dm^2 was reported with a standard deviation of 5.9%. Applying the prorating procedure, this would have constituted an average of

11.18 g active material/dm^2.

Actually, we found an average level of

$$12.26 \text{ g active material/dm}^2$$

with a standard deviation of 5.3%.

The difference of $12.26 - 11.18 = 1.08$ g/dm^2 is definitely far beyond any analytical error, specifically in the light of the accuracy considerations made earlier in this chapter.

On the other hand, the difference can be easily explained by an assumed corrosion of the metallic sinter structure in the course of the cycling regime where the loss of metallic nickel observed would have been equivalent to 1.20 g active material/dm^2.

Results of Visual Inspection. At the same time when the plate packs were disassembled and the individual electroded identified, the following cell components were visually inspected for defects:

- Separator bags
- Negative electrodes
- Positive electrodes

In the course of this procedure, the following pertinent observations were made:

1. All separators were free from defects and the positive electrodes could be easily removed from the bags.
2. With the exception of the old 20 Ah cells #3L and #1, respectively, the separators did not stick to the surfaces of the negative plates.
3. The 4,200+ cycles acquired with these cells had obviously led to an ingrowing of negative plate material into the separators; however, no physical damages to the negative plate surfaces were detectable.
4. All positive electrodes looked good in the wet state, but shed some black powders when dry. The amount of active material lost was less than 1% of the total and was free from all metallic traces.
5. All positive electrodes were free from visible signs of corrosion, like blister, metal flakings, etc. Only in the course of the subsequent chemical analysis the occurrence of nickel attack in the old 20 Ah cells could be detected.

6. Without any exception, the positive plate thicknesses were increased above the average value of .0522 cm after roller compression which had a standard deviation of 1.3% (Table 20 for the 20 Ah-size plates). The corresponding values for the 50 Ah-size materials were .0525 cm with a standard deviation of 1.2% (Table 21).

7. The new average thicknesses in cm and their standard deviat-tions in per cent of the averages are arranged by cycle life as follows:

GROUP	THICKNESS	SIGMA
Reconditioned 7 cycles	.0606	3.2
5-hour rate new 20 Ah 648 cycles	.0652	4.3
Low earth orbit new 20 Ah 1,953 cycles	.0653	2.8
Low earth orbit old 20 Ah 4,273 cycles	.0793	6.1
Low earth orbit 50 Ah	.0659	4.2

These new average values will be used in the calculation of the positive electrode volumes needed in the computation of final specif-if capacities of reconditioned and rejuvenated cells.

8. Several things are apparent, namely,

- The thickness of the positive plate material of this experimental construction increas ·· ooth with cycling and mere open circuit stand, see for instance the reconditioned cells.

- In the majority of cases, the thickness bounced only back to the range which is close to the thickness prior to roller compression.

- However, with an increasing number of cycles, as for instance observed with the old 20 Ah cells, the swelling process continues, possible aided by the corrosion process. The overall increase in thickness of the electrode pack became so pronounced as to make the removal of the pack from the cell rather difficult.

b. Individual Results

Organization of Tables. The detailed chemical results obtained are presented for all 20 Ah nominal capacity cells in the following sequence:

TABLE	CELL	HISTORY
47	6	Reconditioned cell
48	2	Reconditioned cell, completely reversed
49	12	Five-hour rate cell
50	10	Five-hour rate cell with resistive discharge
51	8	Five-hour rate cell with overcharge
52	18	Five-hour rate cell, rejuvenated
53	19	Five-hour rate cell, rejuvenated twice
54	3	Five-hour rate cell, fully charged
55	13	Low earth orbiting regime, plus resistive discharge
56	16	Low earth orbiting regime, plus resistive discharge
57	Old 3L	Low earth orbiting regime, plus resist. disch. LiOH
58	Old 1	Low earth orbiting regime, plus resist. disch. nor.

Within each table the organization is uniform, as follows:

- The upper parts represent the negative electrode composition.
- The lower, part that of the positive electrodes.
- The columns are:

C_r residual charge	metallic cadmium or trivalent nickel hydroxide
C_u uncharged material	cadmium hydroxide or nickel hydroxide
C_t theoretical capacity	based upon a two-electron transfer in the case of the negatives and based upon a one-electron transfer for the positive electrodes

- The letters A, B, C, and D refer to the location of the punches.

- The numbers at the sides represent the relative location of the electrode in the cell pack.

- The numbers inside the individual boxes are capacities in Ah per dm^2 geometric electrode area, one-sided.

- The discharge capacities C_- and C_+, respectively, in Ah/dm^2 were obtained by dividing the final discharge capacity by the total geometric area of the corresponding polarity. This procedure tacitly assumed that the discharge was uniform over the whole electrode surfaces.

The values in the three capacity columns of the tables were obtained by means of computer processing the actual analytical data. In the course of this processing, the results were also plotted in the conventional bar-graph form, representing the composition of the pairs of opposite polarity punches analyzed.

A review of the pertinent data and plots showed they were independent from the relative position of an electrode in the plate stack. However, at the same time, a very strong dependence of the composition of the negative samples on the punch position was detected.

When average values for the four punch positions of each cell were calculated, it was found that a bar-graph plotting of those average results very well reflected the actual composition of the electrode materials. In addition to that, the overall composition of a cell was also calculated and presented in bar-graph form.

In Tables 59 - 65 and 68, the cell history and condensed chemical results are presented in the following manner:

- Column CELL contains the cell identification.

- Column TREATMENT reflects the cycling history.

- Column DISCHARGE MODE contains the pertinent cycling conditions.

- Column CAPACITY represents the Ah values obtained at the corresponding deep discharges.

- Column BEHAVIOR identifies the overall cell performance at those deep discharges.

TABLE 47

RESULTS OF CHEMICAL ANALYSIS

NEW 20 Ah # 6, RECONDITIONED

	C_r	C_u	C_t	C_r	C_u	C_t (TAB -)	
D 4	.96	2.97	6.03	.88	3.34	6.32	1 A
8	1.11	3.70	6.91	.82	2.56	5.48	5
12	.65	3.18	6.93	.92	2.70	5.72	9
C 3	1.73	2.58	6.41	1.51	2.18	5.79	2 B
7	1.15	2.23	6.48	1.63	1.35	5.08	6
11	1.93	1.99	6.02	1.62	2.50	6.22	10

$C_- = 2.10$

	C_r (TAB +)	C_u	C_t	C_r	C_u	C_t	
D 4	.47	0	2.76	.54	-.25	2.58	1 A
8	.51	.02	2.82	.53	.30	3.12	5
	X	X	X	.30	.44	3.03	9
C 3	.39	.30	2.98	.45	-.11	2.63	2 B
7	.51	.01	2.81	.46	-.19	2.56	6
11	.46	.11	2.86	.28	.19	2.76	10

$C_+ = 2.29$

TABLE 48

RESULTS OF CHEMICAL ANALYSIS

NEW 20 Ah # 2, RECONDITIONED

$C_- = 2.96$

		Cr	Cu	Ct	Cr	Cu	Ct (TAB −)		
D	4	.92	2.71	6.59	.55	2.46	6.15	1	A
	8	.91	2.60	6.47	.79	2.32	6.07	5	
	12	.50	2.73	6.19	.91	2.64	6.51	9	
C	3	.70	1.34	5.00	.72	1.28	4.76	2	B
	7	.82	2.54	6.32	.83	2.13	5.92	6	
	11	.93	2.30	6.19	.78	2.65	6.37	10	

$C_+ =$

		Cr (TAB +)	Cu	Ct	Cr	Cu	Ct		
D	4	.39	-.27	2.44	.53	-.20	2.65	1	A
	8	.66	-.23	2.75	.41	-.14	2.58	5	
		X	X	X	.59	-.21	2.70	9	
C	3	.46	.08	2.86	.45	-.11	2.66	2	B
	7	.57	-.39	2.50	.59	-.27	2.59	6	
	11	.55	-.11	2.76	.54	-.31	2.55	10	

TABLE 49

RESULTS OF CHEMICAL ANALYSIS

NEW 20 Ah #12, FIVE-HOUR RATE

						TAB -	
	C_r	C_u	C_t	C_r	C_u	C_t	
D 4	1.16	3.94	6.43	1.52	2.38	5.23	1 A
8	1.33	3.38	6.04	1.24	3.62	6.19	5
12	.62	4.28	6.23	1.10	4.03	6.46	9
C 3	2.36	2.87	6.56	2.73	2.30	6.36	2 B
7	1.64	2.70	5.67	1.82	3.13	6.28	6
11	1.16	3.62	6.11	1.67	3.17	6.17	10

$C_- = 1.35$

	TAB +						
	C_r	C_u	C_t	C_r	C_u	C_t	
D 4	.27	.99	2.71	.30	.96	2.71	1 A
8	.36	1.23	3.04	.27	1.27	2.99	5
	X	X	X	.40	1.03	2.88	9
C 3	.14	1.30	2.89	.36	.98	2.79	2 B
7	.38	1.08	2.91	.23	.90	2.58	6
11	.24	.96	2.65	.29	1.17	2.91	10

$C_+ = 1.45$

TABLE 50

RESULTS OF CHEMICAL ANALYSIS

NEW 20 Ah CELL #10, FIVE-HOUR RATE

TAB –

	C_r	C_u	C_t	C_r	C_u	C_t	
D 4	.95	3.48	5.91	.58	3.73	5.97	1 A
8	.83	6.04	6.35	.93	3.81	6.22	5
12	.51	6.35	6.34	.75	3.53	5.76	9
C 3	1.73	2.77	5.98	1.50	3.28	6.26	2 B
7	1.85	2.85	6.18	1.69	2.67	5.84	6
11	2.35	2.71	6.54	1.74	2.63	6.05	10

$C_- = 1.48$

TAB +

	C_r	C_u	C_t	C_r	C_u	C_t	
D 4	.23	.76	2.61	.27	.83	2.74	1 A
8	.28	.90	2.80	.24	.82	2.68	5
	X	X	X	.43	.68	2.53	9
C 3	.24	.77	2.63	.23	.99	2.84	2 B
7	.68	.72	2.82	.24	.86	2.72	6
11	.37	.88	2.87	.67	.84	2.93	10

$C_+ = 1.62$

TABLE 51

RESULTS OF CHEMICAL ANALYSIS

NEW 20 Ah CELL # 8, FIVE-HOUR RATE

TAB -

	C_r	C_u	C_t	C_r	C_u	C_t	
D 4	1.84	.98	4.28	.86	2.74	5.06	1 A
8	1.98	2.55	5.99	1.57	3.27	6.30	5
12	1.07	3.42	5.95	1.45	3.14	6.05	9
C 3	2.15	1.98	4.89	1.88	2.71	6.05	2 B
7	1.98	1.40	6.86	2.03	2.30	5.79	6
11	1.85	.80	4.11	2.17	1.53	5.16	10

$C_- = 1.46$

TAB +

	C_r	C_u	C_t	C_r	C_u	C_t	
D 4	.56	.78	2.93	.66	.38	2.63	1 A
8	.54	.58	2.71	.59	.52	2.70	5
	X	X	X	.77	.60	2.76	9
C 3	.63	.50	2.72	.61	.72	2.92	2 B
7	.73	.67	2.79	.61	.56	2.76	6
11	.57	.61	2.57	.65	.58	2.86	10

$C_+ = 1.59$

TABLE 52

RESULTS OF CHEMICAL ANALYSIS

NEW 20 Ah CELL #13, REJUVENATED

TAB -

	C_r	C_u	C_t	C_r	C_u	C_t	
D 4	2.60	1.23	5.92	1.17	2.89	6.15	1 A
8	2.35	1.43	5.87	2.24	1.14	5.47	5
12	.96	2.92	5.97	1.82	1.97	5.88	9
C 3	2.65	.56	5.30	2.30	1.37	5.76	2 B
7	2.93	.96	5.98	2.40		4.44	6
11	2.30	1.65	6.04	2.57	1.06	5.72	10

$C_- = 2.09$

TAB +

	C_r	C_u	C_t	C_r	C_u	C_t	
D 4	1.18	-.36	3.10	1.10	-.76	2.62	1 A
8	.72	-.13	2.87	1.14	-.41	3.01	5
	X	X	X	1.14	-.58	2.84	9
C 3	1.11	-.46	2.93	1.08	-.45	2.91	2 B
7	.78	-.38	2.68	1.05	-.50	2.83	6
11	1.13	-.73	2.68	.98	-.65	2.81	10

$C_+ = 2.28$

TABLE 53

RESULTS OF CHEMICAL ANALYSIS

NEW 20 Ah CELL #19, REJUVENATED

	C_r	C_u	C_t	C_r	C_u	C_t (TAB -)	
D 4	2.06	1.66	6.07	.98	2.79	6.12	1 A
8	2.18	1.71	6.24	1.86	1.79	6.00	5
12	.80	2.57	5.72	1.65	1.68	5.68	9
C 3	2.44	.88	5.67	1.69	.53	4.57	2 B
7	3.21	.28	5.84	1.99	.64	4.98	6
11	1.69	1.60	5.64	1.78	1.11	5.24	10

$C_{-} = 2.35$

	C_r (TAB +)	C_u	C_t	C_r	C_u	C_t	
D 4	.92	-.59	2.89	.72	-.52	2.76	1 A
8	.57	-.29	2.84	.85	-.38	3.03	5
	X	X	X	.62	-.38	2.80	9
C 3	.89	-.76	2.69	.80	-.52	2.84	2 B
7	1.09	-.70	2.95	.73	-.36	2.93	6
11	.56	-.33	2.79	.75	-.41	2.90	10

$C_{+} = 2.56$

TABLE 54

RESULTS OF CHEMICAL ANALYSIS

NEW 20 Ah CELL # 3, FIVE-HOUR RATE

TAB -

		C_r	C_u	C_t	C_r	C_u	C_t		
D	4	3.22	3.22	6.44	1.51	4.09	5.60	1	A
	8	3.10	1.20	4.30	2.70	3.31	6.01	5	
	12	1.18	4.17	5.35	2.94	2.40	5.34	9	
C	3	3.21	2.63	5.84	2.38	3.15	5.53	2	B
	7	3.67	.98	4.65	3.54	1.44	4.98	6	
	11	3.29	2.58	5.87	3.56	2.68	6.24	10	

$C_- = 0$

TAB +

		C_r	C_u	C_t	C_r	C_u	C_t		
D	4	2.46	.64	2.90	2.45	.43	2.88	1	A
	8	2.20	.69	2.89	2.34	.35	2.69	5	
		X	X	X	2.24	.53	2.77	9	
C	3	2.37	.49	2.86	2.17	.61	2.58	2	B
	7	2.16	.68	2.84	2.25	.53	2.78	6	
	11	2.25	.63	2.88	2.17	.72	2.89	10	

$C_+ = 0$

TABLE 55

RESULTS OF CHEMICAL ANALYSIS

NEW 20 Ah CELL #13, LOW EARTH ORBIT

						TAB -	
	C_r	C_u	C_t	C_r	C_u	C_t	
D 4	1.98	2.05	5.61	.65	3.46	5.89	1 A
8	1.89	2.44	6.11	1.99	2.09	5.86	5
12	.62	2.77	5.17	1.61	2.59	5.98	9
C 3	2.25	2.05	6.08	2.23	1.71	5.72	2 B
7	2.14	1.31	5.23	2.47	1.92	6.17	6
11	1.95	1.85	5.58	2.19	1.50	5.47	10

$C_- = 1.78$

	TAB +						
	C_r	C_u	C_t	C_r	C_u	C_t	
D 4	.81	.03	2.78	.74	.17	2.85	1 A
8	.72	.12	2.78	.95	.18	3.08	5
	X	X	X	.82	.16	2.92	9
C 3	.75	.01	2.70	.89	.13	2.96	2 B
7	.87	.01	2.82	.85	.04	2.87	6
11	.67	.20	2.81	.89	.15	2.98	10

$C_+ = 1.94$

TABLE 56

RESULTS OF CHEMICAL ANALYSIS

NEW 20 Ah CELL #16, LOW EARTH ORBIT

TAB -

	C_r	C_u	C_t	C_r	C_u	C_t	
D 4	1.75	2.08	5.65	.78	2.62	5.22	1 A
8	1.65	2.21	5.68	1.86	2.14	5.82	5
12	.69	2.77	5.28	1.44	2.29	5.55	9
C 3	2.07	1.57	5.46	1.85	2.12	5.79	2 B
7	2.17	1.73	5.72	1.87	.98	4.67	6
11	1.80	2.80	6.42	2.00	1.96	5.70	10

$C_- = 1.82$

TAB +

	C_r	C_u	C_t	C_r	C_u	C_t	
D 4	.84	.09	2.91	.61	.32	2.91	1 A
8	.83	.28	3.09	.80	.19	2.97	5
	X	X	X	.75	.15	2.88	9
C 3	.76	.17	2.91	.80	.20	2.98	2 B
7	.93	-.10	2.81	.90	.23	3.11	6
11	.82	.34	3.14	.67	.41	3.06	10

$C_+ = 1.98$

TABLE 57

RESULTS OF CHEMICAL ANALYSIS

OLD 20 Ah # 3L, LiOH-

TAB -

	C_r	C_u	C_t	C_r	C_u	C_t	
D 4	1.43	1.27	5.94	1.30	1.88	5.42	1 A
8	1.52	1.30	5.06	1.55	1.57	5.36	5
12	1.36	1.85	5.45	1.26	1.18	4.68	9
C 3	2.85	.40	5.49	2.20	1.20	5.64	2 B
7	2.77	.53	5.54	2.22	1.39	5.85	6
11	2.63	.09	4.46	2.20	1.35	5.79	10

$C_- = 2.24$

TAB +

	C_r	C_u	C_t	C_r	C_u	C_t	
D 4	1.05	.13	3.62	1.39	-.59	3.24	1 A
8	1.09	.23	3.76	1.20	-.4[illegible]	3.16	5
	X	X	X	1.11	-.08	3.47	9
C 3	1.12	-.26	3.30	1.16	-.39	3.21	2 B
7	1.15	-.12	3.47	1.13	-.34	3.23	6
11	1.24	.09	3.77	1.19	-.13	3.50	10

$C_+ = 2.44$

TABLE 58

RESULTS OF CHEMICAL ANALYSIS

OLD 20 Ah # 1, NORMAL

TAB −

	C_r	C_u	C_t	C_r	C_u	C_t	
D 4	1.67	1.48	5.23	1.35	2.18	5.61	1 A
8	1.74	1.61	5.43	1.81	1.43	5.32	5
12	1.27	2.19	5.54	1.87	1.40	5.35	9
C 3	2.47	.50	5.05	2.10	.93	5.11	2 B
7	2.59	.84	5.51	2.67	.28	5.13	6
11	2.56	.29	4.95	2.58	.72	5.38	10

$C_- = 2.08$

TAB +

	C_r	C_u	C_t	C_r	C_u	C_t	
D 4	1.10	.31	3.68	1.05	.29	3.61	1 A
8	1.08	.24	3.59	.98	.26	3.49	5
	X	X	X	.93	.24	3.44	9
C 3	.91	.47	3.65	.74	.91	3.92	2 B
7	.94	.69	3.90	.97	.49	3.73	6
11	1.00	.31	3.58	1.03	.24	3.54	10

$C_+ = 2.27$

The right sides of the tables contain the five bar-graphs representing overall cell composition and the averages for the four punch locations with all numerical values given in Ah per decimeter square. The left portion of each double-block represents the negative electrode as follows:

- Lowest section is the residual capacity, C_r.
- Uppermost section is the uncharged capacity, C_u, or the charge reserve.
- Middle section, if present, is the discharge capacity of the negative electrodes divided by the total geometric area of that polarity, C_-.
- Total height of the block is equal to the theoretical capacity, C_t, i.e., the sum of all partial capacities.

The right portion of each double-block represents the positive electrode in a similar way:

- Lowest section is the residual capacity, C_r.
- Uppermost section is either the uncharged capacity, C_u, or if preceded by a minus sign, the amount of high valency material, HVM.
- Middle section, if present, again is the discharge capacity of the positive electrodes divided by their total geometric area, C_+.
- Total height of the block is either the theoretical capacity, C_t, or in the presence of a negative sign for the topmost section, the sum of $C_u + C_+ +$ HVM.

Reconditioned 20 Ah Cells As Standards. In Table 59, the pertinent results for cells #6 and #2 are presented.

Cell #6 had an original formation capacity of 24.7 Ah, and after a successful reconditioning procedure delivered an almost identical amount of 23.9 Ah. The cell was positive electrode discharge-limiting, and based upon the final volume of the positive electrodes, a specific capacity for the positives of 6.2 Ah/in^3 was calculated.

The discharge capacity, C_d, of 23.9 Ah was equivalent to a utilization of the positive active material of 81.5%, i.e., $\frac{C_d}{C_t} = \frac{23.9}{29.3} \times 100$ without considering the residual charge level.

TABLE 59

CELL HISTORY AND CONDENSED CHEMICAL RESULTS

CELL	TREATMENT	DISCHARGE MODE		CAPACITY	BEHAVIOR
20 Ah #6	FORMATION	C.C.	10A	24.7	NORMAL
	STORAGE	-		-	
	RECONDITION	C.C.	10A	23.9 TO.6	NORMAL
20 Ah #2	FORMATION	C.C.	10A	24.3	NORMAL
	STORAGE	-		-	
	RECONDITION	C.C.	10A	24.2 .6V	NORMAL
	COMPLETE REVERSAL			NEG. 33.7	

OVERALL COMPOSITION — PUNCH LOCATION A, B, C, D

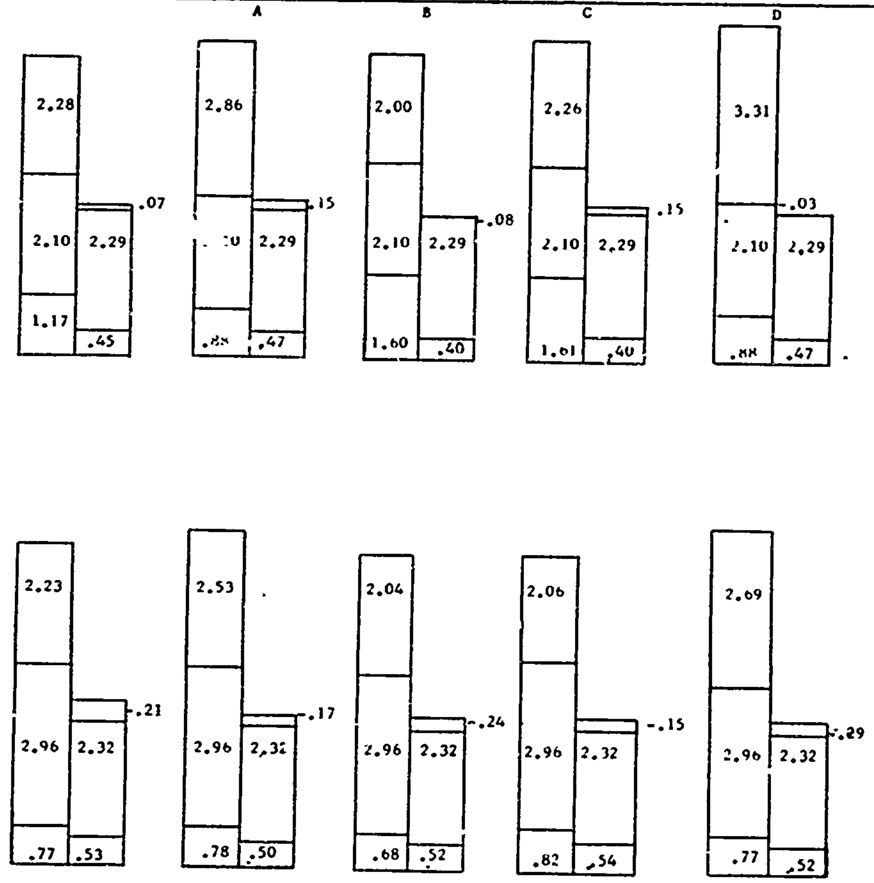

The chemical analysis found uncharged active material in 7 out of 11 positive sample locations. This resulted in an overall value for the complete cell of .07 Ah/cm^2.*

In calculating the total amount of this term for the 11 positive electrodes with 95 cm^2 geometric area, we arrived at a value of

$$.07 \times 11 \times .95 = .7 \text{ Ah}$$

which is close to the difference between formation and reconditioning of .8 Ah.

The amount of residual charge within the positives was very uniform throughout the cell and totaled 4.7 Ah which could no longer be discharged at the nominal two-hour discharge rate of ten amperes.

The composition of the negative electrodes varies with the location of the sample site. Positions A and D, respectively, punched from the upper half of the plates and therefore closer to the current collecting tab, have lower levels of residual charge, or in other words, were deeper discharged than their lower portion counterparts. The difference between these two sections was in excess of .5 Ah/dm^2.

The amounts of uncharged material, C_u, the so-called charge reserve of the negative, was sufficiently large as to permit a proper operation of this cell.

The original formation capacity of the reconditioned cell #2 was 24.3 Ah, which also was achieved in the course of the reconditioning cycle, i.e., 24.2 Ah to an endpoint of .6 volt. This was equivalent to 6.25 Ah/in^3 for the positive specific capacity.

Only in one out of 11 sample locations a rather minute amount of uncharged positive active material could be detected. On an average, the sum of discharge capacity and residual charge present after discharge was about .21 Ah/dm^2 greater than the theoretical capacity, C_t. Since the calculations for the composition of the active material of the positives are based upon a one-electron transfer, i.e., the operation between the bivalent and trivalent state of the nickel hydroxide, the appearance of a "negative" term can only mean that portions of the active material utilized valency levels greater than 3+. We tentatively call this fact the presence of high valency materials (HVM), which is always assumed to exist when this balancing of the electrode composition shows a negative sign.

---

* It should be noted that the term "uncharged active material" refers to the state of charge of those portions in both polarities prior to the final deep discharge.

The level of residual charge in the positives was unaffected from the sample location, and compared with the situation at cell #6 was obviously not further reduced by the fact that the cell was driven into complete reversal upon exhaustion of its useful capacity.

This forced reversal resulted in an additional capacity removal of 9.5 Ah from the negative electrodes only. This left the residual charge in these species at a lower level than in the case of cell #6, and also had a kind of leveling effect on the location dependence of this term.

The conclusions we draw from the analysis of these reconditioned cells, for all practical purposes having to be considered as "uncycled", are as follows:

- At the end of a charge period, the positive electrodes have no or only very minute amounts of uncharged active material.
- More typically, the chemical analysis will indicate the presence of significant amounts of high valency material (HVM).
- The level of residual charge in the discharged positive electrodes is independent from the location of the sample site.
- The composition of fresh negative electrodes is always dependent on the sample location. Areas closer to the current collecting tabs are deeper discharged, i.e., contain less residual negative charge than their more distant counterparts.
- A continuation of discharge beyond the point of delivery of useful capacity into complete cell reversal eliminates those variations in negative electrode composition.
- The fact that these differences are present in the first place indicates that the discharge current densities are dependent on the location of the electrode area with respect to the tabs.
- The amount of uncharged active material in negative electrodes, i.e., their charge reserve, was sufficiently high as to permit a proper operation of these cells.
- Due to the increase in positive electrode volume, the specific capacities for this polarity dropped from a starting value of 7.4 Ah/in^3 to 6.2 Ah/in^3.

20 Ah Cells on Five-Hour Rate Regime. Cell #12 was found to be memorized at the first deep discharge at cycle 2.3, and again at its final discharge at cycle 213, and again at its final discharge at cycle 468. The capacity obtained to .6 volt at six amperes was only 15.2 Ah as compared with a formation value of 25.7 Ah. Table 60 contains the respective repetitive cycle information and the bar-graphs for both overall cell composition and average sample location.

All positive electrodes had significant amounts of uncharged active material with an average value of 1.09 Ah/dm^2, which for all practical considerations was independent of the location of the punch site. This is equivalent to a total of

$$1.09 \times 11 \times .95 = 11.4 \text{ Ah}$$

for the complete cell. The difference between formation capacity and final discharge capacity was

$$25.7 - 15.2 = 10.5 \text{ Ah}$$

which we consider as a reasonably good agreement.

The distribution of residual charge among the positive sample locations was very uniform and had an average value of only .28 Ah/dm^2, which was below that one found in reconditioned cells.

The amount of residual charge found in the negatives had a higher average value than in the standards, i.e., 1.53 Ah/dm^2 versus 1.17 Ah/dm^2 observed in cell #6. The term also howed a dependence on the location of the sample site, that is, an average range of 1.06 - 1.32 Ah/dm^2 for the upper portions versus 1.7 - 2.1 Ah/dm^2 for the lower portions of the plates.

Cell #10 had, at its final cycle, a discharge capacity to .6 volt of 13.7 Ah. An additional amount of charge was obtained at a subsequent resistive discharge which brought the overall capacity up to 16.9 Ah. At the initial formation, 25.5 Ah were delivered, but the difference of 8.6 Ah can very well be explained by the presence of large amounts of uncharged active material in the positive electrodes. The average value of .79 Ah/dm^2 is equivalent to

$$.79 \times 11 \times .95 = 8.2 \text{ Ah}$$

The residual charge found in the positives was low, of the same order as in cell #12, and independent of the original sample location.

The negative electrodes again showed their location-dependent levels of residual charge, however, with a lower average value than

TABLE 30

CELL HISTORY AND CONDENSED CHEMICAL RESULT

CELL	TREATMENT	DISCHARGE MODE			CAPACITY		BEHAVIOR
20 Ah #12	FORMATION	C.C.	10A		25.7		NORMAL
	REP. CYCLING	212	4A 50%		-		
	DEEP DISCHARGE	+ 2	4A .6 .		12.9/23.7		MEM./NORMAL
	REP. CYCLING	253	4A 50% 1.2				
	DEEP DISCHARGE	+ 1	4A .5		15.2		MEMORY
		468	TOTAL				
20 Ah #10	FORMATION	C.C.	10A		25.5		NORMAL
	REP. CYCLING	212	4A 40%				
			1.20 O.C.P.				
	DEEP DISCHARGE	+ 1	4A .6		12.9		MEMORY
		+1	4A .6		23.6		NORMAL
	REP. CYCLING	+294	4A 50% 1.2		.		
		+ 1	4A		13.7		MEMORY
			+short			16.9	
		509	TOTAL				

OVERALL COMPOSITION PUNCH LOCATION

A B C D

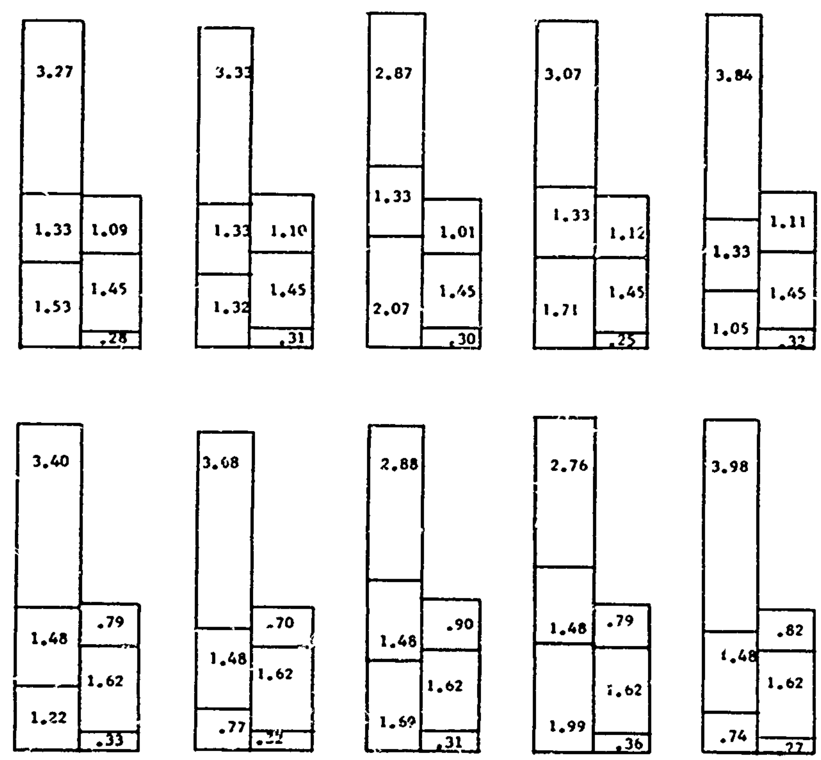

before. This was obviously caused by the incremental discharge in the course of the resistive discharge.

Since the two cells described in this group were both heavily "memorized" with respect to capacity deliverance and voltage performance, the corresponding results of the chemical analyses are an invaluable contribution to the explanation of that phenomenon.

The useful discharge of these cells was terminated by the positive electrodes as indicated by the respective reference electrode measurements reported earlier. If an electrode limits the discharge, it can either be caused by an inefficiency during the preceding charge period(s) or by an inefficiency during the last discharge period. The latter would result in increased levels of residual charge, the former in the presence of uncharged active material which obviously was the case here.

In other words, the experimental conditions of the cycling regime applied were not sufficient to return enough charge to the cell in the course of the charge periods required to maintain the initial state of charge of the active material of the positive electrodes. Consequently, these positives became discharge limiting. The influence of the cycling conditions on the performance of the negative electrodes was apparently of a different nature. As indicated by the corresponding potential curves for the negatives of these two cells, a very persistent change in the discharge mode was induced, as for instance presented in Figures 20 and 21, respectively, by the traces of the potential versus time curves during the final discharges.

The pertinent results of this chapter are:

- At the end of the final charge period, the positive electrodes contained considerable amounts of uncharged active material.

- Expressed as a capacity, the total amount of this uncharged material is very close to the deficit between formation and final discharge values.

- The level of residual charge in the positives was low and independent of the original sample location.

- The composition of the negative electrodes was again dependent on the location of the punch.

- The level of residual charge in the negative electrodes was higher than that of reconditioned cells.

Attempts to Remedy the "Memory" Phenomenon. Since the capacity aspects of the occurrence of memory could be attributed to a decay in charge acceptance or utilization of the amount of charge offered, the most obvious remedy appeared to be to increase this amount. In the final charge period for cell #8, the charge period was increased to 6 hours, and thus twice the amount of charge normally returned was put back in. End of charge voltage and pressure did not increase over the previously observed values, an indication that the cell still was operating properly.

The cell was positive electrode discharge-limiting and discharge capacity obtained after the prolonged charge was disappointing, as only 16.6 Ah could be removed to .6 volt. That was only 1.4 Ah more than obtained at the final discharge of cell #12, in spite of the fact that 12 additional Ah were offered. The capacity loss based upon formation performance of this cell was

$$25.3 - 16.6 = 8.7 \text{ Ah.}$$

At an average level of .54 Ah/dm^2 of uncharged positive material, (See Table 61) chemical analysis could only account for

$$.54 \times 11 \times .95 = 5.7 \text{ Ah.}$$

However, the approximate doubling of the level of residual charge in the positive electrodes by 3 - 4 Ah in the complete cell could easily account for the difference.

Distribution of the residual charge in the negatives showed the usual pattern of sample location dependence with an average slightly higher than observed before.

In some instances of lower total amounts of negative active material, this resulted in rather marginal levels for the charge reserve of these electrode sections, albeit the overall value of this term was still sufficient to permit proper operation of the cell.

The increase of the length of the charge period is not a suitable method to overcome memory. Of the additional 12 Ah provided, only 1.4 Ah were recovered as discharge capacity; another increment of 3 - 4 Ah was stored in an inaccessible manner in the residual charge of the positives, and more than 50% of the additional charge must have gone into oxygen evolution from the positives and immediate recombination at the negatives, since the cell pressure did not increase.

At cycle 596, cell #18 was deep discharged at four amperes to .6 volt. It was positive electrode discharge-limiting (see Figure 23), had severe distortions in the potential and voltage curves, and delivered only 13.2 Ah. In other words, it was memorized.

TABLE 61

CELL HISTORY AND CONDENSED CHEMICAL RESULTS

CELL	TREATMENT	DISCHARGE MODE		CAPACITY	BEHAVIOR	OVERALL COMPOSITION	PUNCH LOCATION
20 Ah #8	FORMATION	C.C.	10A	25.3	NORMAL		
	REP. CYCLING	212	4A 50% 1.20				
	DEEP DISCHARGE	+ 1	4A .6	(4.9)	MEMORY		
		+ 1		23.4	NORMAL		
	REP. CYCLING	+319	4A 50% 1.20				
	OVERCHARGE		4A 3 HRS.				
	DEEP DISCHARGE	+ [illegible]	4A .6	16.[illegible]			
		534 TOTAL					

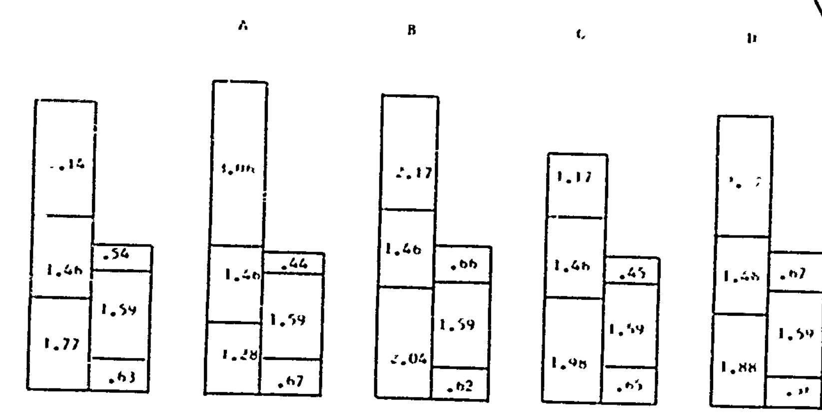

In Table 62, the pertinent history data and the results of a chemical analysis are given which were performed after the cell went through a long open circuit rest, a recharge, and another discharge at cycle 597. Although there were still some distortions in the negative potential left, the capacity of 23.8 Ah obtained at this cycle compared favorably with the formation capacity of 25.0 Ah for this particular cell. The specific capacity of the positives was only 5.7 Ah/in^3, due to the increase in electrode volume.

The chemical analysis showed the presence of HVM in all 11 locations sampled; that is to say, the cell looked like new, with an average value of -.46 Ah/dm^2 for this term. Although this is slightly higher than the value of -.21 Ah/dm^2 found in fresh cells, it is of the same order of magnitude. This means the determination of this component alone cannot differentiate between fresh and rejuvenated cells.

However, another observation might help here. The level of residual charge in the positives, although as always before independent of location of a sample, was much higher here than in uncycled cells.

The amount of negative residual charge showed its usual location-dependent distribution, however, at considerably higher levels. This resulted in an average value for this term of only 1.39 Ah/dm^2, and in one location, B6, the charge reserve was virtually nonexistent.

The results of the deep discharge of cell #19 at the end of its scheduled cycling regime were also disastrous. All indications for memory were present, i.e., distorted cell voltage and only 14.1 Ah delivered to the endpoint of .6 volt.

A low resistance short stand for 69 hours, conditions in Table 62, removed only 2.5 additional Ah. But on the subsequent recharge and discharge regime, 24.7 Ah were delivered, followed by another 2.5 Ah on a subsequent resistive discharge. These 24.7 Ah were equivalent to 5.94 Ah/in^3 for the positives.

The last cycle saw 24.0 Ah delivered to .6 volt, followed by 2.8 Ah by resistor discharge.

The chemical analysis indicated the presence of HVM at an average level of -.45 Ah/dm^2, as an indication for either fresh or rejuvenated cells. Since the average level of residual charge was higher than in fresh cells, albeit a bit lower than in cell #18, the cell must definitely be considered as rejuvenated.

The negative electrodes exhibited their usual location-dependent distribution of their residual charge with an average value of 1.86 Ah/dm^2. This was lower than in cell #18, and with all other composition details the same, the charge reserve of the negatives was greater.

TABLE 62

CELL HISTORY AND CONDENSED CHEMICAL RESULTS

CELL	TREATMENT	DISCHARGE MODE		CAPACITY	BEHAVIOR
20 Ah #18	FORMATION	C.C.	10A	25.0	NORMAL
	REP. CYCLING	212	4A 50% 1.2		
	DEEP DISCHARGE	+ 1	4A .6	11.6	MEMORY
	DEEP DISCHARGE	+ 1	4A .6	23.2	NORMAL
	REP. CYCLING	+381	4A 50% 1.2		
	DEEP DISCHARGE	+ 1	4A .6	13.2	MEMORY
	REVUVENATION	OC	59 HR +21 H 2.5A		
	DEEP DISCHARGE	+ 1		23.8	NORMAL
		597	TOTAL		
20 Ah #19	FORMATION	C.C.	10A	25.0	NORMAL
	REP. CYCLING	212	4A 50% 1.2		
	DEEP DISCHARGE	+ 1		13.7	MEMORY
	DEEP DISCHARGE	+ 1		23.5	NORMAL
	REP. CYCLING	+381			
	DEEP DISCHARGE	+ 1		14.1	MEMORY
	REJUVENATION	SHORT	69 HR +21 H 2.5	+3.5	
	DEEP DISCHARGE	+ 1		2.47	NORMAL
	REJUVENATION			+2.5	
	DEEP DISCHARGE	+ 1		2.40	NORMAL
				+2.8	
		598	TOTAL		

OVERALL COMPOSITION — PUNCH LOCATION: A, B, C, D

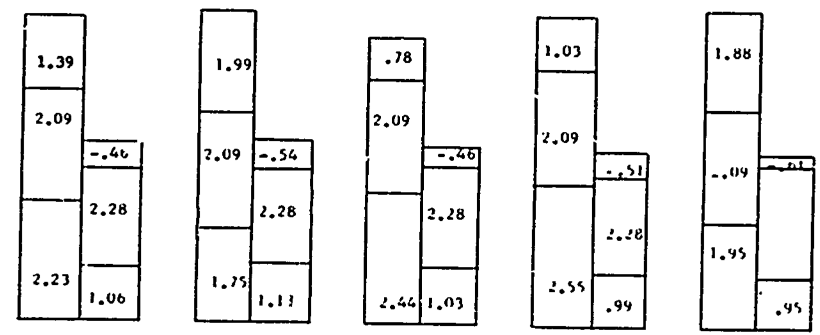

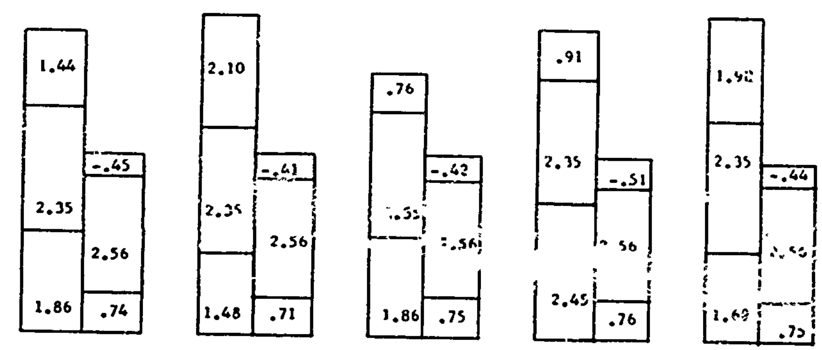

In conclusion of this chapter, we can state:

- Extending the final charge period did not eliminate the symptoms of memory.

- Uncharged positive active material was found in all punch locations of cell #8.

- The additional charge input was roughly distributed as follows:

  10% as an increase in discharge capacity
  30% as an increase in the residual positive charge
  60% went into additional oxygen evolution

- A recharge after several days of open circuit stand of cell #18, in the discharged state, restored the formation capacity performance at a subsequent cycle; i.e., this procedure constitutes an effective measure.

- HVM was present again, but the level of residual charge in the positives was larger than in fresh cells.

- Another rejuvenation means appeared to be a stand in the discharged state with a low ohm resistor across the terminals. Upon recharge, the capacity was restored to formation levels and HVM was present again.

- The negative electrodes of all cells exhibited their sample location dependency of composition.

Analysis of "Fully" Charged Cells. Cell #15 was removed from its repetitive cycling regime at the end of the charge period of cycle 584, and it was immediately processed through the preparation steps of the chemical analysis.

The results obtained for the negative electrode material were reasonable in the light of previously collected data.

- The average theoretical capacity of 6.70 Ah/dm^2 was in good agreement with previous observations.

- The average value of the charge reserve of 2.60 Ah/dm^2 guaranteed a proper operation of this cell.

- The amount of residual charge varied with location of the sample site.

° The average amount of residual charge at 3.20 Ah/dm well accounted for the sum of discharge capacities obtained with other cells under these conditions plus the pertinent levels of residual charge observed after a final discharge.

However, the results of the analysis of the 11 positive samples were completely inconclusive; that is to say, the amounts of residual charge found in all locations were far too small to account for the previously found sums of discharge capacity plus residual charge left. In numbers, an average of .91 Ah/dm^2 for the residual charge level was found versus a typical sum of about 2 Ah/dm^2 for discharge capacity plus residual charge of memorized cells.

At the time of the analysis of this cell, it was thought that possibly secondary reactions between the charged active material of the positives and the separator bags were responsible for the discrepancies observed. This notion was supported by the fact that in many contact areas between the two components severe degradations of the separator material had been observed which originated in the course of the drying process of the plates.

To resolve these inconsistencies, the test was repeated in an identical manner with cell #3, and fortunately, the actual problem was detected right in the beginning of the sample preparation procedure.

Routinely, the plate packs removed from the cell cases had been washed with hot distilled water in the 70 - 80°C range in order to remove the KOH electrolyte. This time it was observed that the insertion of the plate pack into the hot washing liquid resulted in an immediate gas evolution from the positive electrodes. This evolution of gas, undoubtedly oxygen, ceased the very moment the pack was transferred to wash water of room temperature. Consequently, the washing of at least the positive plates in the course of this preparation procedure was continued, using room temperature distilled water.

As indicated by the data presented in Table 63, this change in procedures resulted in acceptable data for the positive electrodes. The average amount of charged positive material found was 2.28 Ah/dm^2, which was large enough to account for the discharge capacity of memorized cells plus their residual charge levels usually found. The distribution of this charged active material across the surfaces of the electrodes appeared to be uniform as indicated by the small standard deviation of 4%.

The amount of uncharged active material in the positives had an average of .53 Ah/dm^2 or 5.3 Ah for the complete cell. This amount would have been large enough to produce the symptoms of memory had this cell been deep-discharged prior to the chemical analysis.

TABLE 63

CELL HISTORY AND CONDENSED CHEMICAL RESULTS

CELL	TREATMENT	DISCHARGE MODE		CAPACITY	BEHAVIOR	OVERALL COMPOSITION	PUNCH LOCATION
20 Ah (?3	FORMATION	C.C.	10A	25.0	NORMAL		
	REP. CYCLING	212	4A 50% 1.2				
	DEEP DISCHARGE	+ 1	4A .6	12.4	MEMORY		
	DEEP DISCHARGE	+ 1	4A .6	22.6	NORMAL		
	REP. CYCLING	+424	4A 50% 1.2				
	NO DISCHARGE AT LAST CYCLE				MEMORY		
		648	TOTAL				

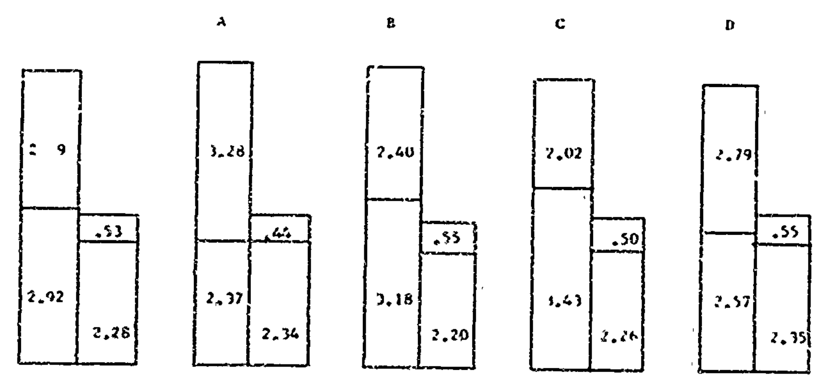

The composition of the negative electrodes of this "fully" charged cell was almost identical with material analyzed in cell #15, and the conclusion drawn there can be applied here accordingly.

In this chapter we observed:

- The charged positive active material of the "fully" charged cells was very susceptible to the washing with hot distilled water. It decomposed under oxygen evolution, i.e., self-discharge, and the amount of charged material found later on by chemical methods was not large enough to account for the previously obtained levels of discharge capacity plus residual charge.

- The washing with distilled water at room temperature prevented this self-discharge. Consequently, the amount of charged positive material found chemically was large enough to provide for the usually obtained ranges of discharge capacity and residual charge of memorized cells.

- Significant amounts of uncharged positive active material were found in all samples, indicating that the symptoms of memory would have occurred upon deep discharge of the cells.

- The composition of the negative electrodes was dependent again on the location of the samples.

<u>20 Ah Cells of Low Earth Orbiting Regime.</u> As mentioned in the testing section, the original group of eight cells on this particular regime was arbitrarily divided into two groups of four each for an easier handling on the final discharges and rejuvenation attempts. One cell from each subgroup was chemically analyzed following a deep discharge at 10.8 amperes to .6 volt and an additional resistor discharge.

Cell #13 was deep discharged at cycle 1,941 with all indications of memory as presented in Figure 15. However, the cell was negative discharge limiting. The capacity obtained to .6 volt was only 11.8 Ah to which an increment of 8.5 Ah could be added by means of a low current resistive discharge for a total of 20.3 Ah. In this additional discharge period, the cell became positive electrode discharge-limiting.

The chemical analysis found uncharged positive active material in all 11 sample locations, i.e., the cell was memorized. The average amount of only .09 Ah/dm^2 was too small to account for the difference of

$$25.3 - 20.3 = 5.0 \text{ Ah}$$

between formation performance and that at final deep discharge (see Figure 15). However, the increase in the average value for residual charge to .83 Ah/dm^2 versus the average of .45 - .53 Ah/dm^2 found in fresh cells can explain the deficit, if lumped together with the total amount of "green" materials found in the cell (Table 64).

The composition of the negative active material followed the now familiar pattern:

- The level of residual charge depends on the location of the punch.

- Its average value was almost 1 Ah/dm^2 higher than that found in fresh cells.

- Average and individual levels of charge reserve were large enough to permit a proper performance of the cell.

Cell #16 was deep discharged at cycle 1,953 with all indications of memory as presented in Figure 17. It was negative electrode discharge-limiting and produced only 11.5 Ah to the endpoint of .6 volt which could be increased by a subsequent resistive discharge to 20.7 Ah. In this portion of discharge, the cell became positive electrode discharge-limiting. The difference between formation and final discharge performance was

$$25.8 - 20.7 = 5.1 \text{ Ah.}$$

In all but one of the 11 sample locations the chemical analysis found uncharged active material in the positives, i.e., corroborated the presence of memory. The average amount of .20 Ah/dm^2 or

$$.20 \times 11 \times .95 = 2.1 \text{ Ah}$$

was too small to explain the missing charge. However, in the same manner as observed with cell #13, the increase of the average level of residual charge to .80 Ah/dm^2 or

$$(.80 - .50) \times 11 \times .95 = 3.1 \text{ Ah}$$

was large enough so that the sum of the two terms can account for the capacity deficit observed.

The negative electrode composition was in strict analogy with that of previously analyzed cells (Table 64).

TABLE 64

CELL HISTORY AND CONDENSED CHEMICAL RESULTS

CELL	TREATMENT	DISCHARGE MODE	CAPACITY	BEHAVIOR	OVERALL COMPOSITION	PUNCH LOCATION
20 Ah #13	FORMATION REP. CYCLING DEEP DISCHARGE RESIST. DISCHG.	C.C. 10A 1940 + 1 10.8A .6 1941 TOTAL	25.3 11.8 +8.5 20.3	NORMAL MEMORY		
20 Ah #16	FORMATION REP. CYCLING DEEP DISCHARGE RESIST. DISCHG.	C.C. 10A 1,952 + 1 10.8A 1,953 TOTAL	25.8 11.5 +9.2 20.7	NORMAL MEMORY		

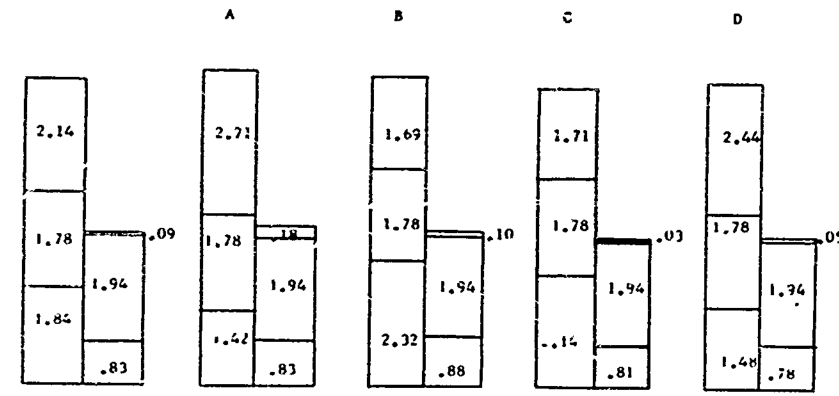

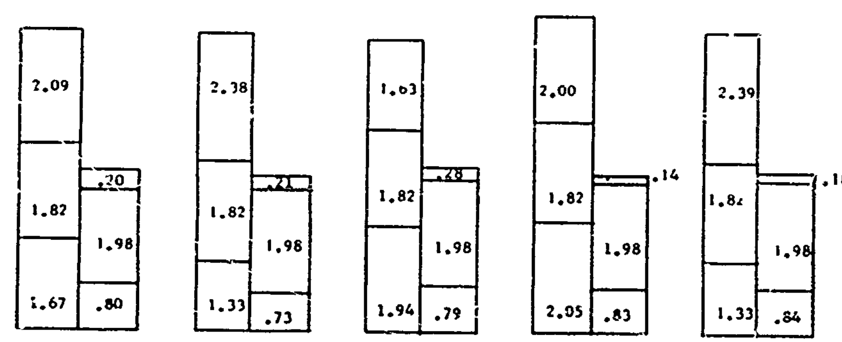

In this subsection we found that:

- Changes in the composition of both negative and positive electrodes were found which were indicative for the presence of memory.

- The results of the chemical analyses thus corroborated the observations of the final deep discharges.

Old 20 Ah Cells on Low Earth Orbiting Regime. In Table 65, the history and the results of the chemical analysis for these two cells are presented.

Cell #3L had an additive of LiOH in its electrolyte. At its final cycle, 4,273 overall, or 4,043 at this low earth orbiting regime, its discharge capacity to .6 volt at 10.8 amperes was only 14.3 Ah. Using the cell can as a reference, it was found that both electrode potentials broke simultaneously (see Figure 12). At a subsequent resistive discharge, another increment of 11.2 Ah was removed for a total of 25.5 Ah, which was slightly larger than the corresponding formation value of 25.0 Ah.

The chemical analysis found HVM in eight out of the 11 positive sample locations, while only three of them had uncharged positive active material. From this observation alone, the cell could not be declared as memorized. However, the amount of residual charge had an average value of 1.17 Ah/dm which was more than twice that found in fresh cells. The resistive charge obviously had resulted in a kind of rejuvenation with regard to HVM levels, and only the good indicator quality of the residual charge level showed that the cell was not fresh.

Residual charge found in the negatives was again very dependent on the original location of the punch. Its average values approached almost twice the amount found in fresh cells. This resulted in an overall low value for the charge reserve of 1.18 Ah/dm^2 and some locations were virtually depleted of uncharged negative active material.

Cell #1 capacity performance was not much different. It delivered 11.6 Ah to .6 volt at 10.8 amperes, and an additional resistive discharge at low currents increased this to 23.7 Ah which was

$$24.5 - 23.7 = .8 \text{ Ah}$$

below the corresponding formation value.

Contrary to cell #3L with its LiOH additive in the electrolyte, uncharged positive active material was found in all 11 punch locations.

TABLE 65

CELL HISTORY AND CONDENSED CHEMICAL RESULTS

CELL	TREATMENT	DISCHARGE MODE	CAPACITY	BEHAVIOR
20 Ah 3L "OLD" W/LIOH ADD.	FORMATION	C.C. 10A	25.0	NORMAL
	REP. CYCLING	SEE FOOTNOTE		
	REJUVENATION		20.8	
	REP. CYCLING	4,042 10.8 32% 1.11		
	DEEP DISCHARGE	+ 1 10.8 .6	14.3	MEMORY
	RESIST. DISCHG.		+11.2	
			25.5	
		230		
		4,043		
		4,273 TOTAL		
20 Ah "OLD" NORM. ELECTROL.	FORMATION	C.C. 10A	24.5	NORMAL
	REP. CYCLING	SEE FOOTNOTE		
	REJUVENATION		21.7	
	REP. CYCLING	4,042 10.8 32% 1.11		
	DEEP DISCHARGE	+ 1 10.3 .6		MEMORY
	RESIST. DISCHG.		+12.1	
			23.7	
		230		
		+4,043		
		4,273 TOTAL		

FOOTNOTE:

TREATMENT				
FORMATION	C.C.	10A		
REP. CYCLING	112	4A	50%	1.2
DEEP DISCHARGE	+ 3	4A	.6	
REP. CYCLING	+112	4A	50%	1.2
DEEP DISCHARGE	+ 3	4A	.6	

OVERALL COMPOSITION

PUNCH LOCATION

A B C D

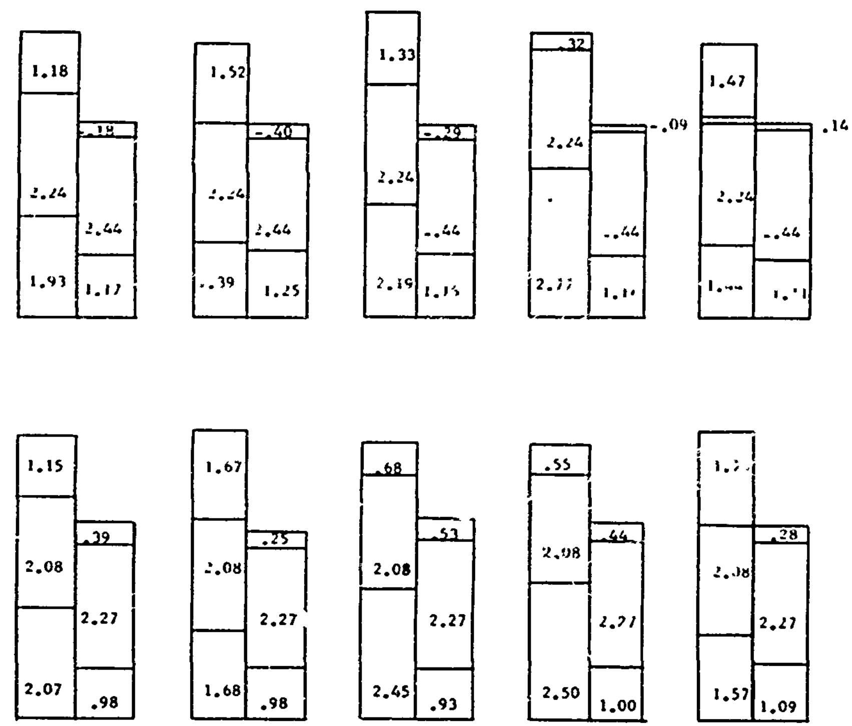

The average value of .39 Ah/dm^2 was equivalent on a whole cell basis to

$$.39 \times 11 \times .95 = 4.1 \text{ Ah}$$

or considerably more than the .8 Ah deficit between formation and final deep discharge capacity.

However, as we recall, the chemical analysis of this positive plate material also established the occurrence of nickel attack and the subsequent production of active material. This additional amount of 1.08 grams $Ni(OH)_2/dm^2$ in theory is equivalent to .31 Ah/dm^2 or to about 3.3 Ah for the complete cell.

The addition of this term to the difference of .8 Ah, i.e., formation capacity minus final total capacity, resulted in a perfect match with the calculated capacity for the green uncharged material.

In conclusion of this chapter we can state:

- The presence of LiOH in the electrolyte of one cell did not prevent the onset of memory but resulted in a slightly different chemical composition of the active material of the positive electrodes.
- High levels of residual charge in the active materials of the positives corroborated the results of the corresponding electrochemical discharges with regard to memory.
- The residual charge in the negative electrodes showed its usual location dependence.
- The averages for this term were lower than in fresh cells which resulted in lower levels for the charge reserve of these electrodes.

Results for Individual 50 Ah Capacity Cells. The results of the chemical analysis of two cells are presented in Tables 66 and 67, respectively, with regard to

- Residual charge, C_r
- Uncharged active material, C_u
- Theoretical capacity, C_t

The organization of these tables is the same as described for the corresponding ones for the 20 Ah cells; however, the physical

TABLE 66

RESUSTS OF CHEMICAL ANALYSIS

50 Ah CELL # 3 LOW EARTH ORBIT

TAB
−

$C_- = 1.58$

	C_r	C_u	C_t
4	.83	4.48	6.89
8	.97	3.91	6.46
12	1.50	3.72	6.80
16	.81	4.38	6.77

D

	C C_r	C C_u	C C_t	B C_r	B C_u	B C_t	A C_r	A C_u	A C_t	
3	1.59	3.44	6.61	1.64	2.87	6.09	1.24	3.38	6.20	1
7	1.69	3.51	6.78	1.80	2.82	6.20	1.30	3.64	6.52	5
11	1.73	3.54	6.05	1.89	3.28	6.75	2.10	3.08	6.76	9
15	2.02	2.93	6.53	2.06	3.22	6.86	3.21	2.19	6.98	13
							2.31	2.90	6.79	17

C B A

TAB
+

$C_+ = 1.68$

	C_r	C_u	C_t
4	.39	.91	2.98
8	.38	.69	2.75
12	.51	.63	2.82
16	.26	.90	2.84

D

	C C_r	C C_u	C C_t	B C_r	B C_u	B C_t	A C_r	A C_u	A C_t	
3	.37	.78	2.83	.38	1.08	3.14	.59	.53	2.80	1
7	.37	.77	2.82	.31	.82	2.81	.20	1.04	2.92	5
11	.32	.66	2.66	.37	.57	2.62	.29	.90	2.87	9
15	.34	.80	2.88	.17	.96	2.82	.16	.88	2.72	13

C B A

TABLE 67

RESULTS OF CHEMICAL ANALYSIS

50 Ah CELL # 4 LOW EARTH ORBIT

TAB
-

$C_- =$ 1.01

D

	C_r	C_u	C_t
4	1.15	4.25	6.41
8	1.72	3.63	6.36
12	2.30	3.07	6.38
16	1.66	3.71	6.38

	C			B			A			
	C_r	C_u	C_t	C_r	C_u	C_t	C_r	C_u	C_t	
3	1.84	3.07	5.92	1.89	3.39	6.29	1.33	4.00	6.34	1
7	3.53	1.44	5.98	3.21	1.83	6.05	3.13	1.87	6.01	5
11	3.37	1.63	6.01	3.12	2.24	6.37	3.28	1.89	6.18	9
15	2.73	2.33	6.07	3.07	.94	6.02	3.38	1.98	6.37	13
							2.02	3.29	6.32	17

TAB
+

$C_+ =$ 1.07

D

	C_r	C_u	C_t
4	1.17	.84	3.08
8	.94	.92	2.93
12	1.23	.55	2.85
16	1.64	.17	2.88

	C			B			A			
	C_r	C_u	C_t	C_r	C_u	C_t	C_r	C_u	C_t	
3	1.11	.81	2.99	1.18	.71	2.96	1.06	.82	2.95	1
7	1.05	.89	3.01	.98	.84	2.89	.96	.89	2.92	5
11	1.04	.94	3.05	.78	1.05	2.90	1.03	.75	2.85	9
15	1.14	.65	2.86	1.01	.82	2.90	1.17	.61	2.85	13

appearance reflects the different location of the punched samples.

A preliminary evaluation of the numbers and bar-graphs showed that the situation for both cells again could be presented by means of an overall bar-graph and averages for the four respective punch locations. Those values are presented in Table 68.

Cell #3 was used only in the second series of the repetitive cycling regime and at cycle 347 was deep discharged to .6 volt at 27 amperes. It was negative electrode discharge-limiting and delivered only 17.3 Ah, or approximately one-third of its original capacity. Another one-third was obtained by means of a subsequent resistive discharge which brought the total capacity removed to 35.2 Ah. In the course of this process the cell became positive electrode discharge-limiting. The difference between recondition and final discharge capacity was

$$51.2 - 35.2 = 16.0 \text{ Ah}$$

The chemical analysis found uncharged positive active material in all 16 sample locations. The values appeared to be free from any location dependence. The average value was .80 Ah/dm^2 or

$$.80 \times 16 \times 1.31 = 16.8 \text{ Ah}$$

which accounts very well for the capacity deficit. The level of residual charge in the positives was low *) and uniform.

The distribution of the residual charge within the negative electrodes varied again with relative distance to the current collecting tab. The three punch areas, A, B, and C, from the lower portion always had higher values than the punch areas from the upper portion, D. The average value of 1.66 Ah/dm^2 appears to be normal for the condition of the cell. The average value and location values for the charge reserve of the negative electrodes were large enough to permit a proper operation of the cell.

Cell #4 was employed in two series of cycling, namely, the second and the third, respectively. At the 590th cycle of the latter, it was deep discharged to almost zero volt at the usual discharge current of 27 amperes. The cell was negative discharge-limiting, as

---

*) Since no uncycled cells of this type were available for analysis, the values found for the 20 Ah cells have to be used for comparison purposes.

TABLE 68

CELL HISTORY AND CONDENSED CHEMICAL RESULTS

CELL	TREATMENT	DISCHARGE MODE				CAPACITY	BEHAVIOR
50 Ah #3	FORMATION	C.C.	25A			50.4	NORMAL
	STORAGE						
	REJUVENATION	C.C.	25A			51.2	NORMAL
	REP. CYCLING	346	27A	32%	1.11		MEMORY
	DEEP DISCHARGE	+ 1	27A	.6V		17.3	MEMORY
	RESIST. DISCHG.					+17.9	
		347	TOTAL			35.2	
50 Ah #4	FORMATION	C.C.	25A			50.4	NORMAL
	STORAGE						
	REJUVENATION	C.C.	25A			51.7	NORMAL
	REP. CYCLING	346	27A	32%	1.11		MEMORY
	DEEP DISCHARGE	+ 1	27A	.6V		17.4	MEMORY
	REJUVENATION					52.5	NORMAL
	REP. CYCLING	+589	27A	32%	1.20		
	DEEP DISCHARGE	+ 1	27A	.8		22.5	MEMORY
		937	TOTAL				

OVERALL COMPOSITION

PUNCH LOCATION

A B C D

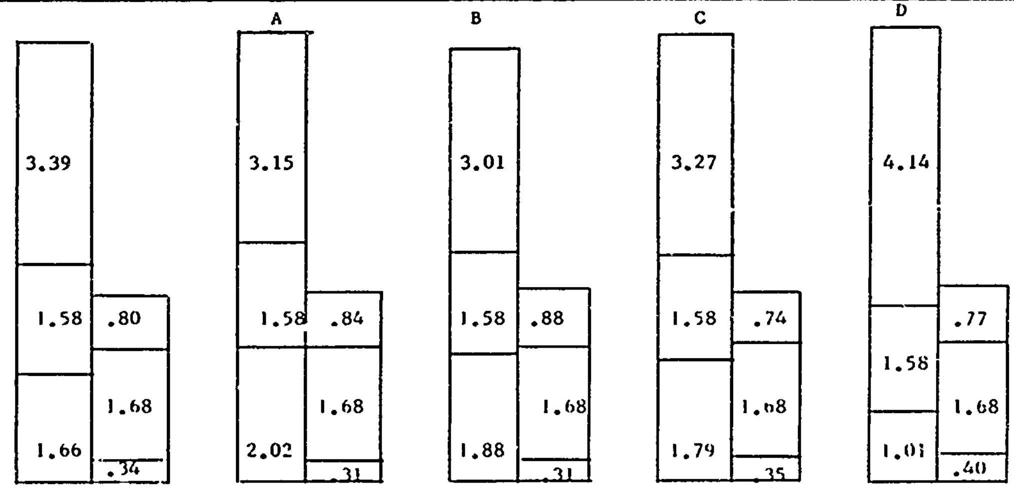

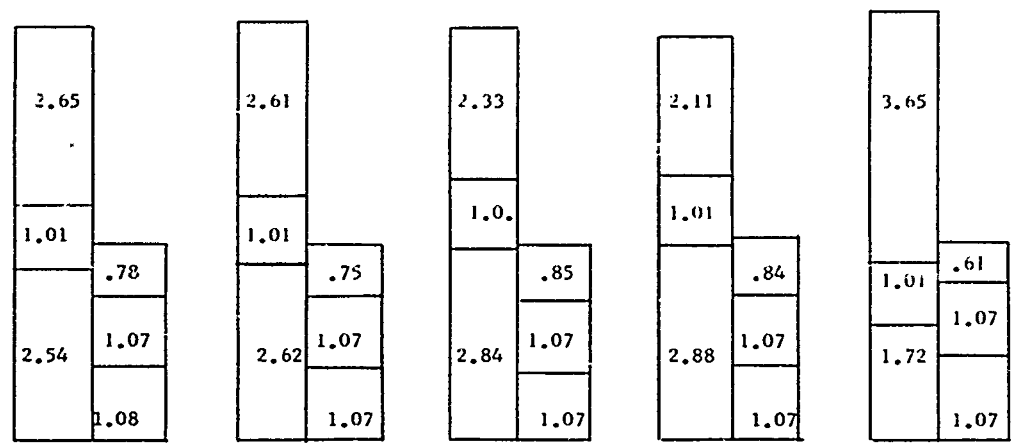

presented in Figure 27, and a capacity of only 22.5 Ah was delivered. The difference between recondition and final capacity was therefore

$$52.5 - 22.5 = 30.0 \text{ Ah}.$$

The chemical analysis found uncharged active material in all 16 punch locations with an average of .78 Ah/dm^2, or for a total

$$.78 \times 16 \times 1.31 = 16.3 \text{ Ah}$$

which means that the difference must have been buried in the residual charge portion of this electrode. This term had an average value of 1.08 Ah/dm^2, or was approximately .70 Ah/dm^2 greater than the corresponding term of cell #3. This would have accounted for

$$.70 \times 16 \times 1.31 = 14.6 \text{ Ah}$$

The sum of both terms of 30.9 Ah for the complete cell would have been an almost perfect match for the deficit in capacity observed.

The levels of residual charge in the negative electrodes were found again to be location dependent. The levels of charge reserve in these electrodes were lower than in the other 50 Ah cell analyzed. Obviously, this was caused by an overall lower amount of active material.

For this experimental cell group, it was found that:

- All positive punch locations contained significant amounts of uncharged positive active material.
- The levels of residual charge in the negative electrodes were again strongly dependent on the sample location.
- The average value for the residual charge was high for cells which, like these, were negative electrode discharge-limiting.
- A possible explanation for that phenomenon has to be sought in the physical state of the active material which resisted an easy discharge.

4. CONCLUSIONS

The reproducibility of the results of the chemical analysis was extremely good, as indicated by the near unity values of the R-factors, i.e., the ratio of amounts given to amounts found chemically.

The analysis of uncycled cells showed the presence of high valency material (HVM) in the positive electrodes, which means that significant portions of the active material had been operated at oxidation states greater than 3+.

The analysis of cycled cells displaying the phenomena of memory, i.e., temporary losses of discharge capacity and voltage distortions, showed that HVM had disappeared, and that significant amounts of uncharged positive active material were present at the end of the charge period immediately preceding the final discharge.

The presence of uncharged positive active material under those conditions indicated that the charge acceptance of the positives had deteriorated in the course of the respective cycling regimes.

By means of suitable reconditioning or rejuvenation procedures, the presence of uncharged positive material could be eliminated and HVM could be restored.

Memorized cells, and those rejuvenated after memory occurred, had levels of residual charge in the positive electrodes which were significantly greater than those found in fresh cells. The level of residual charge in the positives can be used to distinguish between fresh cells and rejuvenated ones.

While the level of residual charge of the positive depended neither on plate nor punch position, the analogous term of the negatives was strongly dependent on the punch locations. Samples stemming from punches close to the current collecting tabs had considerably lower levels of metallic cadmium than those removed from the lower parts of the electrodes.

This observation undoubtedly indicates that the discharge was conducted with location-dependent different current densities.

Although in general the negative electrodes displayed sufficient levels of charge reserve to permit a proper operation of the sealed system, in some cases levels of insufficient magnitude were found. This was always caused by a greater than normal increase in the charged portion of the negative active material.

In the case of negative electrode discharge-limiting 50 Ah cells, large amounts of residual charge were found in the negative electrodes. The only feasible explanation for this fact is that the physical state of this charged material was such as not to permit its complete discharge.

The chemical analysis of the old 20 Ah sealed cells with 4,200+ duty cycles detected the presence of nickel attack or the corrosion of the sintered structure in the course of the repetitive cycling. The amount of metallic nickel still present at the end of the regime was significantly lower than that found at plate making time and, consequently, the amount of active material increased considerably in the course of cycling. The theoretical conversion factor for metallic nickel with nickel hydroxide is 1.58, and in the cases investigated here was almost completely achieved.

The increase in plate thickness upon cycling, and obviously even upon prolonged open circuit stand, increased the overall volume of the positives to an extent that a large reduction in the specific capacity, Ah/in^3, occurred, i.e., from initial values of 7.5 Ah/in^3 down into the 5.8 - 6.2 Ah/in^3 range.

SECTION VII

GENERAL CONCLUSIONS AND RECOMMENDATIONS

The previously developed constant potential electro-deposition process for positive nickel hydroxide nickel sinter electrodes was improved and refined with regard to ease of manufacturing. Chemical analyses showed an excellent uniformity of the active material distribution across the electrodes and the absence of any corrosion of the sinter structure. Consequently, the level of the cobalt additive was also uniform and in the optimized range as provided by the composition of the impregnation solution.

The impregnation of so-called master plaques for both 20 Ah-size and 50 Ah-size electrodes, respectively, was successfully completed. In the course of evaluating the process data, it was found that an excellent current utilization was achieved. In a typical lab bench-style operation, about 12 square feet of finished electrode material was produced in a one shift, five-day work week. Chemical analyses corroborated again that the same good material quality was obtained as in the scale-up phase, i.e., uniformity of active material and additive, and the absence of nickel attack.

The existing equipment was laid out as to permit the simultaneous treatment of two master plaques at any given processing station. It is felt that the output of such an impregnation chain can easily be increased three to four times by means of just providing a larger number of vessels at each treatment station without interfering with the quality of the material produced.

Should it be necessary to produce even larger amounts of finished electrode material per unit of time, the set-up of more such chains is preferred over an expansion of the chain length. This is recommended in order to avoid possible electrical interference among the larger number of vessels connected in series.

Another possibility to enlarge the quantity output is seen in the investigation of a continuous process with a porous sinter strip moving through the various processing stations.

Early in the application of the C.P.E.D. process it was found that a compacting of the impregnated porous nickel sinter structures was necessary in order to meet the specific capacity requirement of 8 - 10 Ah/in^3. Although this objective could easily be achieved by a simple roller compression of the plates by about 20% of its initial thickness, the inherent area increase of the material required a trimming of excesses in both width and length to plate and cell design

dimensions. The resulting loss of active material reduced the overall gain in specific capacity to only about 10% over the level present in the uncompressed material.

Consequently, the evaluation of other existing and/or the development of new plaque structures is recommended which will not require a compression-trimming operation in order to achieve specific capacity goals and meet dimensional specifications.

The actual building of sealed cells of both 20 Ah and 50 Ah nominal capacity, respectively, proceeded well, once the initial difficulties were overcome. The nickel wire screen substrate used had numerous protruding tips which resulted in internal cell shorts when normal cell building procedures were applied. It took great and tedious efforts to overcome this obstacle so successfully that in the subsequent testing phase no internal shorts occurred.

It is absolutely mandatory that in future plate making tasks a better suited substrate material will be used, as for instance, expanded, flattened nickel. This improved substrate is then to be used as a mere replacement in the current plaque structure or in conjunction with a new, still to be developed, sinter structure, in order to eliminate also the compression-trimming step.

The current compressed and trimmed electrode material permitted the introduction of an additional electrode pair plus separator into the electrode pack. Although it was not possible to optimize this new design with respect to electrolyte volume, concentration, and composition, the use of the thinner high capacity positives opened up a new avenue towards higher energy density per unit volume of the cell.

The formation process of the cells resulted in very good absolute discharge capacities and in specific capacities for the positive electrodes in the 7.4 to 8.2 Ah/in^3 for operation in the sealed state.

In the cell testing phase, the 20 Ah nominal capacity cells containing the experimental positive electrodes were submitted to two repetitive cycling regimes; namely,

- A five-hour rate regime which had been previously applied in the evaluation of C_S-size cells and which was originally specified.

- A low earth orbiting regime, the necessity of which was emphasized in the course of the contract work.

The overall outcome of these tests is that all 20 Ah cells performed flawlessly under the specified experimental conditions. However, when the discharge periods, at the same current as was used in the corresponding repetitive regime, were extended beyond the normal end of discharge, severe shortcomings became apparent; namely,

- Voltage depressions in the 100-200 mV range occurring in the vicinity of the normal end of discharge.

- Discharge capacities to one and .6 volt were only a fraction of their respective formation values.

These two facts were a definite manifestation of the memory phenomenon long sought after.

The cell voltage distortions could in all cases be traced back to the negative electrodes, while the polarity of the electrode responsible for the end of useful discharge varied with the experimental conditions. However, it was common to all cells subsequently submitted to low current resistive discharges that their positive electrodes were discharge limiting.

The two deviations mentioned were only of a temporary nature, and they could be remedied by means of suitable procedures like long time open circuit stand or shorter stands with externally applied resistors. Based upon formation performance, the capacities were completely restored, while the voltage steps caused by the negative electrodes lingered on; however, the areas of capacity removed far beyond the normal end of discharge of the respective cycle regime. It is felt that these deviations ultimately might have been eliminated by means of electrical treatments not suitable for hermetically sealed cells.

The 50 Ah nominal capacity cells were on the low earth orbiting regime only, and under the experimental conditions applied, failed, i.e., with increasing number of repetitive cycles, the end of discharge voltages approached and went below the one volt level at the end of normal discharge.

Both cell voltage distortions and the limiting of the useful discharge were traced back to the negative electrodes by means of the reference electrode measurement.

The disturbing effects were of a temporary nature, too, and formation performance could be restored by means of appropriate rejuvenation procedures, again, completely with regard to capacity, and to a lesser degree, voltage-wise.

In the light of the data presented and the results discussed in detail in the testing section of this report, it appears that the occurrence of memory is correlated to the design and the internal geometry of the cells, that is to say, under the limited experimental conditions applied.

This notion about the influence of cell geometry on performance certainly deserves more attention in the future.

The majority of the cycled cells was submitted to a very thorough chemical analysis of their plate materials of both polarities. This procedure was performed with the cells in various states of charge and degrees of performance.

The results of the chemical analysis were rather conclusive; namely,

- In uncycled cells, the presence of high valency material (HVM) in the positive material was detected.

- In cycled memorized cells, HVM was absent and replaced by significant amounts of uncharged positive active material.

- In rejuvenated cells, HVM was present again; however, the level of residual charge in the positives was considerably increased over that found in uncycled cells.

- The positive electrodes of the old 20 Ah cells suffered corrosion or nickel attack in the course of 4,200 + repetitive cycles. This was indicated both by the loss of metallic nickel and an almost stoichiometric increase of the level of active material.

- The composition of the active material of the negative electrodes displayed a strong dependence on the location of the sample. Punches taken from areas closer to the current collecting tabs had considerably lower levels of residual charge than those taken from more distant areas. This finding undoubtedly indicates the non-uniformity of the current distribution.

- The discharge-limiting negative electrodes of the 50 Ah cells had very high levels of residual charge at the end of their regular discharge periods. The material could only be discharged at very low currents in the course of resistive discharges. This observation means that the charged active material of these negative electrodes must have been in a physical state which did not permit a complete discharge.

The visual inspection of the plates of both polarities gave no indications for any material defects. However, the increases in plate thickness of the positives were so significant as to reduce their specific capacity values from the initially satisfactory range down to the 6 Ah/in^3 area.

Although this increase in thickness in the course of repetitive cycling did not interfere with the performance of the cells, it is recommended that in future work the phenomenon of positive electrode swelling should be investigated.

SECTION VIII

ADDENDUM TO FINAL ANNUAL REPORT

C.P.E.D. PROCESS INSTRUCTIONS

1.0 PLAQUE PREPARATION

1.1 Objective

This operating step has to provide two things; namely,

1. A sufficiently large amount of porous nickel sinter on a suitable substrate by means of an appropriate sintering process.

2. The processing of the continuous sinter strip into master plaques of appropriate size for the subsequent impregnation procedure.

1.2 Equipment Requirements

A suitable sintering furnace for continuous operation.

Cutting devices, i.e., shears or paper cutter, etc.

Thickness measurement device Lhomargy M102.

Steel ruler.

Analytical balance - Mettler H15.

1.3 Material Requirements*

Nickel wire mesh screen: 20 mesh, .007" wire diameter.

Die Mesh Corporation 17.1 cm (6-3/4") wide, in length of not less than 150 feet.

---

* A process flow diagram is presented in Figure A1 covering the plate making procedure.

The symbols have the following meaning:

Circle = Material Input
Square = Operational Step
Triangle = Quality Control

These will be used in the same manner in subsequent diagrams.

C.R.E.D. PROCESS
PLAQUE MAKING

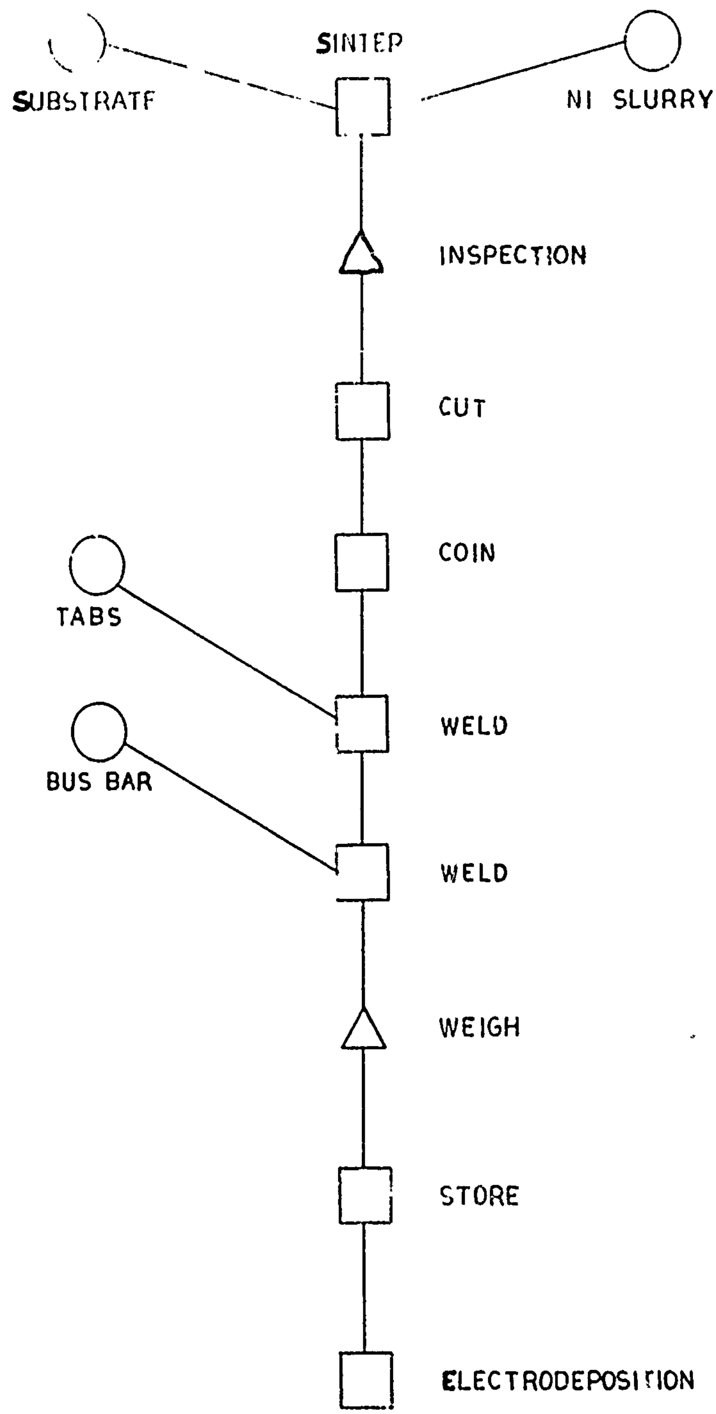

FIGURE A1

Unit area weight 3.66 g/dm^2

Viscous nickel slurry of suitable composition.

Nickel tab material: Thickness, .0127 cm (.005"); Supplier, Phizer Co., Wallingford, Conn.

1.4 Sinter Strip

The nickel slurry is applied to the moving substrate and sintered at the elevated temperature range of 800 - 1000°C. Experimental conditions are selected so that a porous material of 80 - 82% overall porosity and .062 - .064 cm thickness is obtained.

The cooled sinter strip is visually inspected for its entire length. Areas of obvious defects are marked and excluded from further processing.

The inspected strip is stored in air-tight plastic bags or containers until time for cutting into master plaques.

1.5 Master Plaque Fabrication

A master plaque is defined as an unimpregnated piece of material containing two or more unit areas of the selected electrode design.

In the work described herein, master plaques for 20 Ah and 50 Ah-size electrodes were prepared containing six and three individual electrode areas, respectively. The individual electrode and overall master plaque dimensions are taken from Figures A2 and A3, respectively, and are as follows:

Type	Overall		Electrode*		
	cm Length	Height	Height	Width	Area cm^2
20 Ah	44.7	17.2 orig		6.95	94.5
	44.7	13.6 prep	13.6		
50 Ah	44.7	17.2 orig			
	44.7	11.0 prep	11.0	11.9	130.9

* The exact electrode areas are marked on the sinter to facilitate the final cutting into plates and the end of the process.

20 AH MASTER PLAQUE

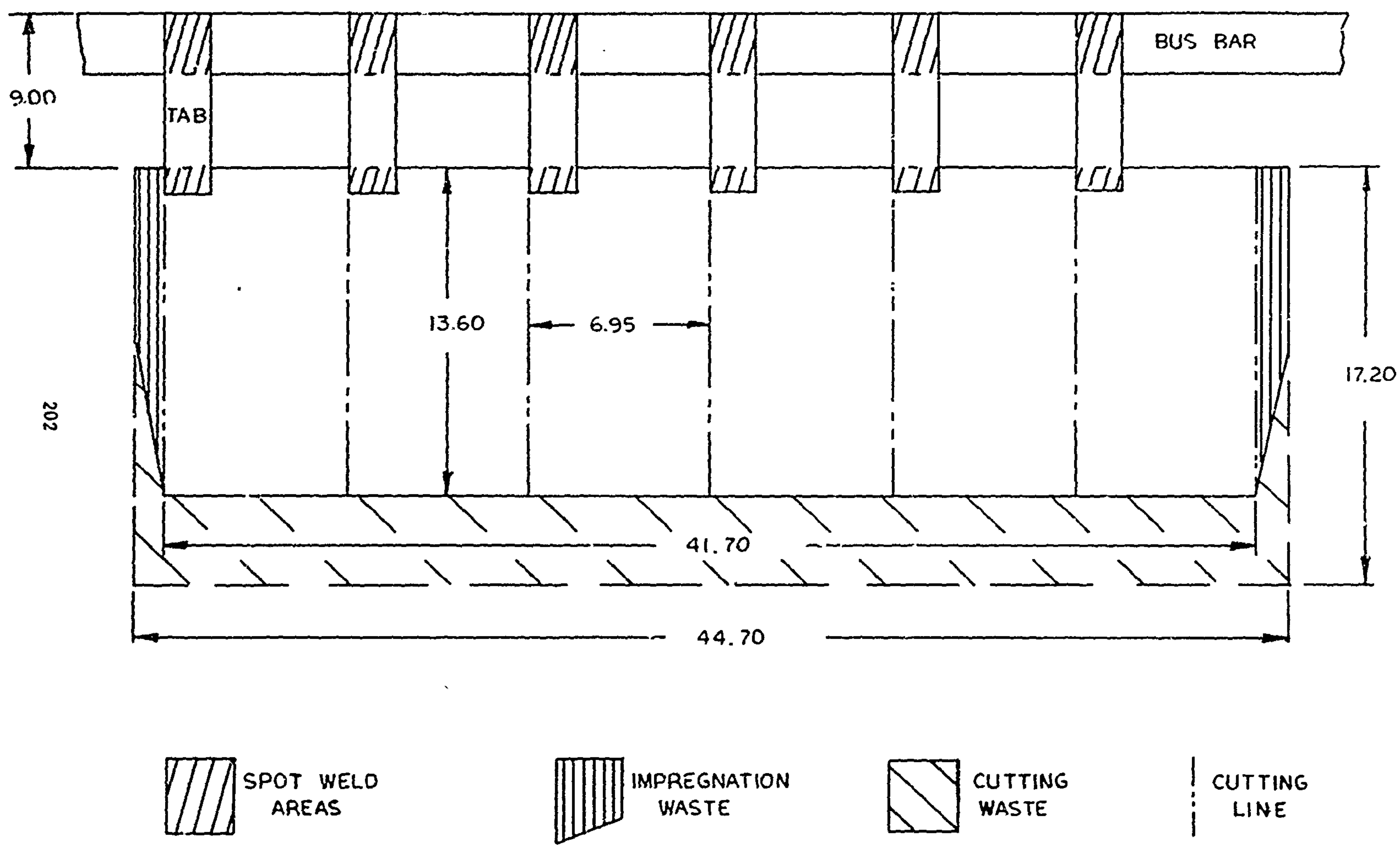

FIGURE A2

50 AH MASTER PLAQUE

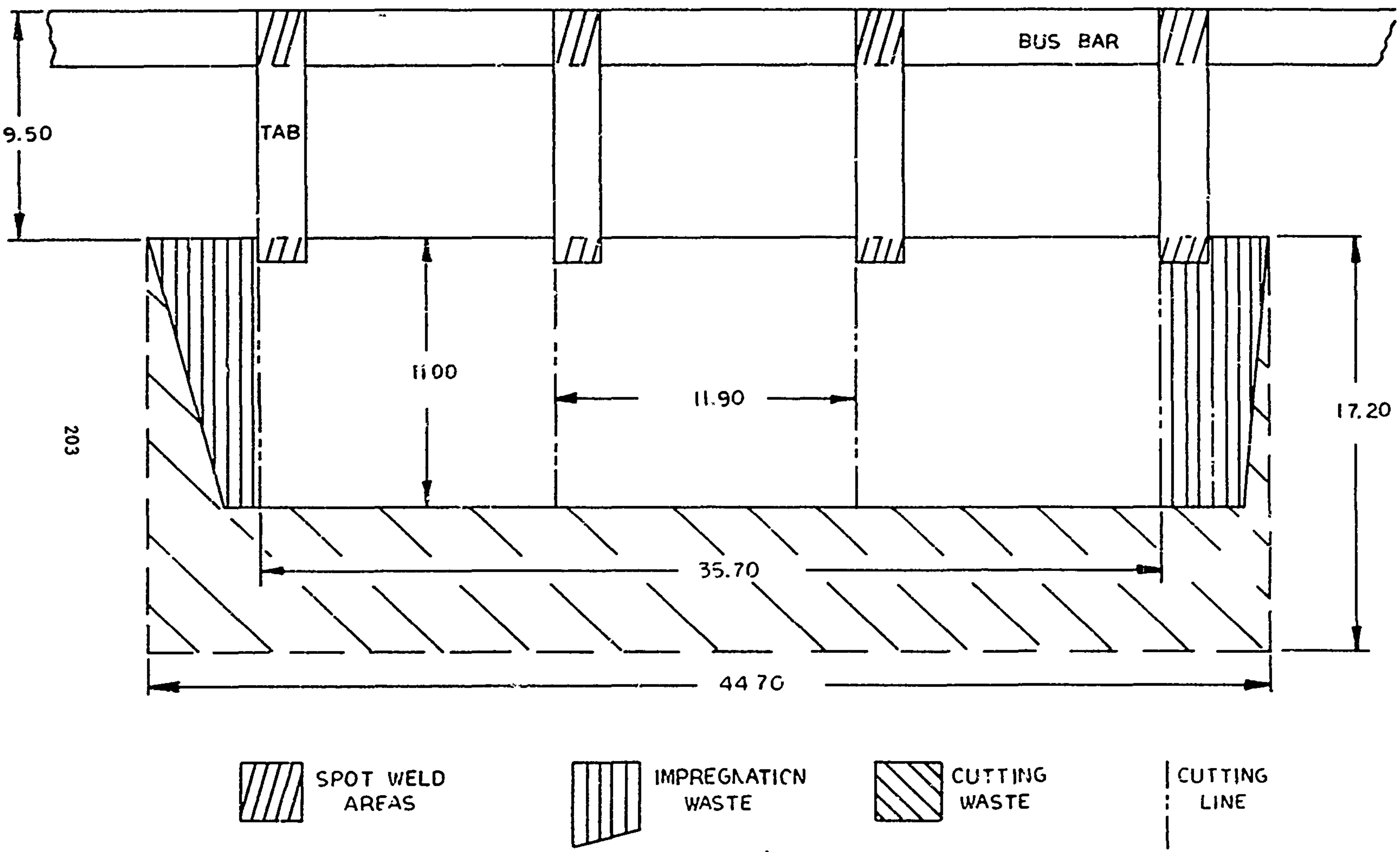

FIGURE A3

Master plaque areas in excess of the single electrode areas are die compacted or coined to minimize deposition of active material in those regions and to increase the mechanical strength of the material.

Small portions of the electrode areas along one long edge were also die compacted to accommodate the vertical tabs.

These nickel tabs are initially "tacked" in position by means of electric spot welding of about 50 W sec. discharges. However, it is mandatory to follow-up with heavier welds, about 500 W sec. discharges, which should be confined to the actual solid tab area to avoid burn-out of the porous uncompacted sinter section.

The vertical electrode tabs are then tacked to the horizontal bus bar by means of 50 W sec. discharges and then secured by several higher power discharges of about 500 W sec.

The finished master plaques are stored in air-tight containers until used for impregnation.

1.6 Quality Control

1. Thickness monitoring at five - six meter intervals during sintering process with appropriate adjustments of slurry thickness.

2. Thickness measurements of finished sinter strip.

3. Determination of overall porosity, P, by cutting known volumes, V, of strip, weighing, W, on analytical balance and calculation with $d_{Ni} = 8.9\ g/cm^2$

$$d_a = \frac{W}{V} \times \frac{1}{d_{Ni}}$$

$$P = 1 - d_a$$

1.7 Time Requirement

The time allotment of all processing steps, excluding quality control, is between 45 and 60 minutes per master plaque.

2.0 IMPREGNATION STATION

2.1 Objective

To provide the physical location for the execution of the four cycle C.P.E.D. process of two master plaques simultaneously.

2.2 Equipment Requirements

Two polycarbonate containers with an approximate volume of 14 liters each - (Vendor: E.H. Sargent Co.), Cat. No. S-752-50, Size D, 6-1/8" deep, 19" long, 10-1/2" wide. This material was selected over other plastic on account of its mechanical strength at the initially anticipated elevated operating temperatures. A perspective view is presented in Figure A4.

Two fitted nickel counter electrodes per container about 1.5 inch spaced. Nickel 270, .056" thick, (Vendor: Elray Manufacturing Co., Glassboro, New Jersey).

Perforated corrugated PVC separator material completely enclosing each of the two counters; (Vendor: Perforating Industries, Inc., Linden, New Jersey).

Power supply capable of delivering 60 - 70 amperes at 3.0 V.D.C. per impregnation cell.

Although 34 Ah aircraft batteries were used in conjunction with a graphite regulating resistor, the necessary effort of keeping the potential across the cells at a constant value makes it desirable to employ a self-regulating electronic power supply, as for instance Hewlett Packard Model 6456B, 0-36V, 0-100 amps.

Wiring by means of insulated copper-standard wire, 8 gauge.

On-off double-pole knife switch, No. 637.

Current shunt 100 mV, 100 A, GE type 140-034-PKAA.

Digital voltmeter for shunt reading, Digitic Model 271A-2, 0-1.999 volt range.

Multirange voltmeter for reading of single and/or multiple impregnation vessel potential readings. Triplet No. 825.

Elapsed time clock with audio signal, Gralab Timer, Model 171, 60 minute cycle.

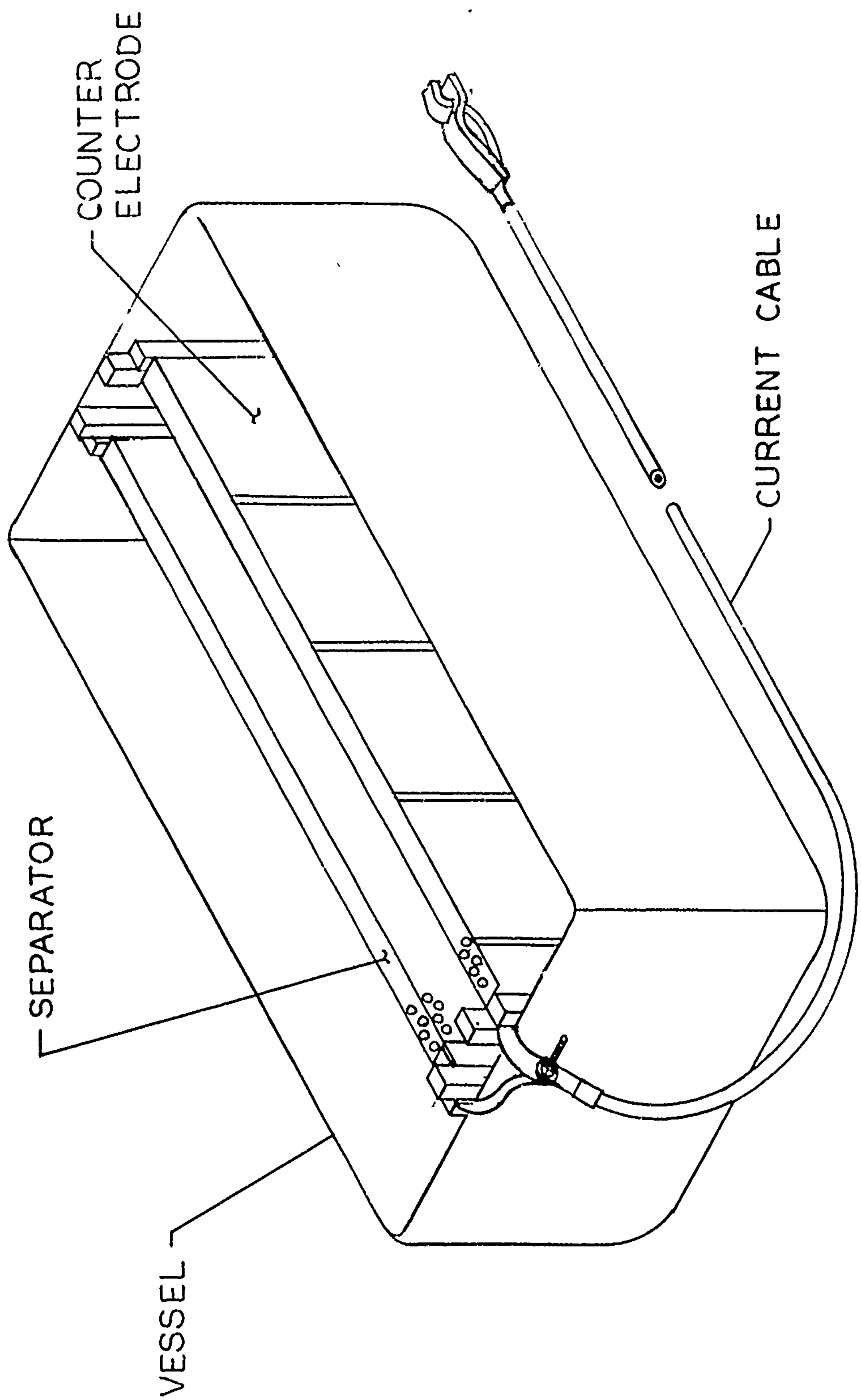

FIGURE A4

Impregnation solution storage tanks made of polyethylene. One 40 liter tank with lid per impregnation vessel, bearing identical labeling as corresponding impregnation vessel.

Impregnation solution pump, Gorman Rupp Industries, Model

Analytical equipment, see details in Section 2.5.

Thermometer divided in °C for readings in 25 - 50°C range.

Timer operated hot plate with magnetic stirring 4 liter glass beaker with watch glass as cover.

Mettler top loading balance with .1 gram accuracy.

2.3 Material Requirements

Master plaques prepared per section 1.0.

4.0 - 4.5 molar nickel nitrate solution containing 8 - 10% cobalt nitrate based upon total molarity of heavy metals.*

Made by dissolving multiples of 240.718g $Ni(NO_3)_2 \cdot 6\ H_2O$ and 29.10 g $Co(NO_3)_2 \cdot 6\ H_2O$ in distilled water and diluting to the corresponding number of liters.

Controlled by appropriate analytical methods, as described in Section 2.5.

Chemicals for analytical procedure; see details in Section 2.5.

2.4 Impregnation Procedure#

1. Fill impregnation vessels with solution from appropriate tanks.

---

* A process flow diagram covering the making, handling, and control of the impregnation solution is presented in Figure A5.

\# Description of the process is done under the assumption that four groups of one or more master plaques receive cycles 1 and 2 on a given day of operation and cycles 3 and 4, respectively, on the next day. A flow diagram for the execution of the whole process is presented in Figure A6.

C.P.E.D. PROCESS
IMPREGNATION SOLUTION

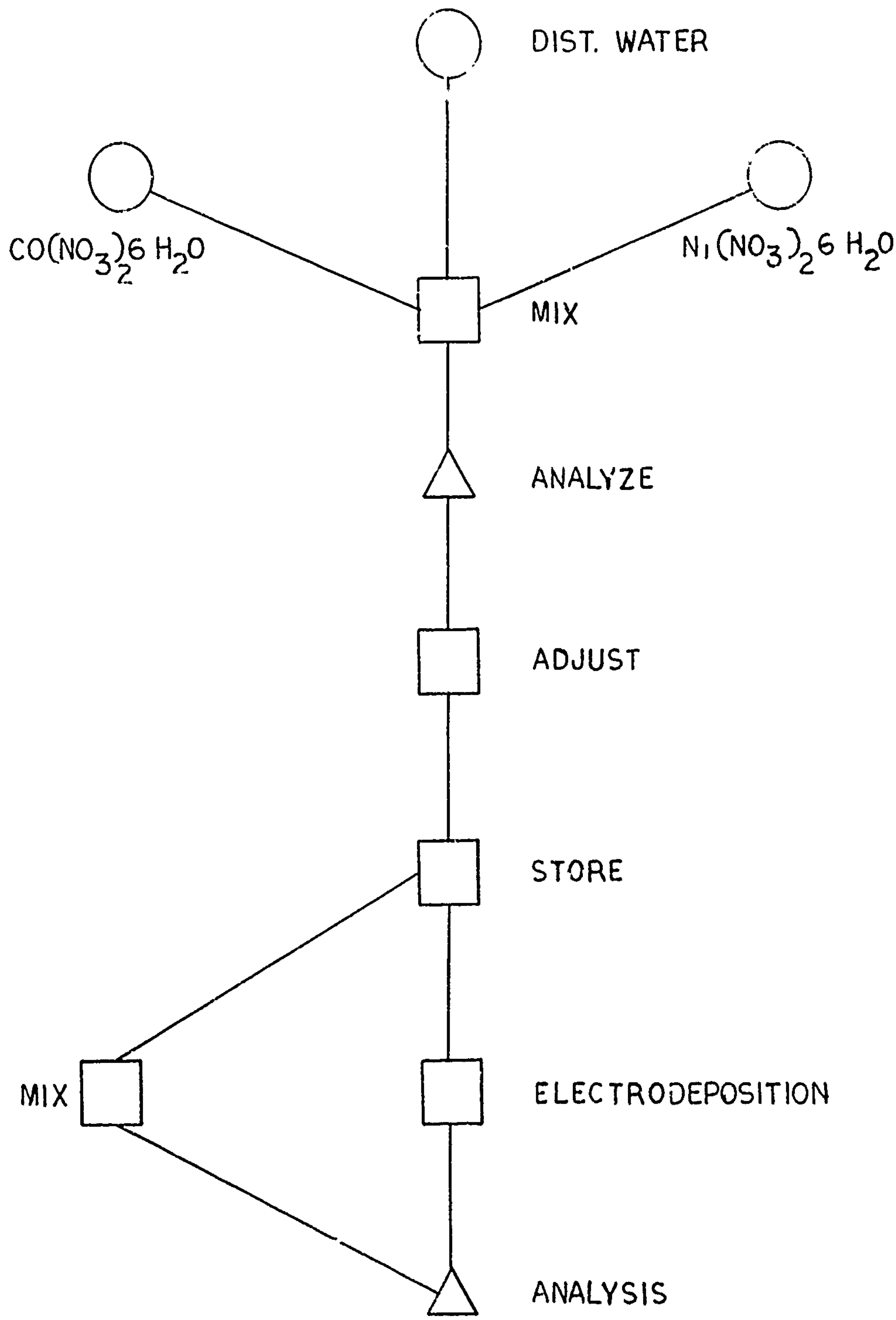

FIGURE A5

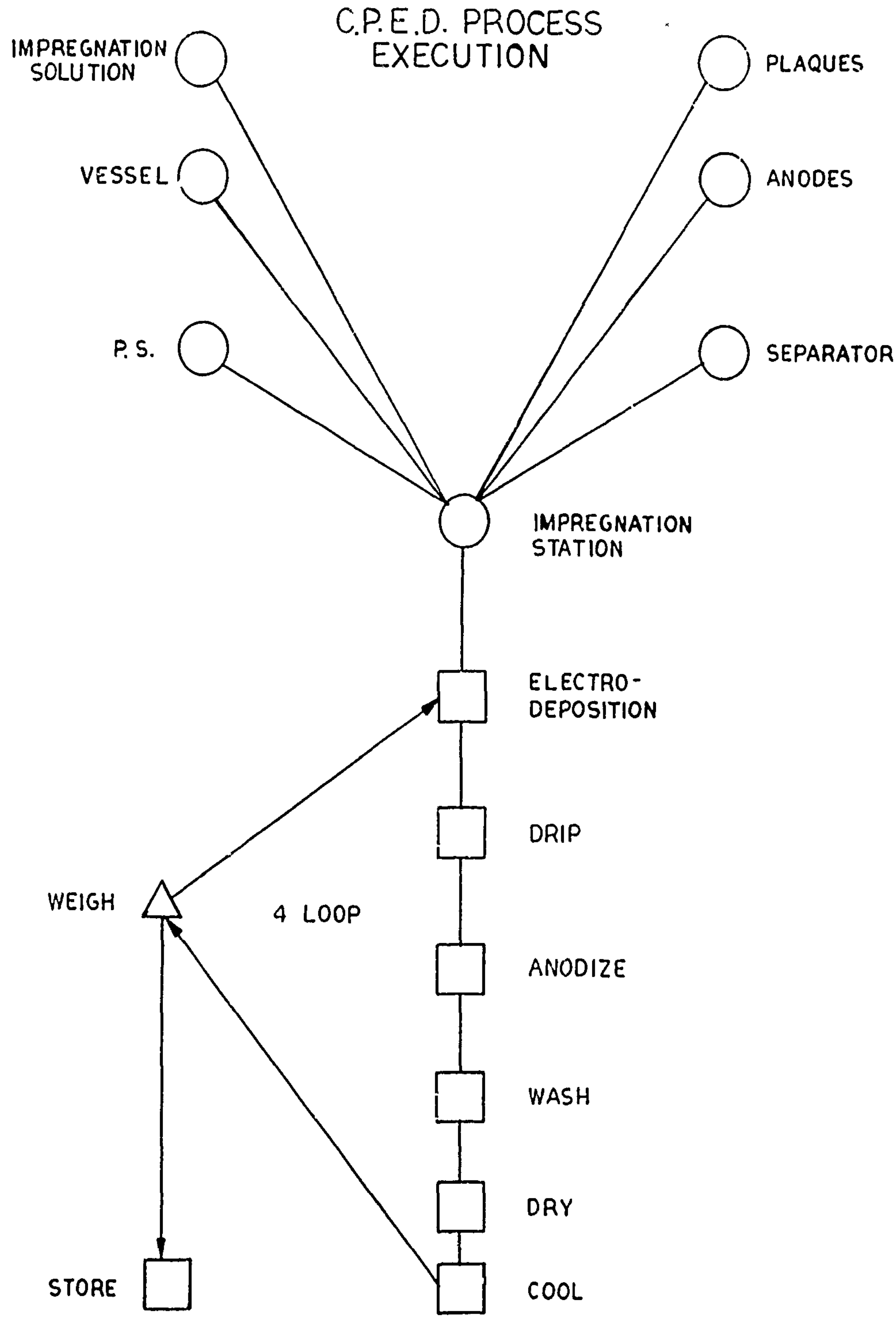
C.P.E.D. PROCESS
EXECUTION
IMPREGNATION
SOLUTION
VESSEL
P. S.
PLAQUES
ANODES
SEPARATOR
IMPREGNATION
STATION
ELECTRO-
DEPOSITION
DRIP
WEIGH
4 LOOP
ANODIZE
WASH
DRY
STORE
COOL

FIGURE A6

2. Transfer two liters solution from each tank into pre-heat glass beaker.

3. Cover beaker with watch glass.

4. Set timer and heater setting so that solution boils prior to start of first cycle.

5. Add hot solution to remainder in impregnation vessel. Stir well to equalize temperature of solution in 33 - 40°C range.

6. Take sample for analysis from each vessel, S_1 and T_1.

7. Weigh two master plaques and record individual weights.

8. Insert plaques into vessels, set timer to five minutes.

9. Make electrical power connections, i.e., master plaques to negative, and counter electrodes to positive pole of power supply. Watch for clean and good contacts! Vessels in series.

10. Connect voltmeter to cells.

11. Start power supply.

12. Close knife switch and set timer as follows:

Cycle	Minutes
1	45
2	30
3	30
4	30

13. Adjust constant potential as follows:

Cycle	Volts/Cell
1	3.0
2	2.75
3	2.5
4	2.5

14. Note initial current and temperature.

15. Watch constancy of potential, make temperature and ampere readings at prescribed intervals and note on appropriate sheet.

16. On signal from timer, open circuits, remove electrical connections, lift plaques out of bath, let drip for 15 seconds, and transfer plate to next processing station. At the first cycle the plaques are greenish in appearance.

17. Repeat parts 7 to 16 above with the next three groups of master plaques.

18. Take sample for analysis from each vessel, S_2.

19. Repeat points 7 and 16 above with the four groups of master plates for their respective second impregnation cycle.

20. Take sample for analysis from each vessel, S_3.

21. Cross-drain solution from impregnation vessel, i.e., A into tank B, B into tank A, etc., by means of solution pump.

22. Go through points 1 through 4 in preparation for next day's work.

23. Proceed with impregnation cycles 3 and 4 as outlined for cycles 1 and 2, respectively.

24. Introduce next four groups of master plaques into cycling operation.

2.5 Process Control

1. Free Acid; samples S1, S2, and S3

1. 5 ml solution from each impregnation vessel.

2. Pipet into 250 ml Erlenmeyer flask.

3. Add 100 ml distilled or de-ionized water.

4. Add 6 drops methylred indicator solution (.2% by weight in alcohol).

5. Titrate with .1 N NaOH from automatic buret until green.

6. Note consumption of titrant.

Note: The consumption of titrant tends to increase in the course of a given day, indicating a production of free acid with increasing amounts of charge passed through the impregnation vessels. This increase is more pronounced on days with impregnation numbers 1 and 2 than on days with cycles 3 and 4, respectively, when the average currents are low.

The cross-drain and mixing procedure at the end of each work day returns consumption of titrant back to initial values.

2. Total molarity of heavy materials; sample T_1

1. 1 ml from each impregnation vessel.
2. Pipet into 250 ml volumetric flask.
3. Fill to mark with distilled water.
4. Pipet 25 ml into 250 ml Erlenmeyer flask.
5. Add 1 - 2 ml concentrated nitric acid.
6. Add concentrated aqueous ammonia from squeeze bottle until solution is blue.
7. Add 100 ml distilled water.
8. Add 6 - 8 drops pyrocatechol violet (PCV) indicator solution (.5% by weight in distilled water).
9. Titrate with .1 molar EDTA solution until solution turns violet.
10. Note consumption of titrant. Its value in ml is equivalent to molarity of nickel plus cobalt.

Note: all practical purposes, the overall molarity of heavy metals remains constant even in the course of prolonged use of the same impregnation solution. However, since the cobalt was removed from the solution and not replenished, an appropriate correction of the composition of the solution appears to be mandatory from time to time.

3. Concentration of cobalt additive; sample T_1

1. 2 ml from diluted sample T_1 per point 3 above.
2. Pipet into 50 ml volumetric flask.

3. Fill to mark with reagent solution (30 g KSCN in 300 ml acetone).

4. Determine absorbance of solution at wavelength of 638 μ using, for instance, a Beckman Spectrophotometer, Model DB.

5. Calculate concentration based upon absorbance reading of known cobalt concentration and overall molarity of the impregnation solution.

Note: Since the non-replenished cobalt concentration tends to fall with length of use time of the impregnation solution, additions of solid cobalt nitrate in appropriate amounts are required in order to keep the concentration of this essential additive at its optimum level.

4. Monitoring of gain in weight

The weighing of the individual master plaques prior to each impregnation cycle is mandatory. It suffices to determine incremental gains in weight to 1/10 of a gram; however, immediate tabulation and comparison with previously acquired data is highly recommended in order to detect serious deviation of the process as soon as possible.

Although individual gains in weight per cycle may differ, the process has a strong leveling effect, and final gains in weight and corresponding theoretical capacities appear to be quite uniform.

2.6 Time Requirement

The processing of the master plaques through the complete impregnation procedure with all its steps requires two full working days of 8-1/2 hours duration. The output of finished plates per day is directly proportional to the amount of plaque processed simultaneously, i.e., the availability of equipment and man power.

3.0 CONVERSION STATION

3.1 Objective

To change the modification of the precipitated material from the hydrated to the denser anhydrous form, thereby providing additional pore volume for the subsequent impregnation steps.

3.2 Equipment Requirements

Two polypropylene vessels of the same dimensions as the impregnation vessels. This material chosen because it is impervious to attack by strong caustic. Vendor: E.H. Sargent Co., Cat. No. S-752-40.

Two fitted counter electrodes about 1.5 inches apart. Made from original porous nickel sinter strip used in the process.

Perforated corrugated PVC separator material completely covering the two counter electrodes.

A constant current power supply capable of supplying a maximum current of 30 amperes. Kepco, Flushing, N.Y., Model KO-45-30-M.

Insulated copper stranded wire, 8 gauge.

On-off double-pole knife switch.

Direct reading ammeter calibrated for the required 15 - 30 A range, GE type D091, Cat. No. 512X76.

Elapsed time clock with audio signal, Gralab Timer Model 171, 60 minute cycle.

Note: Equipment should be assembled in well ventilated area, preferably a laboratory hood, since significant amounts of H_2 are developed at the counter electrode and hazardous spraying of caustic mist can occur.

3.3 Material Requirements

Concentrated aqueous potassium hydroxide solution in the 20 - 31% by weight range.

Note 1: In principle, the less expensive NaOH in the same concentration range can be used. However, no information is currently available about possible influences of absorbed Na^+ ions on the performance of the finished electrode material.

Note 2: Since 7 - 8 gallons of concentrated caustic solution are freshly introduced into the process every second day, care should be taken to provide adequate disposal facilities for the spent caustic which also contains significant amounts of ammonia and solids stemming from external depositions.

3.4 Conversion Procedure

1. Fill vessels with the selected caustic solution to such a level that master plaques later on are completely covered.

2. Transfer master plaques from impregnation station after the 15 second drip period.

3. Insert master plaques between counters of the vessels and make sure that they are completely covered by liquid.

4. Connect master plaque to positive terminal and counters to negative terminal of regulated DC power supply. Two or more vessels in series operation.

5. Start timer at 30 minutes setting for all cycles and complete circuit by means of knife switch.

6. Regulate current to the following setting:

Cycle	Amperes
1	30
2	20
3	15
4	15

Note: These currents pertain to the geometric areas of the two types of master plaques treated. They were experimentally determined, and have to be prorated for other dimensions in order to avoid damage to the plate structures by means of too high values or insufficient conversion of the active material due to too low currents.

7. Open circuit by means of knife switch on signal from timer.

8. Disconnect wiring and remove plaques from vessels, letting excess caustic drip off for 15 - 30 seconds.

9. Transfer plaques to washing station. The plaques are deep black with occasional green spots on the surface.

3.5 Process Control

This is a non-critical processing step as long as the following precautions are taken:

- Electrically connect plates in proper order.
- Maintain prescribed currents.

- Keep plaques covered with liquid.
- Replace caustic every second day.
- Keep vessels covered when not in use to minimize carbonization of the caustic solution.

3.6 Time Requirements

The 30 minutes charging time, plus increments for assembly and disassembly, are part of the time requirements for a given impregnation cycle.

Abbreviation of treatment time by means of increasing the current density appears to be feasible, but is restricted with respect to the capability of the sinter structure to withstand any excessive currents.

4.0 WASHING STATION

4.1 Objective

To remove caustic and nitrogen compound containing solution from the surface and the pores of the plaques in preparation for the subsequent process steps.

4.2 Equipment Requirements

Two polypropylene containers as described in Section 3.2.

Four 3 to 4 liter Pyrex glass beakers.

Four fitting watch glasses.

Two hot plates for pre-heating. Any brand with regulation and power output of 750-1000 watts.

Two large Bunsen burners for after-heating, complete with tripods and asbestos wire nets.

Elapsed timer with audio signal - Gralab Timer, Model 171, 60 minute cycle.

Asbestos gloves for handling hot beakers.

4.3 Material Requirements

Adequate sources for deionized and/or distilled water to provide about 16 liters per master plaque processed in an eight hour working period.

Note: The demand on water supply can be cut back to about half by re-using water from a second washing for the first wash of the next plaque. However, this would require a reheating of the used water.

4.4 Washing Procedure

1. Start heating of water sufficiently ahead of time so that it is available when needed.

2. Place master plaque into cleaned and rinsed polypropylene container.

3. Cover plaque with 3 - 4 liters of boiling, or at least 90°C, deionized or distilled water heated on Bunsen burner.

4. Start timer at 20 minute mark.

5. Move distilled water beaker from hot plate spot to Bunsen burner, fill empty beaker with deionized or distilled water and place on hot plate with watch glass cover.

6. Move plaques gently through the water at regular intervals.

7. At end of 20 minute period, take plaques out of vessel and let drip while disposing of used water and rinsing out vessel to remove solids.

8. Return plaque to vessel.

9. Cover with 3 - 4 liter boiling distilled water from Bunsen burner location.

10. Start timer for second 20 minute wash.

11. Move wash beaker from pre-heating to after-heating position.

12. Gently move plaques in vessel at regular intervals.

13. On signal from timer, remove plaque from vessel, let drip for 15 seconds and transfer to drying process step.

14. Dispose of used water and clean vessel for next washing procedure.

4.5 Process Control

The following points have to be kept in mind.

1. At the moment of addition, the washing water should be boiling, but by no means colder than 90°C.

2. It is recommended to check, from time to time, the pH value of the water at the end of each washing period by means of either pH paper or a pH meter.

   Values of pH = 11 and pH = 8 are acceptable at the end of the first and second wash period, respectively. In case that greater values are consistently observed, the dripping time at the previous station should be increased and/or one additional rinse with cold water included prior to the two hot water washing steps.

4.6 Time Requirements

The two periods of 20 minutes each appear to be the minimum for the process as is. It is feasible, however, that washing in flowing hot water might constitute a saving in time.

5.0 DRYING STATION

5.1 Objective

To remove liquid water from pores and surfaces of the plaques in order to obtain a constant weight of the material.

5.2 Equipment Requirements

Any forced air oven with stable temperature setting in the 105 - 120°C range.

A suitable support device permitting hanging of the plaques unrestrained in the oven.

Note: While standing or leaning against the walls, the plaques appear to be prone to considerable warping.

An elapsed time timer with audiosignal: Gralab Model 171, 60 minute cycle.

Tongs or tweezers for removing hot plaques.

5.3 Material Requirements

None.

5.4 Drying Procedure

1. Freely suspend the dripped-off plaques in the hot oven at 110°C.

2. Close door and start timer at 20 minute mark.

3. At signal from timer, remove plaques from oven and transfer to cooling/weighing station.

5.5 Process Control

Occasionally check proper temperature setting and reading.

5.6 Time Requirements

The 20 minute drying period cannot be abbreviated, since experiments with both impregnated and unimpregnated porous material have shown that the weight becomes constant around 15 minutes drying time and a certain safety margin of about 5 minutes appears to be desirable.

6.0 COOLING AND WEIGHING STATION

6.1 Objective

To permit cooling to room temperature prior to the determination of the new weight of the plaques.

6.2 Equipment Requirements

A top loading balance with .1 g reading capability.

Mettler Model P4.

A soft brush for cleaning plate surfaces.

A suitable temporary storage device, for instance, ringstand with clamps.

6.3 Material Requirements

None.

6.4 Cooling and Weighing Procedure

1. Put hot plaques on clamps of temporary storage.

2. Let cool for 10 - .20 minutes.

3. Remove external flakes by means of gentle brushing with soft brush.

4. Weigh on top loading balance and note weight in proper place.

6.5 Process Control

Check zero-point of balance before each weighing. This is especially important when balance is used by several people.

6.6 Time Requirement

A cooling time of 10 minutes is sufficient.